Flanders
State of
the Art

18_037_1
FH reports

Methodology for Hydraulic Boundary Conditions and Safety Assessment 2021

SWAN v41.20 validation report for a higher wave climate

DEPARTMENT
MOBILITY &
PUBLIC
WORKS

www.flandershydraulics.be

Methodology for Hydraulic Boundary Conditions and Safety Assessment 2021

SWAN v41.20 validation report for a higher wave climate

Suzuki, T.; Trouw, K.; De Roo, S.

Flanders Hydraulics
Flanders State of the Art

Cover figure © Eddy Baete

Legal notice

Copyright and citation

This publication should be cited as follows:

Suzuki, T.; Trouw, K.; De Roo, S. (2025). Methodology for Hydraulic Boundary Conditions and Safety Assessment 2021: SWAN v41.20 validation report for a higher wave climate. Version 4.0. FH Reports, 18_037_1. Flanders Hydraulics: Antwerp.

Document identification

Customer:	MDK aKust	Ref.:	WL2025R18_037_1
Keywords (3-5):	SWAN, Belgian continental shelf model, wave transformation, wind waves		
Knowledge domains:	Coastal safety against extreme storms > hydrometeo climate of extreme storms > numerical modelling		
Text (p.):	130	Appendices (p.):	8
Confidential:	☒ No	☒ Available online	

Author(s):	Suzuki, T.

Control

	Name	Signature
Reviser(s):	De Roo, S. Trouw, K.	De Roo Sieglien Getekend door:Trouw Koen Jacobus M Getekend op:2025-06-04 17:40:38 +02:00 Reden:I approve this document Trouw Koen
Project leader:	De Roo, S.	Getekend door:Sieglien De Roo (Signatur Getekend op:2025-06-04 11:37:16 +02:0 Reden:Ik keur dit document goed De Roo Sieglien Vlaamse overheid

Approval

Head of Division:	Bellafkih, K.	Getekend door:Abdelkarim Bellafkih (Sign Getekend op:2025-06-04 11:30:29 +02:0 Reden:Ik keur dit document goed Vlaamse overheid

Abstract

In a safety assessment or design project, wave boundary conditions are necessary nearshore. In order to obtain them, a model for estimation of offshore to nearshore wave transformation and wind-generated waves needs to be applied. In the last two safety assessments (i.e. Safety Assessment 2007 and Safety Assessment 2015), the spectral phase-averaging model SWAN was used as the wave model since it is open source software and requires less computational resources (compared to phase resolving models).

Based on these arguments, SWAN will also be used in the Safety Assessment 2021.

Validation of an extensive data set of the higher wave climate showed that a change of the value of several input parameters could improve SWAN's estimation result (e.g. GEN3, breaking, time lag and wind speed reduction).

In this report, the selection of the extensive data set is explained, SWAN settings and associated results are discussed and eventually settings for the use of SWAN to calculate the wave boundary conditions nearshore are formulated.

Contents

List of tables

List of figures

1 Introduction

The SWAN model was used for estimation of offshore to nearshore wave transformation and wind-generated waves in order to obtain the wave boundary conditions at -5 m TAW or 1500 m from the dike (in the Safety Assessment 2007 and 2015; IMDC, 2007 and Suzuki *et al.*, 2016 respectively - here after SA07 & SA15). SWAN is a phase averaged wave model and thus it can simulate wave propagation and wind-generated waves with much lower computational cost compared to phase resolving wave models such as e.g. a Boussinesq-type model (like Mike21BW) or a non-hydrostatic wave model (like SWASH).

Note that wind-generated waves can only be properly estimated by such a phase averaged wave model: phase resolving wave models are expanding the capability to include wind-generated waves but it is not yet fully validated. Until today, a large number of studies have been conducted using SWAN in coastal engineering projects all over the world, thanks to its capabilities (i.e. most of main wave physics are implemented in the SWAN source code) and accessibility (i.e. open source). SWAN has been intensively used also in FHR. Apart from SWAN, another phase-averaging model TOMAWAC is now under investigation at FHR as an alternative wave transformation model (project 15_068), however, the number of validation cases is still limited.

Taking into account the feasibility and reliability, the SWAN model is selected to obtain wave boundary conditions for Safety Assessment 2021 (here after SA21). Relying on continued model developments and specific use of the model, it is still favourable to improve or optimize the present SWAN model for SA21.

In principle, the SWAN model and associated settings used for the last Safety Assessments (i.e. SA15) show good performance (De Roo *et al.*, 2016). However, further validation is required, especially for its related purpose here, i.e. transformation of the higher wave and wind climate, using one of the latest SWAN versions. Therefore, further optimization of the SWAN settings to be used for SA21 is conducted.

In this report, the original field measurement data sets and the procedure for cases' selection are explained, and in addition, SWAN settings and associated results are discussed taking into consideration the SA21 model application. Eventually, an update of SWAN settings is proposed for the estimation of the nearshore wave conditions.

2 Literature review

SWAN has a long history of practical applications of wave estimation under different conditions (e.g. deep/shallow water, high/mild wave climate) and different settings were investigated and validated in order to estimate wave climate under the target conditions. Thus these methods and techniques are relevant to this investigation. Note that the model has also been continuously developing, and therefore the same settings might not always work in different versions.

2.1 SWAN reports in FHR

In this section, a literature review mainly focused on the SWAN reports available in FHR is conducted to have an idea which parameters/settings can be important/relevant for this study.

Wave climate Ostend (Technum *et al.*, 2002)

One of the early works that SWAN was applied for Ostend harbour, at the Belgian coast (Technum *et al.* (2002)). This report investigated hydrodynamic boundary conditions using SWAN. The summary of the output is listed below. The difference of the present study is also noted at each line in italic.

- SWAN version 40.11
  - *One of the latest version 41.20.AB is used in the present study*
- SWAN in 2D stationary mode
  - *Same in the present study*
- Minimum 20 iteration in order to get good Tm02 value.
  - *Default iteration setting in 41.20.AB in the present study (also tested some cases)*
- Problem of rotation of the coordinate if each 5 degree is used – to avoid it, 24.9 deg was used
  - *Rotation of 25.5 degree is used in the present study*
- Offshore wave spectrum JONSWAP, gamma=3.3
  - *Same in the present study*
- Wind data is rescaled using a factor 0.9 taking into account the log law for the wind speed.
  - *Log law (to obtain u at 10 m from the sea surface at each time step) is applied in the present study (see section 3.1.2)*
- Wind input is every 6h between 1977 to 1983 and every 15 min between 1983 to 1994: most relevant input is used (i.e. 6h for 6h, 15 min for 15 min)
  - *Every 30 min data from 1994 to 2019 is used in the present study (see section 3.1.2)*
- Wind speed (average of MP7 and MP0) between N and NE is rescaled using a factor 1.07 since MP7 gives smaller value. But not for Ostend: those are not relevant.
  - *Such modification is not applied in the present study*
- Nesting is used. The coarse grid offshore is 250 m for along-shore and 100 m for cross-shore direction. 30 m x 30 m grid is used close to the target location.
  - *Nesting is not used in the present study*
- Bathymetry measured in 2002 is used. Note that this is not the exactly the same as BCP2002. However the difference is supposed to be small.
  - *BCP2015 is used, and comparison between BCP2002 and BCP2015 is conducted.*
- When the measurement parameter for significant wave height is H33 (significant wave height obtained from time domain analysis), a correction factor 1.06 is used to get equivalent value as Hm0.
  - *Same applied in the present study (see section 3.1.1)*
- Triads is not activated since the accuracy is not good enough.

  - *Tested in the present study*
- Quadruplets always on.
  - *Same applied in the present study*
- Conclusion: the value of the slope 'a' of y=ax regression line is 0.98 for Hm0 and 0.97 for Tp, and 0.89 for Tm-1,0 at the Ostend measurement
  - *See conclusions*

Safety assessment 2007 (IMDC, 2007)

This is the report of SA07. The difference of the present study is also noted at each line in italic.

- SWAN version 40.41
  - *One of the latest version 41.20.AB is used in the present study*
- SWAN in 2D stationary mode
  - *Same in the present study*
- Calculation and bathymetry input grid 250 m
  - *Same in the present study*
- Frequency domain 38 bins
  - *Same in the present study*
- JONSWAP spectrum with gamma=3.3
  - *Same in the present study*
- Directionel spreiding 30°
  - *This study is a validation case, and therefore actual directional spreading value is used*
- 3rd generation mode KOMEN
  - *Tested in the present study (Westhuysen, Komen)*
- Whitecapping OFF
  - *In this study GEN3 is activated and therefore whitecapping is also activated*
- Triads OFF
  - *Tested in the present study*
- Brekingsindex 0.73
  - *Different breaking command tested in the present study*
- FRICTION Jonswap coëfficiënt 0.067m²s-3 (voor sea wave condities)
  - *Tested in the present study (0.038, 0.067)*

Wave climate for Belgian coast (IMDC's work)

The series of this study produced 8 reports in the period between 2005-2009

Afstemming Vlaamse en Nederlandse voorspelling golfklimaat op ondiep water

- Deelrapport 1: Voorbereiding tijdsreeksen met randvoorwaarden. (International Marine and Dredging Consultants, 2005)
- Deelrapport 2: Voortzetting Validatie Numeriek Model : Tekst. (International Marine and Dredging Consultants, 2006)
- Deelrapport 3 Ontwikkeling van post processing tools. (International Marine and Dredging Consultants, 2009a)
- Deelrapport 4 : Technisch Wetenschappelijke Bijstand : Technisch wetenschappelijke bijstand: traject golfklimaat. (International Marine and Dredging Consultants, 2009b)
- Deelrapport 4 : Technisch Wetenschappelijke Bijstand : Technisch wetenschappelijke bijstand: traject onderzoek. (International Marine and Dredging Consultants, 2009d)
- Deelrapport 5: Rapportage jaargemiddeld golfklimaat. (International Marine and Dredging Consultants, 2009c)

From those reports it is concluded the recommended settings listed below. The difference of the present study is also noted at each line in italic.

- SWAN version 40.72
  - *One of the latest version 41.20.AB is used in the present study*
- Offshore wave height input is 1 hour averaged data
  - *Every 30 min data is used in the present study*
- The time lag of wave propagation from offshore to the target location is 1 hour
  - *Advanced time lag settings are tested in the present study (see section 6.2)*
- Wind input is 30 min averaged data
  - *The same time stamp is used for offshore wave and wind input (every 30 min data) in the present study (see section 6.2)*
- Wind data is rescaled using a factor 0.94 taking into account the log low for the wind speed to obtain wind speed at 10 m level, instead of 0.9 (Technum *et al.*, 2002).
  - *Log law is applied in the present study (see section 3.1.2)*
- The highest value of the wave height (i.e. 5 m) was calculated
  - *Not applied in the present study (see section 3.1.2)*
- Directional spread of 30 degrees was used
  - *This study is a validation case, and therefore actual directional spreading value is used*
- Grid resolution 250x250 m
  - *Same in the present study*
- Frequency between 0.025 and 0.85, msc = 37 (38 bins)
  - *Same in the present study (also tested other settings, see 6.2.10)*
- Offshore wave spectrum JONSWAP, gamma=3.3
  - *Same in the present study*
- Bathymetry BCP2002 (prepared by KUL & WL (2004) in wgs84 - mTAW)
  - *Tested in the present study (BCP2002, BCP2015)*
- Wave characteristics of Westhinder are also used for the western edge
  - *By default it is used in the present study (for SW, WSW it is tested, see 6.5.2)*
- For wind growth, WESTHUYSEN is used instead of KOMEN
  - *Tested in the present study*
- STOPC function with default setting (maximum 50 iterations[1])
  - *Tested in the present study*
- The resolution of direction is 10 degree instead of 4 degree
  - *Same in the present study*
- Triads is not activated (confirmed by Prof. Zijlema)
  - *Tested in the present study*
- Bottom friction 0.038 for swell and 0.067 for sea-waves
  - *Tested but no separation between swell and sea-waves*

Het hydraulisch randvoorwaardenboek – Achtergrondrapport (De Roo *et al.*, 2016)

This is the report of SA15. The difference of the present study is also noted at each line in italic.

- Swan in 2D stationary mode
  - *Same in the present study*
- Calculation and bathymetry input grid 250 m
  - *Tested in the present study*

[1] In De Roo *et al.* (2016), it is stated minimum 50 iterations but seeing the SWAN input listed in C.5, it is maximum 50 iterations (default) – in order to force 50 times, fraction [npnts] needs to be more than 100 %.

- Frequency domain 38 bins
  - *Tested in the present study*
- JONSWAP spectrum with gamma=3.3
  - *Same in the present study*
- 3rd generation mode WESTHUYSEN
  - *Tested in the present study*
- Triads OFF
  - *Tested in the present study*
- Brekingsindex 0.73
  - *Tested in the present study*
- FRICTION Jonswap coëfficiënt 0.067 m^2s-3
  - *Tested in the present study*

Taking into account that SA15 is the latest methodology for the estimation of a higher wave climate for the Belgian coast, most of the settings of (De Roo et al., 2016) are kept (exception: bottom friction) in the basic case (see detail settings in Section 4.3).

2.2 Broersbank reports

In this section, a literature review on the Broersbank reports is conducted to have an idea which parameters/settings can be important/relevant for this study.

Broersbank report from KUL (Ortega & Monbaliu, 2015; **Komijani *et al.*, 2016**)

- SWAN version 40.91 in combination with WAM V4.5.3
  - *One of the latest version 41.20.AB is used in the present study*
- Offshore boundary condition is from WAM
  - *Wave properties from WHI (JONSWAP with gamma=3.3 is assumed)*
- Unstatinary mode
  - *Stationary mode*
- Input time step for SWAN is 10 min
  - *The time lag is taken into account since the present study is based on stationary mode*
- ERA-Interim wind field (at 10 m height) is used
  - *Measured value at MP7 at 10 m height (corrected by log law) is applied in the present study. Note that Comparison of the ERA-Interim wind data with the measured values shows that the ERA-Interim corresponds fairly well with the measured wind data both in size and direction.*
- Grid resolution 250x250 m
  - *Same in the present study*
- Frequency between 0.05 and 0.5, msc = 24 (25 bins)
  - *Frequency between 0.025 and 0.85, msc = 37 (38 bins)*
- Bathymetry WL 14_KZ (CM50): originally from Marebasse project and some additional adaptation incorpolating the data from Flemish Hydrography
  - *The present study used BCP2015*
- Lateral boundary is naturally modelled by the WAM
  - *Lateral boundary is artificially modelled in the present study*
- For wind growth, WESTHUYSEN is used
  - *Westhuysen and Komen are tested in the present study*
- 98 % accuracy with maximum 20 times iteration
  - *Tested in the present study*
- The resolution of direction is 12 degree
  - *The resolution of direction is 10 degree*

- Triads is activated
  - *Triads is NOT activated*
- Bottom friction 0.067 (half value 0.0335 is also tested)
  - *0.067 and 0.038 are tested*

TOMAWAC report from FHR (Kolokythas *et al.*, 2018: WL2018R15_068_7)

- TOMAWAC model is used
  - *SWAN is used in the present study*
- Offshore wave input : spectral data from Westhinder bouy (WHIDW1)
  - *Wave properties from WHI (JONSWAP with gamma=3.3 is assumed)*
- Unstatinary mode
  - *Stationary mode*
- Simulation time step is 1 min
  - *The time lag is taken into account since the present study is based on stationary mode*
- ERA5 and MP7 wind field (at 10 m height) are used
  - *Measured value at MP7 at 10 m height (corrected by log law) is applied in the present study.*
- Unstructured grid is used
  - *Grid resolution 250x250 m in SWAN*
- Frequency from 0.025 (34 bins)
  - *Frequency between 0.025 and 0.85, msc = 37 (38 bins)*
- Bathymetry 'Scaldis-coast' model (Smolders et al., 2016, depeloped in WL project 13_131)
  - *The present study used BCP2015*
- No 'lateral' boundary since it is unstructured grid
  - *Lateral boundary exist in SWAN structured grid*
- For wind growth, Cavaleri and Malanotte-Rizzoli (1981) is used
  - *Westhuysen and Komen are tested in the present study*
- The resolution of direction is 10 degree
  - *The resolution of direction is 10 degree*
- Triads is NOT activated
  - *Triads is NOT activated in the present study*
- Bottom friction Formula of WAM cycle 4 is used
  - *0.067 and 0.038 are tested*

3 Data

3.1 Available data set

All the available data is listed below. The metadata in tree structure and original filenames can also be found in Appendix A (ALD.mat: data set used for this study).

3.1.1 Wave data

Measured wave data (every 30 minutes for the directional waverider and directional wavec buoy, 15 min for the waverider buoy) are obtained from Meetnet Vlaamse Banken (Vlaamse Hydrografie, 2014a). The coordinates of the locations, measurement data period, bottom level and normal distance to the coast line are summarized in Table 3.1. The wave parameters obtained at those locations are summarized in Table 3.2. Note that Waverider sometimes gives H1/3 value (significant wave height in time domain analysis), and therefore they are translated to spectral significant wave height Hm0 by multiplying factor 1.06 ($H_{m0}/H_{1/3}$) as used in De Roo *et al.* (2016).

Wave parameters are used for further analysis/simulations. Note that we selected WHI, AKZ, TRG, OST and BVH for the input/output locations for the validation. Each location in xy-coordinate WGS84UTM31 used in SWAN is calculated in the OpenEarth toolbox and listed in Appendix B.

As stated earlier, only parameter input is used for the validation since 1) spectral data is not directly available, and 2) thinking about the application where only parameter output will be used for the present safety assessment.

Instead of using spectral input, we are going to analyze the cases categorizing them into two:

- the cases where main wave direction and main wind direction are the same (less than 30 degree)
- the cases where main wave direction and main wind direction are different (more than 30 degree).

Doing that we can evaluate the performance of the parameter input (i.e. standard JONSWAP spectrum shape). In case the parameter input is not good enough, spectrum input can be explored for the further study.

Table 3.1 – Data type, name, location and time window from wave buoys: bold letters are selected locations*** (Vlaamse Hydrografie, 2014a)

sensor	Code	Location	Position N (WGS84)	Position E (WGS84)	Used Measurement data****	Bottom level [m TAW]	Normal dist. to coast [km]
Waverider	**TRG**	**Trapegeer**	**51° 8'15.04"N**	**2°34'58.97"E**	**1994.1-2019.10**	**-3.80**	**3**
	OST	**Oostende Oosterstaketsel**	**51°14'48.60"N**	**2°55'39.60"E**	**1997.4-2015.11**	**-5.92**	**1**
	WDL	Wandelaar	51°23'31.80"N	3° 3'1.80"E	1995.4-2014.10		
	A2B	A2-Boei	51°21'34.80"N	3° 7'11.40"E	1994.1-2014.10		
	SWI	Scheur Wielingen	51°24'5.40"N	3° 18'8.40"E	1995.3-2014.10		
	ZOK	Zand Opvangkade Zeebrugge	51°21'20.40"N	3° 11'34.20"E	2009.4-2014.10		
	AKZ	**Akkaert***	**51°25'5.40"N**	**2° 48'4.20"E**	**1994.1-2012.6**	**-26.43**	**22**
	KWI	Kwintebank	51°21'0.00"N	2° 42'21.00"E	2003.6-2010.10		
Dir. waverider	ONS	Oostende Noodstrand	51°14'17.00"N	2° 54'31.00"E	2004.8-2013.8		
	BVH	**Bol van Heist**	**51°23'30.60"N**	**3° 12'1.50"E**	**2005.4-2019.10**	**-9.29**	**6**
	OST	**Oostende Oosterstaketsel**	**51°14'48.60"N**	**2°55'39.60"E**	**2002.7-2006.4 2016.8-2019.10**	**-5.92**	**1**
	AKZ	**ZW-Akkaert**	**51°25'5.40"N****	**2° 48'4.20"E****	**2012.7-2019.10**		
	KWI	Kwintebank	51°21'0.00"N	2° 42'21.00"E	2010.11-2014.10		
	RAV	Raversijde	51°13'17.70"N	2° 42'30.00"E	2012.10-2014.10		
	WHI	**Westhinder**	**51°22'51.72"N**	**2° 26'20.82"E**	**2006.1-2019.10**	**-24.25**	**32**
Wavec	**BVH**	**Bol van Heist**	**51°23'30.60"N**	**3° 12'1.50"E**	**1993.6-2005.3**	**-9.29**	**6**
	WHI	**Westhinder**	**51°23'12.00"N**	**2° 26'52.00"E**	**1990.7-2011.12**		
	ODK	Oostdyck-bank	51°16'24.00"N	2° 26'44.00"E	2011.5-2014.10		

*AKZ POSITION IN SWAN SIMULATION WAS FIXED AT THIS POINT

**COORDINATE OF AKZ IS CORRECTED SINCE THE ORIGINAL DOCUMENT INDICATED THE SAME LOCATION AS A2B

*** SELECTED LOCATIONS CAN BE FOUND AT SENTION 2.3

**** ORIGINAL FILE NAME AND PERIOD CAN BE FOUND IN THE APPENDIX

Table 3.2 – Wave parameters and description (Vlaamse Hydrografie, 2014a)

Parameter Code	Omschrijving	Eenheid
E10	Laagfrequente golfenergie (0.03 Hz - 0.1 Hz)	cm².s
GEM	Energie maximum van het spectrum	cm².s
GTZ	Gemiddelde golfperiode	s
HLF	Hoogte golven met een periode > 10 seconden	cm
HM0	Significante golfhoogte berekend uit het spectrum	cm
HM1	Gemiddelde hoogte 10% hoogste golven berekend uit het spectrum	cm
HMM	Gemiddelde golfhoogte berekend uit het spectrum	cm
REM	Richting van de frequentiecomponent met de hoogste energie	graden
RHF	Richting van de hoogfrequente golven (periode tussen 2 en 5 seconden)	graden
RLF	Richting van de laagfrequente golven (periode groter dan 10 seconden)	graden
TPE	Periode van de golven met de hoogste energie	s
TZW	Zeewatertemperatuur	°C
SEM	Spreidingshoek van de frequentiecomponent met de hoogste energie	graden

Parameter Code	Omschrijving	Eenheid
H33	Gemiddelde hoogte van de 33.3% hoogste golven	cm
H10	Gemiddelde hoogte van de 10% hoogste golven	cm
H01	Gemiddelde hoogte van de 1% hoogste golven	cm
GTZ	Gemiddelde golfperiode	s
E10	Laagfrequente golfenergie (0.03 Hz – 0.1 Hz)	cm².s
HLF	Hoogte golven met een periode groter dan 10 seconden	cm
TPE	Periode van de golven met de hoogste energie	s
GEM	Energie maximum van het spectrum	cm².s

3.1.2 Wind data

Wind measurement data (every 10 minutes) are also obtained from the Meetnet Vlaamse Banken (Vlaamse Hydrografie, 2014b). The coordinates of the locations are shown in Table 3.3. The parameters and description are shown in Table 3.4.

In this study we selected MP7 and MP0, to represent the wind field of the entire calculation domain. The measurement data of MP7 are obtained at z=26.143 m TAW (East, MP7/WI1 – WL1 indicates the name of data, obtained at the east side of the wind sensor) and 26.156 m TAW (West, MP7/WI2). MP7/WI0 gives information of highest wind speed of the two (Vlaamse Hydrografie, 2014b): it shoud be noted that, even though MP7/WI0 should be the highest wind speed of the two theoretically there is a difference between MP7/WI0 and the calculated maximum of the measuring sensors WI1 and WI2, see Figure 2-9 in De Roo *et al.*, 2016). The data MP7/WI0 is used and further processed to obtain the velocity at 10 m above the sea level at the time step using the log-law equation shown below. Since there is no sea level data each time step at MP7/WHI, OST maregraph data which has longest data (see Appendix A) was used for this processing.

$$u(z_2) = u(z_1)\frac{\ln((z_2 - d)/z_0)}{\ln((z_1 - d)/z_0)},$$

where $u(z_1)$, $u(z_2)$ are the wind speed at the position z_1 and z_2 respectively, d the zero plane displacement (in metres), z_0 is the surface roughness (in meters). In this calculation d=0 m, z_2=(height of the measurement point) - (OST sea level at the time step) m, z_2=10 m and z_0=0.001 m were applied (De Roo et al., 2016b). The value can be changed according to the sea state and wind speed, and therefore it is not an optimum value but we assume it is an acceptable value. For further accuracy the value can be further optimized if necessary.

The measurement data obtained at MP0 are summarized in Table 3.5. Note that the wind speed till 2014 has been corrected to 10m reference level as explained above (after 2014 the measurement data is already corrected). Therefore data in ALD.mat (Appendix A) is velocity at 10 m above the sea level at the time step. The correction is done based on the equation above.

Table 3.3 – Data type, name, location and time window from anemometers: bold letters are selected locations (Vlaamse Hydrografie, 2014b)

Type of sensor	Code	Location	Position N (WGS84)	Position E (WGS84)	Measurement data
Wind	**MP0**	**MP0 - Wandelaar**	**51° 23'40.04"N**	**3°2'44.82"E**	**1994.4-2014.10** **2014.1-2019.10**
	MP4	MP4 – Bol van Heist	51°25'6.08"N	3°17'54.88"E	2010.3-2014.10
	MP7	**MP7 – Westhinder**	**51°23'18.74"N**	**2° 26'16.18"E**	**1994.3-2014.10** **2014.1-2019.10**
	ZDI	Daminstrumentatie Zeebrugge	51°21'15.00"N	3° 10'20.00"E	1998.5-2014.10
	ZMP	Meteopark Zeebrugge	51°20'7.00"N	3° 13'11.00"E	1993.6-2014.10

Table 3.4 – Wind parameters and description (Vlaamse Hydrografie, 2014b)

Data	Parametercode 10-minuut data (herh.tijd=010)	Eenheid data	Opmerkingen
- Gemiddelde windsnelheid	WVS	m/s	
- Max. 3sec windstoot	WG3	m/s	
- Max. 1sec windstoot	WG1	m/s	Enkel op de meteoparken
- Gemiddelde windrichting	WRS	°	

Table 3.5 – Wind measurement period, sensor and height for MP0 (Vlaamse Hydrografie, 2014b)

Periode	Data	Geplaatste sensor	Hoogte sensor tov TAW
01/04/1994-21/01/1997	WI1	NBA	22.636m
21/01/1997- 16/06/2000	WI1	Friederichs 4433.210	19.2m
Vanaf 16/06/2000	WI1	Vaisala Type WAA151 en WAV151	19.2m
Vanaf 28/03/2002	WI1	Vaisala Type WAA151 en WAV151	19.877m
	WI2	Vaisala Type WAA151 en WAV151	27.547m
05/08/2004-03/11/2004	Renovatie meetpaal 0: bijgevolg geen data		
Vanaf 03/11/2004	WI1	Vaisala Type WAA151 en WAV151	25.068m
	WI2	Vaisala Type WAA151 en WAV151	27.568m
05/10/2009-nu	WI1	Vaisala Type WAA151 en WAV151	25.731m

3.1.3 Water level data

Water level data (every 5 minutes) are also obtained from the Meetnet Vlaamse Banken. The coordinates of the locations are shown in Table 3.6. As can be seen, WL-OST has more detailed data between 1992-2000.

Table 3.6 – Locations of the water level data

Type of sensor	Code	Location	Position N (WGS84)	Position E (WGS84)	Measurement data
Water level	WL_ZLD	Zeebrugge Leopold II dam	51° 20' 46.00"N*	3° 12' 01.00"E*	2000-2010 2011-2014 2014-2019
Water level	WL_OST	Ostend harbor maregraph	51° 14' 03.00"N**	2° 55' 36.00"E**	1992-2000 2000-2019
Water level	WL_NPT	Nieuwpoort	51° 09' 02.00"N*	2° 43' 41.00"E*	2000-2010 2011-2019

*POSITION COORDINATE IS BASED ON THE PRESENT MEASUREMENT LOCATION

** THE POSITION WAS MOVED SOME YEARS AGO FROM THE WEST SIDE OF THE HARBOUR TO THE EAST SIDE (THE COORDINATE LISTED HERE IS THE PRESENT ONE)

3.2 Data selection

3.2.1 Introduction of data selection

From all available data explained in the last section, we selected the relevant cases to be of use for the validation. Selection is done in two different ways, namely a selection starting from offshore and a selection starting from nearshore.

The selection from offshore is to focus on big events from offshore and labelled as the standard selection (593 cases). This method is rather straightforward when we take into account the time lag (wave delay between WHI and the nearshore measurements, see detail definition at page 24): the time lag can be explicitly calculated from the offshore boundary conditions (wave direction and period) at the time of the biggest event offshore.

We learned that the biggest waves offshore do not always lead to big events nearshore. In order not to miss important events nearshore, an extra selection is added to the standard selection (99 cases). In this case, time lag calculation is rather complex (time lag is a function of the offshore wave direction and group wave celerity). To avoid too much complication, we made one assumption: we use the offshore boundary conditions (wave direction and period) at the time of the biggest event nearshore to calculate the time lag.

a) example: standard selection

First we look at the offshore time series at WHI:

	0:00	0:30	1:00
WHI	4m, NNW, 10s	**5m, NNW, 10s**	4m, NNW, 10s
		(biggest Hm0)	

In this case we can find the peak of significant wave height at 0:30. Then the time lag is calculated based on the wave direction and period at the peak, NNW and 10s taken into account the wave front distance between WHI and TRG. This resulted in 30 min delay, then we use TRG data after 30 min for the comparison.

TRG	1m, NNW, 11s	1m, NNW, 10s	**2m, NW, 10s**

b) example: extra selection

In this case we first look at the nearshore time series at TRG (or OST, BVH):

	0:00	0:30	1:00
TRG	1m, N, 11s	1m, NNW, 10s	**2m, NW, 10s**
			(biggest Hm0)

Seeing the biggest event in TRG, we do not know the time lag a priori, since wave direction nearshore includes some influence of the nearshore bathymetry. Instead of using this nearshore wave direction, we look at the wave direction offshore and the wave period to decide the time lag.

WHI	4m, NNW, 10s	5m, NNW, 10s	4m, **NNW, 10s**
			(same time as nearshore biggest event)

Then, the time lag is calculated based on wave direction NNW and peak wave period 10 s taking into account the wave front distance. If it gives 30 min, then the offshore data at 0:30 is used as the input of the simulation.

WHI	4m, NNW, 10s	**5m, NNW, 10s**	4m, NNW, 10s

It might not always be very correct but most of the time the wave period and direction are the same for a few hours.

3.2.2 Selection from offshore (standard selection)

The selection from offshore (i.e. standard selection) is made based on the *findpeaks* command from ®Matlab. After applying the *findpeaks* over the entire time series of Hm0 at WHI, we set the thresholds for the selection criteria to select a limited number of big storm events. The criteria are shown below.

Hm0 peaks (WHI) by the peak detection algorithm

+ a criterion of, at least, half a day interval between the peaks

+ a minimum Hm0 (depends on wave direction: see details below)

criteria	Hm0 +	number of sample
SW	3.5 m	65 points
WSW	2.7 m	62 points
W	2.1 m	65 points
WNW	2.0 m	69 points
NW	1.8 m	68 points
NNW	1.9 m	65 points
N	3.0 m	65 points (35 points: 0-11.25°, 30 points: 348.75-360°, cf. Figure 3.2)
NNE	2.8 m	66 points
NE	2.0 m	67 points

+ wave direction only SW, WNW, …, NE

+ Tp, dir, spreading data also available

+ Wind data MP7 available

+ Water level data WL-OST available

These criteria lead to a total of 593 points (each wave direction > 60 samples). See the selected points in Figure 3.1 and the number of the cases of the selected direction in Figure 3.2.

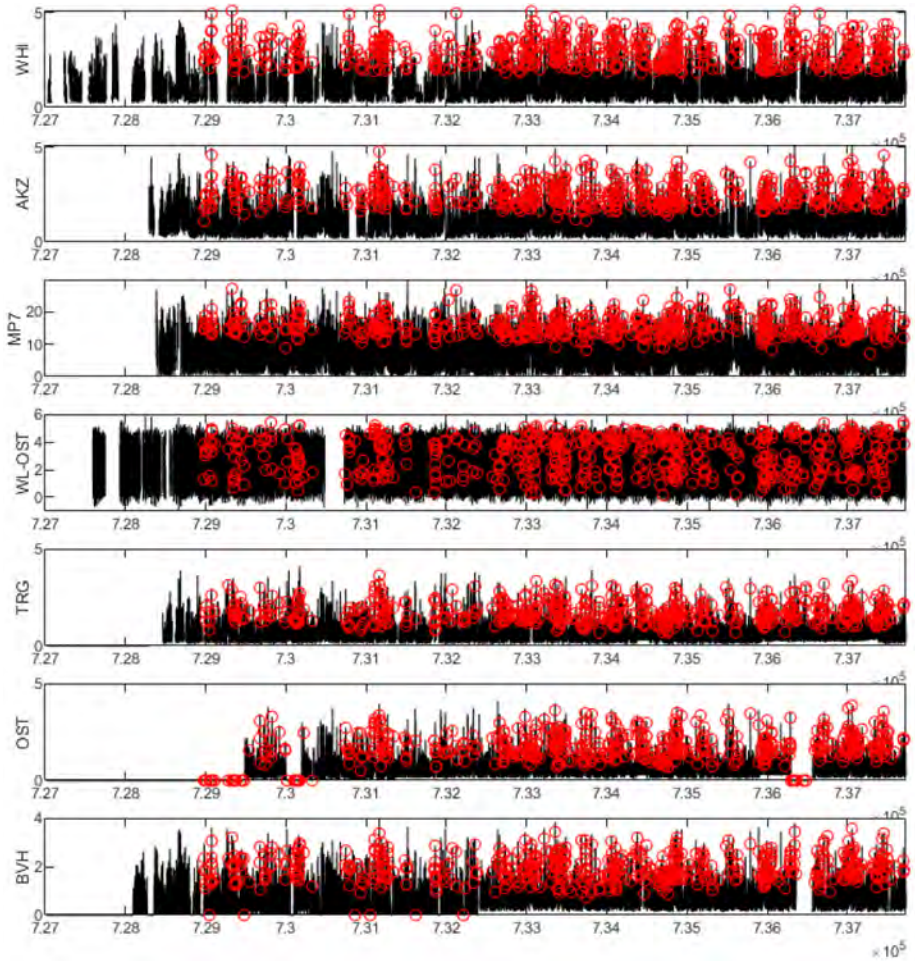

X AXIS IS SERIAL DATE NUMBER. THE FIGURE SHOWS THE DATA OF 1990-2019.

Figure 3.1 – Standard data selection (593 data)

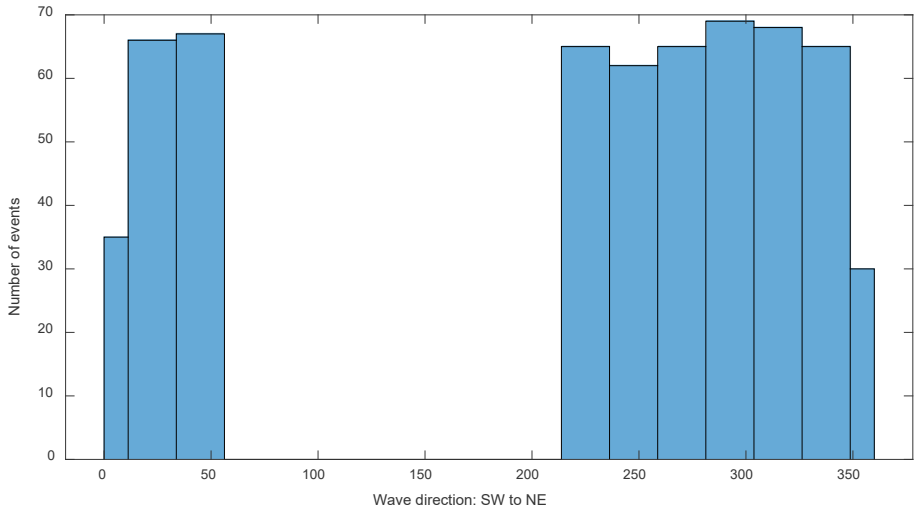

DIRECTION N IS THE SUMMATION OF DATA 0-11.25 AND 348.75 - 360.

Figure 3.2 – Selected wave direction and number of events (standard cases)

3.2.3 Selection from nearshore (extra selection)

The selection from nearshore is also made based on the *findpeaks* algorithm. After applying the *findpeaks* over the entire time series of Hm0 at TRG/OST/BVH, we set the thresholds for the selection criteria to select a limited number of big storm events. The criteria are shown below.

Hm0 peaks (TRG, OST, BVH) by the peak detection algorithm, applying a fixed Hm0 threshold of 3.1m

+ a criterion of, at least, half a day interval between the peaks

+ a minimum Hm0

criteria Hm0 + number of sample		
SW	total	66 points
WSW	total	63 points
W	total	67 points
WNW	total	74 points
NW	total	79 points
NNW	total	81 points
N	total	114 points (59 points: 0-11.25°, 55 points: 348.75-360°, cf. Figure 3.4)
NNE	total	80 points
NE	total	67 points

+ offshore wave direction at the same time of the nearshore peak only SW, WNW, …, NE

+ Tp, dir, spreading at the same time of the nearshore peak also available

+ Wind data MP7 at the same time of the nearshore peak available

+ Water level data OST at the same time of the nearshore peak available

These criteria lead to a total of 99 points and eventually the cases are extended to total 692 points. See the selected points in Figure 3.3 and the number of the cases of the selected direction in Figure 3.4.

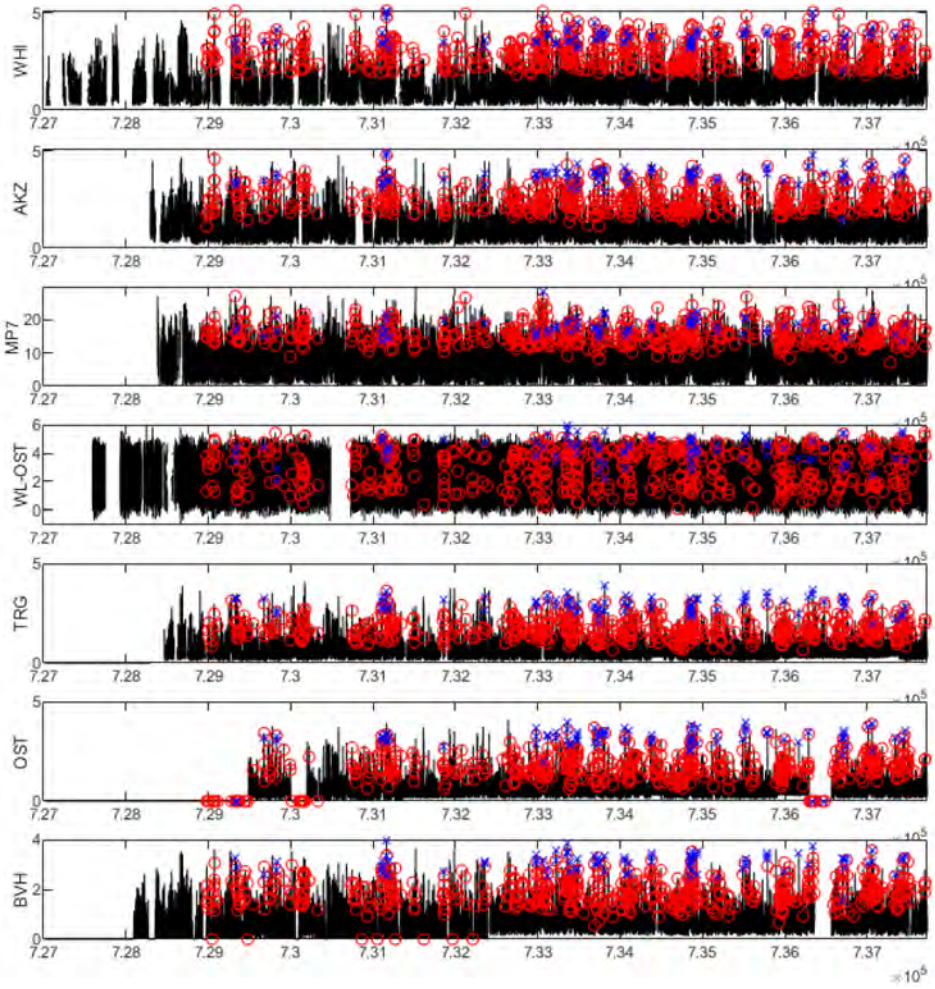

Figure 3.3 – Standard (= red) +extra data (= blue) selection (692 data)

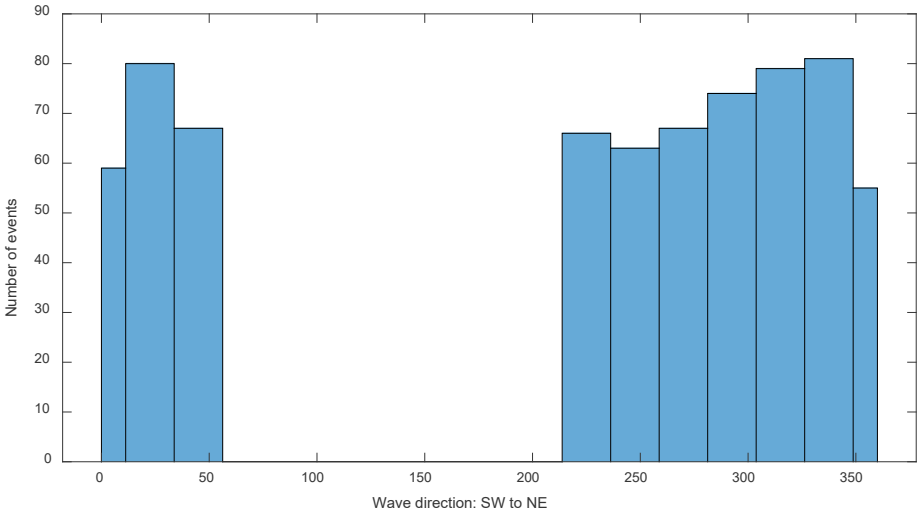

Figure 3.4 – Selected wave direction and number of events (standard+extra cases)

4 Model

4.1 SWAN model

SWAN (Simulating WAves Nearshore) is a third-generation wave model, developed at Delft University of Technology, which computes random short-crested wind-generated waves in coastal regions and inland waters (Booij *et al.*, 1999). This model is based on the numerical solution of the wave action balance equation and accounts for physics such as wave propagation, shoaling refraction, wave generation by wind, transmission through and reflection against obstacles and diffraction. It has to be noted that wave diffraction is modelled in a simplified manner, by use of a phase-decoupled refraction-diffraction approach proposed in Holthuijsen *et al.* (2003) in order to describe (qualitatively rather than quantitatively) the behavior of spatial variation in wave direction.

4.2 Version of the model

In SA15, SWAN version 41.01 was used for wave transformation from the offshore boundary (~30 km from the coastline to -5m TAW/1500 m distance from the coast) (De Roo *et al.*, 2016). On the other hand SWAN version 40.41 was used for SA07 (IMDC, 2007). The differences of the versions are expected to be minor (personal oral communication with M. Zijlema on 15/2/2019). However, according to Zijlema, one of the major upgrades from version 40 to 41 was the improvement of whitecapping, which results in roughly the same wave height but a shorter wave period. Other updates have minor influence on the output. Note that the latest user guide book of the SWAN (The SWAN team, 2019b) recommends to use the bottom friction of 0.038 (now it is the default value instead of 0.067, which was the default value in the older versions before version 40).

SWAN version 41.01 was tuned for SA15, however, the number of validation points for higher waves (Hs >= 3.8m at WHI) was limited, i.e. only 209 events from the time window 1997-2005 (mostly wave direction from north) and, additionally, sensitivity analysis was not fully conducted. Thus it is recommended to further validate and calibrate the model by means of bigger data set including different wave directions in order to have better validated wave boundary conditions at – 5 m TAW/1500 m location points.

In this report, further comparisons between the latest stable version 41.20.AB and the older version 40.85 are conducted (note that v.40.85 and v.41.10 are the only archived versions on the FHR's cluster: therefore no comparison has been made for v.41.01 which was used for SA15).

4.3 Basic calculation settings

Dimension and direction

Two dimensional mode is used since the computational domain is 2DH. The Nautical convention for wind and wave direction (SWAN input and output) is used instead of the default Cartesian convention. The Nautical convention uses the direction where the wind or the waves come from, measured clockwise from geographic North. Note that directions are in degrees and not in radians.

Stationary mode

The above mentioned validated models, applied for SA07 and SA15, are used in stationary mode. It means that SWAN calculates the saturated wave condition in the domain. Non-stationary mode can be more appropriate if it is only for the validation purpose since we have time evolution of wind, waves and water levels at each measurement location. However, stationary mode is used in this study for the validation since the model in the end will be used to obtain hydraulic boundary conditions for high and extreme events for which we do not know the time evolution: we only assume offshore wave conditions according to extreme wave statistics. Since we use stationary mode for the validation, we need to think of a possible time lag between offshore and nearshore waves for the validation.

Computational grid and frequency resolution

The default computational grid settings of the model are summarized in Table 4.1. The Cartesian coordinates with fixed grid size is used. The coordinate of the domain is based on WGS84 – UTM31. The model is referred to as 'Belgian coast model'. See details in De Mulder *et al.* (2004).

The spectral wave directions cover the full circle and the resolution is 10 degree (i.e. 36 bins for direction). The frequency domain is between 0.025 and 0.85 Hz with 38 bins by default.

Table 4.1 – Default domain settings of the Belgian coast model

Origin of X coordinate (WGS84UTM31) [m]	Origin of Y coordinate (WGS84UTM31) [m]	Rotation [deg]	Domain size in X [m]	Domain size in Y [m]	Number of grid in x	Number of grid in y
438116.00	5639190.00	25.50	125000	39000	500 (dx=250 m)	156 (dy=250 m)

Bathymetry

The model bathymetries of the Belgian coast (both BCP2002, top figure and BCP2015, bottom figure) are shown in Figure 4.1. The grid resolution of both bathymetries in x-direction and y-direction is identical and equals to 250 m; the number of the data points is 157 and 501 (i.e. calculation grid +1 to cover the region with 156x500 grid cells), respectively. On the map, the used measurement locations from Meetnet Vlaamse Banken have been placed to give their overview in the domain.
In this study, the SWAN bathymetry file based on BCP2015 (BCP=Belgisch Continentaal Plat; filename 'wgs84_taw_swan2015.dep'; see more details in De Roo *et al.*, 2016) is mainly used for the validation, taking into account the fact that BCP2015 was developed based on the surveys between 1997 and 2015. This time window matches good with the selected validation data set from 1995 to 2019. BCP2002 (filename 'wgs84_taw_swan.dep'; see details in De Mulder *et al.,* 2004) has been used for the validation for SA07 and SA15, however, the SWAN bathymetry file based on BCP2002 has been made based on the survey till 2002 (detailed year unknown) and thus it is not representing better than BCP2015.
Note that the difference between the bathymetry of the BCP2002 and the BCP2015 is not significant according to Figure 4.2 (the difference between two bathymetries is mostly around -0.5 to 0.5 m). This trend -the bathymetry did not significantly change over the last decades - is also confirmed in Janssens *et al.* (2013).

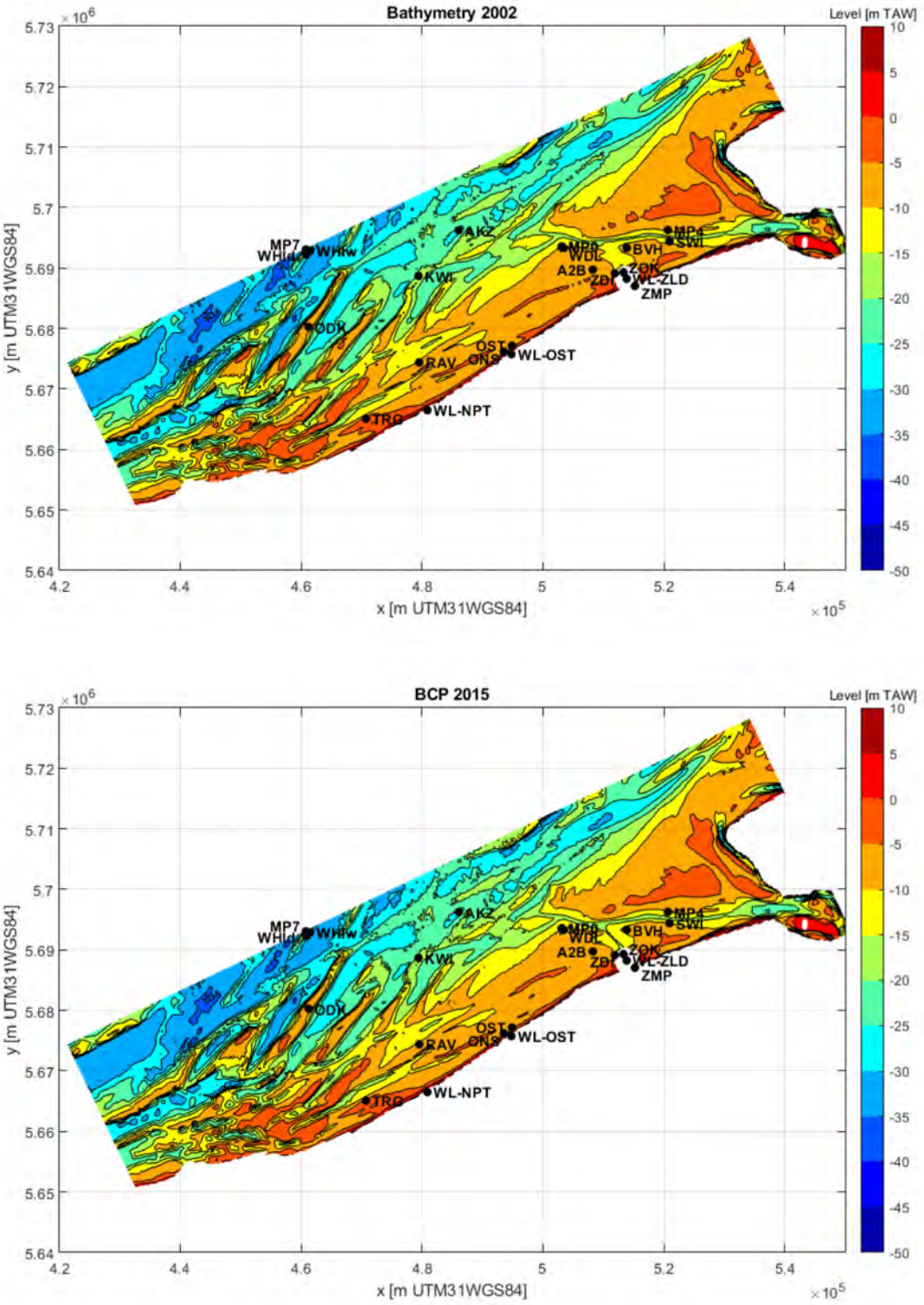

SEE THE DETAILS OF THE MEASUREMENT POINT IN SECTION 3.1

Figure 4.1 – The Belgian coast model with measurement locations obtained by Meetnet Vlaamse Banken. BCP2002 (above) and BCP2015 (below)

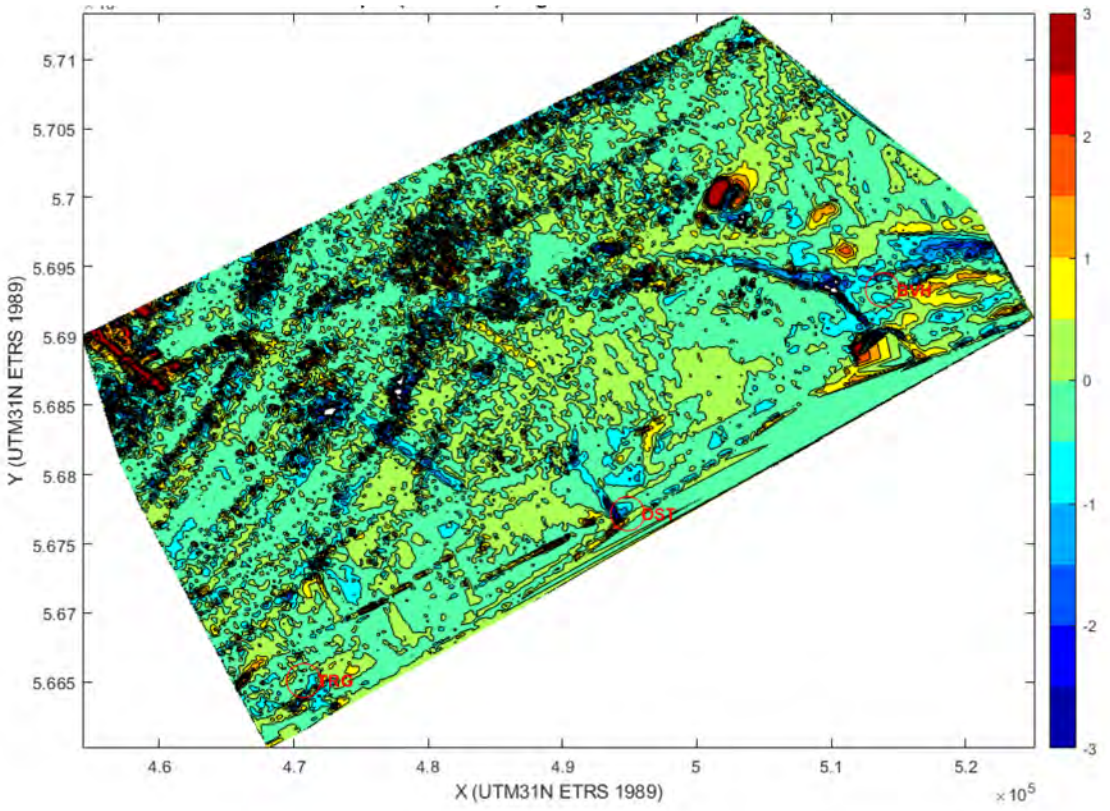

NOTE THAT THE DOMAIN SHOWN HERE IS NOT THE SAME AS FIGURE 4.1

Figure 4.2 – Difference (in [m]) between BCP2002 and BCP2015 (value=BCP2015-BCP2002)

Water level

In the model, the relevant water level is used based on the field measurement data in the harbour. By default the maregraph in the Ostend harbor (tide measurement in TAW; WL-OST) is selected as basic water level point since it is located more or less the center geographically in the calculation domain. The detailed specification and discussion is found at Section 4.4.

Offshore spectrum shape

Offshore spectrum peak is assumed to be a JONSWAP spectrum with gamma factor 3.3 as default. The directional distribution is often expressed as $\cos^m(\theta)$ where m is directional spreading factor. In SWAN it is also possible to express the directional spreading in degree, which is used for the input in this study. Note that the directional spreading is a (one sided) standard deviation of the spreading function.

In the reality the spectrum shape can be different from the theoretical spectrum shape. For example a two peaks spectrum can be observed when swell direction and wind direction is different. Therefore the influence of wind direction is investigated in this study. Yet, the standard shape is kept as a JONSWAP spectrum with gamma factor 3.3. In the validation, the measured directional spreading value (SEM) is used.

Wave boundary conditions

Wave boundary condition parameters (i.e. significant wave height, peak period, main wave direction, directional spreading) are decided based on the measurement at WHI as default. The same wave properties are also imposed at the lateral boundaries for the validation.

3rd generation mode

The model runs in third-generation mode for wind input, quadruplet interactions and whitecapping. Westhuysen (nonlinear saturation-based whitecapping combined with wind input of Yan, 1987) is selected for the run as selected in De Roo et al. (2016b). Note that Whitecapping, Quadruplet automatically is included if no declaration OFF WCAP, OFF QUAD. Triads, which is nonlinear three wave interaction – see details in section 4.4, was not activated as default following the past methodologies SA07 and SA15.

Wave breaking

Depth induced wave breaking is activated. A constant breaker index is used, with the value of alpha (proportionality coefficient of the rate of dissipation) =1.0 and gamma (the breaker index, i.e. the ratio of maximum individual wave height over depth)=0.73 as default as selected in De Roo et al. (2016b). Different methods are also tested in this study.

Bottom friction

JONSWAP with a constant friction coefficient is applied. By default 0.038 m^2s^{-3} is applied, since the domain is sandy bottoms as recommended in the SWAN user manual (The SWAN team, 2019b). Different bottom friction factor/methods are also tested in this study.

Wind input

Wind input in SWAN includes direction and velocity at the point of 10 m above the sea level at the time step. The measurement data is used for the wind input. See details of the pre-processing of the wind speed in Section 3.1.2.

Numerics

Default numeric settings are applied.

Output

Selected output point are Trapegeer (TRG), Oostende Oosterstaketsel (OST) and Bol van Heist (BVH). They are representative of the eastern (Dutch side), center, and western (French side) coastline and located nearshore, see locations in Figure 4.1.

Furthermore, these locations were used for the validation of SA15 settings (De Roo *et al.*, 2016). Note that the bottom levels differ – TRG -3.80 m TAW, OST -5.92 m TAW and BVH -9.29 m TAW, which variability is also useful for the discussion of the quality of the results. See details about the location in Section 3.1.

Note that the typical nearshore output location in the Safety Assessment is around – 5 m TAW. Taking into account the extreme water level (e.g. +7 m TAW), and the extreme significant wave height (e.g. 5 m), an output location at -5 m TAW is close to the wave breaking point (depth 12m * breaker index 0.73 / Hmax ratio 1.8 = significant wave height 4.9 m). This fact needs to be carefully considered in the decision of the final settings for SA21.

Output parameters in SWAN are the spectral significant wave height Hm0, the spectral peak period Tp, the spectral average wave period Tm02 and the main wave direction dir (SWAN output DIR: mean wave direction) while output parameters of the field measurements are the spectral significant wave height Hm0, the spectral peak period Tp, the spectral average wave period GTZ and the main wave direction of the energy maximum dir (REM). Note that Waverider sometimes gives H1/3 value (significant wave height in time domain analysis), and therefore they are translated to spectral significant wave height Hm0 by multiplying factor 1.06 ($H_{m0}/H_{1/3}$) as used in De Roo *et al.* (2016). GTZ is comparable to Tm02 most of the time (till 1998, GTZ is comparable to 1.1*Tm01 for the wavec data, see details in Vlaamse Hydrografie, 2014a).

4.4 Possible improvements / parameter to be tested

Possible improvements for SWAN model are listed below. Sensitivity analyses and validation are conducted based on the selected cases from the measurement data set of Meetnet Vlaamse Banken (see details in Appendix A).

Extended number of cases

The number of selected test cases for the validation is extended from 209 (SA15) to 692 cases (SA21, this study). Furthermore, the selection of the cases is based on the offshore wave direction, so that enough data is available for each direction to be evaluated, see details in Section 3.2.

Different versions (version 41.20.AB vs 40.85)

The present latest stable release version of SWAN is 41.20.AB (at the moment of January 2020). By default we use version 41.20.AB. Together with version 40.85 (older version used and archived at FHR), comparisons are made.

Different grid sizes (grid sizes)

In SA15, the grid size of 250 m (Cartesian coordinate) has been used for SWAN after comparing it with a finer grid resolution (dx=250 m, dy=125 m), taking into account that the latter model setup did not significantly improve the results. The coarser resolution was thus preferable for the computational cost. Nevertheless the finer resolution cases (250x125, 125x125 m)are tested in this study using BCP2020, to check if the mentioned extended data set leads to a different conclusion.

Different bathymetry (BCP2002 vs BCP2015)

There are two bathymetry files, i.e. BCP2002 and BCP2015, based on (combined) surveys of different time windows; 2002 and 2015 being the last year included in the bathymetry resp. These are compared.

Input of wave data (WHI vs AKZ)

Wave data measured at WHI or AKZ, can be used as the input of the offshore wave climate since WHI is very close to the offshore boundary lie of the Belgian continental shelf and AKZ is also not too far. However, much more data is available from WHI compared to AKZ since the measurement buoy in AKZ was a non-directional one till 2012, and therefore we take WHI as main input for the validation (for the validation we need not only the significant wave height and peak period but also the main direction and directional spreading).

Even though the number of the cases is less for AKZ, the quality of the output is evaluated by the difference between the input points. Note that De Roo *et al.* (2016) shows that there is not so much difference between the significant wave heights of WHI and AKZ.

Input of wind data (MP7 vs MP0)

Applying two different wind inputs using MP7 (Westhinder) and MP0 (Wandelaar) can improve the model performance. The input of wind is evaluated.

Wind data measured at MP7 (Westhinder) and MP0 (Wandelaar) can be used as input for the wind field (in SWAN, the input wind field is uniform over the entire domain). MP7 is very close to WHI and thus very close to the offshore boundary of the Belgian continental shelf. MP0 is located in between AKZ and BVH.

The quality of the output is evaluated by the difference of the input points. Note that De Roo *et al.* (2016) shows that there is not so much difference between the wind speed at MP7 and MP0.

Bottom friction (bottom friction parameter 0.038 vs 0.067)

Hasselmann et al. (1973) found Cb = CJON = 0.038m^2s^{-3} which is in agreement with the JONSWAP result for swell dissipation. However, Bouws and Komen (1983) suggest a value of CJON = 0.067m^2s^{-3} for depth-limited wind-sea conditions in the North Sea. This value is derived from revisiting the energy balance equation employing an alternative deep water dissipation. Recently, in Zijlema et al. (2012) it was found that a unified value of 0.038m^2s^{-3} can be used if the second order polyomial fit for wind drag of Eq. (2.35) is employed. So, in SWAN 41.01 this is default irrespective of swell and wind-sea conditions (The SWAN team, 2019a).

Applying different bottom friction values using the JONSWAP bottom friction approach is evaluated: both the present default value of 0.038 (in version 41) and the higher value of 0.067 which was the default value in the older versions (till version 40).

Different frequency resolution (number of frequency bin 38 vs 60 vs 44)

According to Miani & Vanneste (2019), the frequency resolution influences the output of Tp nearshore. Their recommendation is to use 60 bins instead of 38 bins (= used for SA15) after the convergence study. The accuracy improvement using 60 bins is discussed. Furthermore, an extra case with frequency bin 44 is also tested. In this case fmax is extended to 1.506 Hz instead of 0.85 Hz, resulted in df/f=0.1, which is the calibrated setting for the DIA approximation of the quadruplet interactions.

Breaking parameter (constant breaker index of 0.73 and 1.00, Westhuysen and Ruessink)

Depth induced wave breaking is a key parameter deciding the significant wave height in the shallow zone. A constant breaker index is often used, with the value of alpha =1.0 and gamma =0.73 (the breaker index). In SA15, SWAN underestimated the high waves (De Roo *et al.*, 2016), so it is interesting to test a higher breaker index value. Furthermore, two extra breaking formulas are of interest, namely Westhuysen (Van Der Westhuysen, 2010) and Ruessink (Ruessink *et al.*, 2003). Here below is the explanation of each model – extract of the abstract from their papers.

Westhuysen: *Recent studies have shown that the spectral wind wave model SWAN (Simulating Waves Nearshore) underestimates wave heights and periods in situations of finite depth wave growth. … this inaccuracy is addressed through a rescaling of the Battjes and Janssen (1978) bore-based model for depth-induced breaking, considering both sloping bed surf zone situations and finite depth wave growth conditions. It is found that the variation of the model error with the BJ breaker index in this formulation differs significantly between the two types of conditions. For surf zones, clear optimal values are found for the breaker index. By contrast, under finite depth wave growth conditions, model errors asymptotically decrease*

with increasing values of the breaker index (weaker dissipation). Under both the surf zone and finite depth wave growth conditions, optimal calibration settings of BJ were found to correlate with the dimensionless depth kpd (where kp is the spectral peak wave number and d is the water depth) and the local mean wave steepness. Subsequently, a new breaker index, based on the local shallow water nonlinearity, expressed in terms of the biphase of the self-interactions of the spectral peak, is proposed. Implemented in the bore-based breaker model of Thornton and Guza (1983), this breaker index accurately predicts the large difference in dissipation magnitudes found between surf zone conditions and finite depth growth situations. Hence, the proposed expression yields a significant improvement in model accuracy over the default Battjes and Janssen (1978) model for finite depth growth situations, while retaining good performance for sloping bed surf zones (Van Der Westhuysen, 2010).

Ruessink: *Since its introduction in 1978, the Battjes and Janssen (BJ) model has proven to be a popular framework for estimating the crossshore root-mean-square wave height Hrms transformation of random breaking waves in shallow water. Previous model tests have shown that wave heights in the bar trough of single bar systems and in the inner troughs of multiple bar systems are overpredicted by up to 60% when standard settings for the free model parameter c (a wave height-to-depth ratio) are used. … a new functional form for c is derived empirically by an inverse modelling of c from a high-resolution (in the crossshore) 300-h Hrms data set collected at Duck, NC, USA. We find that, in contrast to the standard setting, c is not cross-shore constant, but depends systematically on the product of the local wavenumber k and water depth h. Model verification with other data at Duck, and data collected at Egmond and Terschelling (Netherlands), spanning a total of about 1600 h, shows that crossshore Hrms profiles modelled with the locally varying c are indeed in better agreement with measurements than model predictions using the cross-shore constant c. In particular, model accuracy in inner bar troughs increases by up to 80%. Additional verifications with data collected on planar laboratory beaches show the new functional form of c to be applicable to non-barred beaches as well. Our optimum c cannot be compared directly to field and laboratory measurements of height-to depth ratios and we do not know of a physical mechanism why c should depend positively on kh.* (Ruessink *et al.*, 2003).

Salmon *et al.* (2015) and Salmon & Holthuijsen (2015) further studied about breaking and concluded that beta-kd scaling with directional partitioning represents depth-induced breaking compared to traditional breaking models (eg BJ78) and bi-phase parametrizations (Westhuysen 2010). Note that the model of Salmon has not been implemented in the present SWAN model.

Time lag (no time lag vs theoretical time lag)

There must be a time lag between WHI and the measurement locations (e.g. offshore WHI 0:00 data is compared to nearshore Ostend 0:30 data if the theoretical delay is 30 min). The theoretical time lag can be calculated as the wave front distance (not just a distance: it is the travel distance of the wave front line, see example of TRG shown in Figure 4.3) between WHI and each measurement stations divided by theoretical wave group celerity.
The wave group celerity is calculated using the measured peak wave period at WHI and a rough estimation of the bathymetry (i.e. representative depth is 20 m in average, cf. the bathymetry map) since each direction of each location has its own trajectory and it is not that easy to calculate the precise representative depth.
Note that we can accept some uncertainties in the theoretical time lag calculation since the measurement data have a time step of 30 min: the time lag is eventually rounded up (e.g. if the time lag is 40 min, then we use it as 30 min delay as it falls into the range of 15-45 min). The group velocity of the intermediate depth is expressed as follows:

$$\frac{1}{2}c_p\left(1+\frac{2kh}{\sinh(2kh)}\right)$$

where c_p is phase velocity.

For SA15, fixed 30 min delay was applied irrespective of the direction and period. In this study, the sensitivity of the time lag is evaluated by comparing no time lag assumption and theoretical time lag assumption.

The time lag is also relevant to the water level input, see details in the next section, Water level (water level data, only WL-OST vs WL-NPT, WL-OST, WL-ZDL).

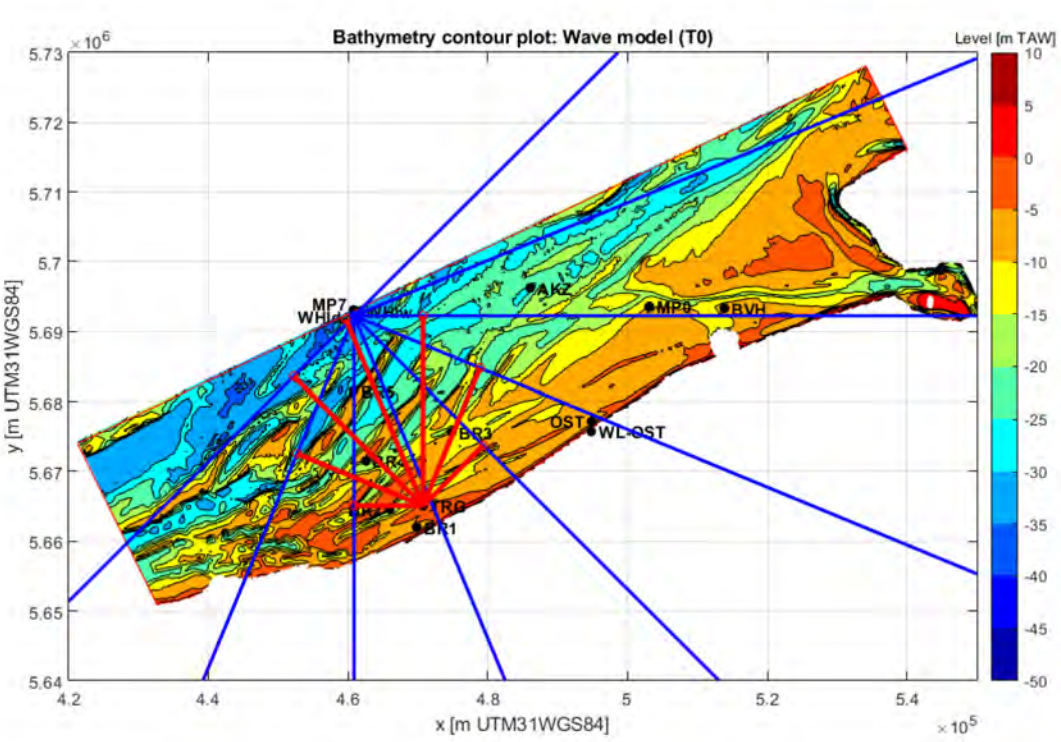

RED LINES SHOW THE TRAVEL DISTANCE OF WAVE FRONT LINE (BLUE LINE) BETWEEN TRG AND WHI FOR EACH DIRECTION

Figure 4.3 – Example of distance between WHI and TRG for each direction (red lines)

Water level (water level data, only WL-OST vs WL-NPT, WL-OST, WL-ZDL)

The location of the water level data is also an important discussion point. By default WL-OST is used since it might be representative of the domain being in the center. Still, it is better to have water levels closer by the output locations. For TRG, WL-NPT is much closer, and for BVH, ZLD is much closer. As a result, the input water level can be different for each station.

Not only the geographical location is of importance, but also the timing of the water level. Thinking about the wave propagation from deep offshore to shallow nearshore waters, wave breaking might play an important role in the wave transformation (especially TRG and OST). If there is a time lag, it is good to use the data of the closest time of the output station (e.g. water level of 0:00 is +4.0 m TAW and 0:30 is +4.5 m TAW, and 30 min delay is expected due to time lag, then +4.5 m is better to be used).

In this study, the sensitivity of the water level input location in combination with the time lag is evaluated by comparing no assumption and theoretical time lag assumption.

GEN3 (Westhuysen vs Komen)

SWAN contains a number of physical processes that add or withdraw wave energy to or from the wave field. The processes included are: wind input, whitecapping, bottom friction, depth-induced wave breaking, dissipation due to vegetation, mud or turbulence, obstacle transmission, nonlinear wave-wave interactions (quadruplets and triads) and wave-induced set-up. SWAN can run in several modes, indicating the level of parameterization. SWAN can operate in first-, second and third-generation mode (The SWAN team, 2019b).

The physical meaning of the interactions is that resonant sets of wave components exchange energy, redistributing energy over the spectrum. In deep and intermediate water, four-wave interactions (so-called quadruplets) are important, whereas in shallow water three-wave interactions (so-called triads) become important. In deep water, quadruplet wave-wave interactions dominate the evolution of the spectrum. They transfer wave energy from the spectral peak to lower frequencies (thus moving the peak frequency to lower values) and to higher frequencies (where the energy is dissipated by whitecapping). In very shallow water, triad wave-wave interactions transfer energy from lower frequencies to higher frequencies often resulting in higher harmonics. Low-frequency energy generation by triad wave-wave interactions is not considered here (The SWAN team, 2019b).

According to Allahdadi *et al.* (2019), *parameterizing the whitecapping effect can be done using the Komen-type schemes, which are based on mean spectral parameters, or the saturation-based (SB) approach of van der Westhuysen (2007), which is based on local wave parameters and the saturation level concept of the wave spectrum.*

In the third-generation mode wind input, whitecapping and quadruplets are activated. The default setting of GEN3 is Komen, while Westhuysen was used in SA15. These settings are tested in this study.

Note that there are some other GEN3 settings in SWAN. One of those is 'ST6' (originally referred to as 'Babanin et al. physics, see details in The SWAN team, 2019a), which is currently used in WW3.

Triads (off vs on)

*The Lumped Triad Approximation (LTA) of Eldeberky (1996), which is a slightly adapted version of the Discrete Triad Approximation (DTA) of Eldeberky and Battjes (1995) is used in SWAN in each spectral direction (*The SWAN team., 2019a). See also the explanation of the Triads in relation to quadruplets above.

In this study, sensitivity of triads is tested in order to see the importance of this command.

Wind friction (default Zijlema vs Wu formula)

Wind drag of Wu (see the difference between default setting, namely 2nd order best fit line, and Wu in Figure 4.4) is also tested to see if the different setting affects to the result.

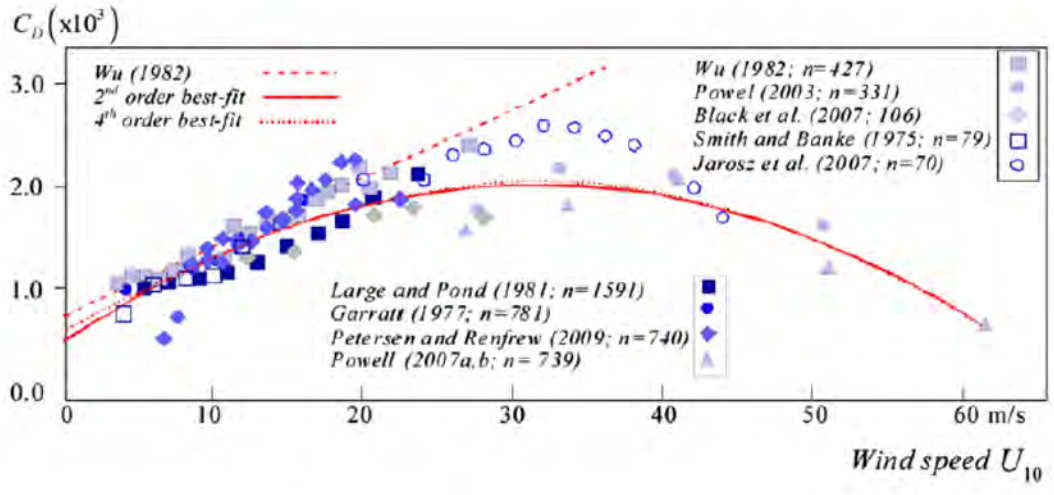

Figure 4.4 – Wind drag (Zijlema *et al.*, 2012)

Numerics (default vs 200 iterations)

As shown in Technum *et al.* (2002), the number of iteration can influence to calculated parameters in SWAN (Figure 4.5). Influence of the iteration is tested to see whether the saturation of calculated parameter can be changed by the number of iteration in the version to be used in SA21.

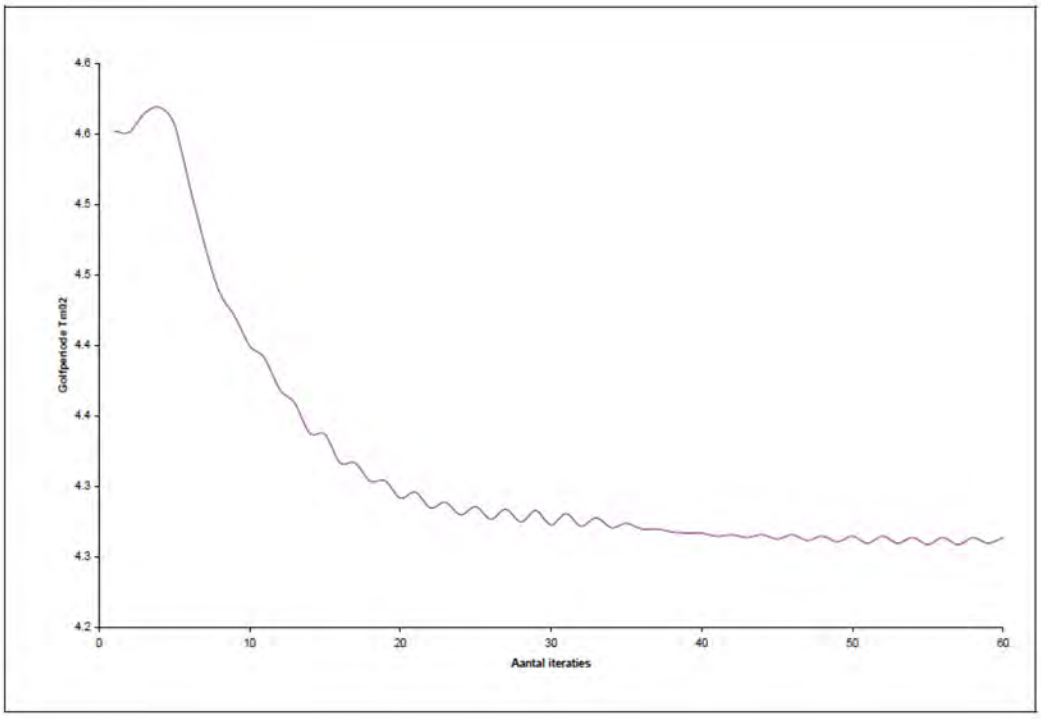

Figure 4.5 – Evolution of the mean wave period Tm02 and number of iteration (Hs=2 m from north, at OST)

5 Pre- and post-processing

5.1 Standard input for SWAN input

The standard input and short explanation of each line is presented below, see details in Section 4.3. Based on the standard case, we try to see the influence of different settings (listed in Section 4.4) and the performance. Further explanation on which parameters are changed is given in Section 2.4, where the model identification code is explained.

SET LEVEL 3.56 ! Water level input from OST and no time lag

SET NAUT ! Same settings as previous SAs

MODE STATIONARY ! Same settings as previous SAs

MODE TWOD ! Same settings as previous SAs

CGRID REG 438116 5639190 25.50 125000 39000 500 156 CIRCLE 36 0.025 0.85 37 ! Same settings as SAs.

INPGRID BOTTOM 438116 5639190 25.50 500 156 250 250 EXC -999 ! Same settings as previous SAs

READINP BOTTOM 1.0 'wgs84_taw_swan2015.dep' 4 0 FREE ! BCP2015 is used.

BOU SHAP JON 3.3 PEAK DEGREES ! Same settings as previous SAs

BOU SIDE N CCW CON PAR 2.88 6.1 295.00 29.0 ! Hs, Tp, dir, spr input from WHI/AKZ

BOU SEGM IJ 500 80 500 156 CON PAR 2.88 6.1 295.00 29.0 ! Hs, Tp, dir, spr input from WHI/AKZ

BOU SIDE W CCW CON PAR 2.88 6.1 295.00 29.0 ! Hs, Tp, dir, spr input from WHI/AKZ

GEN3 WESTHUYSEN ! Same settings as previous SAs

Note that Whitecapping, Quadruplet is automatically included if no declaration OFF WCAP, OFF QUAD. Triads was not activated.

BREAK CON 1.00 0.73 ! Same settings as previous SAs, constant breaker index, default values

FRIC JON 0.038 ! Bottom friction values (0.038 and 0.067) were tested

WIND 14.7 289.9 ! Standard wind input is MP7. u is at 10 m level.

NUM STOPC STAT 50! Default setting

5.2 Model identification code

In order to run the model in a systematic way, tested parameters are included in the model identification code. Doing that the it is easy to recognize which case are tested and displayed in the following chapters. See details in Section 4.4.

Model identification code (the standard case, stated earlier): V2_G2_15_WP_7_JZ_38_BD_NNN_WO

SWAN version (V1: version 40.85, V2: 41.20.AB)

Grid resolution (G1: 125x125 m, G2: 250x250 m, G4: 250x125)

Bathymetry (02: BCP2002, 15: BCP2015)

Offshore wave input (WP: WHI + parameter input, AP: AKZ + parameter input)

Wind input (0: MP0, 7: MP7)

Bottom friction (JD: JONSWAP 0.067, JZ: JONSWAP 0.038)

Frequency bins (38, 44, 60)

Breaking (BD: breaker index 0.73, B1: breaker index 1.0, BW: Westhuysen, BR: Ruessink)

No delay / delay (NNN: no delay, TRG/OST/BVH: delay at each location)

Water level (WN: water level from WL-NPT, WO: water level from WL-OST, WZ: water level from WL-ZLD)

5.3 Cases to be tested

Based on the basic case V2_G2_15_WP_7_JZ_38_BD_NNN_WO, following cases are tested as sensitivity analysis including the influence of the time lag (see page 24) and water level input location (see page 25). The case to be tested is shown as follows (only examples).

V2_G2_15_WP_7_JZ_38_BD_NNN_WO	**Basic case**
V1_G2_15_WP_7_JZ_38_BD_NNN_WO	to check sensitivity of the version
V2_**G1**_15_WP_7_JZ_38_BD_NNN_WO	to check sensitivity of the grid resolution
V2_G2_**02**_WP_7_JZ_38_BD_NNN_WO	to check sensitivity of the bathymetry (250 m grid)
V2_G2_15_WP_7_JZ_38_BD_NNN_WO_**NEWB**	50 m grid resolution of BCP2020
V2_G2_15_**AP**_7_JZ_38_BD_NNN_WO	to check sensitivity of the wave input
V2_G2_15_WP_**0**_JZ_38_BD_NNN_WO	to check sensitivity of the wind input
V2_G2_15_WP_7_**JD**_38_BD_NNN_WO	to check sensitivity of the bottom friction
V2_G2_15_WP_7_JZ_**60**_BD_NNN_WO	to check sensitivity of the number of frequency bin
V2_G2_15_WP_7_JZ_38_**B1**_NNN_WO	to check sensitivity of the breaker index
V2_G2_15_WP_7_JZ_38_**BR**_NNN_WO_NNNN	to check sensitivity of the breaker index
V2_G2_15_WP_7_JZ_38_**BW**_NNN_WO_NNNN	to check sensitivity of the breaker index
V2_G2_15_WP_7_JZ_38_BD_**TRG**_WO	to check the time lag influence
V2_G2_15_WP_7_JZ_38_BD_**OST**_WO	to check the time lag influence
V2_G2_15_WP_7_JZ_38_BD_**BVH**_WO	to check the time lag influence
V2_G2_15_WP_7_JZ_38_BD_**TRG_WN**	to check the water level influence
V2_G2_15_WP_7_JZ_38_BD_**BVH_WZ**	to check the water level influence
V2_G2_15_WP_7_JZ_38_BD_NNN_WO_**BOU1**	to check wave boundary for SW and WSW
V2_G2_15_WP_7_JZ_38_BD_NNN_WO_**GEN3**	to check Gen3 based on Komen
V2_G2_15_WP_7_JZ_38_BD_NNN_WO_**TRIA**	to check triads
V2_G2_15_WP_7_JZ_38_BD_NNN_WO_**WDWU**	to check wind drag of Wu's formula
V2_G2_15_WP_7_JZ_38_BD_NNN_WO_**I200**	to check the numerics

5.4 Post-processing

Post-processing is conducted in a systematic way, using the same rule. Each plot has different colours for the main wave direction (REM) and different symbols for the difference between the wave and wind directions, see further definition below. Evaluation is done in two different ways, namely, y=ax linear regression line and y=ax+b linear regression line in combination with R^2 and RMSE calculation.

The example output figure with some explanation is shown in Figure 5.1.

Plot

- different colours: different wave directions (only SW-NE)
- Different symbols: o ---- abs(wave dir-wind dir) < 30 deg

  x ---- abs(wave dir-wind dir) > 30 deg

Evaluation

Two expressions:

- Y=aX *linear regression, intercept (b value) was set zero*
- Y=aX+b *linear regression, including intercept b*

for each, extra parameters are added to see the performance.

- R^2 *decision coefficient: ~0.2 no correlation, ~0.4 weak, ~0.7 correlation, ~1 strong, negative value possible as negative correlation, 1 is the best.*
- RMSE *root mean square error, smaller is better*

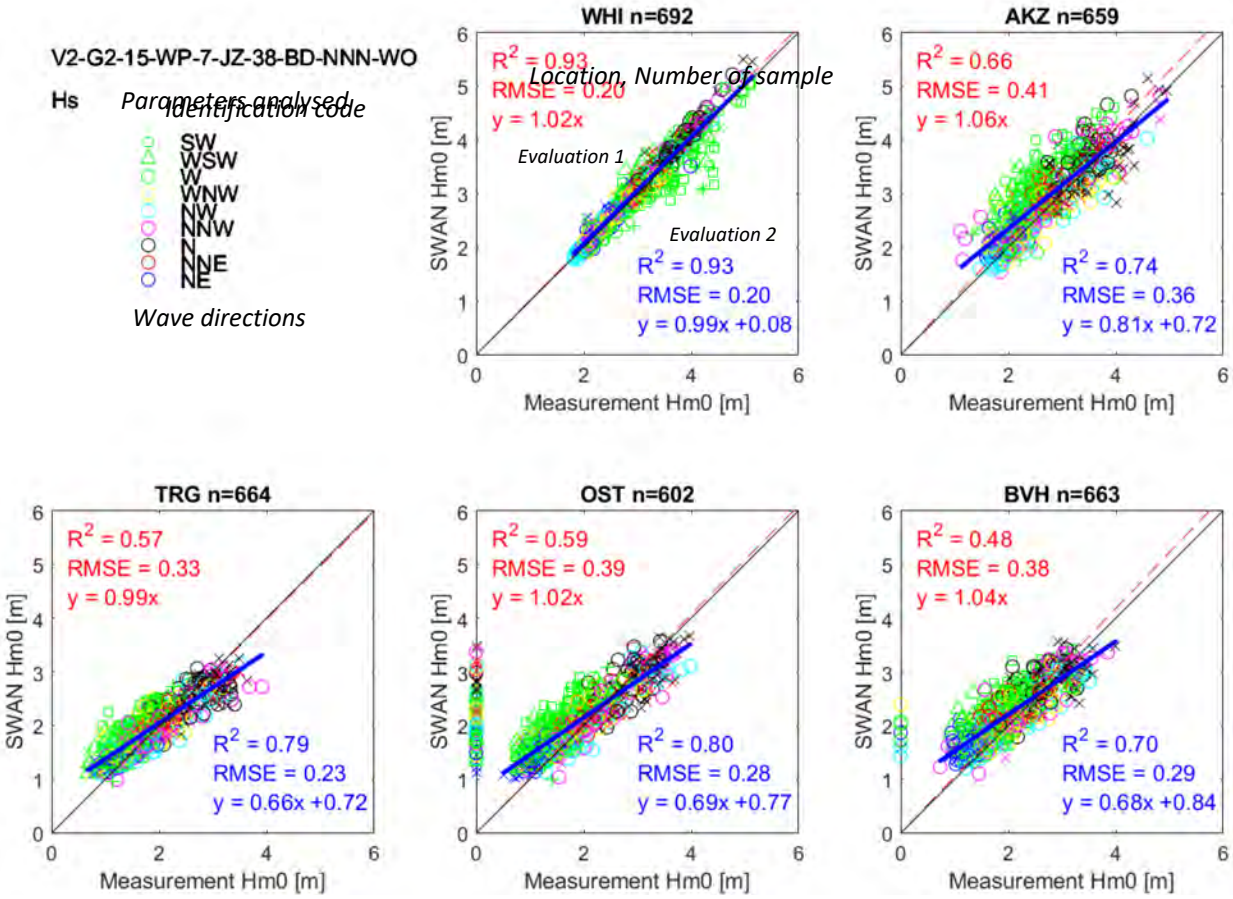

Figure 5.1 – Example of output figure (explanation is added in italic)

6 Model performance

6.1 Basic case

In total 692 cases were run, and all the results of the basic case (i.e. V2_G2_15_WP_7_JZ_38_BD_NNN_WO) were obtained.

Figure 6.1 shows its performance to estimate the significant wave height Hm0. Note that *the wave parameters in the output of SWAN are computed from the wave spectrum over the prognostic part of the spectrum with the diagnostic tail added. Their value may therefore deviate slightly from values computed by the user from the output spectrum of SWAN which does not contain the diagnostic tail* (The SWAN team, 2019b).

All the runs had SWAN output in this here. WHI had all measurement data points for the selected time step therefore n indicated in the figure is 692 at WHI. AKZ, TRG, OST and BVH have less data than 692 because some measurement values are missing at the selected time step.

Estimation results (R^2, RMSE, a value), in general, are very good for WHI case. It is logic since WHI measurement value is used at the offshore boundary which is located very close to WHI. However, looking at directions WSW and SW, the performance is not always good. This is due to the fact that the wave boundary in this direction is very far (if a line is drawn from WHI to the direction SW, the line does not cross the offshore boundary but it crosses the lateral boundary – the distance is much larger compared to the other directions).

The performance of AKZ is less good compared to WHI but better than TRG, OST and BVH. This is logic since AKZ is geographically closer to the offshore boundary.

Looking at the value of the slope 'a' of y=ax regression line for TRG, OST and BVH, it is actually very good (=close to 1.0) but it is not representing the overall trend. In that sense it is more meaningful to see the slope 'a' and intercept 'b' values of y=ax+b regression line since we have enough data points (when number of data points is limited y=ax form can be also very useful, while y=ax+b form can give extreme values of a and b: imagine if only two points). Yet the slope 'a' of y=ax regression line is also useful parameter for sensitivity analysis to check the cloud of the point is moved upward or downward.

In general, SWAN output are overestimated for lower wave height and underestimated for higher waves. Taking a closer look to the performance of the validation results for SA15 (Figure 6.2), the plots show a similar cloud as the basic case. The performance of the basic case is thus comparable to it, although the slope 'a' values are different (SA15 TRG a=0.9, OST= 0.95, BVH= 0.98; basic case TRG a=0.99, OST= 1.02, BVH= 1.04 – these differences result from a different number of points and a different case selection, namely less directions taken into account).

Until now, we only looked at the overall performance (i.e. omnidirectional). In reality, the performance of the model will depend on the wave (and wind) direction (see Figure 6.3,). This figure shows the performance of each wave direction per each nearshore location. In general, the data points of W-SW direction are located above the 1:1 line (= overestimation). The other directions are generally located close to the 1:1 line; however, the slope 'a' value of y=ax+b form is not close to 1.

Based on these results, it can be concluded that the basic case is a good benchmark in this study.

A sensitivity analysis is conducted in the following section based on the performance of the basic case result discussed here (concretely, slope 'a', R^2 and RMSE from y=ax, and slope 'a', intercept 'b', R^2 and RMSE from y=ax+b are used to discuss the sensitivity for different settings).

Table 6.1 – Sensitivity of SWAN version – significant wave height Hm0

Location	Case	Y=ax			Y=ax+b					
		Slope 'a'	R^2	RMSE	Slope 'a'	Intcpt 'b'	R^2	RMSE	Est_x=5	Ratio
TRG	Basic case	**0.99**	0.57	0.33	0.66	0.72	0.79	0.23	4.02	-
OST	Basic case	**1.02**	0.59	0.39	0.69	0.77	0.80	0.28	4.22	-
BVH	Basic case	**1.04**	0.48	0.38	0.68	0.84	0.70	0.29	4.24	-

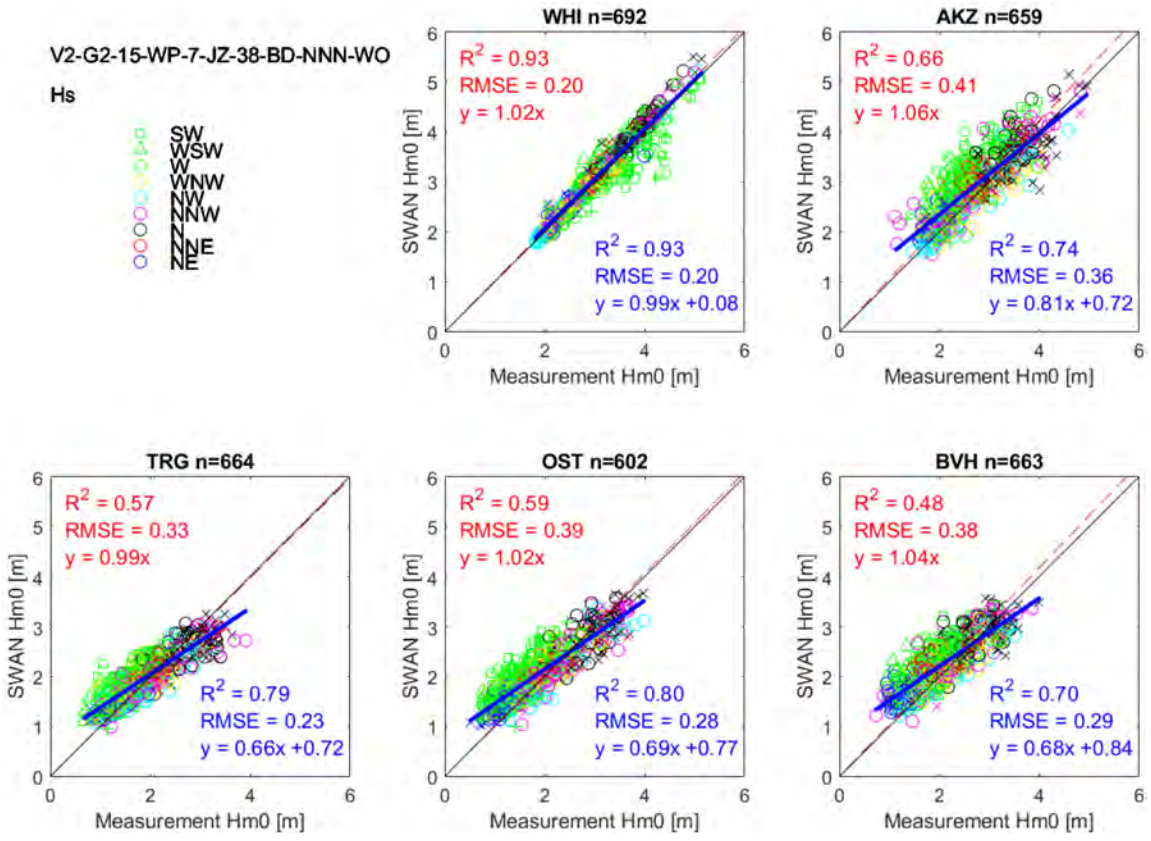

Figure 6.1 – Model performance of the basic case – significant wave height Hm0

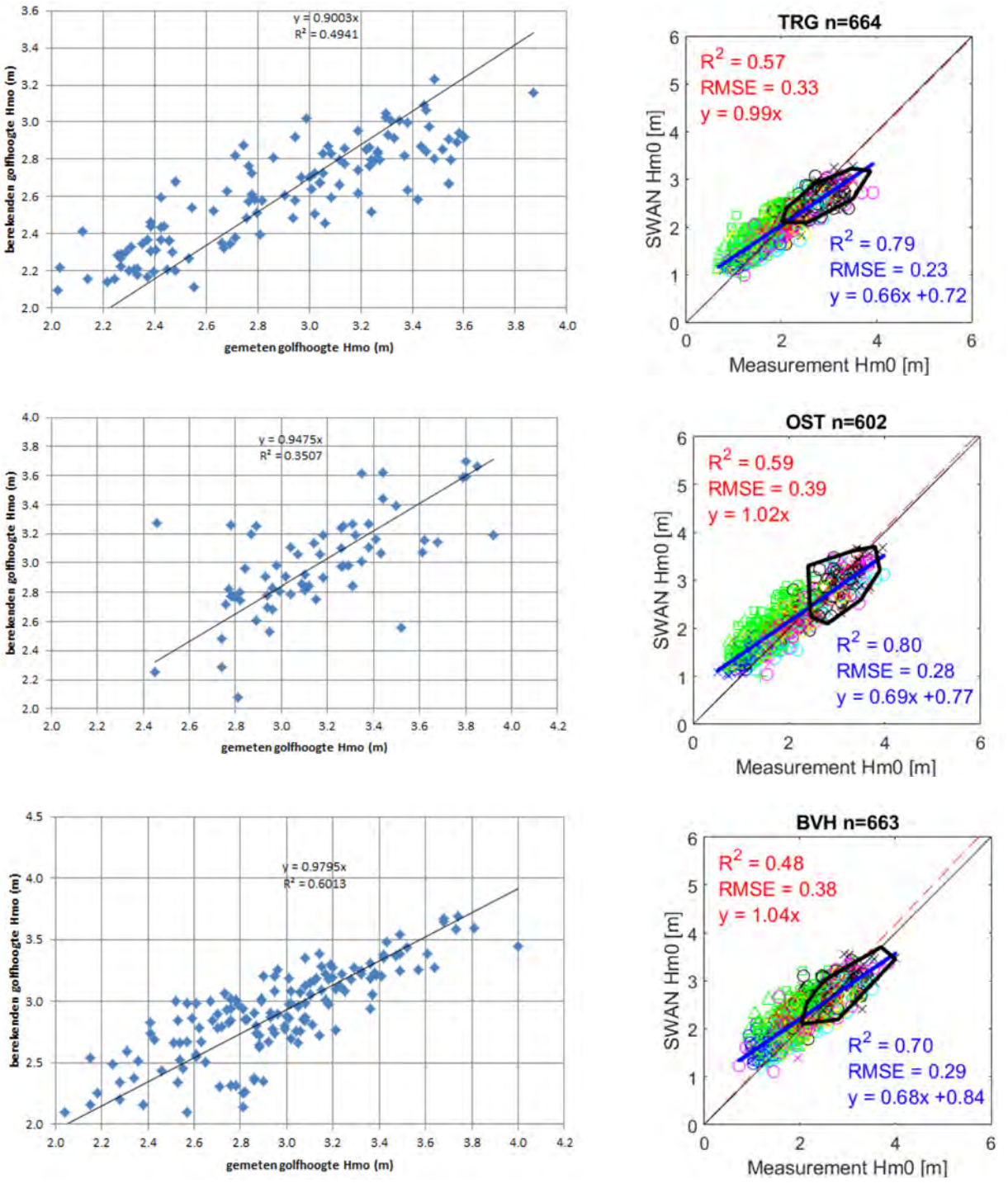

Figure 6.2 – Model performance of SA15 validation case (209 cases in total), left: original SA15 validation, right: SA15 (black line derived from outer points of the scatterd results in the left figure) vs basic case – significant wave height Hm0

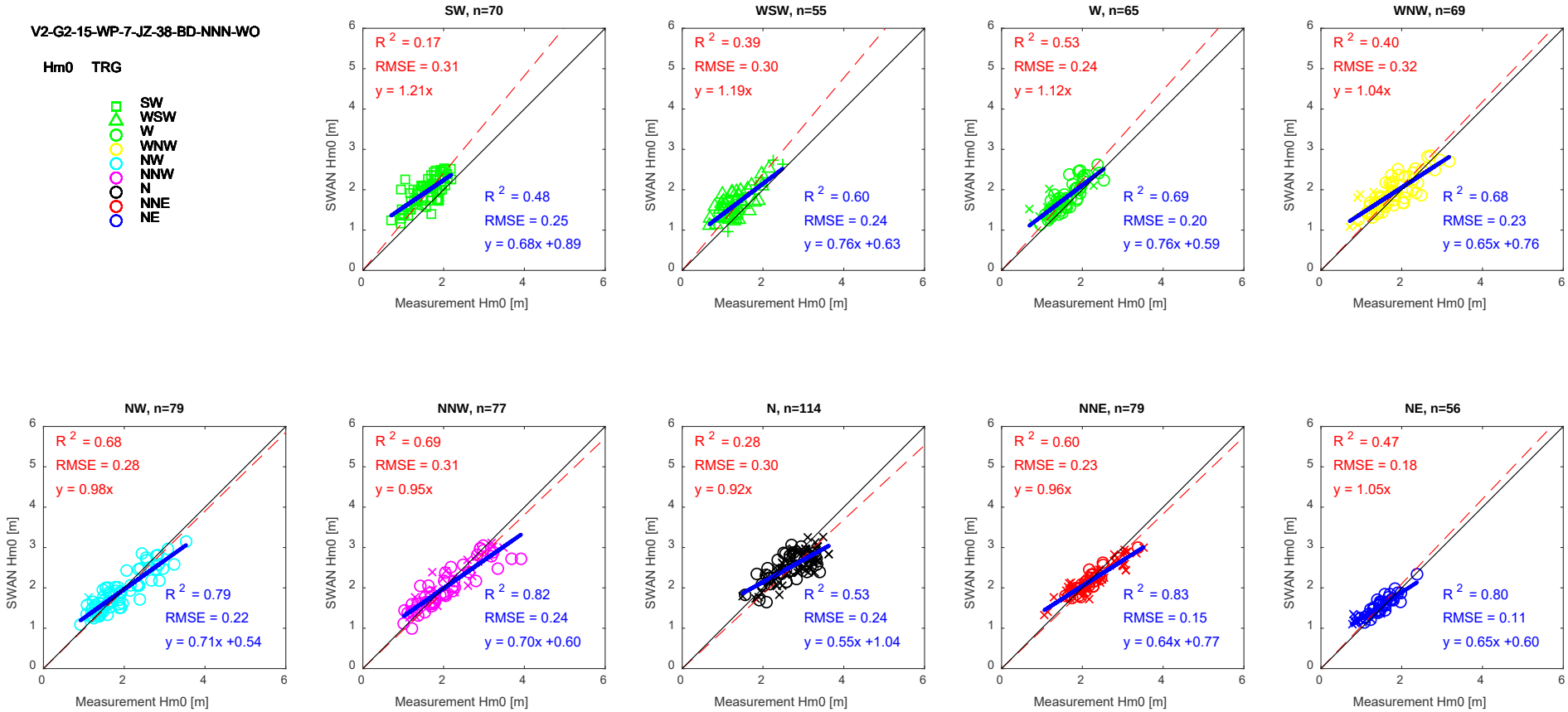

Figure 6.3 – Model performance of the basic case for each direction at TRG – Significant wave height Hm0

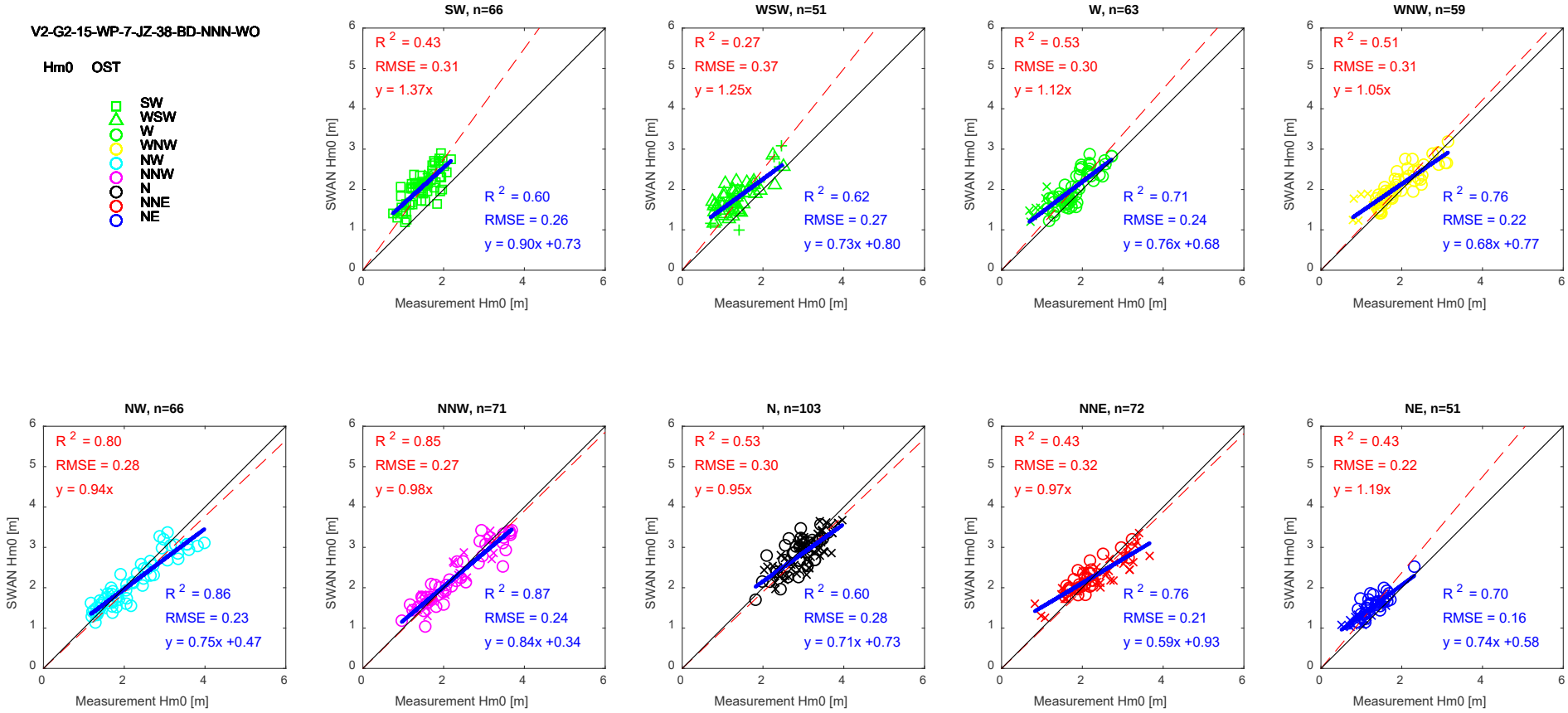

Figure 6.4 – Model performance of the basic case for each direction at OST – Significant wave height Hm0

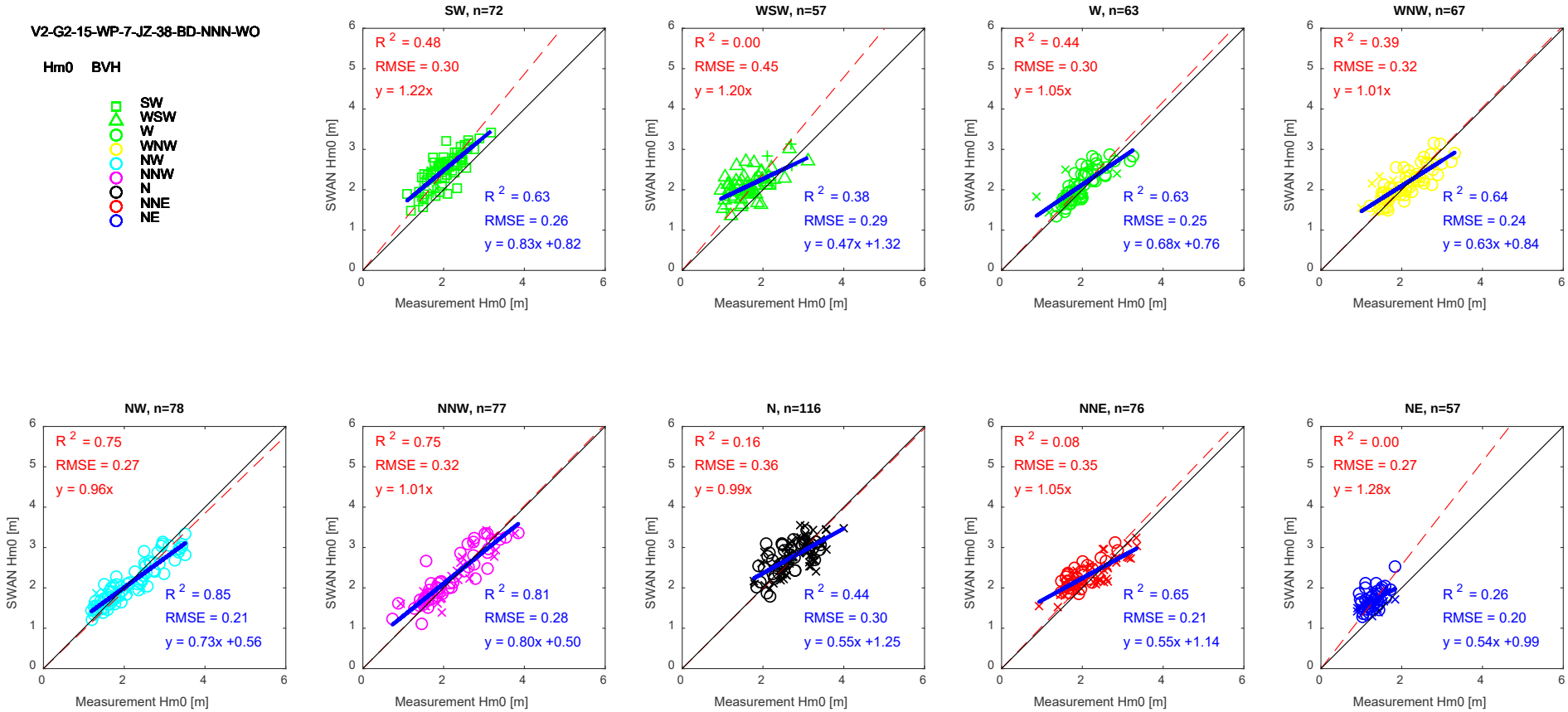

Figure 6.5 – Model performance of the basic case for each direction at BVH – Significant wave height Hm0

Figure 6.6 shows the overall model performance for the peak wave period in the basic case (e.g. 38 frequency bins) and Figure 6.7 shows the one for the smoothed peak wave period. The peak wave period has some scatter and a similar trend as seen in the significant wave height analysis seeing the regression lines: SWAN output is overestimated for lower wave periods and underestimated for higher wave periods in general. The slope 'a' is smaller and intercept 'b' is bigger at BVH compared to the ones in TRG and OST. The difference might be due to the geographiscal location, or water depth, but it is not clear. The scatter can also be related to the fact that our offshore wave input is idealized spectrum shape (i.e. JONSWAP 3.3).

Figure 6.8 shows a limited number of cases (subset of Figure 6.6) where the wave direction and wind direction are similar: the difference between the offshore main wave direction and the main wind direction at MP7 is less than 30 deg ('single peaked spectrum case'). Even though the slope 'a'values of the y=ax+b form are not close to 1 and the scatter is still rather high, most of the cloud around the higher wave periods are located around 1:1 line, or slightly higher. It indicates that the 'single peaked spectrum case' focusing on higher peak wave periods mostly gives an acceptable estimation (if the overestimation at TRG is acceptable) for the basic case (here the assumption is made that if wind and wave direction are similar, the spectrum has a single peak).

Figure 6.9 shows that the 'basic case' model for the mean wave period generally underestimates.

Figure 6.10 shows the model performance for the wave direction (DIR and PDIR) for the basic case. The estimation of the wave direction is in general good, given that the number of the directional wave datais limited data. Note that some data points are far from the 1:1 line (e.g. some data can be seen around (360,0) and (0,360), being physically very close to one another, this is due to the expression of the direction ranging from 0-360 degree.

Figure 6.11 shows the model performance for the directional spreading for the basic case. The estimation of the directional spreding is not good as shown in the figure. All the SWAN result at OST and BVH are concentrated around 20-30 degrees. Note that SEM is representing directional spreading at the highest energy frequency component by definition, see Table 3.2.

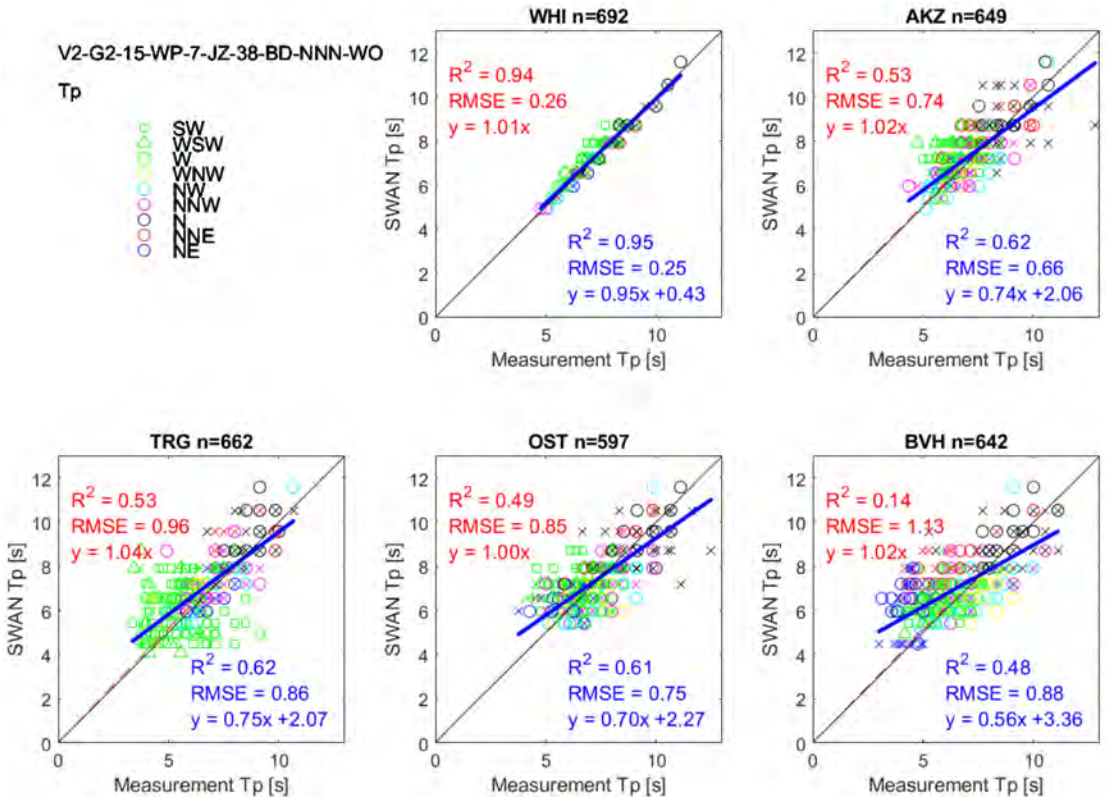

Figure 6.6 – Model performance of the basic case – peak wave period Tp from RTP (wave peak period)

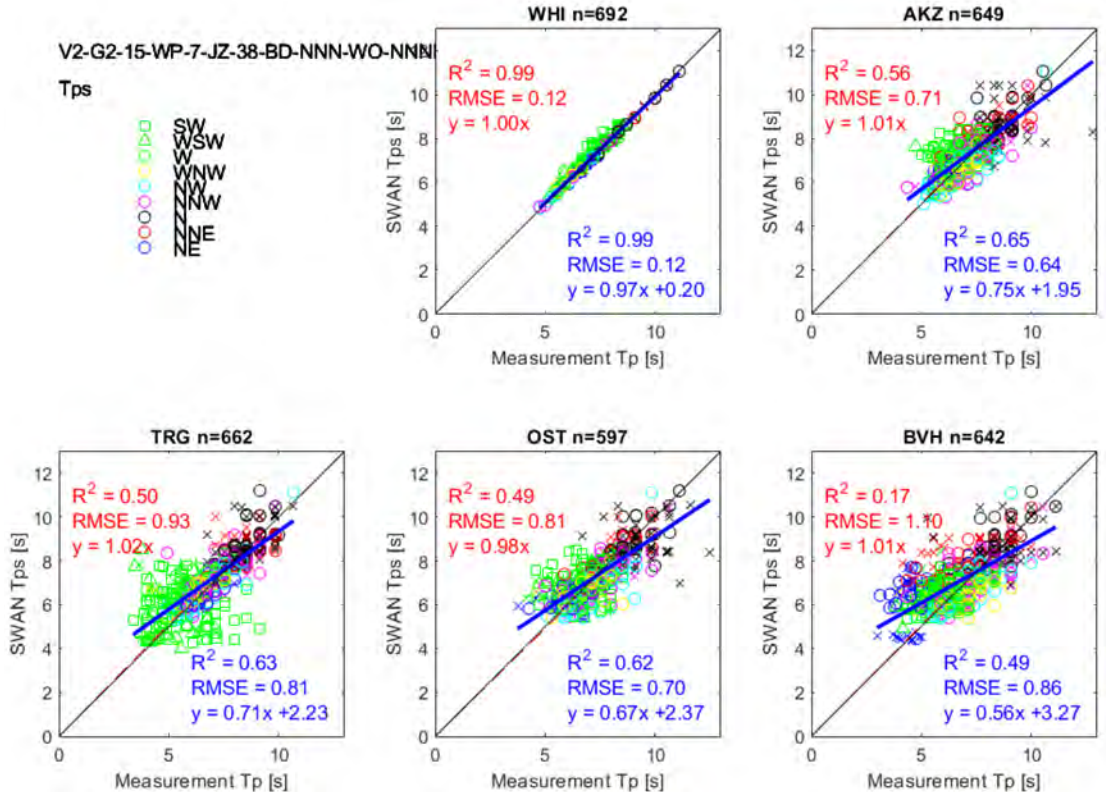

Figure 6.7 – Model performance of the basic case – peak wave period Tp from TPS (smoothed peak wave period)

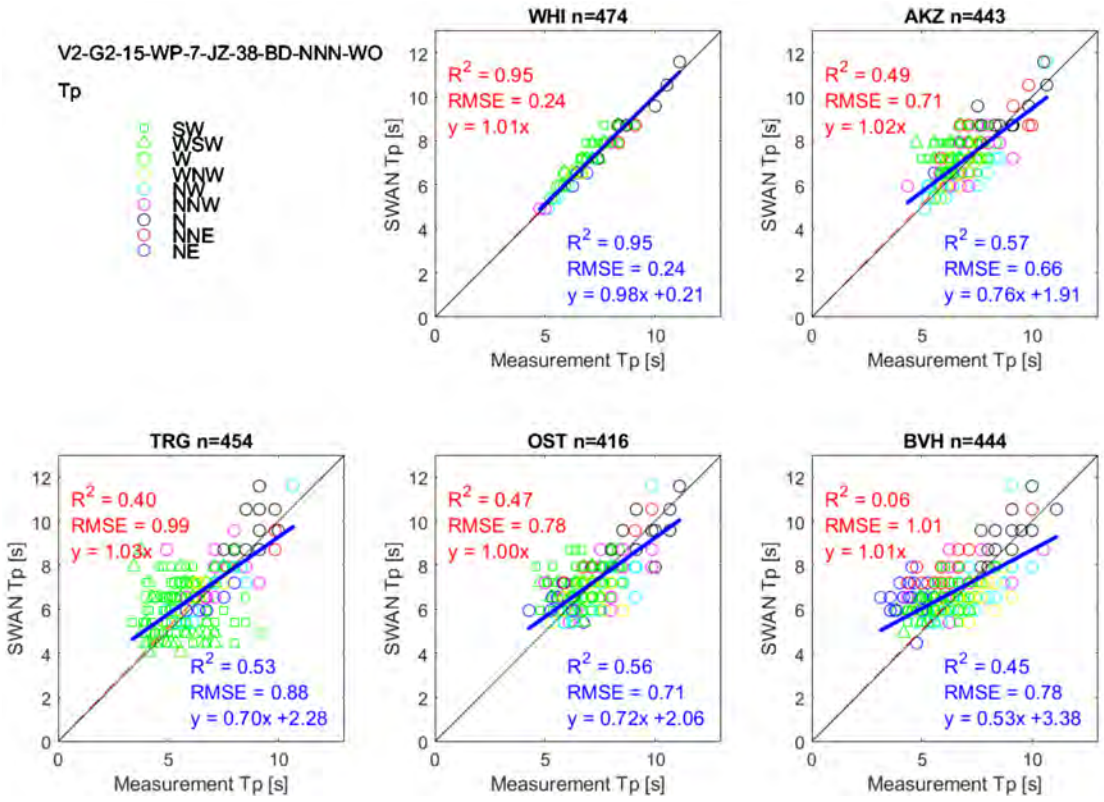

Figure 6.8 – Model performance of the basic case – Tp, limited to cases of (main wave dir – main wind dir) < 30 deg

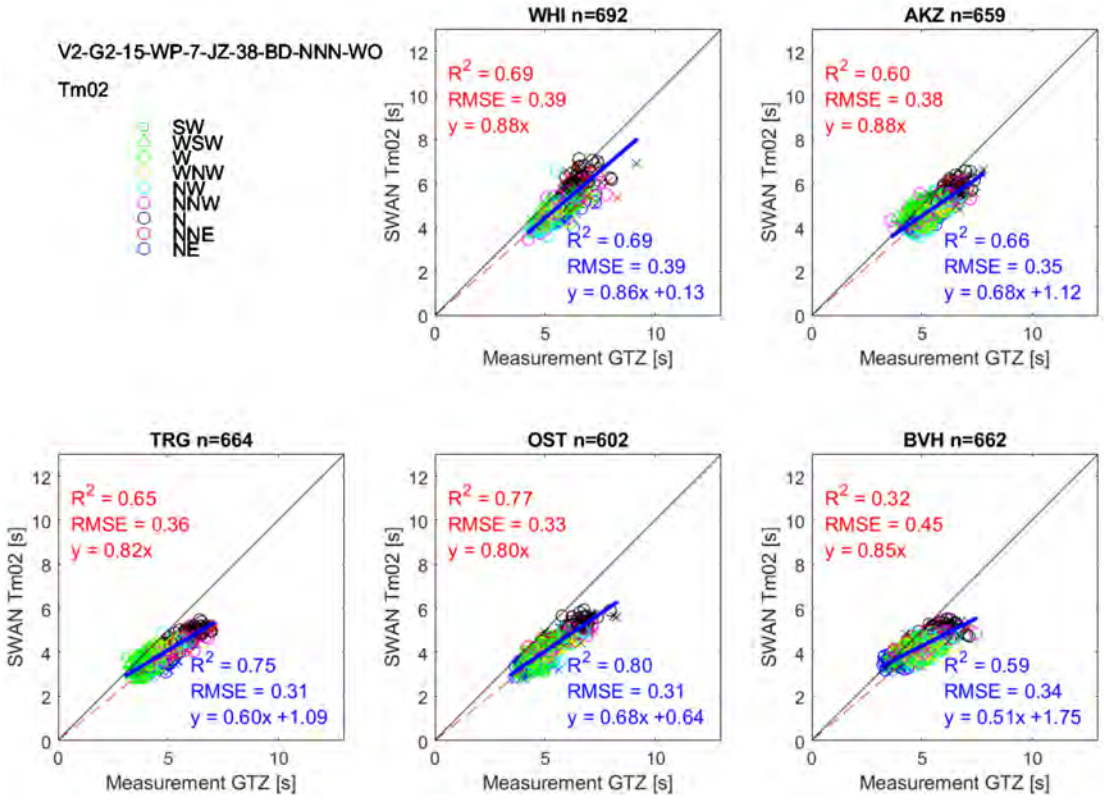

Figure 6.9 – Model performance of the basic case from parameter output- mean wave period Tm02

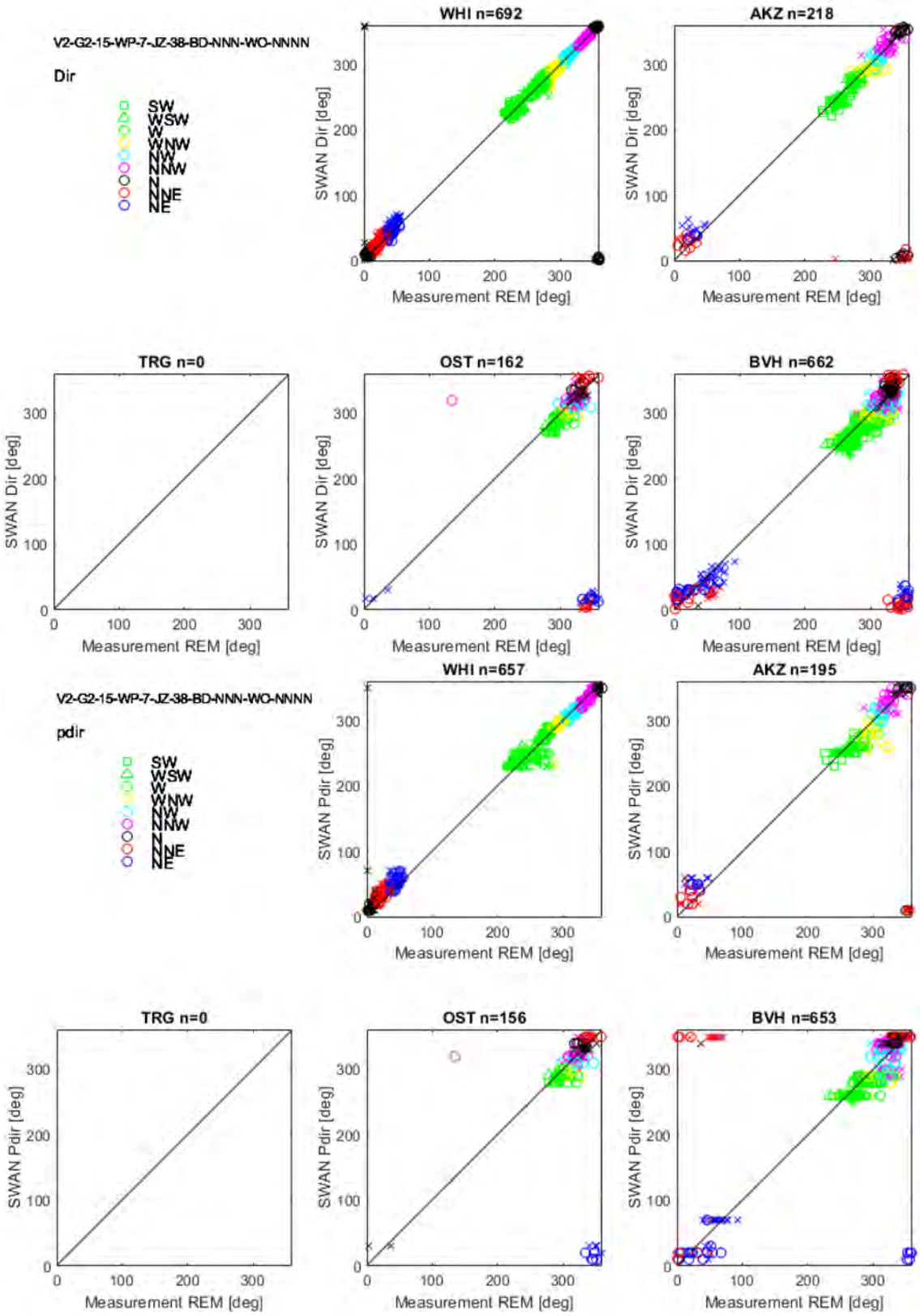

Figure 6.10 – Model performance of the basic case – wave direction Dir (upper) and PDIR (lower)

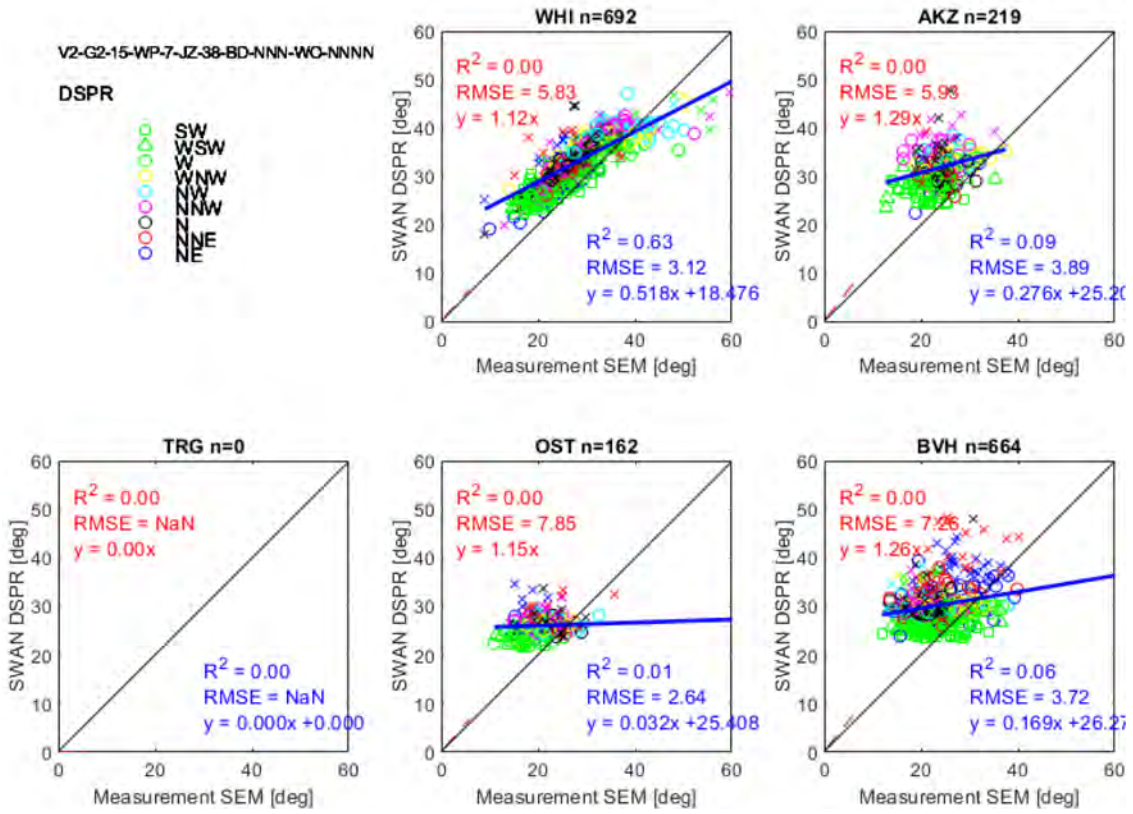

Figure 6.11 – Model performance of the basic case – directional spreading

6.2 Sensitivity analysis for input parameters

6.2.1 Sensitivity of SWAN version

Comparison of the significant wave height between version 40 (40.85) and the basic case - version 41 (41.20.AB) is shown in Table 6.2 and Figure 6.11. The difference is not significant (at most 2% looking at the slope ‘a’ of y=ax regression line, see the red bold value; and at most 2% looking at the ratio of estimation value for x=5 – Hm0=5 m -, see the blue bold value).

According to Zijlema, the difference between both version 40 and 41 is the wave period (Section 4.2) rather than the wave height. In order to check it, a comparison of the mean wave period (GTZ for measurement and Tm02 for SWAN output) between version 40 (40.85) and version 41 (41.20.AB) is shown in Figure 6.12 and Table 6.3. The wave period (Tm02) became shorter, as the slope ‘a’ of y=ax is 1-3% higher in the old version and also the estimation ratio is 2-6% higher in the old version, as Zijlema mentioned.

We continue to use version 41.20.AB for further analysis since it is one of the most recent versions of the SWAN model.

Table 6.2 – Sensitivity of SWAN version – significant wave height Hm0

Location	Case	Y=ax			Y=ax+b					
		Slope 'a'	R^2	RMSE	Slope 'a'	Intcpt 'b'	R^2	RMSE	Est_x=5	Ratio
TRG	Basic case	**0.99**	0.57	0.33	0.66	0.72	0.79	0.23	4.02	-
	Version 40.85	**1.00**	0.53	0.35	0.65	0.75	0.77	0.24	4.00	**1.00**
OST	Basic case	**1.02**	0.59	0.39	0.69	0.77	0.80	0.28	4.22	-
	Version 40.85	**1.01**	0.54	0.41	0.67	0.81	0.78	0.29	4.16	**0.99**
BVH	Basic case	**1.04**	0.48	0.38	0.68	0.84	0.70	0.29	4.24	-
	Version 40.85	**1.06**	0.52	0.38	0.70	0.82	0.72	0.29	4.32	**1.02**

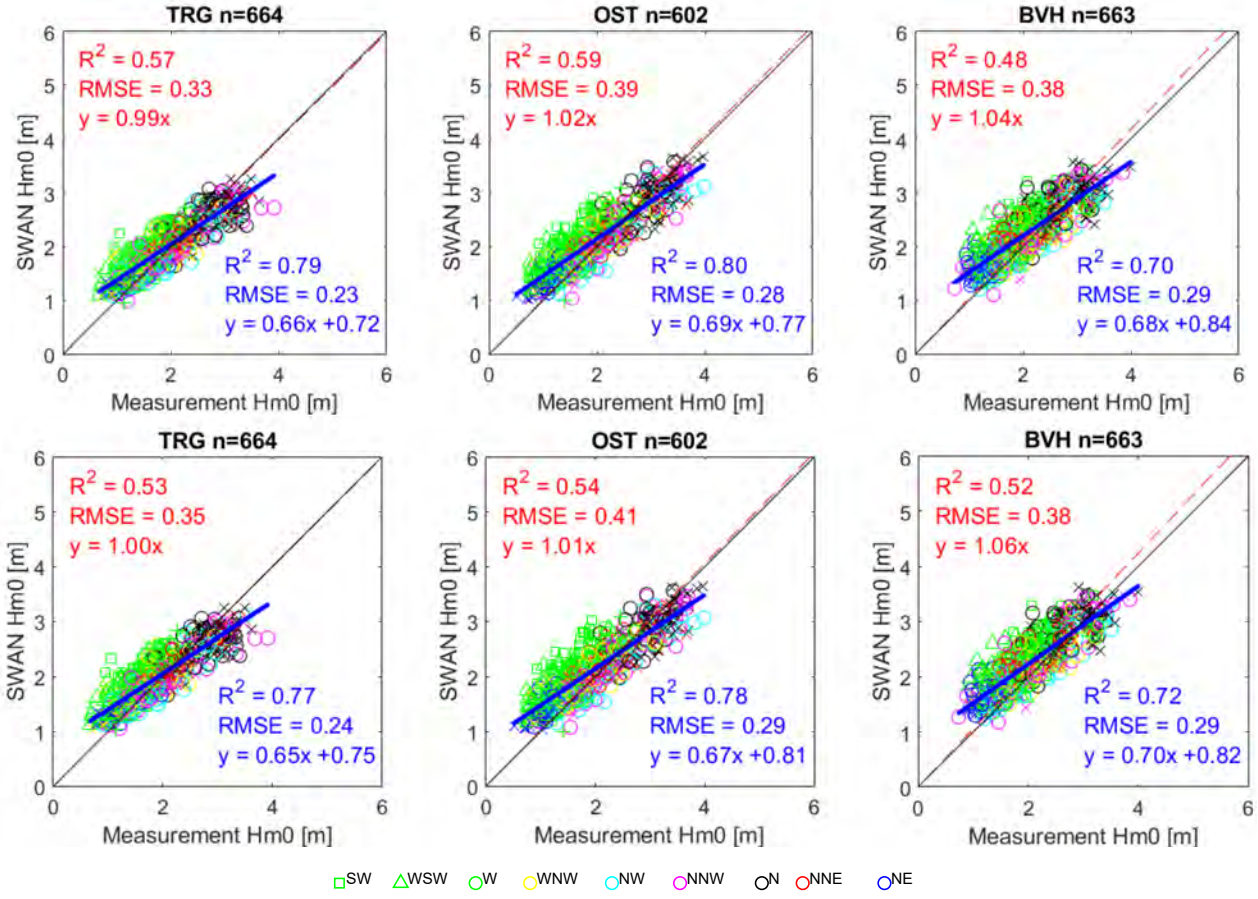

Figure 6.12 – Sensitivity of version (upper: version 41.20.AB, lower: version 40.85) – significant wave height Hm0

Table 6.3 – Sensitivity of SWAN version - Tm02

Location	Case	Y=ax			Y=ax+b					
		Slope 'a'	R^2	RMSE	Slope 'a'	Intcpt 'b'	R^2	RMSE	Est_x=5	Ratio
TRG	Basic case	**0.82**	0.65	0.36	0.60	1.09	0.75	0.31	7.69	-
	Version 40.85	**0.84**	0.66	0.37	0.62	1.08	0.75	0.31	7.92	**1.03**
OST	Basic case	**0.80**	0.77	0.33	0.68	0.64	0.80	0.31	8.14	-
	Version 40.85	**0.81**	0.78	0.33	0.70	0.60	0.80	0.32	8.35	**1.02**
BVH	Basic case	**0.85**	0.32	0.45	0.51	1.75	0.59	0.34	7.34	-
	Version 40.85	**0.88**	0.43	0.44	0.57	1.59	0.63	0.35	7.81	**1.06**

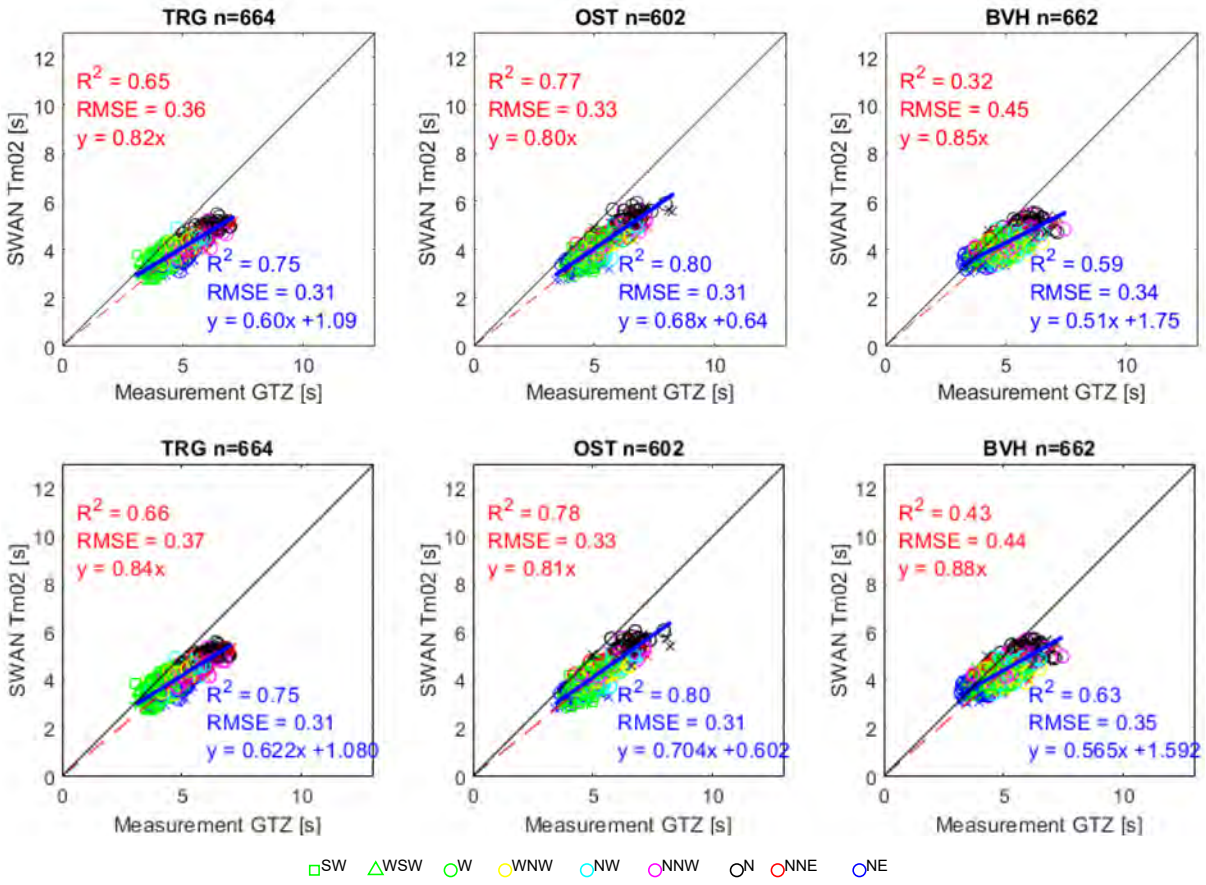

Figure 6.13 – Sensitivity of SWAN version (upper: version 41.20.AB, lower: version 40.85) - mean wave period

6.2.2 Sensitivity of bathymetry input (BCP2002 vs BCP2015)

Comparison of significant wave height between BCP2002 (input dx=dy=250 m) and BCP2015 (input dx=dy=250 m) is shown in Table 6.4 and Figure 6.13. Note that the computational grid is dx=dy=250 m in this case. As can be seen in the table, the difference is not significant (at most 1% difference looking at the slope 'a' of y=ax regression line, see the red bold value; and at most 1% difference looking at the ratio of estimation value for x=5 of y=ax+b regression line, see the blue bold value).

Small trend differences at Ostend (the slope 'a' and the intercept 'b' of y=ax+b regression line) can be explained by the difference of the new navigation channel. There are not so much difference in general, however looking at the R^2 value of both y=ax and y=ax+b regression line, the measurement data are better predicted using BCP 2015 (basic case) for OST.

Comparison of mean wave period (GTZ for measurement and Tm02 for SWAN output) between BCP2002 (input dx=dy=250 m) and BCP2015 (input dx=dy=250 m) is shown in Figure 6.15 and Table 6.5. As can be seen in the table, the difference is not significant (at most 1% difference looking at the slope 'a' of y=ax regression line, see the red bold value; and at most 3% difference looking at the ratio of estimation value for x=11 – Tm02=12 s/1.1 - of y=ax+b regression line, see the blue bold value).

From this test it can be concluded that BCP2015 is the input file to validate this data set.

Table 6.4 – Sensitivity of bathymetry input – significant wave height Hm0

Location	Case	Y=ax			Y=ax+b					
		Slope 'a'	R^2	RMSE	Slope 'a'	Intcpt 'b'	R^2	RMSE	Est_x=5	Ratio
TRG	Basic case	**0.99**	0.57	0.34	0.66	0.72	0.79	0.23	4.03	-
	BCP2002	**1.00**	0.57	0.33	0.67	0.71	0.79	0.24	4.05	**1.00**
OST	Basic case	**1.02**	0.59	0.39	0.69	0.77	0.80	0.28	4.21	-
	BCP2002	**1.03**	0.46	0.44	0.65	0.89	0.75	0.30	4.16	**0.99**
BVH	Basic case	**1.04**	0.48	0.38	0.68	0.84	0.70	0.29	4.25	-
	BCP2002	**1.04**	0.50	0.38	0.69	0.83	0.71	0.29	4.26	**1.00**

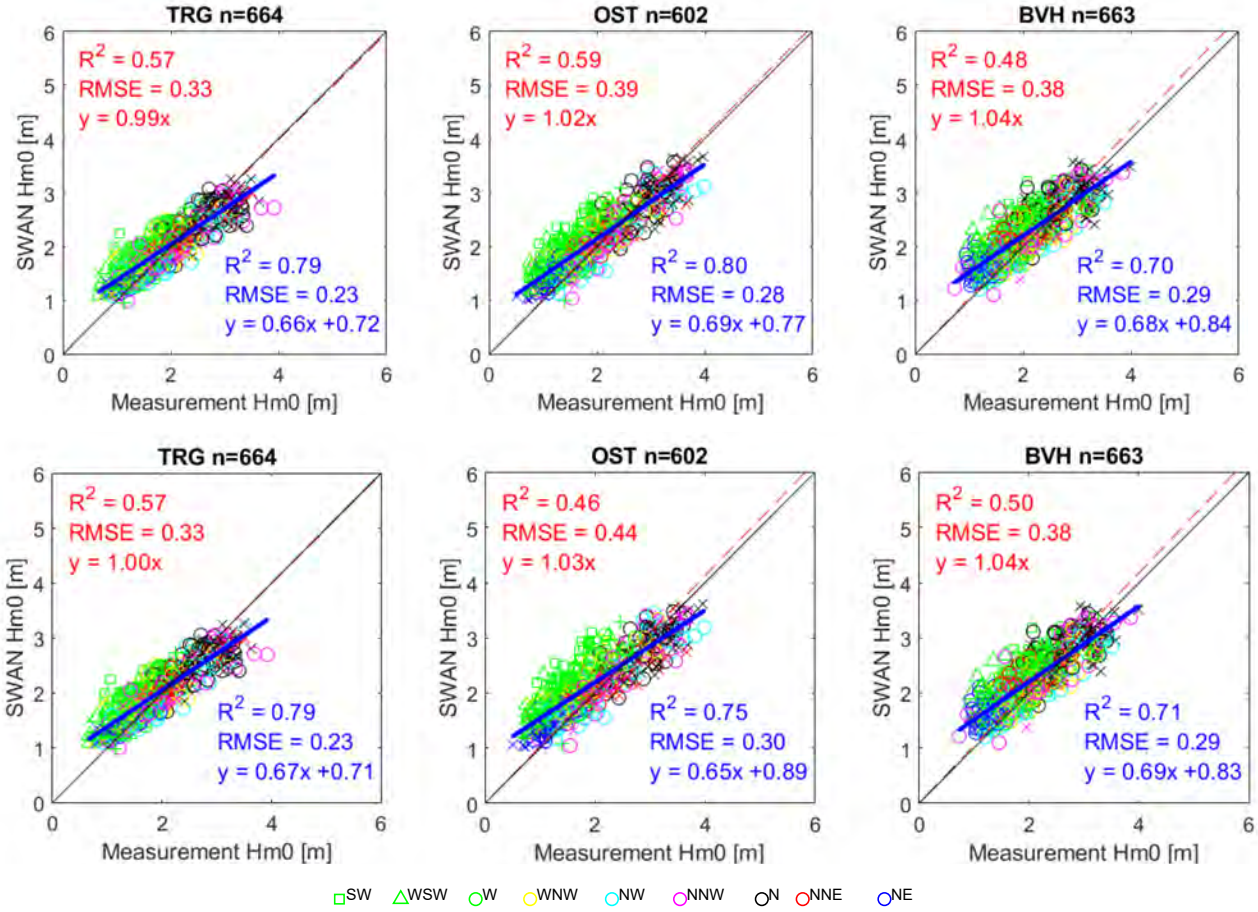

Figure 6.14 – Sensitivity of bathymetry input (upper: BCP 2015, lower: BCP 2002) – significant wave height Hm0

Table 6.5 – Sensitivity of bathymetry input – mean wave period Tm02

Location	Case	Y=ax			Y=ax+b					
		Slope 'a'	R^2	RMSE	Slope 'a'	Intcpt 'b'	R^2	RMSE	Est_x=11	Ratio
TRG	Basic case	**0.82**	0.65	0.36	0.60	1.09	0.75	0.31	7.69	-
	BCP2002	**0.82**	0.67	0.36	0.61	1.05	0.76	0.31	7.80	**1.01**
OST	Basic case	**0.80**	0.77	0.33	0.68	0.64	0.80	0.31	8.14	-
	BCP2002	**0.81**	0.71	0.35	0.63	0.96	0.77	0.31	7.94	**0.97**
BVH	Basic case	**0.85**	0.32	0.45	0.51	1.75	0.59	0.34	7.34	-
	BCP2002	**0.85**	0.34	0.44	0.52	1.71	0.60	0.35	7.38	**1.01**

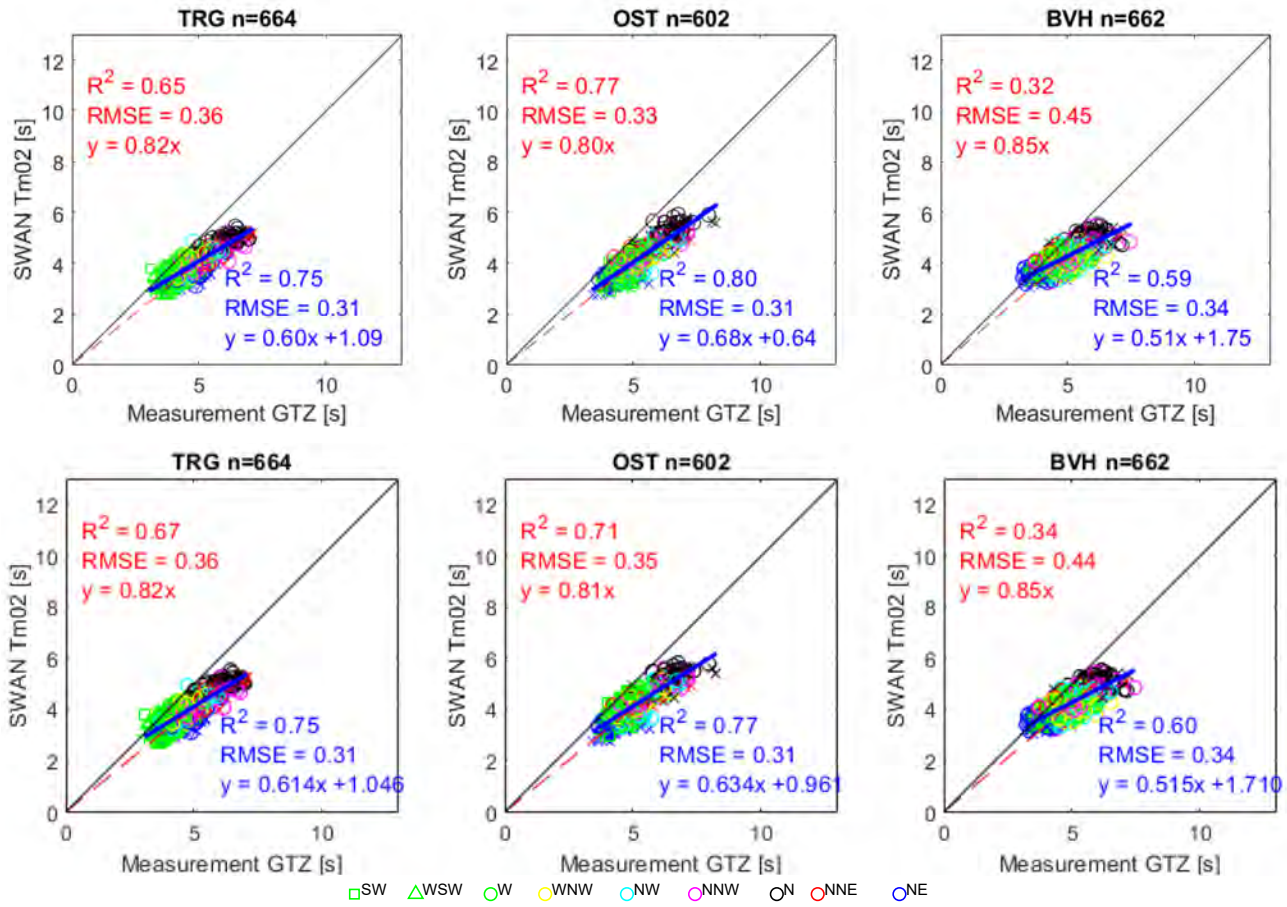

Figure 6.15 – Sensitivity of bathymetry input (upper: BCP 2015, lower: BCP 2002) – mean wave period Tm02

6.2.3 Sensitivity of computational grid size

In this section sensitivity of computational grid size is investigated. In the past study De Roo *et al.* (2016) indicated that 250x125 m computational grid gives at most 3 % differences in significant wave height at -5 m contour line where hydraulic boundary condition is calculated, and concluded that the influence of the gird is minor, and therefore 250x250 m grid was used for SA15. Note that the computational grid was based on a bathymetry grid of 250x250 m, and therefore 250x125 m is achieved by linear interpolation by SWAN. In this study, different grid sizes are tested from 500x500 m in order to investigate the grid convergence more systematically.

Comparison of significant wave height between computational grid size 500x500 m, 250x250 m, 250x125 m (along-shore direction 250 m, cross-shore direction 125 m) and 125x125 m (all based on a newly created bathymetry 'BCP2020' which included recent update of the bathymetry and input grid resolution is 50 m, see Figure 6.15) is shown in Figure 6.16 and Table 6.6. Grid size 500x500 leads to some deviation from other grid sizes while 250x250 m, 250x125 m and 125x125 m give similar outputs.

From the result above, it can be concluded that the computational grid size of 250x250 m has already reached to the saturation for the estimation of wave climate at TRG, OST and BVH. However, one concern is if there are rapidly changing bathymetries (e.g. gully and access channel) around the output points of the hydraulic boundary conditions, and they influence to the estimation result significantly.

In order to investigate it, an example calculation is conducted. Note that this calculation is done using an example input: Water level=7.0 m TAW, Hm0=5 m, Tp=12 s, wave dir=NNW, wind speed=26 m/s, wind dir=NNW, with the setting of GEN3 KOMEN and BREAK Ruessink (see details in section 6.6.4). The output locations (HBC output points in SA15, and 1500 m line) are shown in Figure 6.17 (pink points are representing 1500 m line, and cyan points are representing HBC output points in SA15). Figure 6.18 (HBC output points in SA15) and Figure 6.19 (1500 m line) show the difference of estimated Hm0 based on different grid sizes. The biggest differences can be found around the port of Zeebrugge. As can be seen in Figure 6.17, 3-4 points are located at the edge or insde the port on the 250x250 m grid (figure is somewhat interpolated by the visualization of matlab). It is logical that the difference between blue (250x250-125x125) and red (250x125-125x125) points are not big around the port of Zeebrugge since the longitudinal grid resolution is the same, dx=250 m. The other big differences can be seen around the point 90 and 170, which show the maximum difference of 5-6% (blue points, 250x250-125x125). The differences are significantly low for the red points (250x125-125x125), since transverse grid resolution is fine, y=125 m. If we have enough distance between the output points close to the port of Zeebrugge, the grid resolution of 250x125 will be acceptable.

Taking into account the computational efficiency, 250x125 m is recommended for the SA21 HBC estimation.

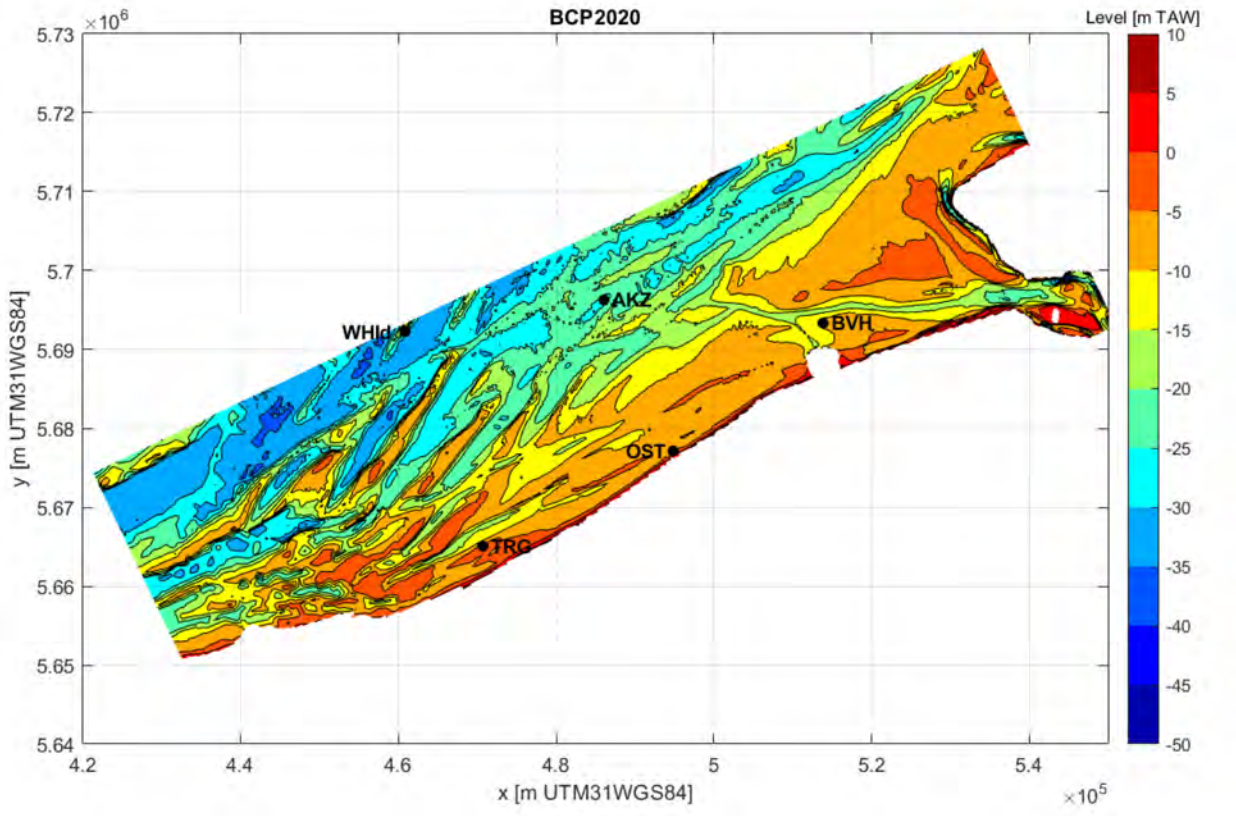

Figure 6.16 – The Belgian coast model with measurement locations obtained by Meetnet Vlaamse Banken. BCP2020 (50x50m).

Table 6.6 – Sensitivity of BCP 2020 bathymetry input grid size– significant wave height Hm0

Location	Case	Y=ax			Y=ax+b					
		Slope 'a'	R^2	RMSE	Slope 'a'	Intcpt 'b'	R^2	RMSE	Est_x=5	Ratio
TRG	500x500 m grid	**1.01**	0.54	0.34	0.66	0.75	0.78	0.24	4.06	**1.00**
	250x250 m grid	**1.00**	0.57	0.34	0.67	0.72	0.79	0.23	4.05	-
	250x125 m grid	**1.00**	0.60	0.33	0.68	0.71	0.81	0.23	4.09	**1.01**
	125x125 m grid	**1.00**	0.55	0.34	0.66	0.74	0.78	0.24	4.03	**1.00**
OST	500x500 m grid	**1.00**	0.46	0.42	0.63	0.87	0.76	0.29	4.01	**0.96**
	250x250 m grid	**1.02**	0.55	0.41	0.67	0.81	0.79	0.28	4.18	-
	250x125 m grid	**1.02**	0.60	0.39	0.69	0.77	0.81	0.27	4.23	**1.01**
	125x125 m grid	**1.02**	0.60	0.39	0.69	0.77	0.81	0.27	4.23	**1.01**
BVH	500x500 m grid	**1.05**	0.52	0.38	0.70	0.81	0.72	0.29	4.31	**1.01**
	250x250 m grid	**1.05**	0.50	0.38	0.69	0.83	0.70	0.29	4.29	-
	250x125 m grid	**1.05**	0.51	0.39	0.69	0.84	0.72	0.29	4.29	**1.00**
	125x125 m grid	**1.05**	0.49	0.39	0.69	0.84	0.70	0.30	4.29	**1.00**

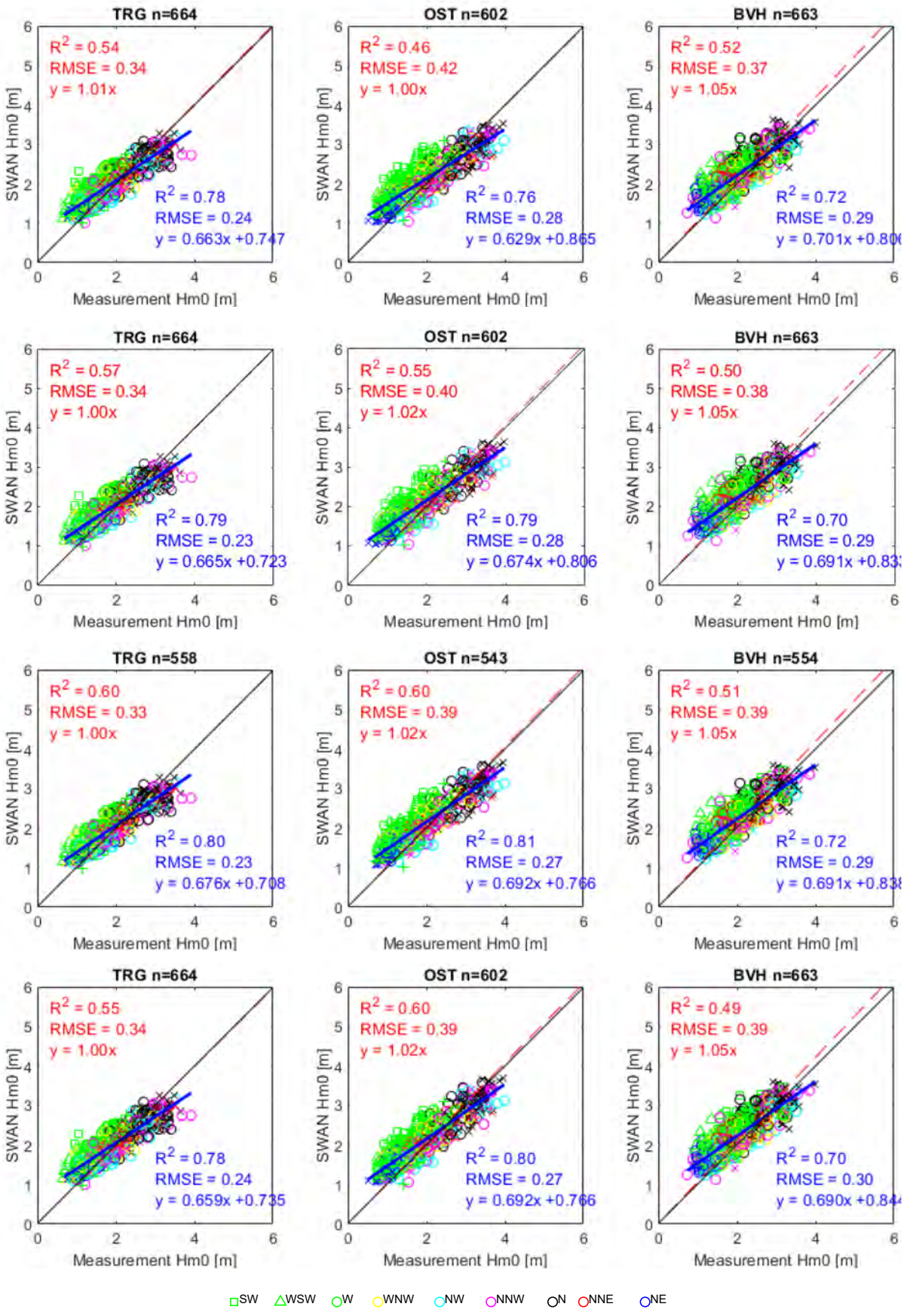

Figure 6.17 – Sensitivity of BCP 2020 bathymetry input (fom the top, 500x500, 250x250,250x125, 125x125 m, respectively) – Hm0

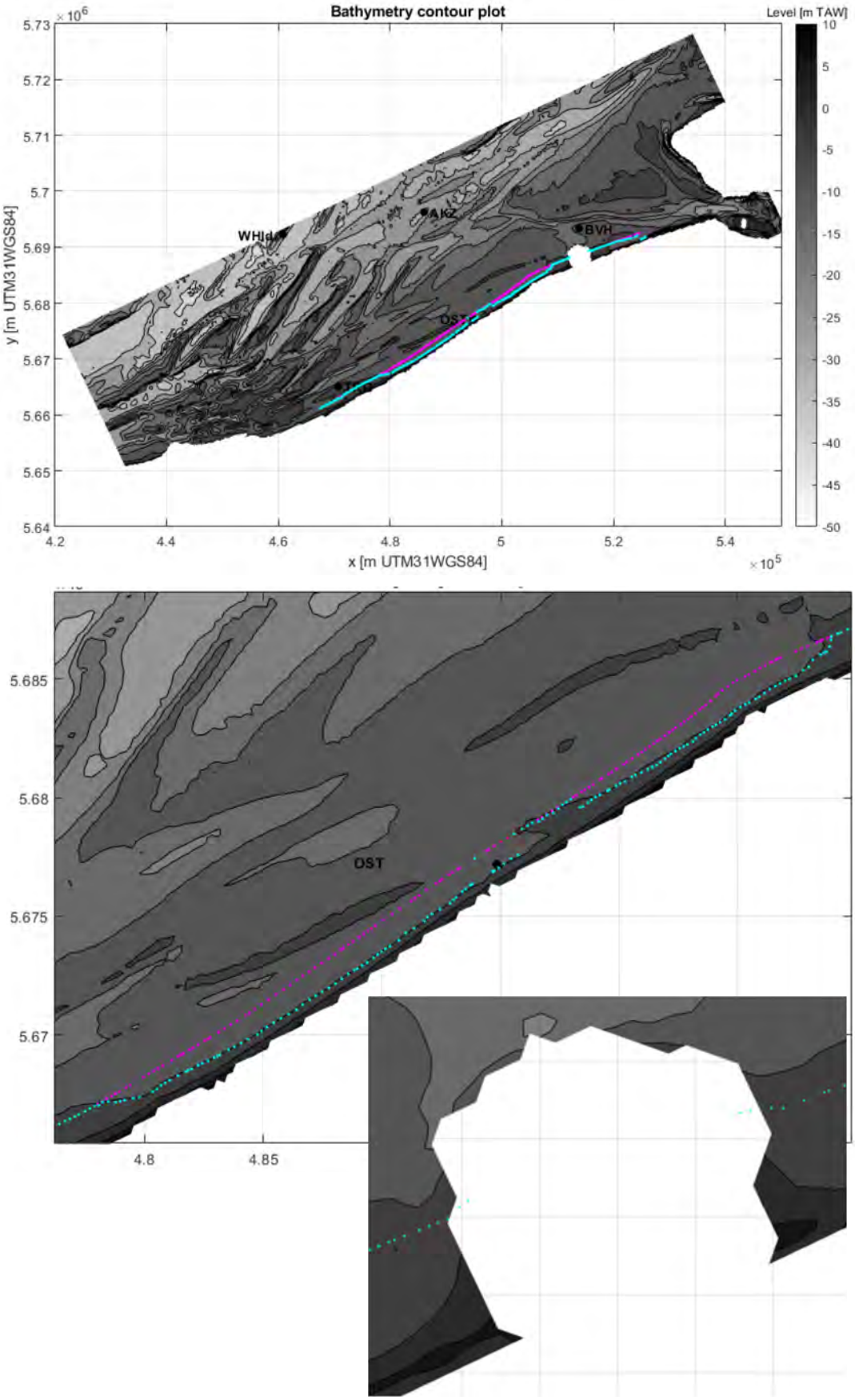

Figure 6.18 – Location of the points (top: entire view, bottom: around Ostend + around Zeebrugge)

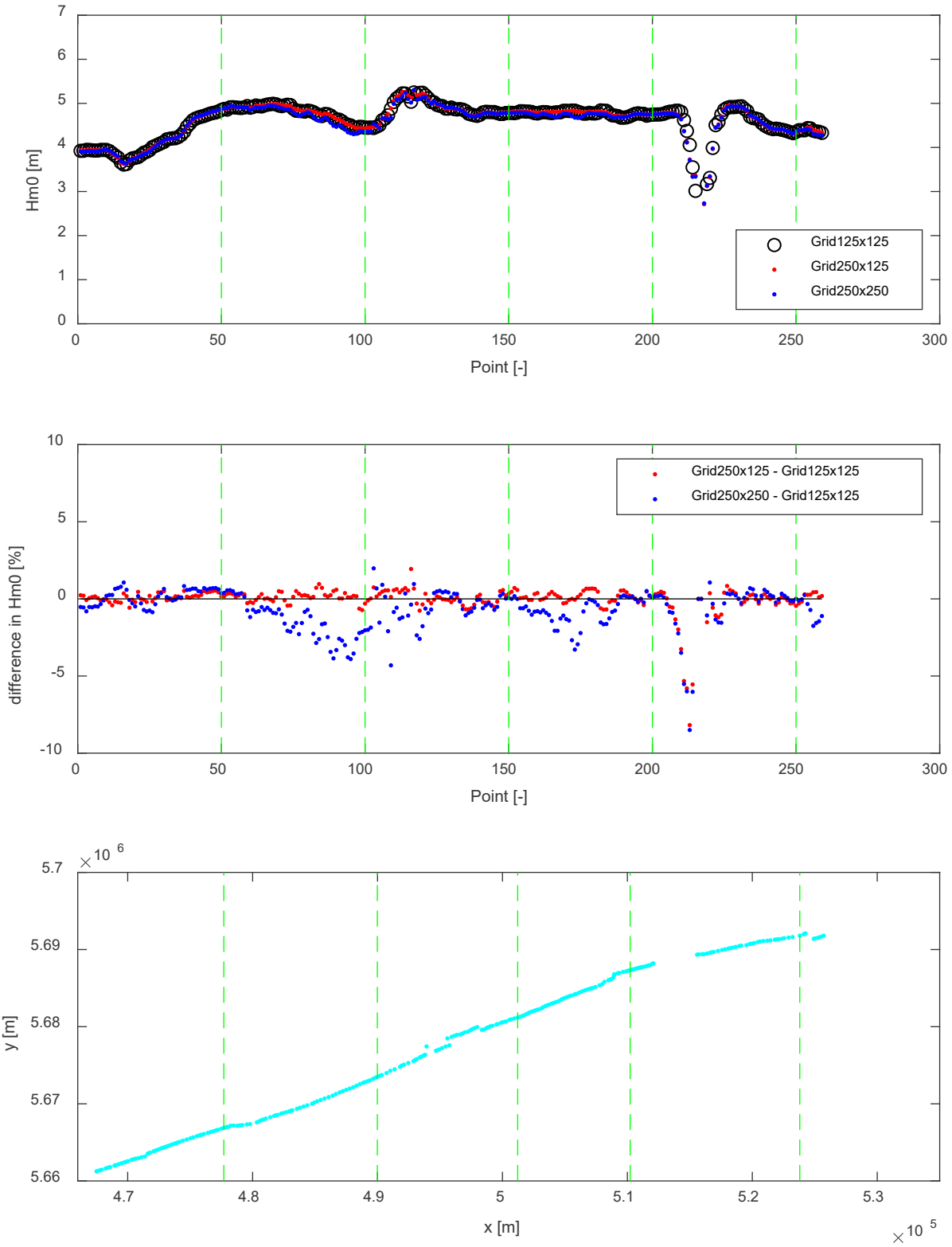

Figure 6.19 – Comparison of BCP 2020 different grid size at HBC output points in SA15
(Top: Hm0, mid: difference, bottom location)

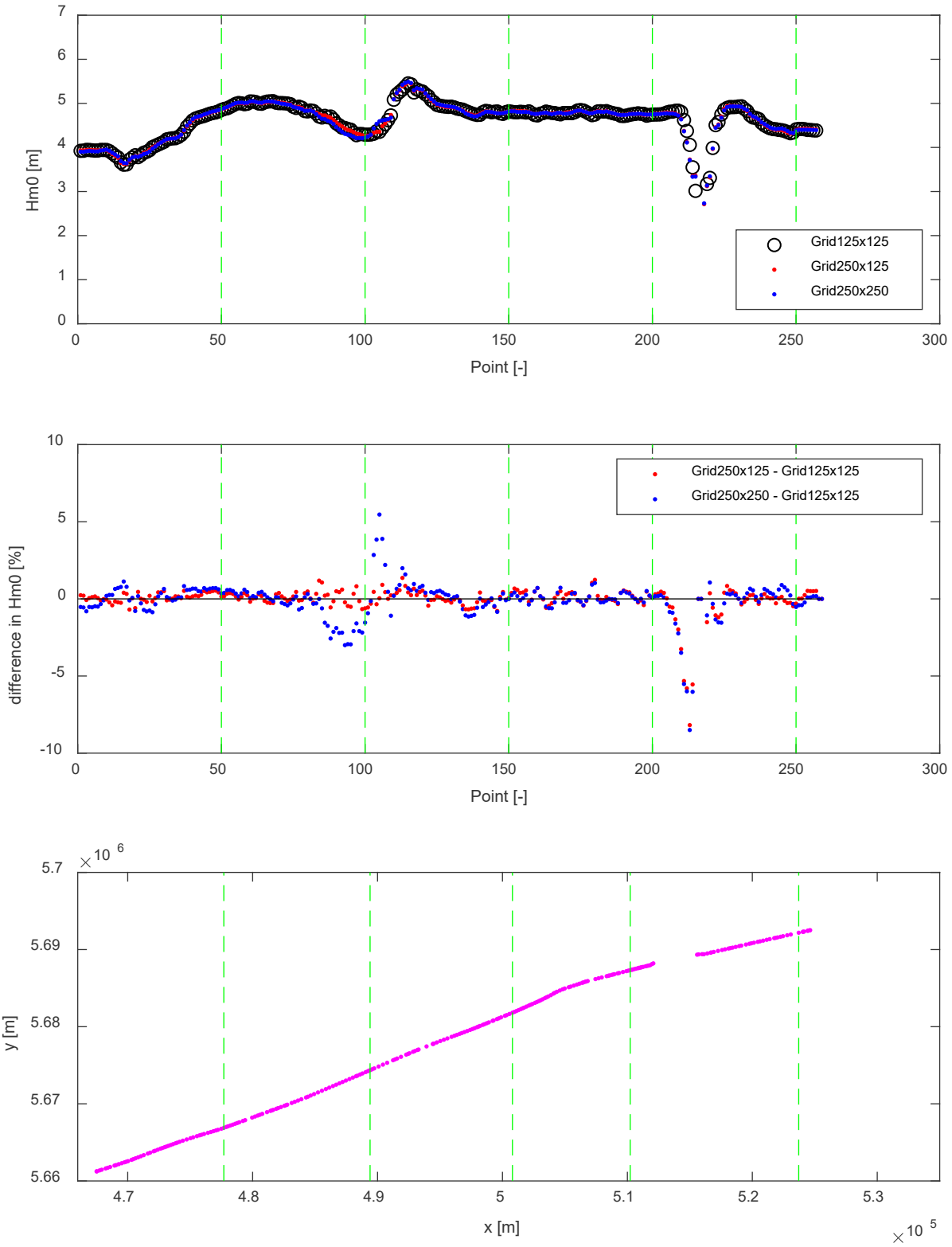

Figure 6.20 – Comparison of BCP 2020 different grid size at HBC output points on 1500 m line
(Top: Hm0, mid: difference, bottom location)

6.2.4 Sensitivity of offshore wave input

Comparison between WHI and AKZ wave input is shown in Table 6.7; the results using AKZ as offshore wave input are depicted in Figure 6.20.

Looking at the estimation value of y=ax+b when x=5m is applied (Est_x=5), some differences are observed for all locations. BVH output from AKZ input gives the best estimation among others. This can be explained by the geographical locations. However, the number of cases is significantly smaller for AKZ input (i.e. 219 against 692 for WHI). A larger dataset is necessary to further verify the differences. For now, it can be concluded that the AKZ input is at least equally good as the WHI input. Note that the WHI measurements might be influenced by the presence of the Westhinder bank. How far this bank plays a role is never fully investigated. For most conditions, the influence of the bank is probably limited. However for the more extreme (largest wave height and longest wave period) conditions that might no longer be the case.

Table 6.7 - Sensitivity of offshore wave input – significant wave height Hm0

Location	Case	Y=ax			Y=ax+b					
		Slope 'a'	R^2	RMSE	Slope 'a'	Intcpt 'b'	R^2	RMSE	Est_x=5	Ratio
TRG	Basic case	0.99	0.57	0.33	0.66	0.72	0.79	0.23	4.02	-
	AKZ input	1.02	0.59	0.33	0.70	0.70	0.78	0.24	4.20	**1.04**
OST	Basic case	1.02	0.59	0.39	0.69	0.77	0.80	0.28	4.22	-
	AKZ input	1.04	0.71	0.34	0.76	0.65	0.83	0.26	4.45	**1.05**
BVH	Basic case	1.04	0.48	0.38	0.68	0.84	0.70	0.29	4.24	-
	AKZ input	1.07	0.61	0.35	0.77	0.70	0.73	0.29	4.55	**1.07**

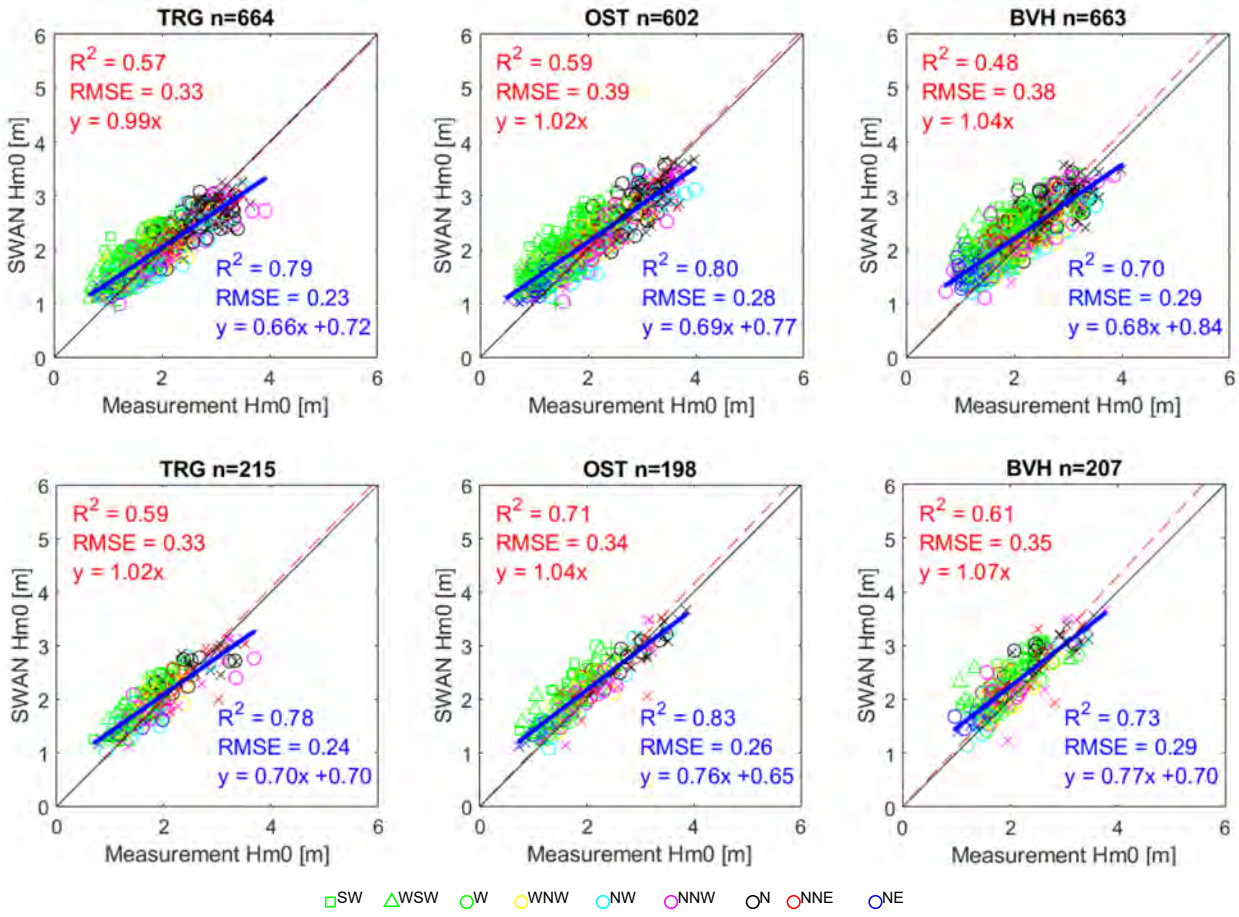

Figure 6.21 – Sensitivity of offshore wave input (upper: WHI input, lower: AKZ input) – significant wave height Hm0

6.2.5 Sensitivity of wind input

Comparison between MP7 and MP0 wind input is shown in Table 6.8 and Figure 6.21. Looking at the estimation value of y=ax+b when x=5m is applied (Est_x=5), it can be seen that the difference is limited. Looking at the R^2 value of y=ax+b, the basic case MP7 gives slightly better estimation for TRG and OST. On the other hand, MP0 leads better estimation for BVH. It can be again explained by the geographical location: BVH is very close to MP0 location. For OST, MP7 and MP0 are equally good.

From this test it can be concluded that the wind input MP0 is equally good as MP7. MP0 data can be also used on top of MP7 data for the extreme value analysis to obtain offshore wave conditions.

Table 6.8 – Sensitivity of wind input – significant wave height Hm0

Location	Case	Y=ax			Y=ax+b					
		Slope 'a'	R^2	RMSE	Slope 'a'	Intcpt 'b'	R^2	RMSE	Est_x=5	Ratio
TRG	Basic case	0.99	0.57	0.33	0.66	0.72	0.79	0.23	4.02	-
	MP0 input	0.97	0.58	0.34	0.67	0.65	0.75	0.26	4.00	1.00
OST	Basic case	1.02	0.59	0.39	0.69	0.77	0.80	0.28	4.22	-
	MP0 input	0.98	0.60	0.39	0.69	0.69	0.77	0.30	4.14	0.98
BVH	Basic case	1.04	0.48	0.38	0.68	0.84	0.70	0.29	4.24	-
	MP0 input	1.01	0.64	0.33	0.73	0.64	0.76	0.27	4.29	1.01

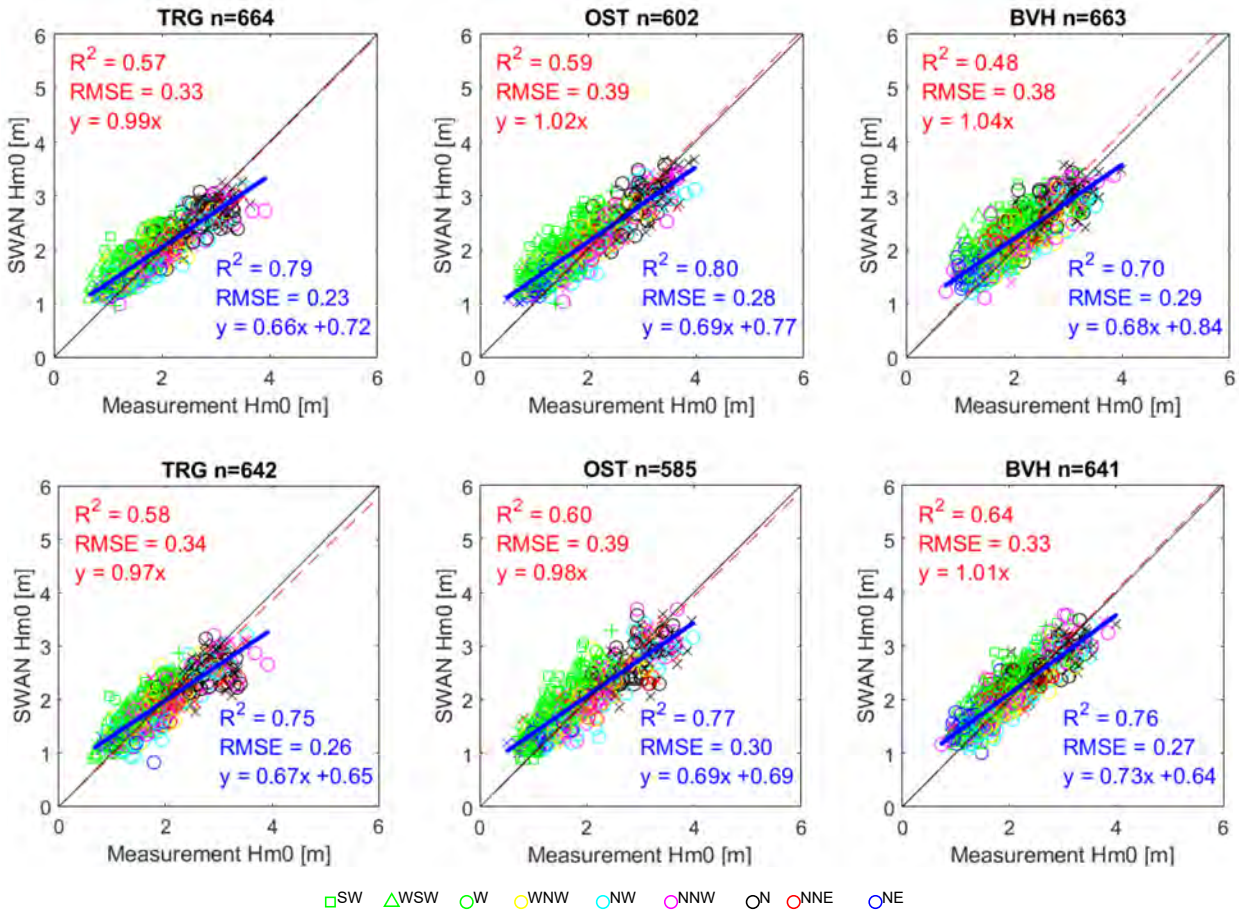

Figure 6.22 – Sensitivity of wind input (upper: MP7 input, lower: MP0 input) – significant wave height Hm0

6.2.6 Sensitivity of wind drag (Default Zijlema FIT setting vs Wu's setting)

Comparison between default FIT setting (Zijlema *et al.*, 2012) and Wu's setting (Wu, 1982) for the wind drag in SWAN is shown in Table 6.9 and Figure 6.22. Wu's setting generally gives higher since the drag coefficient is always higher than one in Zijlema's as shown in Figure 4.4, while the difference is not significant (within 3% looking at the ratio of y=ax+b when x=5m is applied).

Wu's setting will influence more for a higher wind speed case since the difference of the drag coefficient is getting bigger as shown in Figure 4.4, while FIT setting follows the observation results better. Therefore it is concluded that the default setting is suitable for the estimation of nearshore waves in the Belgian coast for a higher wave climate.

Table 6.9 – Sensitivity of wind drag – significant wave height Hm0

Location	Case	Y=ax			Y=ax+b					
		Slope 'a'	R^2	RMSE	Slope 'a'	Intcpt 'b'	R^2	RMSE	Est_x=5	Ratio
TRG	Basic case	0.99	0.57	0.33	0.66	0.72	0.79	0.23	4.02	-
	Wu's setting	1.02	0.54	0.35	0.67	0.76	0.78	0.24	4.11	1.02
OST	Basic case	1.02	0.59	0.39	0.69	0.77	0.80	0.28	4.22	-
	Wu's setting	1.04	0.55	0.42	0.69	0.82	0.78	0.29	4.27	1.01
BVH	Basic case	1.04	0.48	0.38	0.68	0.84	0.70	0.29	4.24	-
	Wu's setting	1.07	0.44	0.41	0.69	0.90	0.68	0.31	4.35	1.03

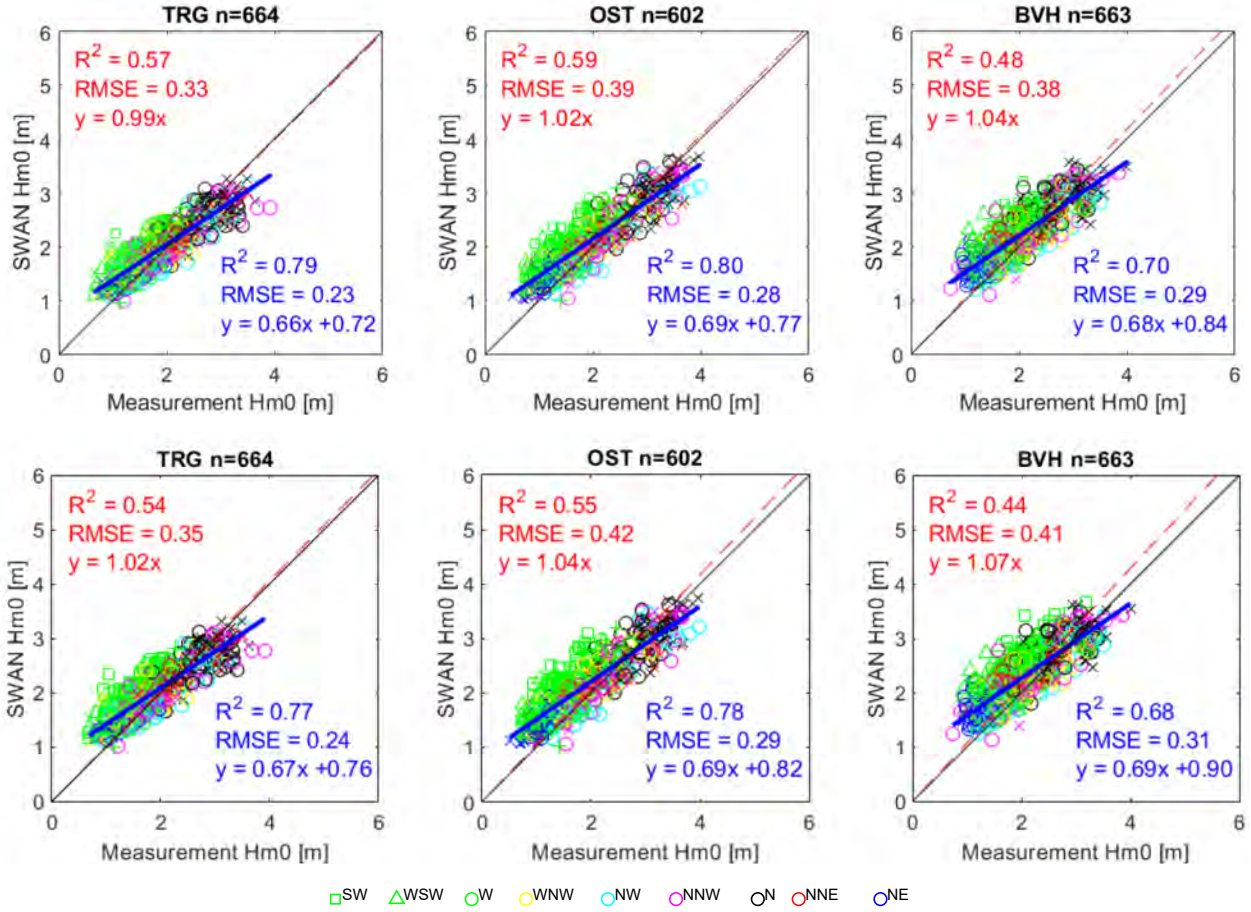

Figure 6.23 – Sensitivity of wind drag (upper: default FIT setting, lower: Wu's setting) – significant wave height Hm0

6.2.7 Sensitivity of GEN3 mode (Westhuysen vs Komen)

Allahdadi *et al.* (2019) did a study about whitecapping using field measurement data and they described it as follows: *Model–data comparisons show that when using the default parameters in SWAN, both Komen and Westhuysen methods underestimate wave height. Simulations of mean wave period using the Komen method agree with observations, but those using the Westhuysen method are substantially lower. Examination of source terms shows that the Westhuysen method underestimates the total energy transferred into the wave action equations, especially in the lower frequency bands that contain higher spectral energy. Several causes for this underestimation are identified. The primary reason is the difference between the wave growth conditions along the east coast during winter storms and the conditions used for the original whitecapping formula calibration. In addition, some deficiencies in simulation results are caused along the coast by the "slanting fetch" effect that adds low-frequency components to the 2-D wave spectra. These components cannot be simulated partly or entirely by available source terms (wind input, whitecapping, and quadruplet) in models and their interaction. Further, the effect of boundary layer instability that is not considered in the Komen and Westhuysen whitecapping wind input formulas may cause additional underestimation.*

Note that Allahadadi's application domain is much deeper (i.e. 5000-40m depth) compared to our case, therefore depth induced breaking is not playing an important role in their case. As for the underestimation of wave height, actually Komen gave larger wave heights that were more consistent with observations.

Our case westhuysen does not give different wave height as Komen but wave period behaviour is the same as his conclusion.

Comparison of significant wave height between Westhuysen and Komen of GEN3 mode based on the present measurement data is shown in Table 6.10 and Figure 6.23. As can be seen in the table, the difference is not significant for the estimation of significant wave height (at most 2% difference looking at the slope 'a' of y=ax regression line, see the red bold value; and at most 2% difference looking at the ratio of estimation value for x=5 of y=ax+b regression line, see the blue bold value; R^2 calue is almost the same). In terms of mean wave period (GTZ for measurement and Tm02 for SWAN output), Komen leads 8-15% higher slope 'a' value of y=ax regression line and 23-29% higher estimation ratio as shown in Figure 6.24 and Table 6.11. These results are in line with the findings of Allahdadi *et al.* (2019).

De Roo *et al.* (2016) stated that: *An alternative formulation for whitecapping is introduced in version 40.51. The dissipation depends on the frequency as opposed to the dissipation which is evenly distributed over it spectrum as in the Komen formulation. This formulation for dissipation can be linked to an adapted formulation for wind wave growth. This custom wind growth formulation is more accurate for young waves than the standard Komen expression. The combination of alternative wind supply and expression for whitecapping is capable of underestimating both the tendency to correct wave periods as the overestimation of sea-waves in combined swell conditions. This combination of formulations is activated with the GEN3 command WESTHuyssen instead of GEN3 KOMEN. In version 40.72 one can opt for the integrated parameters (eg significant wave height, wave direction, etc.) at a user-defined frequency interval [fmin; fmax].*

Even though Westhuysen is recommended in version 40.72 in De Roo *et al.* (2016), the settings can be more suitable for young waves. Therefore taking into account the outcome it is concluded that Komen gives better estimation especially for mean wave period (while wave height is almost the same) and thus suitable for the further investigation.

Table 6.10 – Sensitivity of GEN3 mode – significant wave height Hm0

Location	Case	Y=ax			Y=ax+b					
		Slope 'a'	R^2	RMSE	Slope 'a'	Intcpt 'b'	R^2	RMSE	Est_x=5	Ratio
TRG	Basic case	**0.99**	0.57	0.34	0.66	0.72	0.79	0.23	4.03	-
	Komen	**1.01**	0.54	0.34	0.66	0.76	0.79	0.23	4.04	**1.00**
OST	Basic case	**1.02**	0.59	0.39	0.69	0.77	0.80	0.28	4.21	-
	Komen	**1.03**	0.60	0.39	0.70	0.78	0.81	0.27	4.28	**1.02**
BVH	Basic case	**1.04**	0.48	0.38	0.68	0.84	0.70	0.29	4.25	-
	Komen	**1.05**	0.47	0.38	0.68	0.88	0.71	0.28	4.26	**1.00**

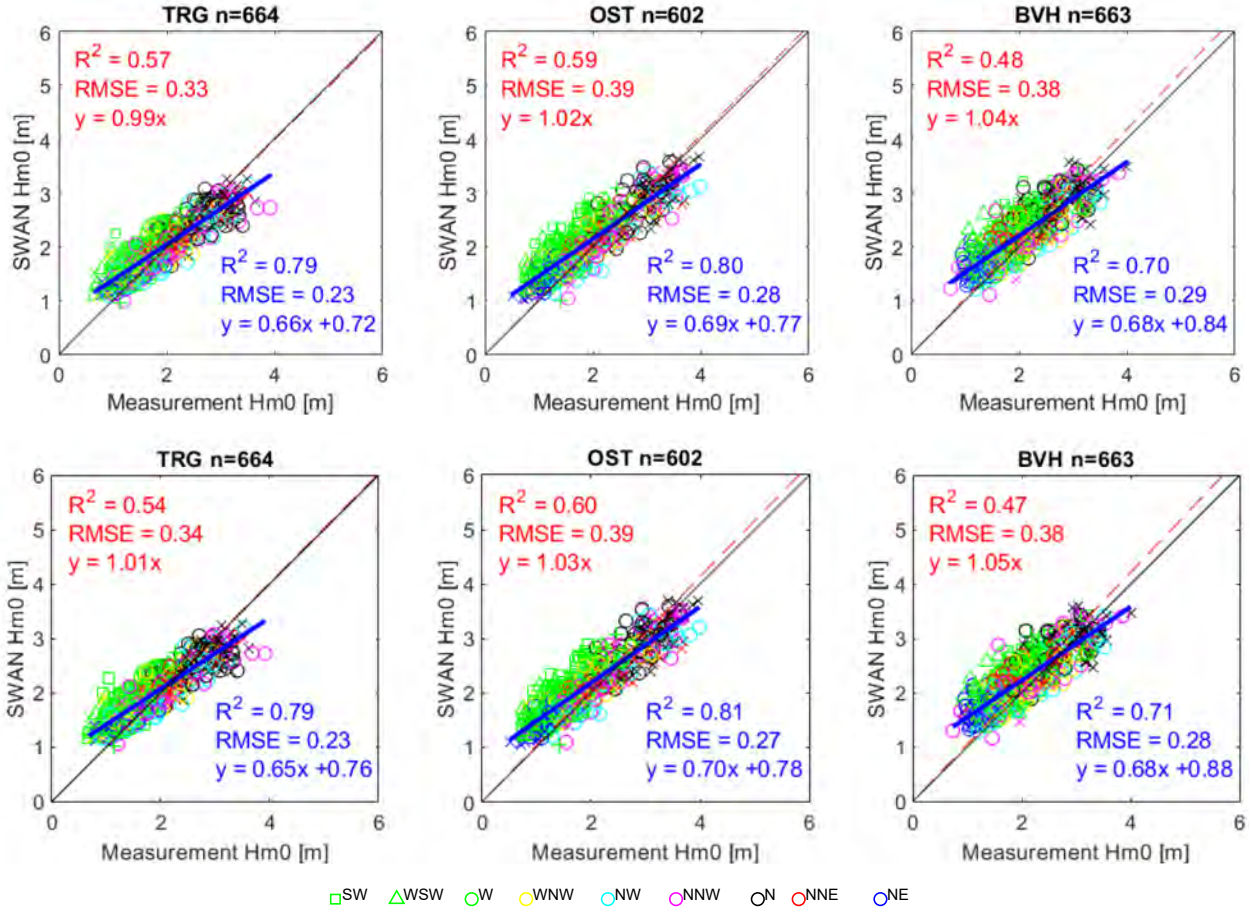

Figure 6.24 – Sensitivity of GEN3 mode (upper: Westhuysen, lower: Komen) – significant wave height Hm0

Table 6.11 – Sensitivity of GEN3 mode – mean wave period

Location	Case	Y=ax			Y=ax+b					
		Slope 'a'	R^2	RMSE	Slope 'a'	Intcpt 'b'	R^2	RMSE	Est_x=12	Ratio
TRG	Basic case	**0.82**	0.65	0.36	0.60	1.09	0.75	0.31	7.69	-
	Komen	**0.95**	0.68	0.46	0.78	0.88	0.71	0.44	9.44	**1.23**
OST	Basic case	**0.80**	0.77	0.33	0.68	0.64	0.80	0.31	8.14	-
	Komen	**0.95**	0.77	0.47	0.96	-0.07	0.77	0.47	10.48	**1.29**
BVH	Basic case	**0.85**	0.32	0.45	0.51	1.75	0.59	0.34	7.34	-
	Komen	**1.00**	0.45	0.52	0.67	1.71	0.61	0.44	9.03	**1.23**

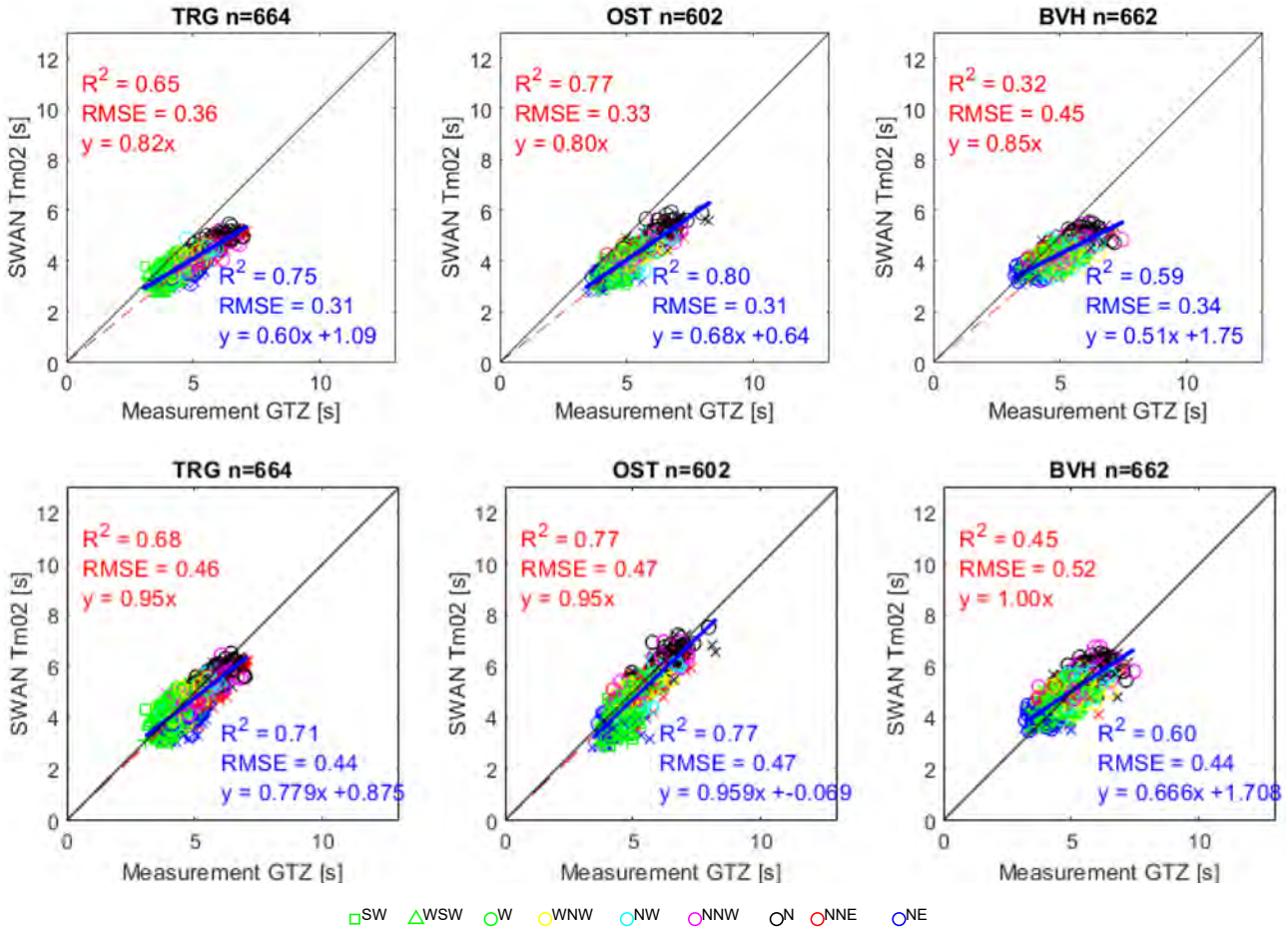

Figure 6.25 – Sensitivity of GEN3 mode (upper: Westhuysen, lower: Komen) – mean wave period

6.2.8 Sensitivity of Triads (off vs on)

Comparison of significant wave height between a case without TRIADS and with TRIADS is shown in Table 6.12 and Figure 6.25. As can be seen in the table, the difference is very small (no difference looking at the slope 'a' of y=ax regression line, see the red bold value; and at most 1% difference looking at the ratio of estimation value for x=5 of y=ax+b regression line, see the blue bold value; R^2 calue is also almost the same).

Figure 6.24 and Table 6.11. show the comparison of mean wave period. TRIADS leads 2% lower estimation ratio of y=ax+b regression line.

Figure 6.27 shows spectrum output comparing with Broesbank measurement data (only limited to 5 cases in one storm peak). All the cases show that the peak energy is lower (partly because wave height is underestimated). When Triads is activated, the peak becomes even lower and the second superharmonic becomes slightly overestimated. It is not very clear but Triads seems to transfer energy (slightly) too much to the higher frequency.

De Roo *et al.* (2016) stated that: *In shallow water, interactions between 3 wave components become important. These so-called triads give rise to higher and lower harmonic wave components. However, the method for triads modeled in SWAN only work for higher harmonic. Experiences of using triads in SWAN indicate that they have accuracy deteriorate rather than improve. Therefore, triads are not activated in SWAN calculations.* This choice is in line with the major studies applied to Flemish coast (e.g. Technum *et al.*, 2002; International Marine and Dredging Consultants, 2009d). On the other hand, collinear approach was made consistent in version 41.01 (Salmon et al. 2016).

The results shown here shows minor differences but the consequence of the choice can give bigger difference for the extreme wave condition (i.e. SA21). Therefore further investigation will be conducted in Section 6.6.2.

Table 6.12 – Sensitivity of TRIADS – significant wave height Hm0

Location	Case	Y=ax			Y=ax+b					
		Slope 'a'	R^2	RMSE	Slope 'a'	Intcpt 'b'	R^2	RMSE	Est_x=5	Ratio
TRG	Basic case	0.99	0.57	0.34	0.66	0.72	0.79	0.23	4.03	-
	TRIADS	0.99	0.56	0.33	0.66	0.72	0.78	0.23	4.00	0.99
OST	Basic case	1.02	0.59	0.39	0.69	0.77	0.80	0.28	4.21	-
	TRIADS	1.02	0.59	0.39	0.69	0.77	0.80	0.28	4.21	1.00
BVH	Basic case	1.04	0.48	0.38	0.68	0.84	0.70	0.29	4.25	-
	TRIADS	1.04	0.48	0.38	0.68	0.85	0.70	0.29	4.23	1.00

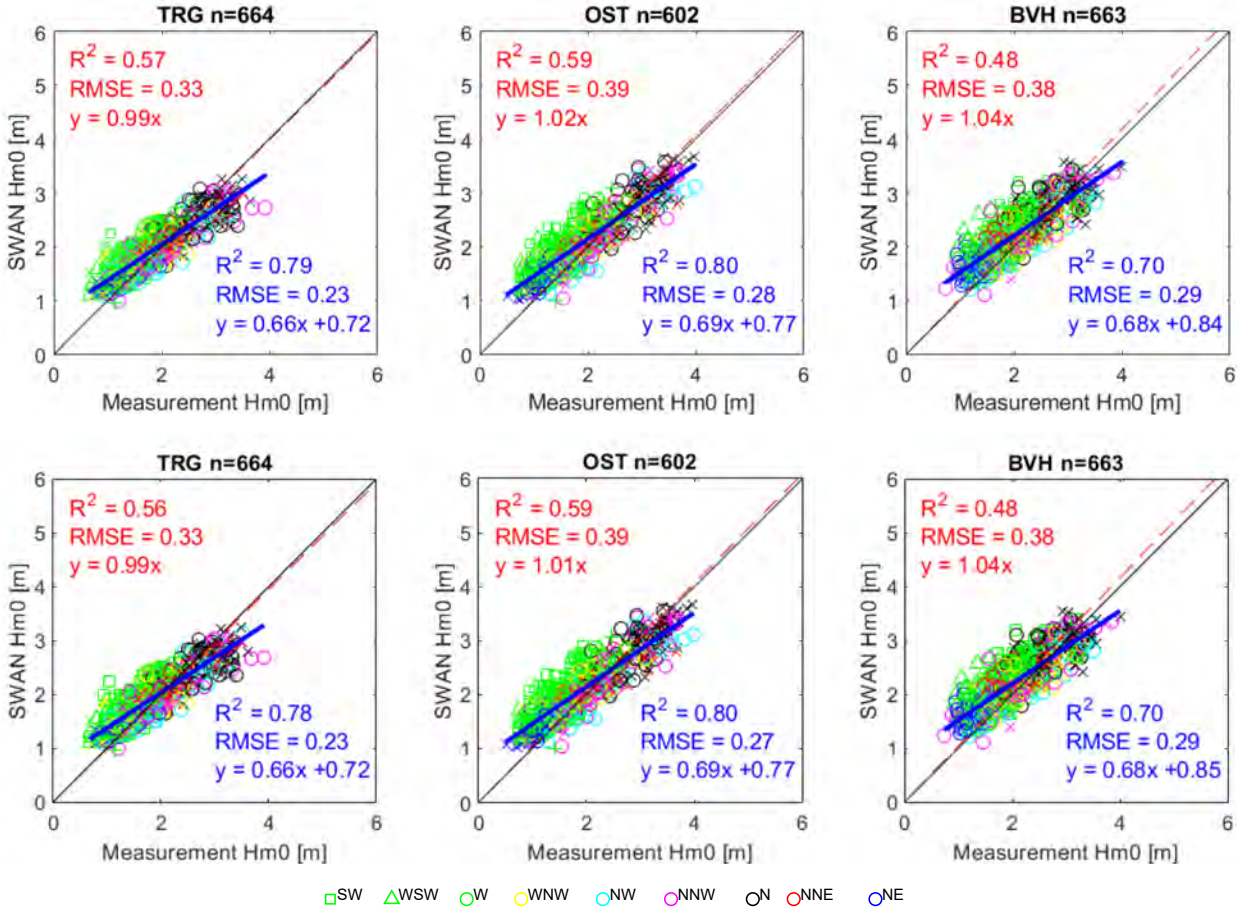

Figure 6.26 – Sensitivity of TRIADS (upper: without TRIADS, lower: TRIADS) – significant wave height Hm0

Table 6.13 – Sensitivity of TRIADS – mean wave period

Location	Case	Y=ax			Y=ax+b					
		Slope 'a'	R^2	RMSE	Slope 'a'	Intcpt 'b'	R^2	RMSE	Est_x=5	Ratio
TRG	Basic case	**0.82**	0.65	0.36	0.60	1.09	0.75	0.31	7.69	-
	TRIADS	**0.81**	0.61	0.37	0.58	1.18	0.74	0.30	7.50	**0.98**
OST	Basic case	**0.80**	0.77	0.33	0.68	0.64	0.80	0.31	8.14	-
	TRIADS	**0.80**	0.75	0.33	0.65	0.77	0.79	0.30	7.96	**0.98**
BVH	Basic case	**0.85**	0.32	0.45	0.51	1.75	0.59	0.34	7.34	-
	TRIADS	**0.85**	0.26	0.45	0.49	1.83	0.58	0.34	7.19	**0.98**

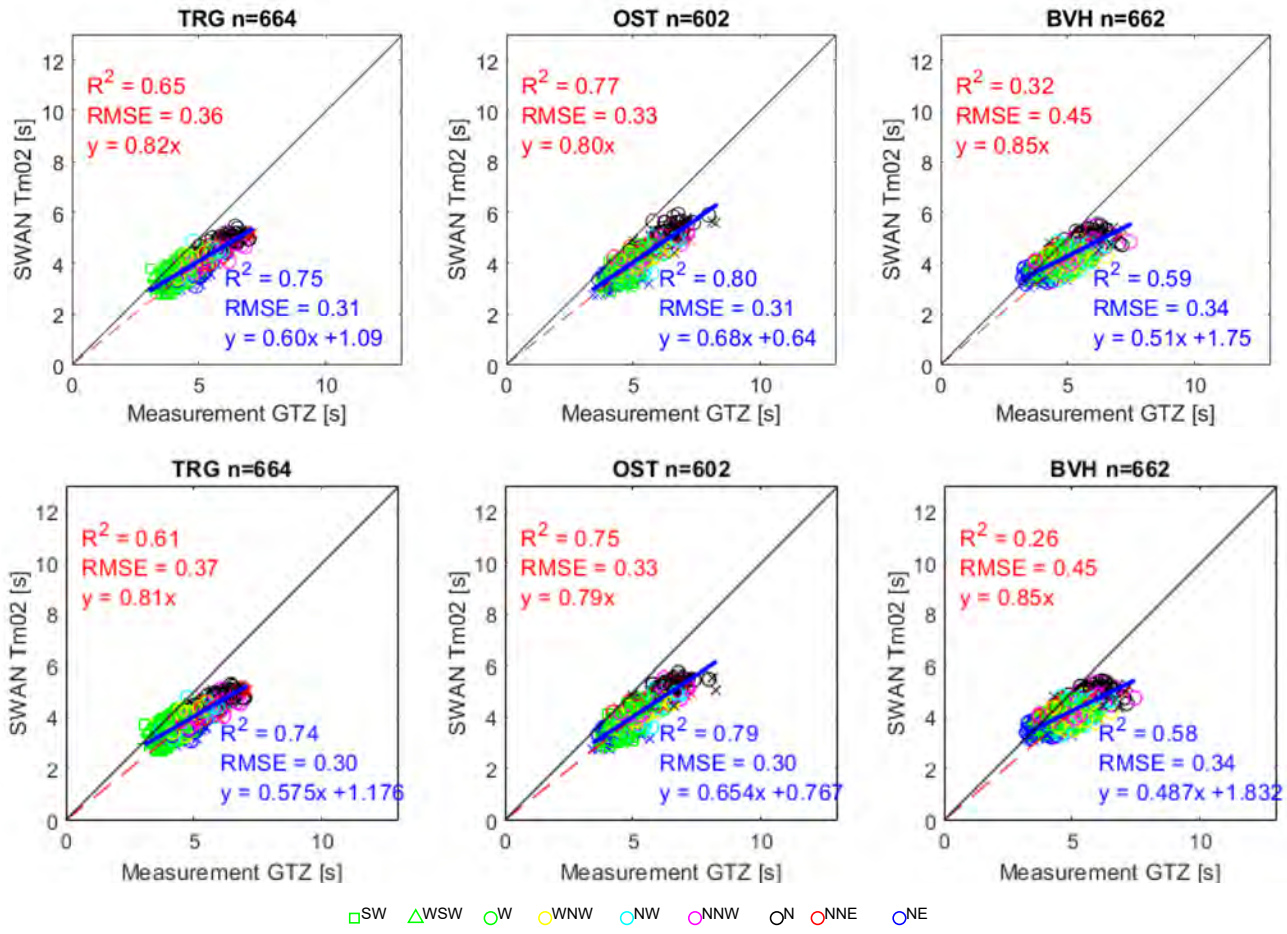

Figure 6.27 – Sensitivity of TRIADS (upper: without TRIADS, lower: TRIADS) – mean wave period

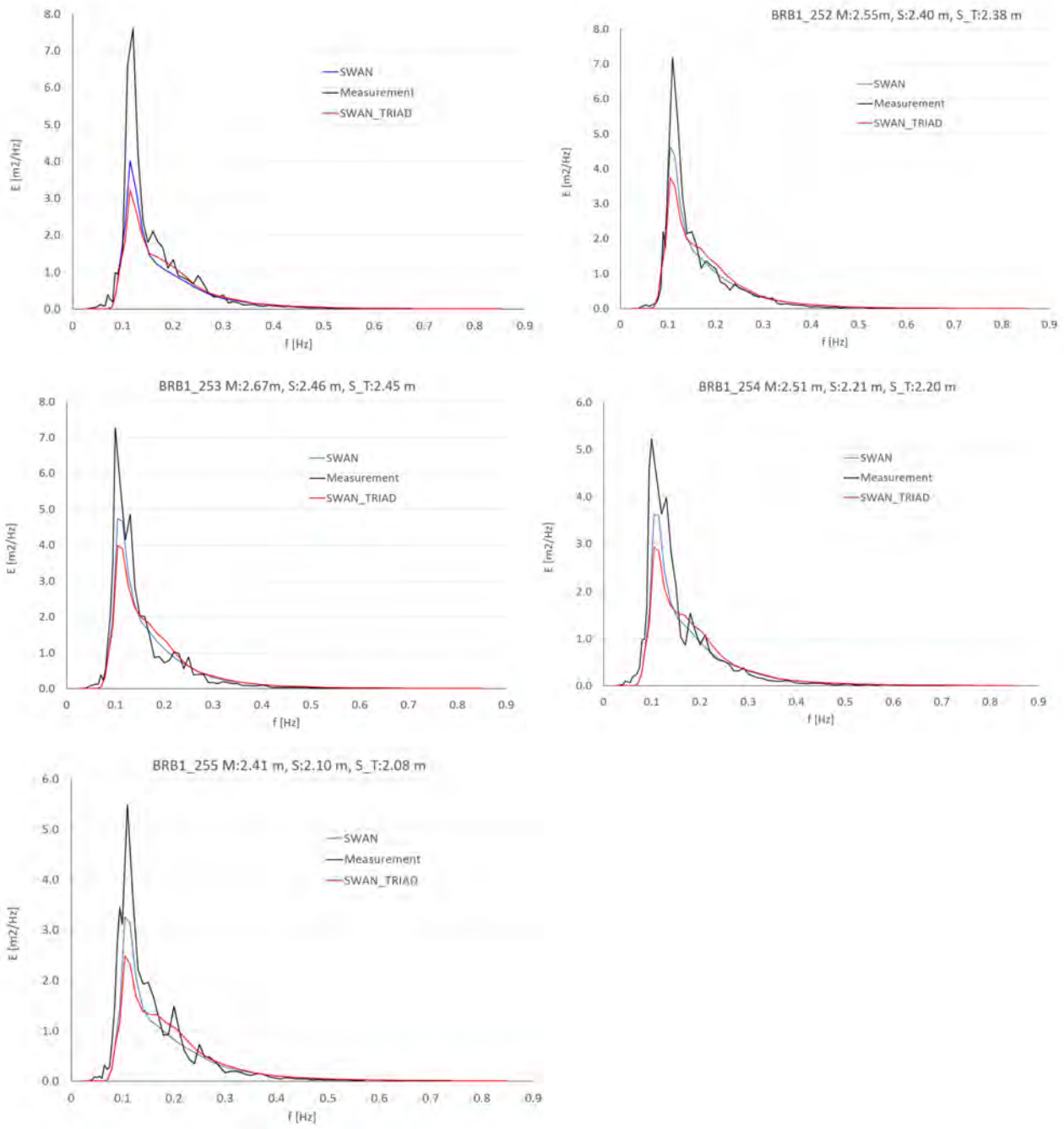

Figure 6.28 – Sensitivity of TRIADS – spectrum shape

6.2.9 Sensitivity of bottom friction

Comparison between the value for bottom friction being 0.038 or 0.067 is shown in Table 6.14 and Figure 6.28.

As can be seen in the table, the slope 'a' values are smaller for the higher bottom friction parameter, logically leading to a smaller wave height, which here leads to an underestimation of the significant wave height. Seeing that the wave height is underestimated at higher waves and thus lower bottom friction will be suitable for SA21, in which even higher waves needs to be estimated.

The default value of 0.038 for version 41 is thus to be used.

Table 6.14 – Sensitivity of bottom friction – significant wave height Hm0

Location	Case	Y=ax			Y=ax+b					
		Slope 'a'	R^2	RMSE	Slope 'a'	Intcpt 'b'	R^2	RMSE	Est_x=5	Ratio
TRG	Basic case	**0.99**	0.57	0.33	0.66	0.72	0.79	0.23	4.02	-
	Bf 0.067	**0.94**	0.59	0.32	0.64	0.65	0.78	0.23	3.85	**0.96**
OST	Basic case	**1.02**	0.59	0.39	0.69	0.77	0.80	0.28	4.22	-
	Bf 0.067	**0.95**	0.59	0.37	0.65	0.70	0.78	0.27	3.95	**0.94**
BVH	Basic case	**1.04**	0.48	0.38	0.68	0.84	0.70	0.29	4.24	-
	Bf 0.067	**0.99**	0.51	0.36	0.66	0.77	0.70	0.28	4.07	**0.96**

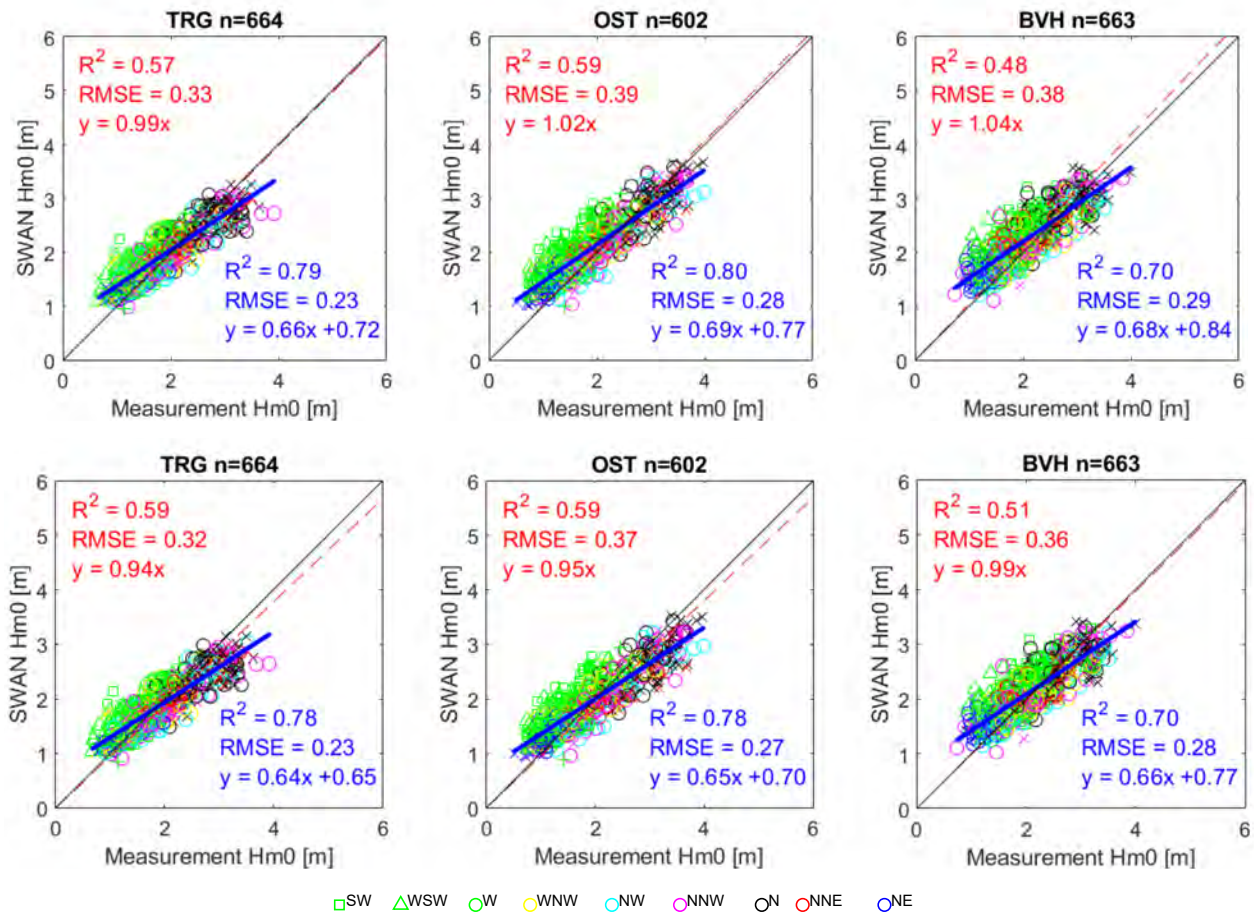

Figure 6.29 – Sensitivity of bottom friction (upper: bottom friction 0.038, lower: 0.067) – significant wave height Hm0

6.2.10 Sensitivity of number of frequency bins

In The SWAN team (2019) it is stated that the quality of the DIA approximation for the quadruplet wave-wave interactions depends on the width of the directional distribution of the wave spectrum and the frequency resolution. The DIA approximation of the quadruplet interactions (activated by GEN3 mode) is based on a frequency resolution of df/f = 0.1 and hence, γ = 1.1. Directional distribution is set 10 degree following the past studies (e.g. De Roo *et al.*, 2016).

Comparison of the significant wave height, peak period, smoothed peak period and mean wave period Tm02 when using 38, 44 and 60 frequency bins are shown in Table 6.15, Table 6.16, Table 6.17 and Table 6.18, and Figure 6.30, Figure 6.31, Figure 6.32 and Figure 6.33. Note that the fmax is set 1.506 Hz for the case frequency bin 44 in order to make df/f=0.1, which is calibrated value for DIA. The case frequency bin 38 is also using df/f=0.1 while the case frequency bin 60 is not following df/f=0.1.

The Tp estimation plot (Figure 6.31) and spectrum shape (Figure 6.29) look more natural (continuous instead of discrete periods) when frequency bin 60 is applied due to the higher frequency resolution however the tables and figures indicate that it does not influence on the result significantly (maximum 1% for the slope 'a' and the estimated ratio).

The case bin 44 in which the behaviour of DIA in GEN3 is guaranteed and fmax is higher (i.e. fmax=1.5006) also shows minor differences (2% difference) for Tm02 compared to the case bin 38. It means that the influence of the higher fmax is also small. Therefore it is concluded that 38 bins with the frequency range of 0.025-0.85 Hz is to be used for SA21. Note that the difference will be even smaller for a case with a higher peak wave period, see extra calculation results in Appendix C (the second analysis).

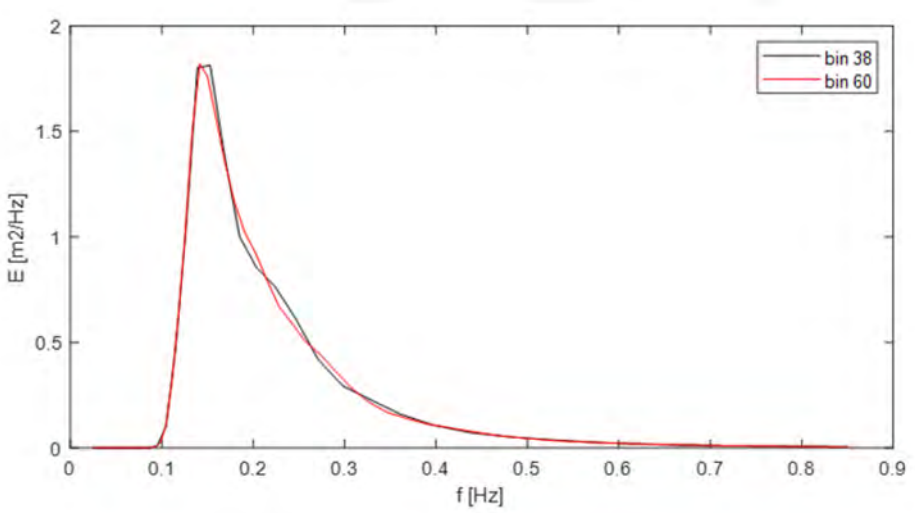

Figure 6.30 – An example of frequency spectral energy density (38 and 60 bins)

Table 6.15 – Sensitivity of number of frequency bins – significant wave height Hm0

Location	Case	Y=ax			Y=ax+b					
		Slope 'a'	R^2	RMSE	Slope 'a'	Intcpt 'b'	R^2	RMSE	Est_x=5	Ratio
TRG	Basic case	**0.99**	0.57	0.34	0.66	0.72	0.79	0.23	4.03	-
	44 bin	**0.99**	0.57	0.33	0.66	0.72	0.79	0.23	4.03	**1.00**
	60 bin	**0.99**	0.57	0.33	0.66	0.72	0.79	0.23	4.03	**1.00**
OST	Basic case	**1.02**	0.59	0.39	0.69	0.77	0.80	0.28	4.21	-
	44 bin	**1.02**	0.59	0.39	0.69	0.77	0.80	0.28	4.22	**1.00**
	60 bin	**1.01**	0.59	0.39	0.69	0.77	0.80	0.28	4.21	**1.00**
BVH	Basic case	**1.04**	0.48	0.38	0.68	0.84	0.70	0.29	4.25	-
	44 bin	**1.04**	0.48	0.38	0.68	0.84	0.70	0.29	4.25	**1.00**
	60 bin	**1.04**	0.48	0.38	0.68	0.84	0.70	0.29	4.24	**1.00**

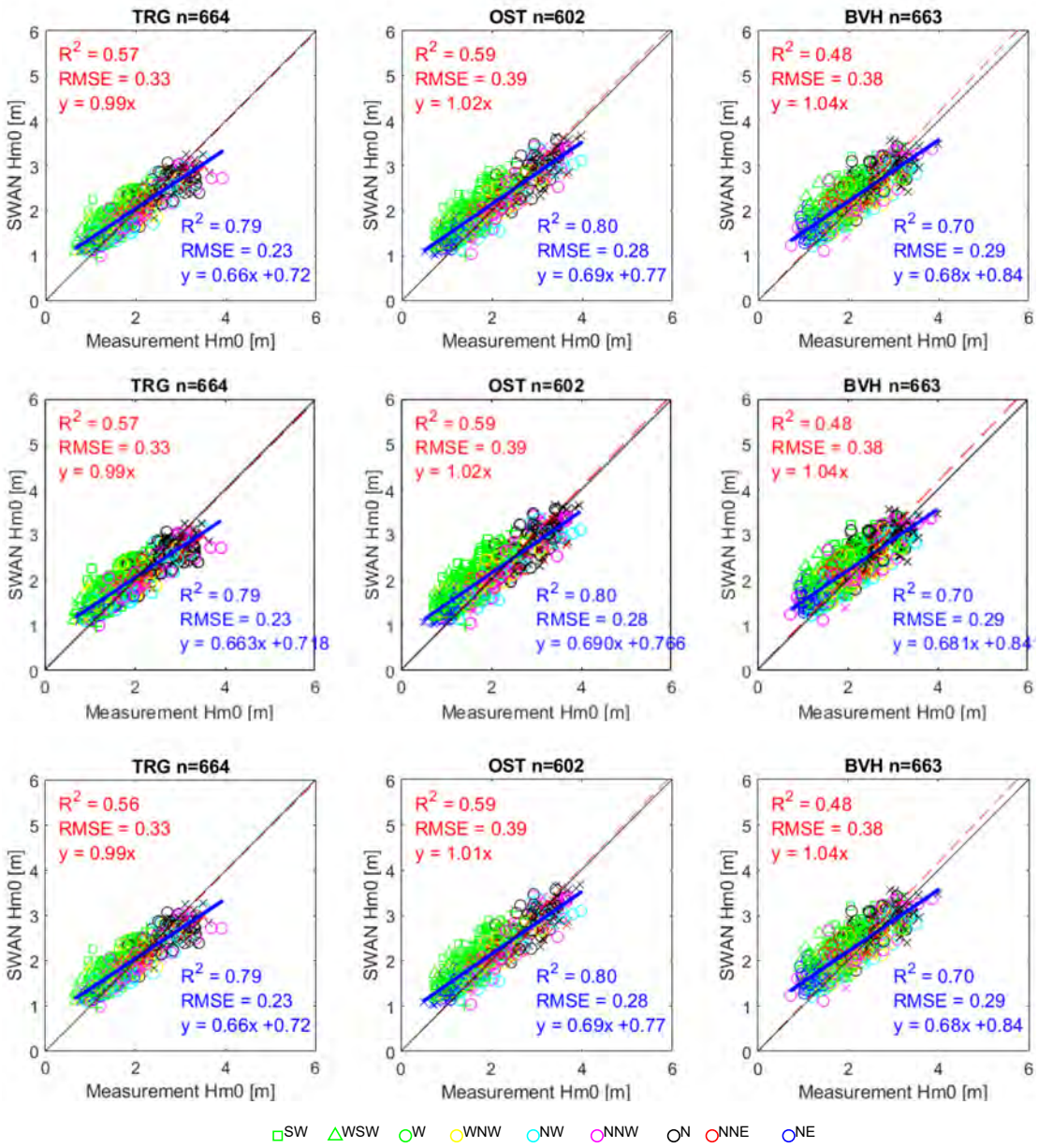

Figure 6.31 – Sensitivity of number of frequency bins (upper: 38, middle 44, lower: 60 bins) – significant wave height Hm0

Table 6.16 – Sensitivity of number of frequency bins – peak wave period Tp

Location	Case	Y=ax			Y=ax+b					
		Slope 'a'	R^2	RMSE	Slope 'a'	Intcpt 'b'	R^2	RMSE	Est_x=5	Ratio
TRG	Basic case	**1.04**	0.53	0.96	0.75	2.07	0.62	0.86	5.81	-
	44 bin	**1.04**	0.53	0.96	0.75	2.06	0.62	0.86	5.81	**1.00**
	60 bin	**1.03**	0.47	0.96	0.70	2.35	0.61	0.83	5.87	**1.01**
OST	Basic case	**1.00**	0.50	0.85	0.70	2.27	0.61	0.75	5.77	-
	44 bin	**1.00**	0.49	0.85	0.70	2.27	0.60	0.75	5.77	**1.00**
	60 bin	**0.99**	0.45	0.84	0.67	2.50	0.60	0.72	5.82	**1.01**
BVH	Basic case	**1.02**	0.14	1.13	0.56	3.36	0.48	0.88	6.16	-
	44 bin	**1.02**	0.13	1.13	0.56	3.37	0.48	0.88	6.17	**1.00**
	60 bin	**1.02**	0.18	1.11	0.57	3.26	0.50	0.87	6.13	**0.99**

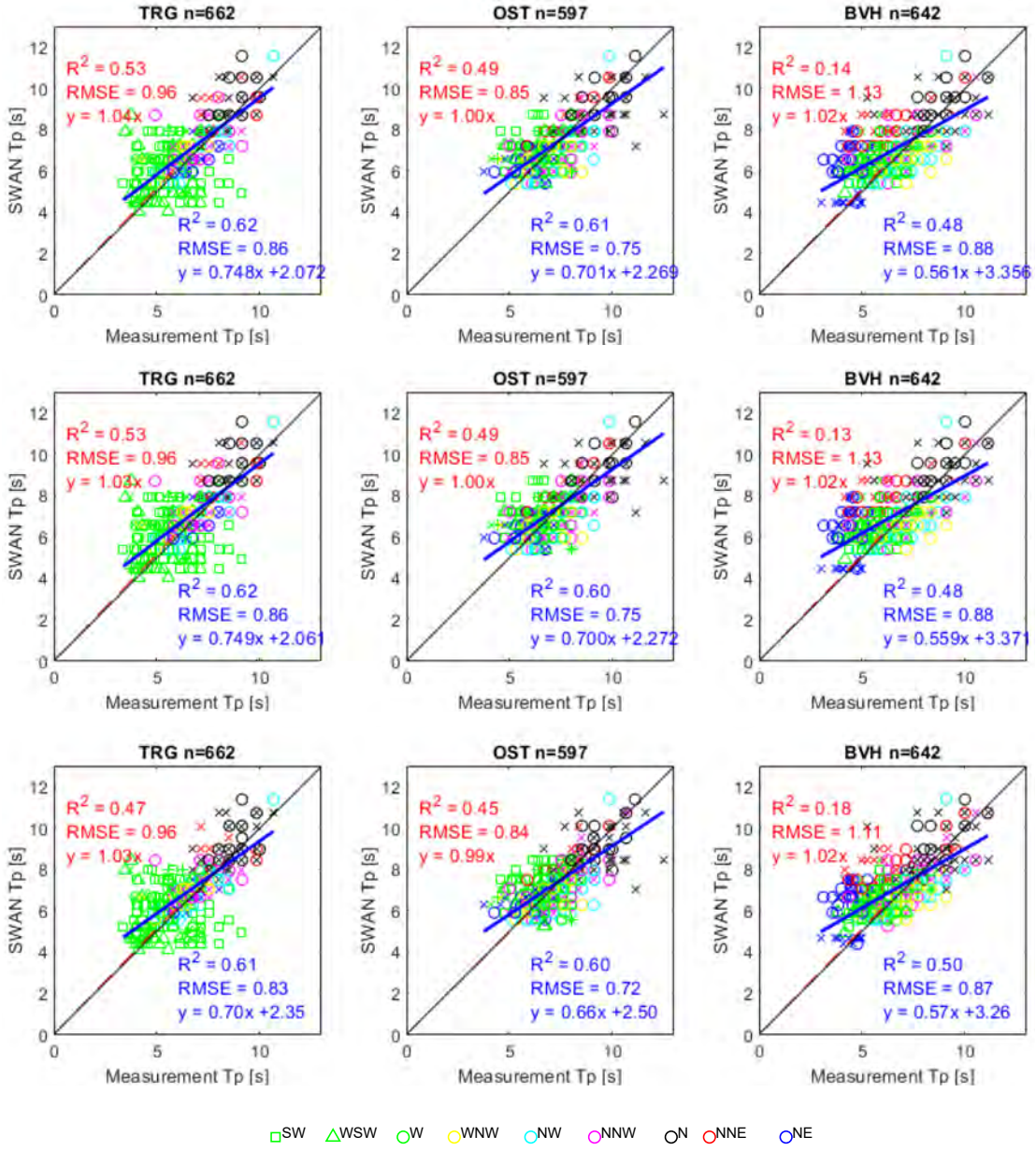

Figure 6.32 – Sensitivity of number of frequency bin (upper: 38, middle: 44, lower: 60 bins) – peak wave period Tp

Table 6.17 – Sensitivity of number of frequency bins – smoothed peak wave period Tps

Location	Case	Y=ax			Y=ax+b					
		Slope 'a'	R^2	RMSE	Slope 'a'	Intcpt 'b'	R^2	RMSE	Est_x=5	Ratio
TRG	Basic case	**1.02**	0.50	0.93	0.71	2.24	0.63	0.81	5.80	-
	44 bin	**1.02**	0.50	0.93	0.71	2.22	0.63	0.81	5.79	**1.00**
	60 bin	**NaN**	NaN	NaN	NaN	NaN	NaN	NaN	-	-
OST	Basic case	**0.98**	0.49	0.82	0.67	2.37	0.62	0.70	5.74	-
	44 bin	**0.98**	0.48	0.82	0.67	2.39	0.62	0.70	5.75	**1.00**
	60 bin	**NaN**	NaN	NaN	NaN	NaN	NaN	NaN	-	-
BVH	Basic case	**1.02**	0.17	1.10	0.57	3.27	0.49	0.86	6.09	-
	44 bin	**1.02**	0.17	1.10	0.57	3.27	0.49	0.86	6.09	**1.00**
	60 bin	**NaN**	NaN	NaN	NaN	NaN	NaN	NaN	-	-

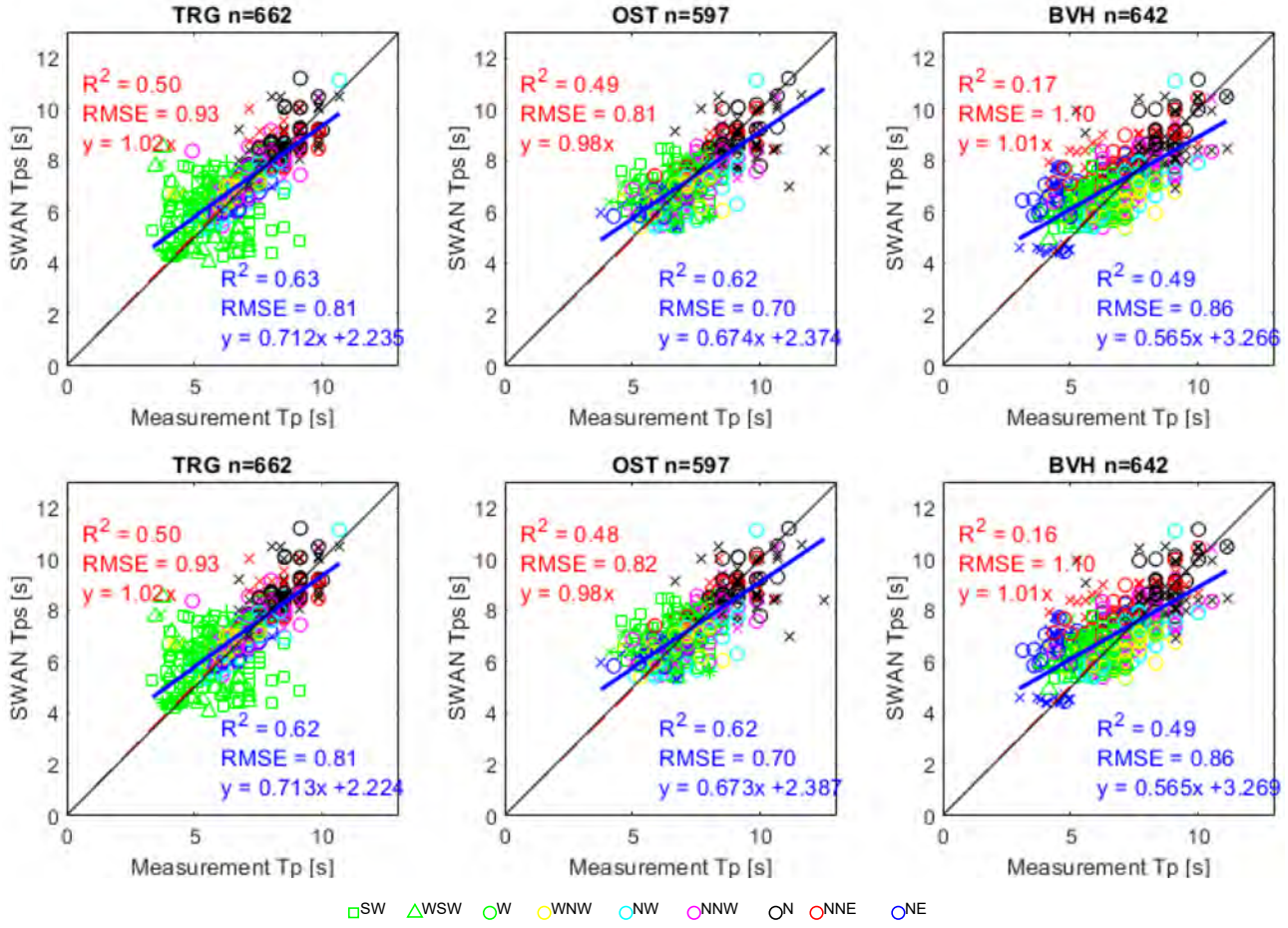

Figure 6.33 – Sensitivity of number of frequency bin (upper: 38, middle: 44, lower: 60 bins) – smoothed peak wave period Tps

Table 6.18 – Sensitivity of number of frequency bins – mean wave period Tm02

Location	Case	Y=ax			Y=ax+b					
		Slope 'a'	R^2	RMSE	Slope 'a'	Intcpt 'b'	R^2	RMSE	Est_x=11	Ratio
TRG	Basic case	**0.82**	0.65	0.36	0.60	1.09	0.75	0.31	7.69	-
	44 bin	**0.83**	0.65	0.37	0.61	1.11	0.74	0.32	7.83	**1.02**
	60 bin	**0.82**	0.65	0.36	0.60	1.08	0.75	0.31	7.71	**0.98**
OST	Basic case	**0.80**	0.77	0.33	0.68	0.64	0.80	0.31	8.14	-
	44 bin	**0.81**	0.77	0.33	0.69	0.66	0.79	0.32	8.27	**1.02**
	60 bin	**0.80**	0.77	0.33	0.68	0.64	0.80	0.31	8.15	**1.00**
BVH	Basic case	**0.85**	0.32	0.45	0.51	1.75	0.59	0.34	7.34	-
	44 bin	**0.87**	0.33	0.45	0.52	1.75	0.60	0.35	7.49	**1.02**
	60 bin	**0.85**	0.32	0.45	0.51	1.75	0.59	0.35	7.34	**1.00**

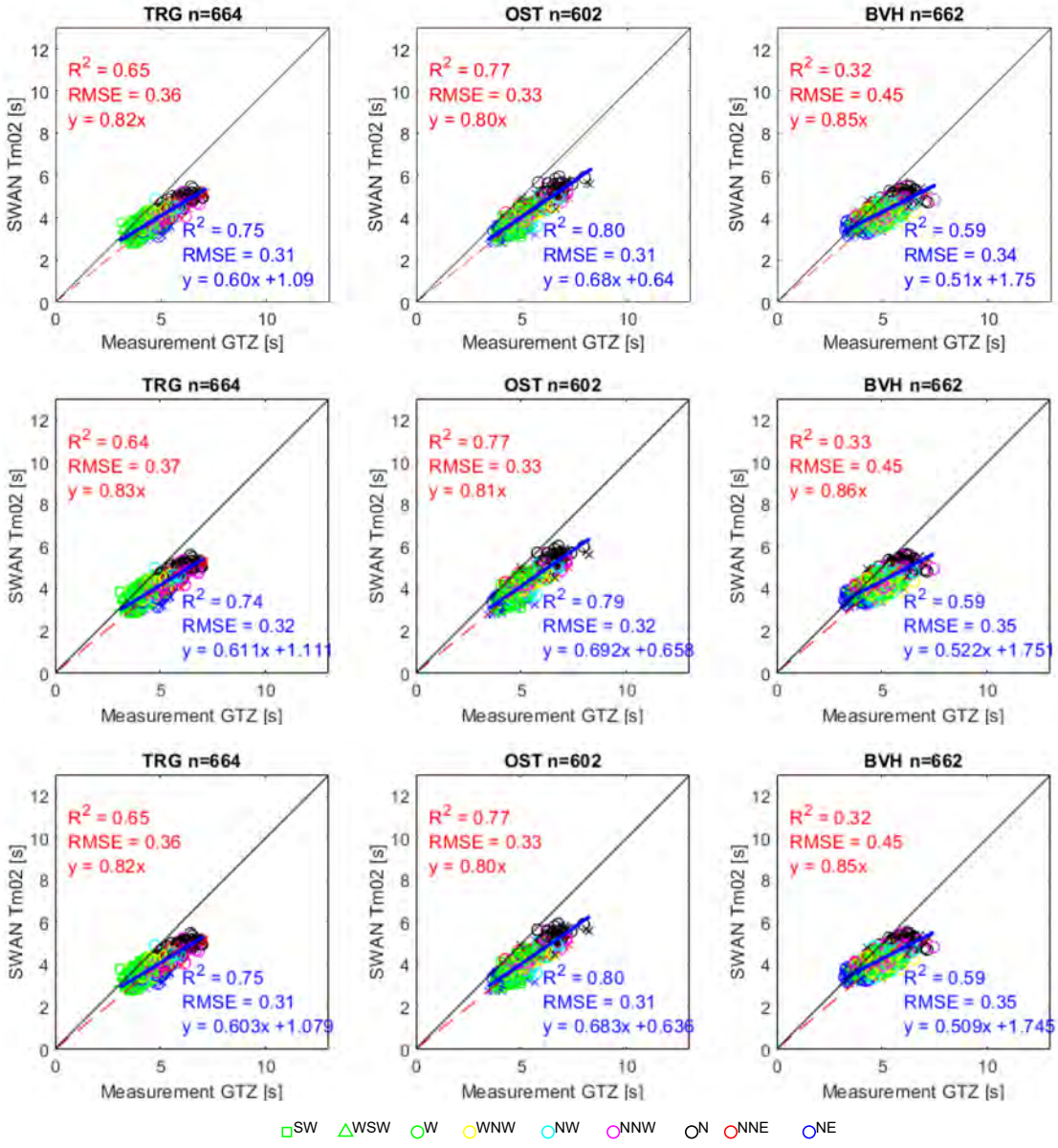

Figure 6.34 – Sensitivity of number of frequency bin (upper: 38, middle: 44, lower: 60 bins) – mean wave period Tm02

6.2.11 Sensitivity of wave breaking

Comparison between constant wave breaking parameter 0.73 and 1.0 (i.e. breaker index parameter), Westuysen and Ruessink is shown in Table 6.19 and Figure 6.34. These indicate that CON 0.73 (i.e. basic case) gives low slope values. On the other hand CON 1.0 gives the highest and Westhuysen and Ruessink are in between: it seems that the performance of Westhuysen and Ruessink gives similar estimation. In terms of R^2 value from y=ax+b regression line, all the results show similar quality. However, in Figure 6.34, an important change can be seen in the higher waves' output (Hm0 >=3.5 m, when more breaking is expected).

Table 6.20 and Figure 6.35 show the performance of estimation on Tm02. The behaviour is the same as significant wave height, CON 0.73 (i.e. basic case) gives low slope values and CON 1.0 gives the highest while Westhuysen and Ruessink are in between.

A further detailed investigation is to be found in the next section 6.4.

Table 6.19 – Sensitivity of breaking – significant wave height Hm0

Location	Case	Y=ax			Y=ax+b					
		Slope 'a'	R^2	RMSE	Slope 'a'	Intcpt 'b'	R^2	RMSE	Est_x=5	Ratio
TRG	Basic case	**0.99**	0.57	0.34	0.66	0.72	0.79	0.23	4.03	-
	CON 1.0	**1.07**	0.66	0.35	0.77	0.64	0.79	0.27	4.50	**1.11**
	Westhuysen	**1.02**	0.61	0.33	0.70	0.69	0.80	0.24	4.21	**1.04**
	Ruessink	**1.02**	0.61	0.34	0.71	0.68	0.78	0.25	4.21	**1.04**
OST	Basic case	**1.02**	0.59	0.39	0.69	0.77	0.80	0.28	4.21	-
	CON 1.0	**1.04**	0.64	0.40	0.74	0.71	0.79	0.30	4.39	**1.04**
	Westhuysen	**1.03**	0.62	0.39	0.72	0.74	0.80	0.29	4.31	**1.02**
	Ruessink	**1.03**	0.63	0.39	0.72	0.73	0.80	0.29	4.33	**1.03**
BVH	Basic case	**1.04**	0.48	0.38	0.68	0.84	0.70	0.29	4.25	-
	CON 1.0	**1.08**	0.57	0.39	0.76	0.74	0.71	0.32	4.53	**1.07**
	Westhuysen	**1.06**	0.53	0.38	0.71	0.80	0.71	0.30	4.37	**1.03**
	Ruessink	**1.06**	0.54	0.38	0.72	0.79	0.71	0.30	4.40	**1.04**

Table 6.20 – Sensitivity of breaking – mean wave period Tm02

Location	Case	Y=ax			Y=ax+b					
		Slope 'a'	R^2	RMSE	Slope 'a'	Intcpt 'b'	R^2	RMSE	Est_x=5	Ratio
TRG	Basic case	**1.08**	0.65	0.48	0.80	1.42	0.75	0.41	11.04	-
	CON 1.0	**1.11**	0.63	0.52	0.82	1.45	0.72	0.45	11.34	**1.03**
	Westhuysen	**1.09**	0.65	0.49	0.81	1.43	0.74	0.42	11.15	**1.01**
	Ruessink	**1.09**	0.66	0.48	0.82	1.41	0.75	0.42	11.19	**1.01**
OST	Basic case	**1.05**	0.71	0.47	0.83	1.17	0.76	0.42	11.18	-
	CON 1.0	**1.06**	0.70	0.48	0.84	1.16	0.75	0.44	11.26	**1.01**
	Westhuysen	**1.05**	0.70	0.47	0.84	1.16	0.75	0.43	11.22	**1.00**
	Ruessink	**1.05**	0.70	0.47	0.84	1.16	0.75	0.43	11.25	**1.01**
BVH	Basic case	**1.09**	0.37	0.59	0.69	2.09	0.58	0.48	10.31	-
	CON 1.0	**1.11**	0.42	0.59	0.73	1.94	0.59	0.50	10.66	**1.03**
	Westhuysen	**1.10**	0.39	0.59	0.70	2.03	0.58	0.49	10.45	**1.01**
	Ruessink	**1.10**	0.39	0.59	0.70	2.03	0.58	0.49	10.47	**1.02**

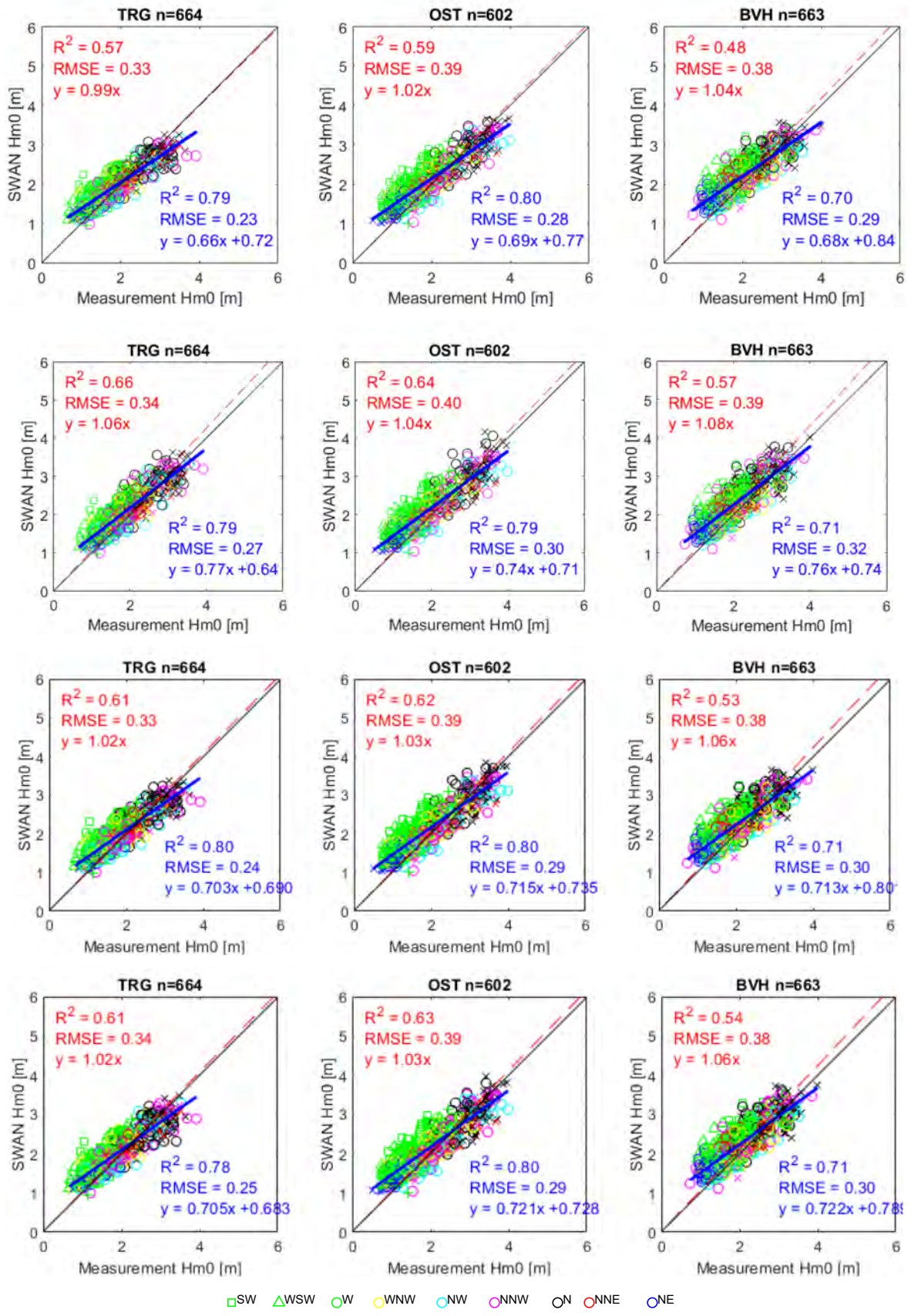

Figure 6.35 – Sensitivity of breaking (from the top, breaker index 0.73, 1.00, Westhuysen, Ruessink) – significant wave height Hm0

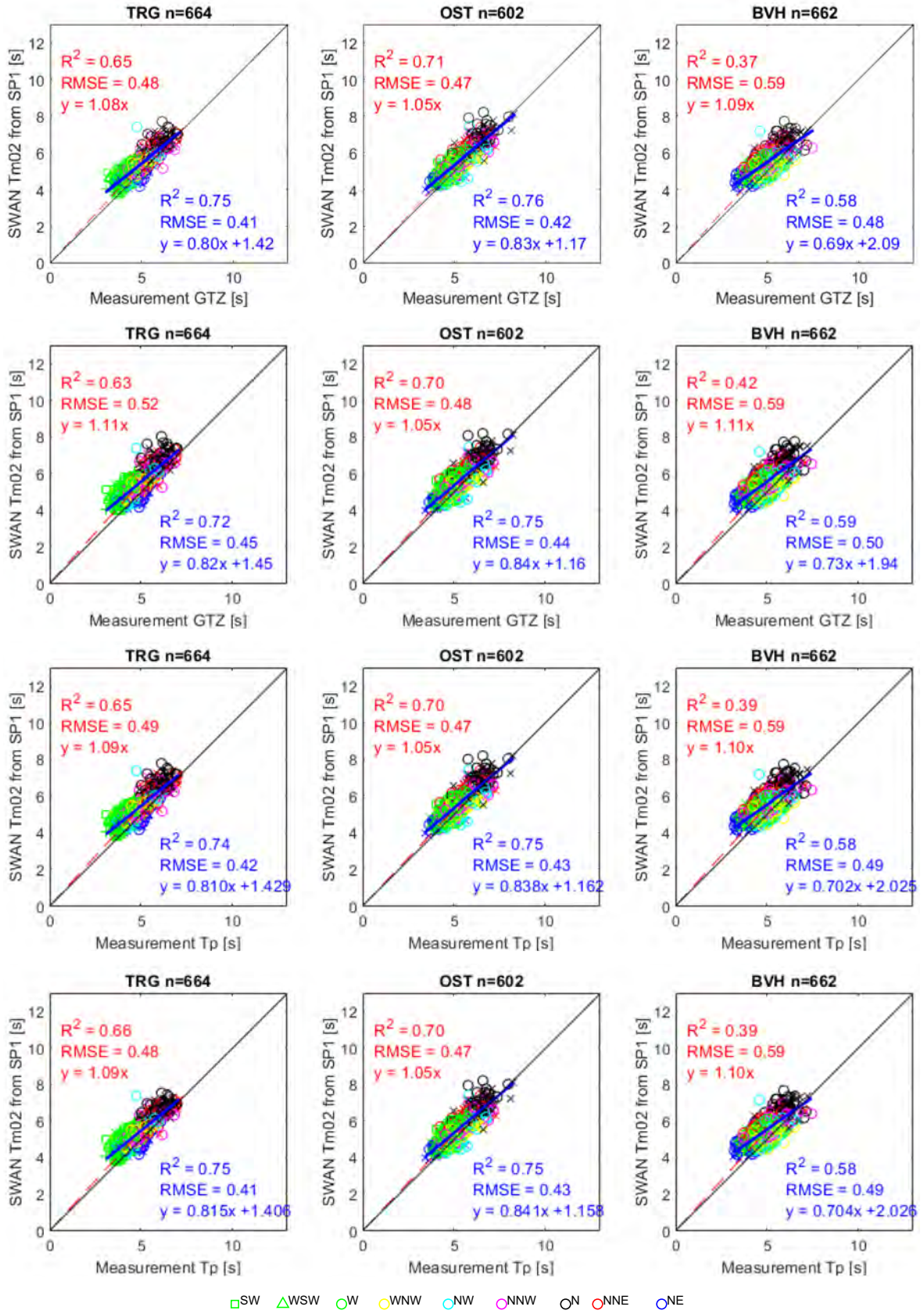

Figure 6.36 – Sensitivity of breaking (from the top, breaker index 0.73, 1.00, Westhuysen, Ruessink) – mean wave period Tm02

6.2.12 Sensitivity of time lag

The theoretical time lag is calculated taking into account the wave travelling distance, the group velocity of waves and the geographical location of each station (TRG, OST and BVH). The results' comparison against the no time lag results (=basic case) is shown in Table 6.21, while Figure 6.36 depicts the time lag results for the nearshore locations.

The scatter for TRG, especially higher waves' output (e.g. Hm0 >3 m) is reduced significantly and this is reflected in the value of R^2 (RMSE change is still minor). The scatter for OST and BVH is also decreased but rather limited compared to one for TRG. This might be explained by the fact that the depth at TRG (and its surroundings) is rather shallow (i.e. closer to wave breaking depth) and thus, results are more sensitive to the appropriate water level which is changed by the time (=time lag).

It is recommended to include the theoretical time lag for validation purposes, which is a function of distance, group velocity and wave direction.

Table 6.21 – Sensitivity of time lag – significant wave height Hm0

Location	Case	Y=ax			Y=ax+b					
		Slope 'a'	R^2	RMSE	Slope 'a'	Intcpt 'b'	R^2	RMSE	Est_x=5	Ratio
TRG	Basic case	**0.99**	0.57	0.33	0.66	0.72	0.79	0.23	4.02	-
	Time lag	**1.00**	0.67	0.30	0.70	0.66	0.85	0.20	4.16	**1.03**
OST	Basic case	**1.02**	0.59	0.39	0.69	0.77	0.80	0.28	4.22	-
	Time lag	**1.02**	0.61	0.38	0.70	0.76	0.81	0.27	4.26	**1.01**
BVH	Basic case	**1.04**	0.48	0.38	0.68	0.84	0.7	0.29	4.24	-
	Time lag	**1.04**	0.52	0.37	0.69	0.81	0.73	0.28	4.26	**1.00**

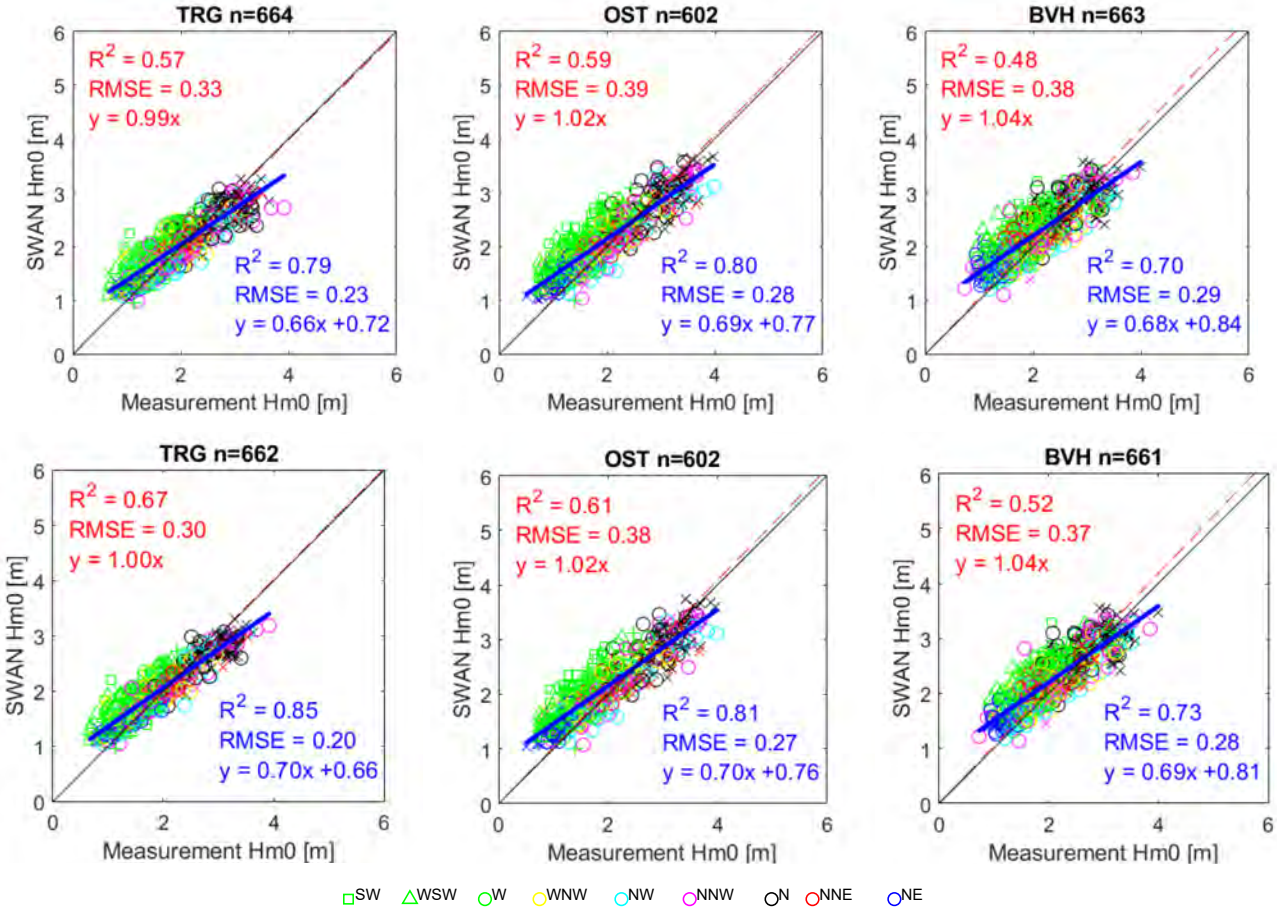

Figure 6.37 – Sensitivity of time lag (upper: no time lag, lower: with time lag each nearshore location) – significant wave height Hm0

6.2.13 Sensitivity of water level input location (incl. time lag)

The water level input location is further investigated for TRG and BVH. The OST case is not considered since the water level measurement is located close (= WL-OST). WL-NPT is used for TRG, and WL-ZLD is used for BVH since these water level measurement locations are then closest to the respective output locations (note that it is not exactly the same point since there is no water level measurement at TRG and BVH respectively while WL-OST is very close to OST). See the results in Table 6.22 and Figure 6.37.

The scatter is further reduced by selecting the closer water level input location. The overall improvement is minor but it is logic that selection of a closer water level location leads to a better estimation.

Therefore, it is recommended to use the closest water level measurement location for validation.

Table 6.22 - Sensitivity of water level input point – significant wave height Hm0

Location	Case	Y=ax			Y=ax+b					
		Slope 'a'	R^2	RMSE	Slope 'a'	Intcpt 'b'	R^2	RMSE	Est_x=5	Ratio
TRG	Basic case	**0.99**	0.57	0.33	0.66	0.72	0.79	0.23	4.02	-
	Water level corr.	**1.01**	0.69	0.3	0.72	0.64	0.86	0.2	4.24	**1.05**
OST	Basic case	**1.02**	0.59	0.39	0.69	0.77	0.8	0.28	4.22	-
	Water level corr.	**1.02**	0.61	0.38	0.7	0.76	0.81	0.27	4.26	**1.01**
BVH	Basic case	**1.04**	0.48	0.38	0.68	0.84	0.7	0.29	4.24	-
	Water level corr.	**1.04**	0.54	0.36	0.69	0.81	0.74	0.27	4.26	**1.00**

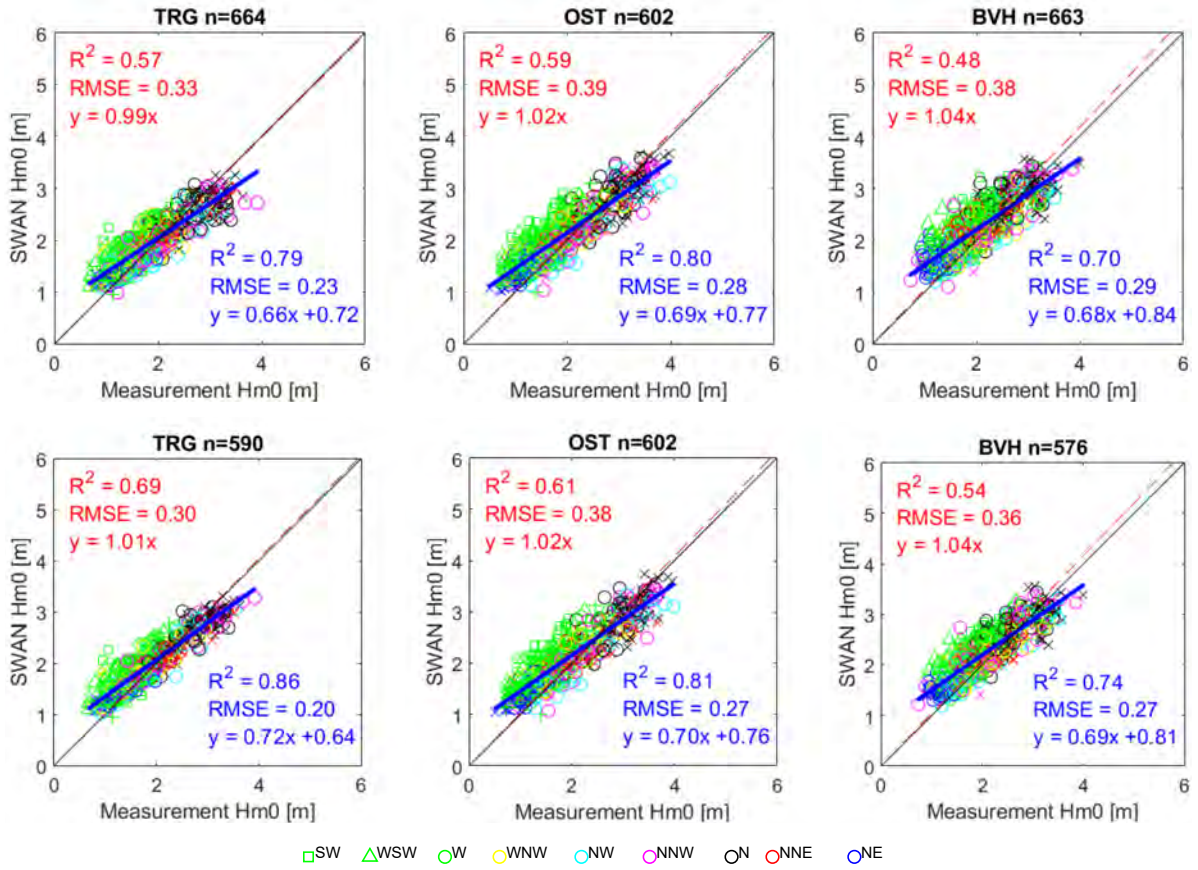

Figure 6.38 – Sensitivity of water level input point (upper: water level OST, lower: NPT, OST, ZLD) – significant wave height Hm0

6.2.14 Sensitivity of numerics (Iteration stop at 99.5 accuracy vs 200 iteration)

The number of iteration can influence to calculated parameters in SWAN. According to De Roo *et al.* (2016), this was a common problem in the earlier version of SWAN but it was improved in version 40.41: an alternative criteria was introduced to end a simulation. The criteria is based on the interation curve of the significant wave height and it is more effective. Nevertheless we investigate it in this section by forcing iteration 200 times (by setting the accuracy 101%, so that the SWAN never 'satisfy' the criteria and continue till thespecified iteration number), see Table 6.23 and Figure 6.38 (significant wave height), Table 6.24 and Figure 6.39 (mean wave period).

As can be in the table, it is clear that the convergence is good enough in the basic setting for the validation cases tested here. Therefore the standard numeric setting (99.5% accuracy with maximum iteration 50 times) is opted for, being computationally faster for the validation cases. Based on this assumption Deltares conducted calculations with extreme wave boundary conditions (e.g. Hm0 offshore is much bigger than 5 m which is observed in the validation cases) however it was found that the saturation is not good enough for those extreme cases even with slightly increased accuracy, 99.7%.

Therefore it is finally recommended to use **101% accuracy with 50 iteration**.Note that the convergence is different for different calculation settings. It was found that the convergence is much slower when triads is activated, see details in Section 6.6.2.

Table 6.23 – Sensitivity of iteration – significant wave height Hm0

Location	Case	Y=ax			Y=ax+b					
		Slope 'a'	R^2	RMSE	Slope 'a'	Intcpt 'b'	R^2	RMSE	Est_x=5	Ratio
TRG	Basic case	**0.99**	0.57	0.34	0.66	0.72	0.79	0.23	4.03	-
	200 iterations	**1.00**	0.56	0.34	0.66	0.72	0.79	0.24	4.04	**1.00**
OST	Basic case	**1.02**	0.59	0.39	0.69	0.77	0.80	0.28	4.21	-
	200 iterations	**1.02**	0.59	0.39	0.69	0.77	0.80	0.28	4.23	**1.00**
BVH	Basic case	**1.04**	0.48	0.38	0.68	0.84	0.70	0.29	4.25	-
	200 iterations	**1.05**	0.48	0.38	0.68	0.85	0.70	0.29	4.26	**1.00**

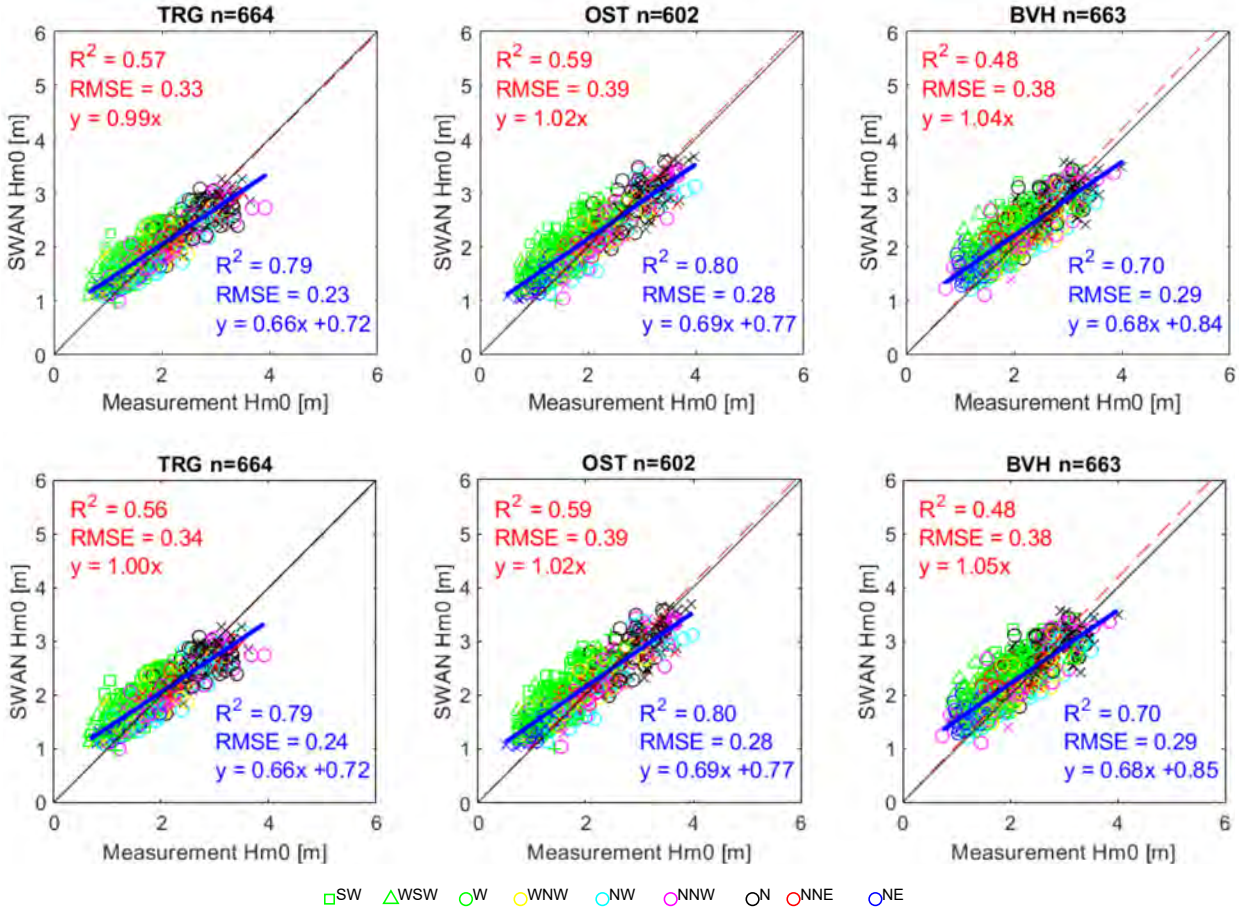

Figure 6.39 – Sensitivity of iteration (upper: default iteration setting – run till 99.5% accuracy, lower: 200 iterations) – significant wave height Hm0

Table 6.24 – Sensitivity of iteration – significant wave height Hm0

Location	Case	Y=ax			Y=ax+b					
		Slope 'a'	R^2	RMSE	Slope 'a'	Intcpt 'b'	R^2	RMSE	Est_x=5	Ratio
TRG	Basic case	**0.82**	0.65	0.36	0.60	1.09	0.75	0.31	7.69	-
	200 iterations	**0.81**	0.64	0.36	0.59	1.13	0.75	0.30	7.63	**0.99**
OST	Basic case	**0.80**	0.77	0.33	0.68	0.64	0.80	0.31	8.14	-
	200 iterations	**0.80**	0.77	0.33	0.67	0.69	0.80	0.31	8.06	**0.99**
BVH	Basic case	**0.85**	0.32	0.45	0.51	1.75	0.59	0.34	7.34	-
	200 iterations	**0.85**	0.28	0.45	0.49	1.80	0.59	0.34	7.23	**0.99**

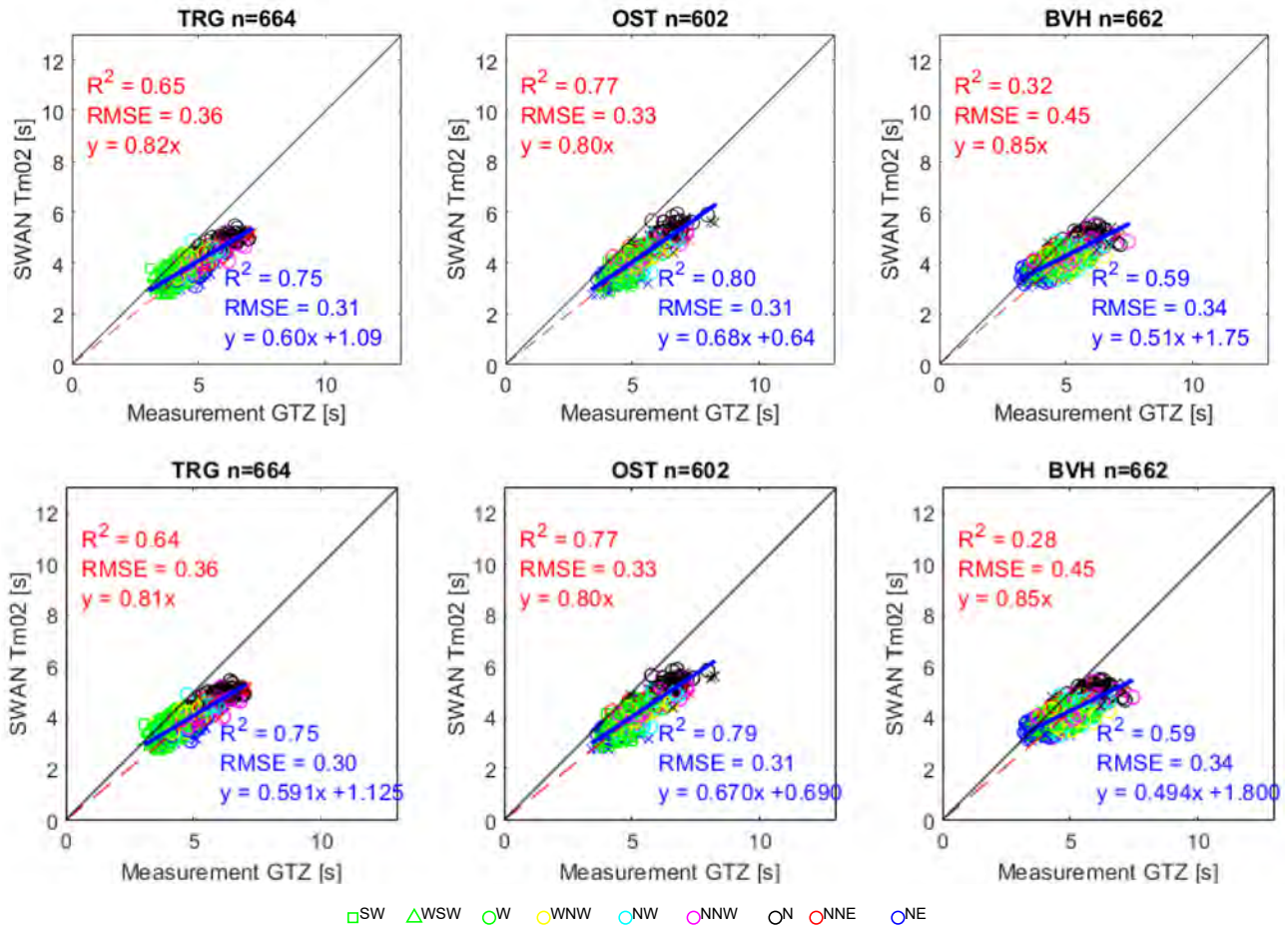

Figure 6.40 – Sensitivity of iteration (upper: default iteration setting – run till 99.5% accuracy, lower: 200 iterations) – mean wave period Tm02

6.2.15 Summary of sensitivity analysis for input parameters

From the sensitivity analyses for input parameters, it can be concluded that

- Version difference is minor: the present stable version 41.20.AB will be used for the further analysis
- BCP2020 is recommended for SA21 while BCP2015 will be used for the further analysis
- 250x125 m grid based on BCP2020 is recommended for SA21 while 250x250 m based on BCP2015 will be used for the further analysis.
- Offshore wave and wind input might be obtained from AKZ and MP0 as well
- Default setting will be used for the wind drag
- The basic case (GEN3 Westhuysen) leads similar significant wave height as GEN3 Komen, however, it leads significantly lower mean wave period Tm02 (~29%) and Komen show a good agreement with the measurement. Therefore Komen will be used for the further analysis.
- Triads leads similar significant wave height but 2% smaller mean wave period compared to the basic case: Triads will not be used for the further analysis
- 38 bin with the frequency range of 0.025-0.85 Hz will be used for the further analysis
- Bottom friction gives the best output using the recommended default value of 0.038 in combination with the listed SWAN settings here.
- An increase in the number of frequency bins does not lead to a significant improvement but further investigation will be conducted.
- Breaking parameter influences the estimation quality for the higher waves. We will continue further investigation in the next section.
- Taking into account the theoretical time lag, the estimation quality is improved.
- In addition, selection of the closest water level location to your output locations leads to a better estimation.

101% accuracy with 50 iteration is recommended in order to obtain stable results

6.3 Model uncertainties

6.3.1 Measurement location

One of the uncertainties of the model is related to the measurement location Trapegeer (TRG). See Figure 6.40. According to Vlaamse Hydrografie, the anchor location of the wave buoy never changed. Yet, throughout the years several coordinates were found in reports. Note that (some of) these differences might be related to the conversion from one coordinate system to another. The distance between the 4 measurement locations is within 1 km, but TRG is located at the edge of a gully so the depth varies a lot: the maximum difference is about 7 m (depth -3.9 m TAW to -10.6 m TAW).

We picked up one simulation with maximum wave height. It shows that the difference of the output does not differ so much. This is due to the fact that the breaking has already happened in front of the gully over the shallow banks.

Even though the location is uncertain, it does not influence the result too much.

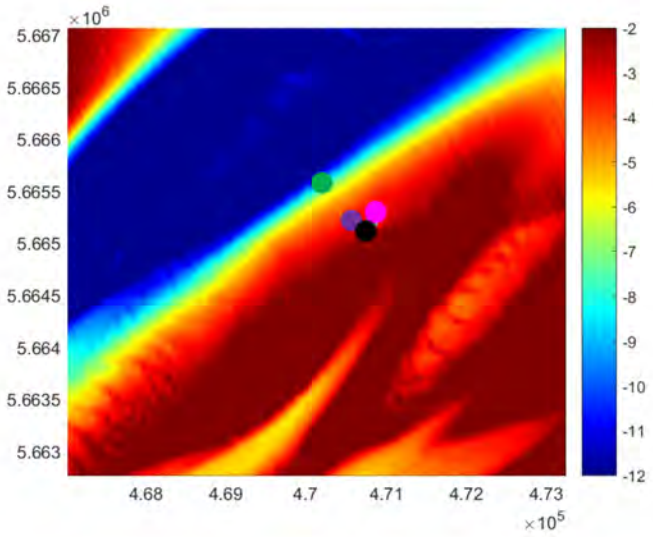

	x	y	distance
measurement	?	?	?
TRG - original location	470723.8	5665106.3	0.0
TRG - Johan 2019	470528.7	5665208.1	220.1
TRG - Koen 1	470174.4	5665571.2	719.7
TRG - Koen 2 (TRG08)	470827.8	5665315.7	233.8

	Hm0	depth	Hm0/d
measurement	3.92	8.72	0.45
TRG - original location	3.17	8.72	0.36
TRG - Johan 2019	3.20	9.51	0.34
TRG - Koen 1	3.21	15.44	0.21
TRG - Koen 2 (TRG08)	3.22	9.48	0.34

Figure 6.41 – Possible TRG locations

6.3.2 Refraction effect on gully

As written in Groeneweg *et al.* (2015), there might be influence of a gully (in his publication it is an access channel). Close to TRG, there is a gully, as indicated in Figure 6.41. Depending on the wave direction, the gully influences the wave transformation conducted by SWAN. According to Groeneweg *et al.* (2015), SWAN does not predict accurately the wave propagation over the gully, being a source of uncertainty. However, measurements near Broersbank show the same underestimation North of the Broersbank, where gullies are less pronounced.

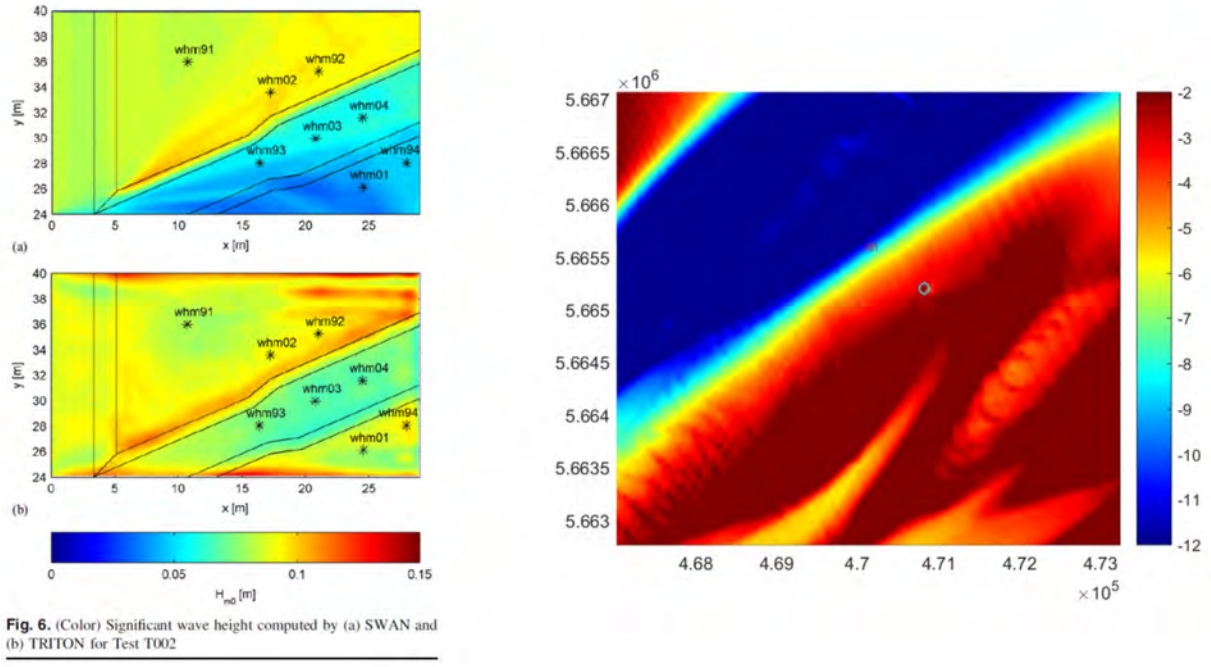

Fig. 6. (Color) Significant wave height computed by (a) SWAN and (b) TRITON for Test T002

Figure 6.42 – Possible refraction effects

6.4 Further investigation of wave breaking

6.4.1 Breaking criteria

It was found that the breaking formulas and associated parameters play an important role for the better estimation of higher waves, especially for TRG and OST where the depth is relatively shallow (-3.9 m TAW and -5.9 m TAW respectively). The higher waves might break before and around these measurement locations.

Taking a closer look to what is the cause of these differences and considering what is the optimum setting to obtain hydraulic boundary conditions at -5 TAW/1500m points given storm conditions (i.e. output locations close to the wave breaking point).

In the SA15, -5m TAW or somewhat shallower (at 1500 m from the coast) was the nearshore output location of the hydraulic boundary conditions. Generally, the significant wave height is around 5 m when the water level is around +7m TAW. Calculating the breaker index under such condition, it is around 0.75 (Hs 5 m * Hmax ratio 1.8 /12 m depth = 0.75). This is logic since a breaking index value of 0.73 was selected for SA15. On the other hand, the selected cases here show that the SWAN estimation using a breaker index of 1.0 represents the measurements better.

(The SWAN team, 2019b) described the following sentence regarding the breaker index. *The maximum wave height Hmax is determined in SWAN with Hmax = γ d, in which γ is the breaker parameter and d is the total water depth (including the wave-induced set-up if computed by SWAN). In the literature, this breaker parameter γ is often a constant or it is expressed as a function of bottom slope or incident wave steepness (see e.g., Galvin, 1972; Battjes and Janssen, 1978; Battjes and Stive, 1985; Arcilla and Lemos, 1990; Kaminsky and Kraus, 1993; Nelson, 1987, 1994). In the publication of Battjes and Janssen (1978) in which the dissipation model is described, a constant breaker parameter, based on Miche's criterion, of γ = 0.8 was used. Battjes and Stive (1985) re-analyzed wave data of a number of laboratory and field experiments and found values for the breaker parameter varying between 0.6 and 0.83 for different types of bathymetry (plane, bar-trough and bar) with an average of 0.73. From a compilation of a large number of experiments Kaminsky and Kraus (1993) have found breaker parameters in the range of 0.6 to 1.59 with an average of 0.79.*

Taking a closer look to what is the cause of these differences and considering what is the optimum setting to obtain hydraulic boundary conditions at -5 TAW/1500m points given storm conditions (i.e. output locations close to the wave breaking point).

In order to investigate it further, the breaking criteria are discussed here. The breaking criteria can be expressed as Hmax/d, where Hmax is the maximum individual wave height (derived from the significant wave height, multiplied by factor 1.8 – assuming typical time duration ~1000 waves) and d the local water depth. To start with, the cases of breaker index 0.73 and 1.0 and other formulas are used + time lag and water level point corrections.

Different breaking formulation and parameters are shown in Figure 6.42 and Figure 6.43.

When the breaker index 0.73 is applied, a flattening can be seen at the top of the data cloud. However, the flat part disappears when the breaker index 1.0 is applied due to the fact that the breaker index is a parameter which decides the limit of higher waves at a certain depth. It is not clear why the flat part in the simulation did not reach to 0.73 (it might be related to the assumption of the ratio of Hmax/Hm0: for now 1.8 is used for the simplification but this value can be different in the surf zone) but it is clear that the breaker index value plays an important role. Good thing is that breaker index 1.0 does not influence to the entire cloud, but pushes up only the high Hmax/d values. As long as we see only this estimation result, breaker index 1.0 seems not a bad choice although it is calculated based on a diagnostic measure.

Other than constant breaker index cases, different breaking calculations (BKD, Nelson, Westhuysen and Ruessink) are also tested. BDK indicates that the breaker index scales with both the bottom slope and the dimensionless depth. Nelson (1987) and Ruessink et al. (2003) use variable breaker parameters. The default values are applied for these cases. The flattening roof part appears clearly when BKD and Nelson is used, while Westhuysen (the executable file provided by Deltares; activated the code by the command BREA WESTH alpha=0.96 pown=2.50 bref=-1.3963 shfac=500.0) and Ruessink (which is available in 41.20.AB while this is not explicitly described in the swan user manual) do not have the flat part.

In order to understand the breaking calculation better, an extra calculation using both the SWAN and SWASH model has been conducted. See Figure 6.44. The model bathymetry represents a shallow sand bank close to the coast (bottom figure). Note that all the slopes in the figure are 1/35 (positive and negative) and that wave gauge notation is based on the depth (e.g. wave gauge -5a is located at -5 m TAW). The top figure shows wave transformation over the shallow sandbank in different models (i.e. SWASH2D, SWAN breaker index 0.73, 1.00, Westhuysen and Ruessink). The result of SWASH2D (note that the Hmax is calculated based on the multiplication of 1.8 to Hm0 for the simplicity instead of actual Hmax from the model) is quite similar to that of SWAN breaker index 0.73, Westhuysen and Ruessink, therefore these must be the most appropriate settings to represent the local wave transformation in such a configuration. The middle figure shows the breaker index from offshore to nearshore calculated by SWAN. The breaker index starts around 0.4 and reaches to around 1.0 at the beginning of the sandbank (-2 m TAW; 9 m depth), even in the case with breaker index 0.73. It starts to decrease over the flat sandbank for 200 m due to breaking. Towards the end of the sandbank, the value decreases even more. This calculation indicated that the Hmax/d value with breaker index 0.73 can also exceed 0.73. Note that Battjes & Stive (1985) obtained the breaker index by calibration and therefore it is possible to have a high breaker index locally. Indeed, their results also included some cases where the breaker index locally reaches close to 1 (much higher than their proposed γ).

6.4.2 Summary of wave breaking

Even though constant 0.73 settting gives a reasonable output in this simplified sand bank configuration as shown in Figure 6.44 (very similar value as a time domain wave model SWASH, where wave breaking is inheriently modelled by the nature of the shock capturing scheme), the sensitivity analysis of breaking (Figure 6.34) and the breaking criteria study (Figure 6.42) show that constant 0.73 gave less good performance compared to the constant 1.0 in terms of most energetic waves in the data cloud (while constant 1.0 gives partly slight overestimation).

By seeing these figures, breaking formula of Westhuysen or Ruessink seem to be a good compromise for the further applications since these outputs do not have a flat part in the breaking criteria figure (they are close to 1:1 line), and also show a good wave transformation in the shallow bank configuration. Note that Westhuysen formula is not available for the default setting in the version 41.20.AB.

Further discussion might be useful to understand the behaviour of wave breaking command. For this purpose, data of the Broersbank field measurement campaign (conducted from 2013-2016 by KUL) could be investigated. However we do not tackle this issue further here, but focus on the discussion on the methodology to obtain appropriate hydraulic boundary condition at -5m TAW points. Further decision is made in section 6.6.3.

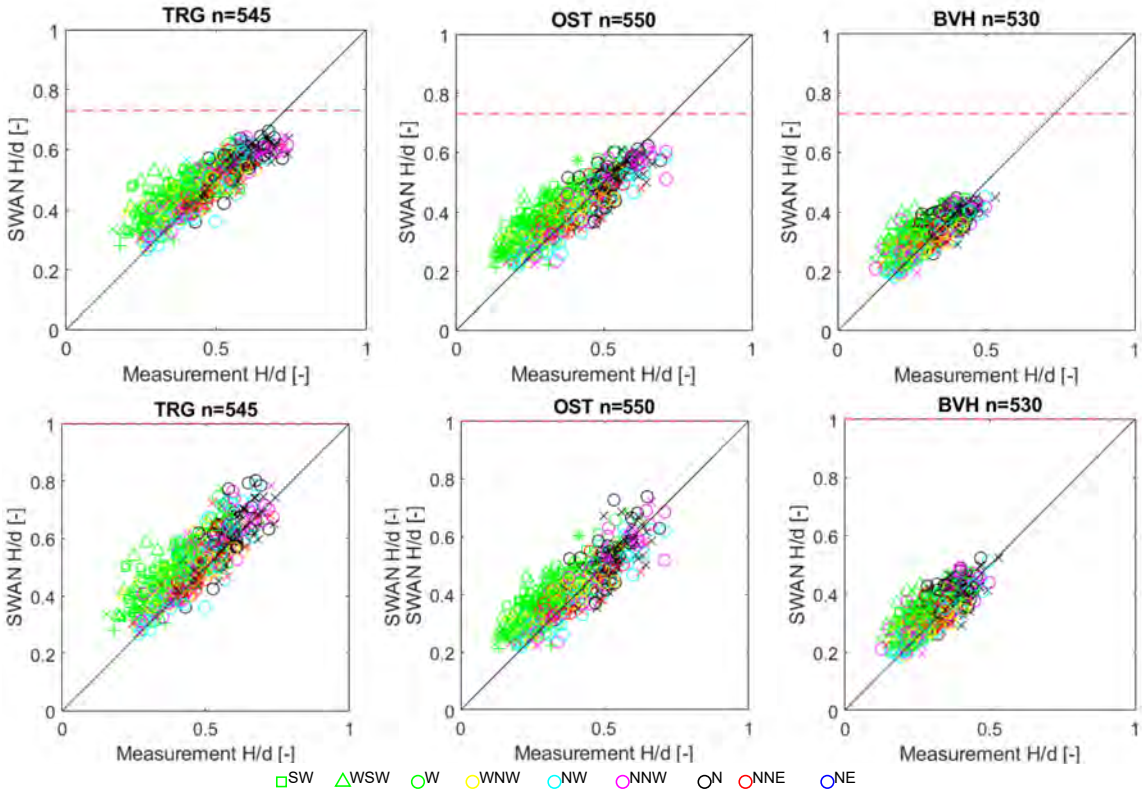

Figure 6.43 – Breaking setting (top; CON 0.73, bottom; 1.00)

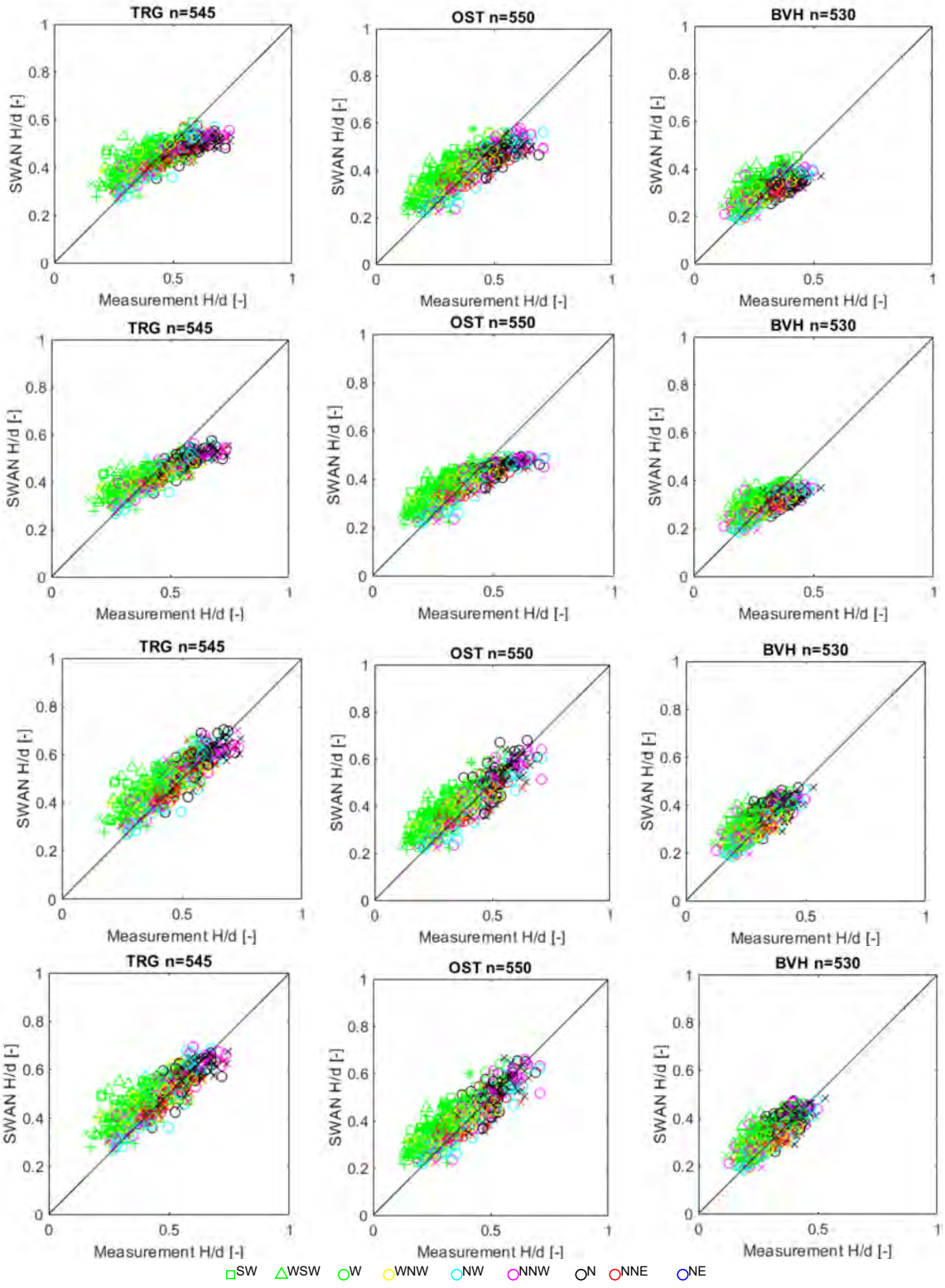

Figure 6.44 – Breaking setting (from the top; BKD, Nelson, Westhuyssen, Ruessink)

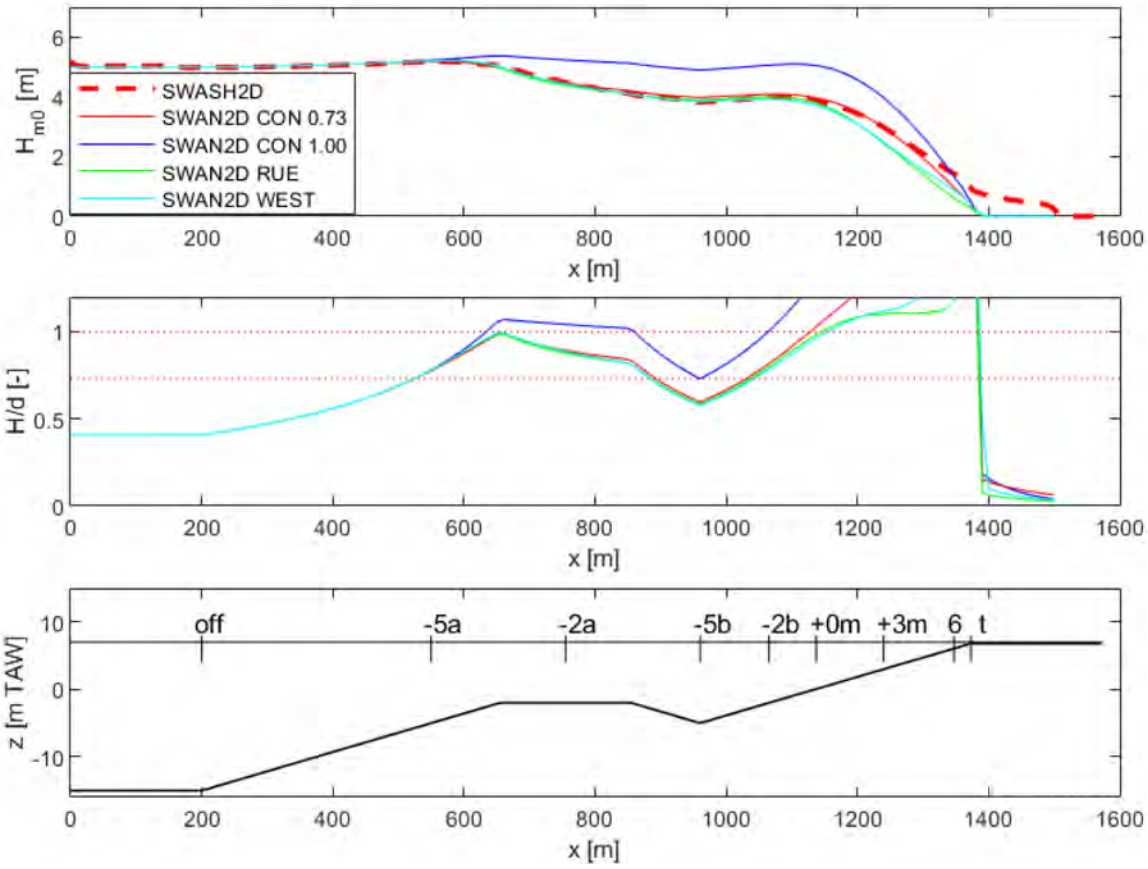

Figure 6.45 – Wave transformation over a shallow nearshore sandbank and breaker index (top: significant wave height, middle: Hmax/d, low: topography)

6.5 Further investigation of highly angled wave/wind directions

6.5.1 Overestimated cases

Looking at the performance of the basic case, some cases give overestimation. These overestimated cases are all highly angled wave directions (i.e. SW, WSW for all 3 locations and NE for BVH, see Figure 6.45). Direction WSW is almost parallel to the Belgian coast (blue dashed line in Figure 6.46) and SW has more angle (red dashed line), Direction NE is less angle but the NE line from the Dutch coast (green dashed line) goes to BVH. The overestimation can be related to the geographical locations, and thus we investigate it further here.

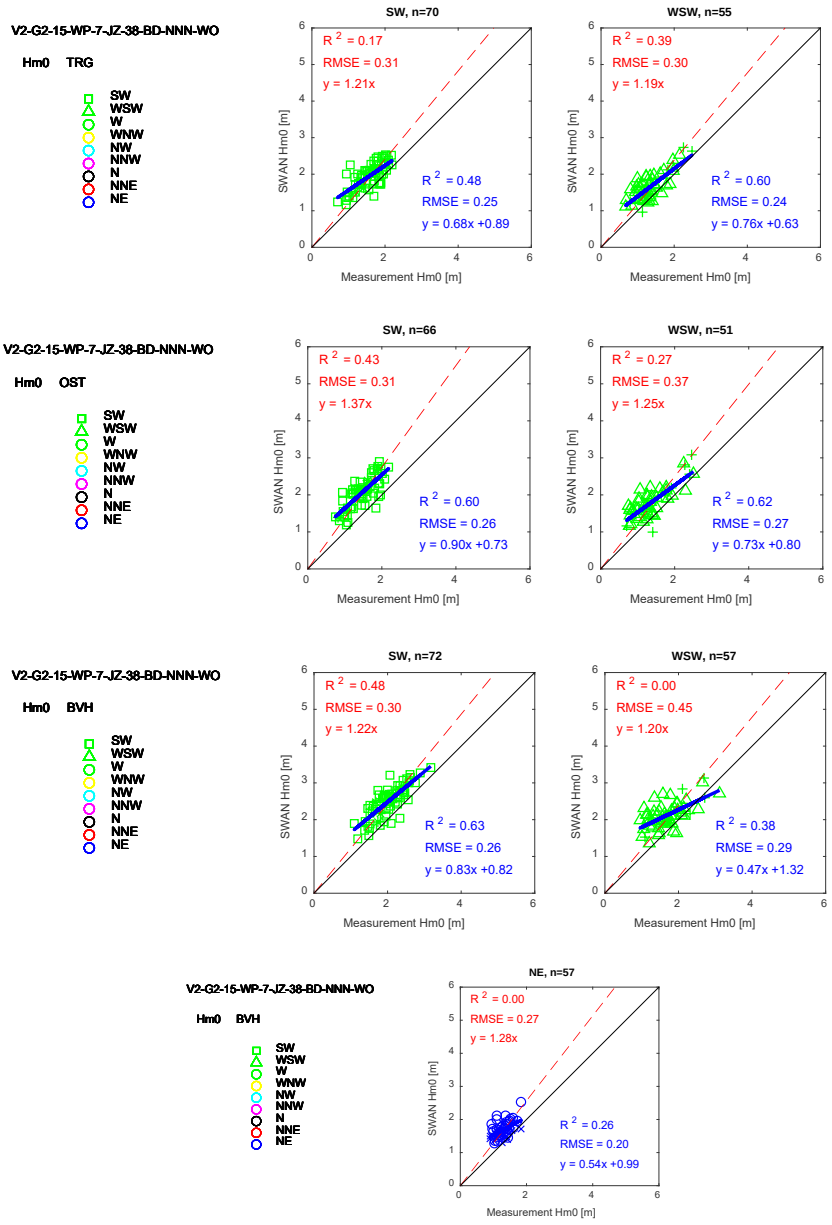

Figure 6.46 – Overestimated cases (basic case settings)

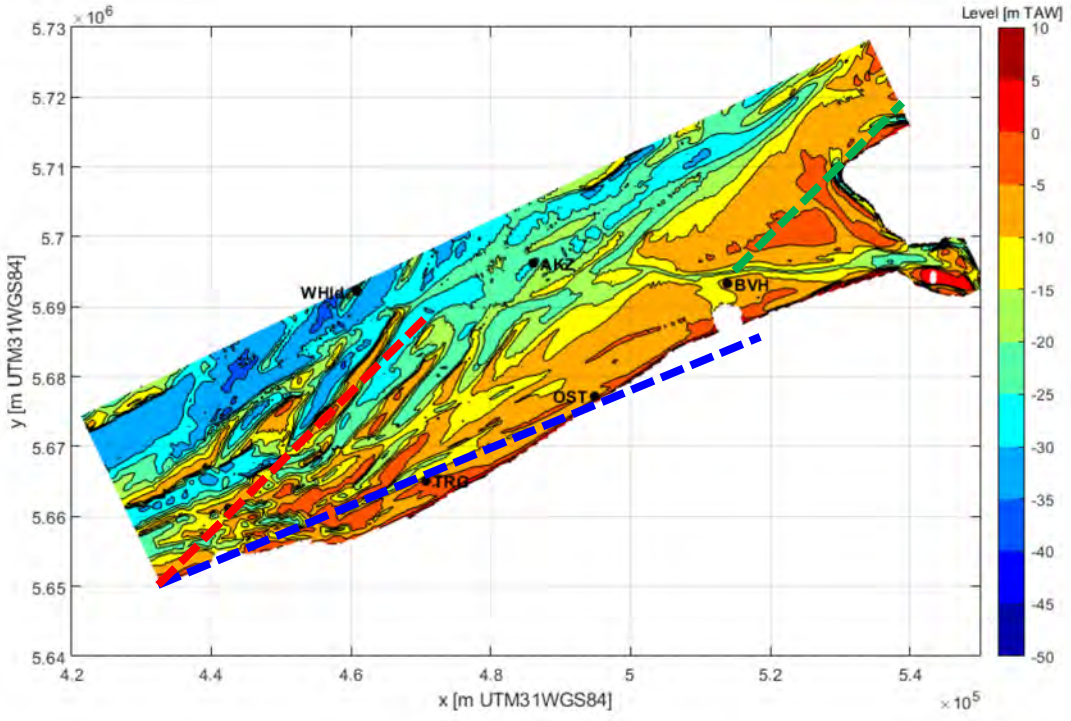

Figure 6.47 – Directions

6.5.2 Wave/wind boundary condition for SW and WSW

In order to have a better estimation, several measures are investigated. These are 1) time lag and water level input correction, 2) switching off the western wave boundary and 3) decreasing the wind speed. 1) is already tested in the sensitivity analysis (see section 6.2.13) but detailed output was not given there.

Time lag and water level input

The influence of the time lag and water level correction is shown in Figure 6.47, Figure 6.48 and Figure 6.49. It is clear that the influence of the time lag and water level correction is limited and thus the change is not enough.

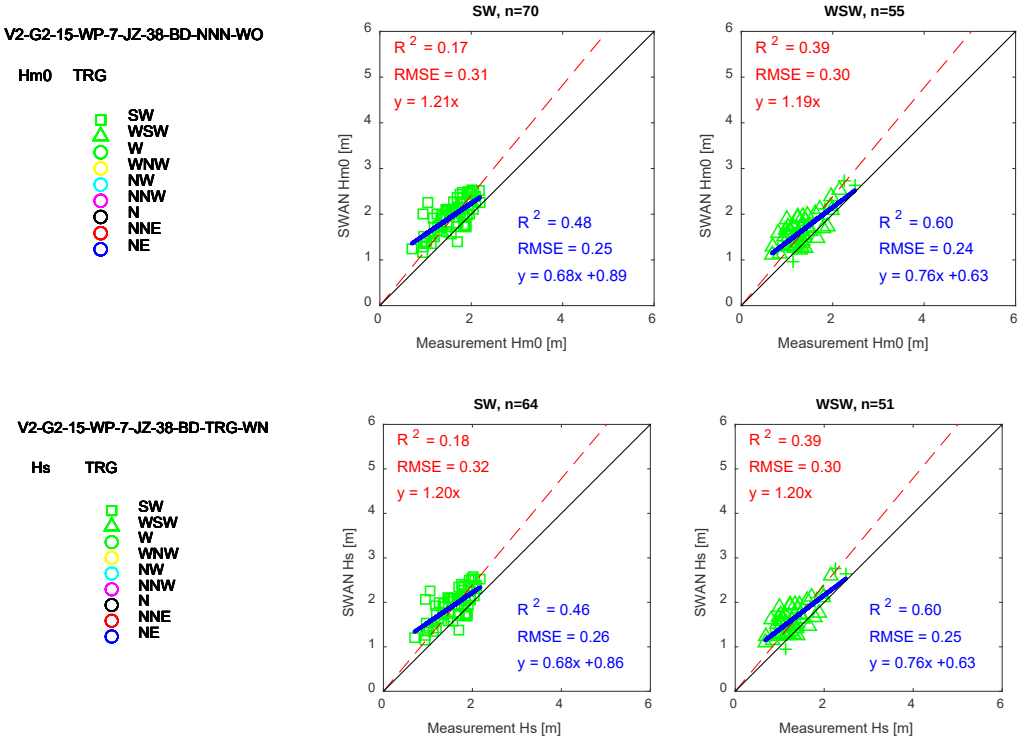

Figure 6.48 – Sensitivity of time lag and water level correction (upper: basic case, lower: time lag + water level correction, TRG)

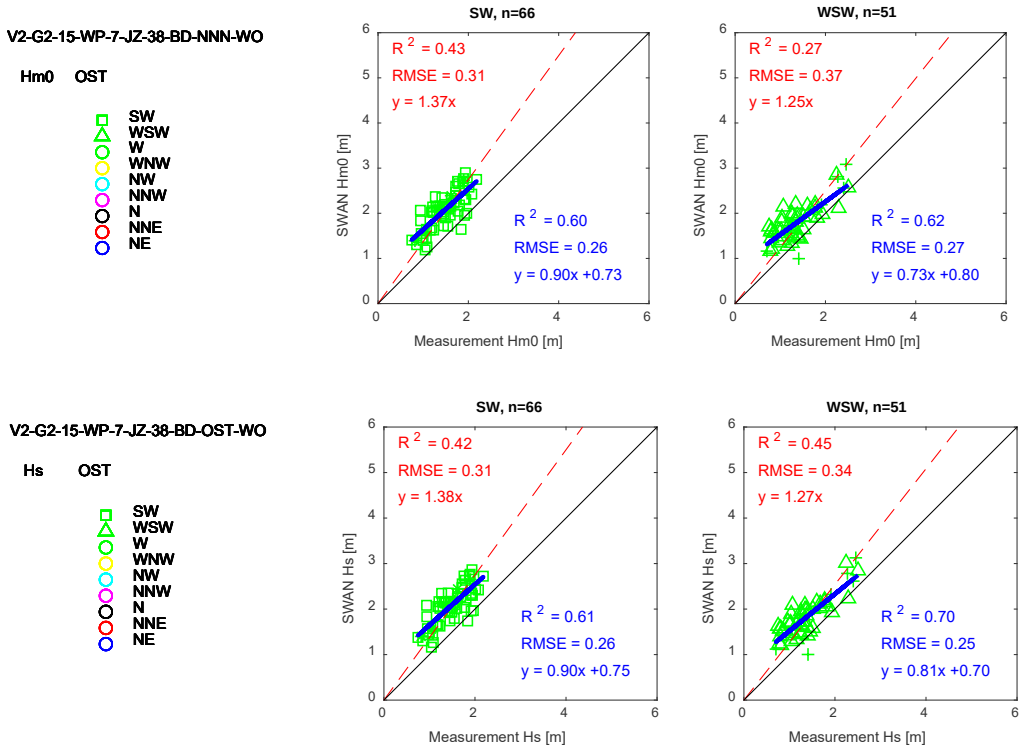

Figure 6.49 – Sensitivity of time lag and water level correction (upper: basic case, lower: time lag + water level correction, OST)

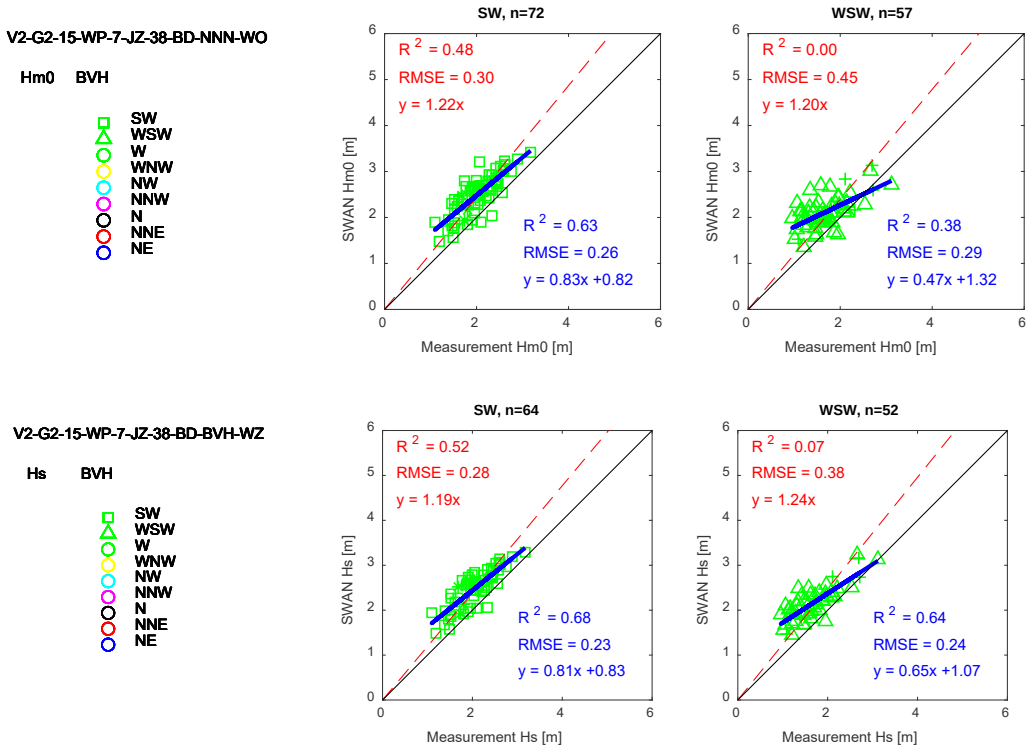

Figure 6.50 – Sensitivity of time lag and water level correction (upper: basic case, lower: time lag + water level correction, BVH)

Switching off the western lateral boundary

Wave boundary conditions are decided based on the measurement at WHI as default in this study. The same wave properties are imposed at the offshore wave boundary and the lateral boundaries. However, this assumption most probably gives more wave energy than the reality: the uniform wave height continues to the coast at the western lateral boundary. It is an attempt to switch off the wave input for western lateral boundary when the wave direction is SW and WSW.

The results are shown in Figure 6.50, Figure 6.51 and Figure 6.52. As shown, the influence of the western wave boundary is getting less towards east. The slope ‘a’ value of y=ax is 7% smaller at TRG, 3% smaller at OST and 2% at BVH for SW, and 2% smaller at TRG, 1% smaller at OST and 1% at BVH for WSW. Nevertheless these decreases are not enough but will be necessary measure especially for SW direction.

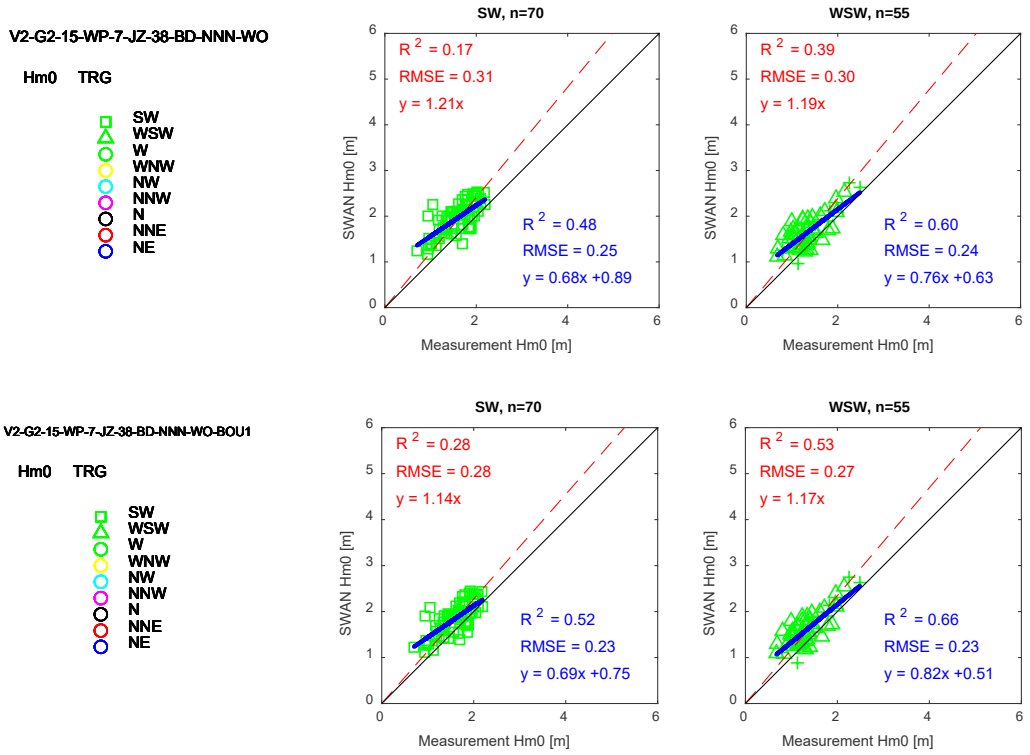

Figure 6.51 – Influence of no wave boundary for SW and WSW (upper: basic case, lower: no wave input for west boundary, TRG)

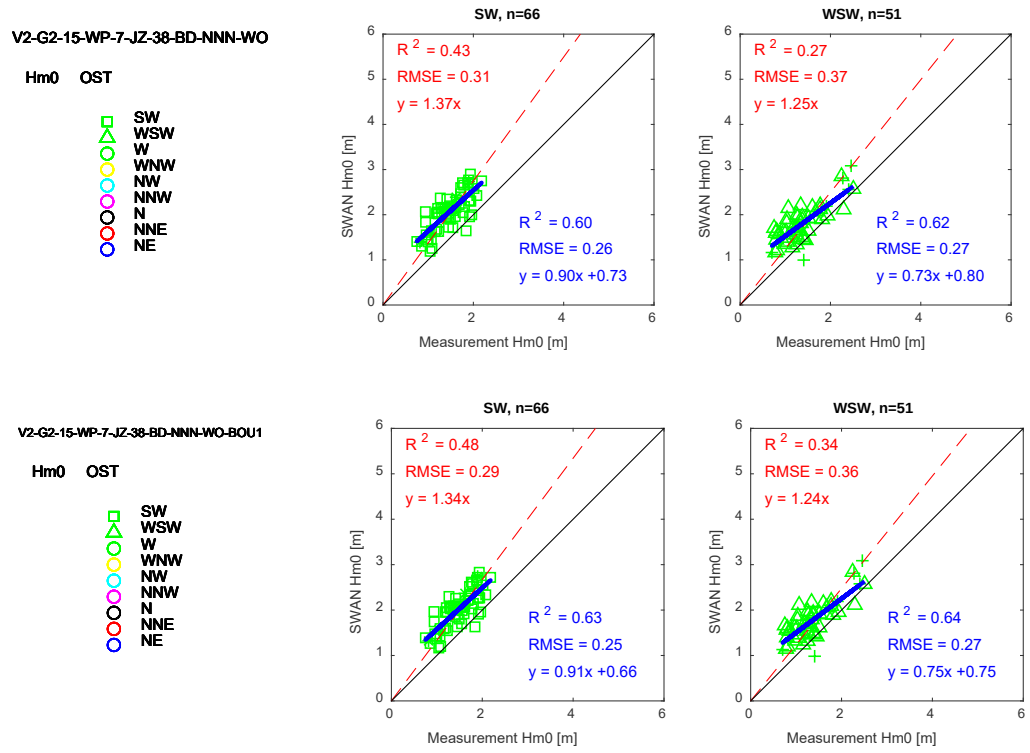

Figure 6.52 – Influence of no wave boundary for SW and WSW (upper: basic case, lower: no wave input for west boundary, OST)

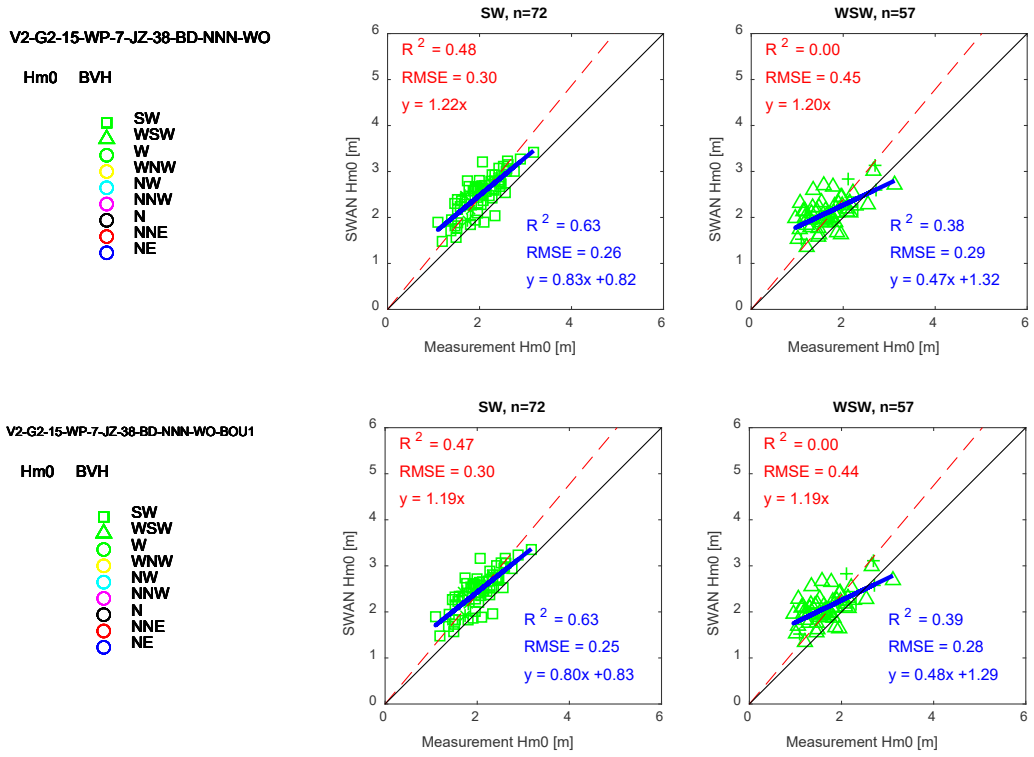

Figure 6.53 – Influence of no wave boundary for SW and WSW (upper: basic case, lower: no wave input for west boundary, BVH)

Decrease wind speed blowing from the land

The last option is to decrease the wind speed blowing from the land boundary, in addition to the first measure switching off the westside lateral wave boundary input for the wave direction SW and WSW.

The input of wind speed is decreased from the original input for the wind direction from 67.5 to 247.5 degree which line is almost parallel to the Belgian coast. In these wind directions the wind speed will be somewhat smaller than one observed in the offshore since the wind blows from the land. According to the land-based Ostend and Zeebrugge wind measurements, the wind speed directing to seaward is 51%, 72% respectively compared to the one in offshore (MP7 or MP7/MP0), see Figure 6.53. Taking into account the wind speed is increased again on the sea, we consider two cases, namely 90% and 80 % wind speed for all locations: TRG (3 km away from the coast: a quick check of NPT's wind measurement indicated the wind speed is higher than ZMP), OST (1 km away from the coast: originally 51%) and BVH (5 km away from the coast: originally 72%). Note that the breakwater of the port of Ostend (since 2008) might also slightly influence to the wind generated waves when wind is blowing from SW, therefore the object lines are defined as shown in Figure 6.54.

The results are shown in Figure 6.55, Figure 6.56 and Figure 6.57. As shown, the best compromise can be found when 80 % is applied: 'a' value in y=ax form is cloest to 1 and most of the estimation plot is situated around 1:1 line.

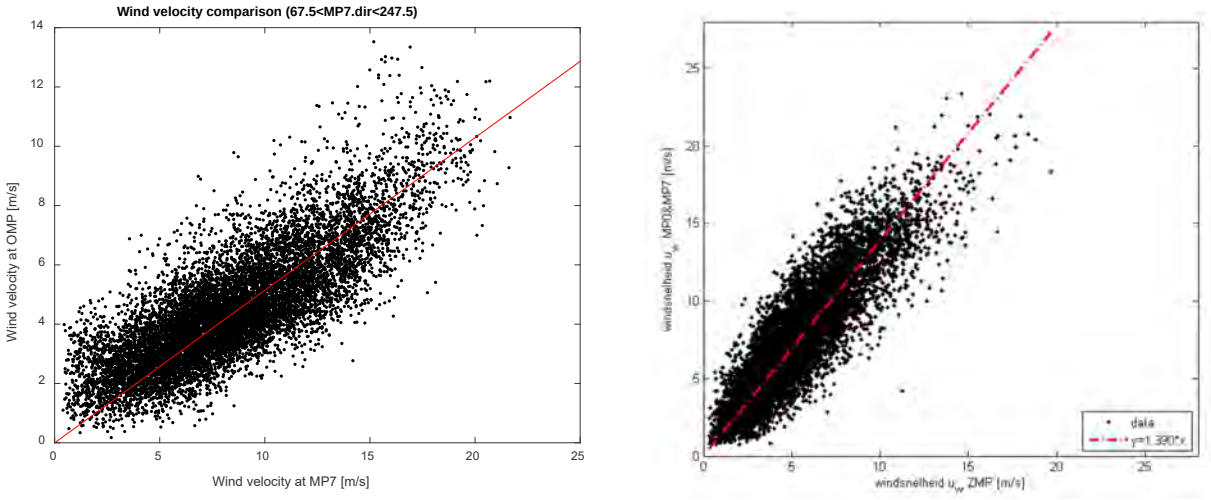

*the anaysis period is about 1 year, starting from Sep 2018.

Figure 6.54 – Ratio of wind speed at OMP* and ZMP compared to offshore stations (51% for OMP and 72% for ZMP) (De Roo *et al.*, 2016))

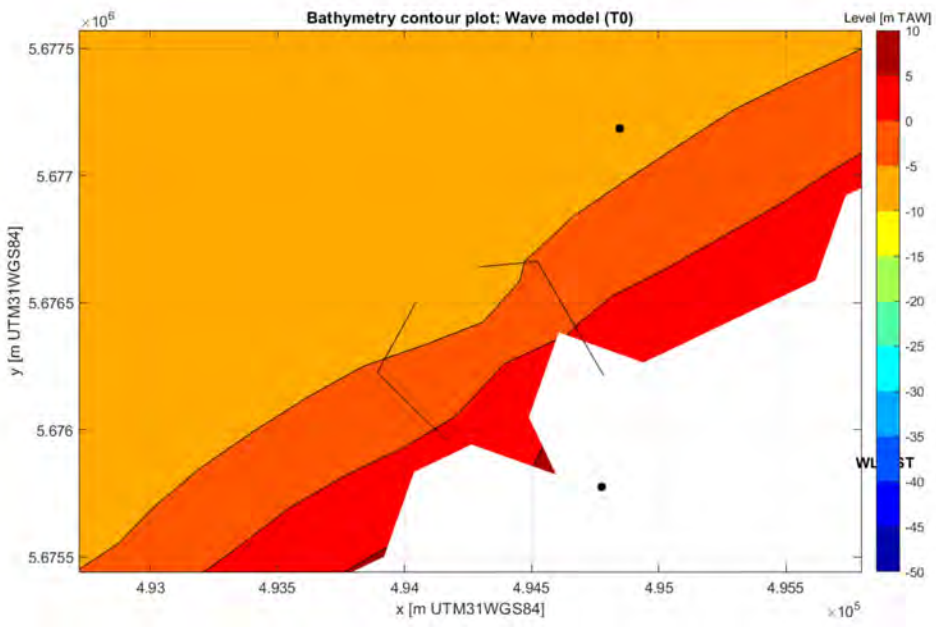

Figure 6.55 – Breakwater location of the port of Ostend

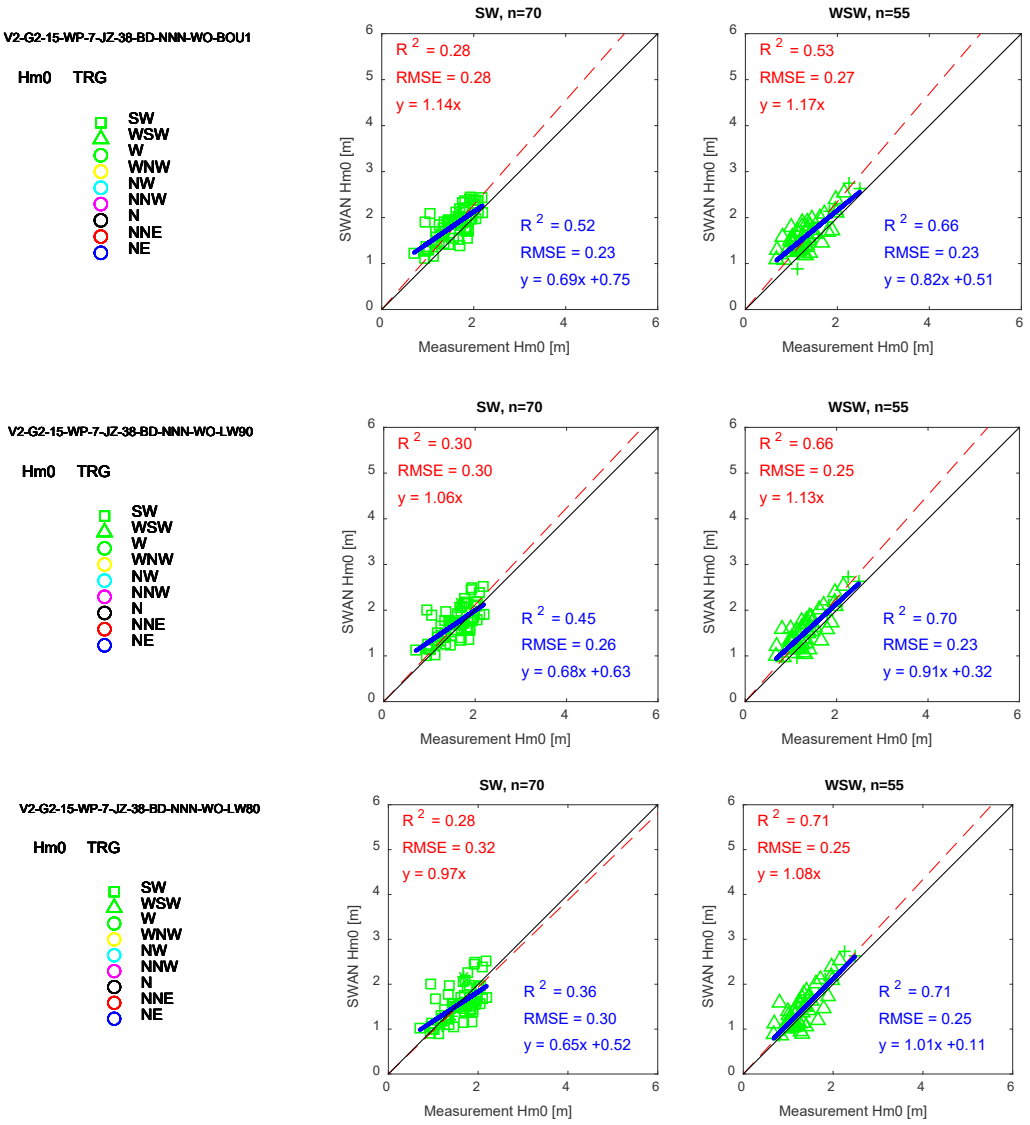

Figure 6.56 – Sensitivity of boundary condition input for SW and WSW (upper: basic case, middle: wind from the land is reduced to 90 %, lower: reduced to 80%) – significant wave height Hm0

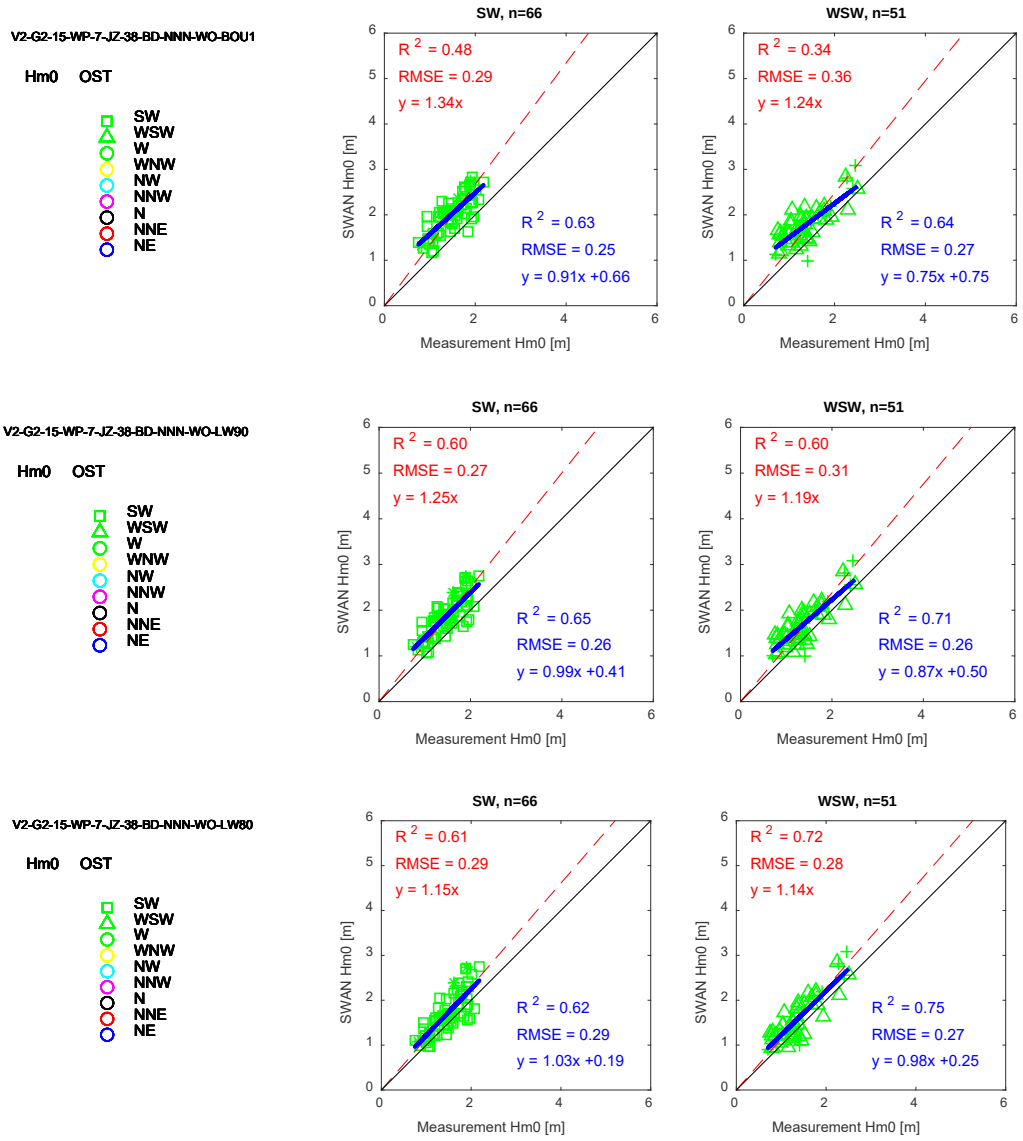

Figure 6.57 – Sensitivity of boundary condition input for SW and WSW (upper: basic case, middle: wind from the land is reduced to 90 %, lower: reduced to 80 %) – significant wave height Hm0

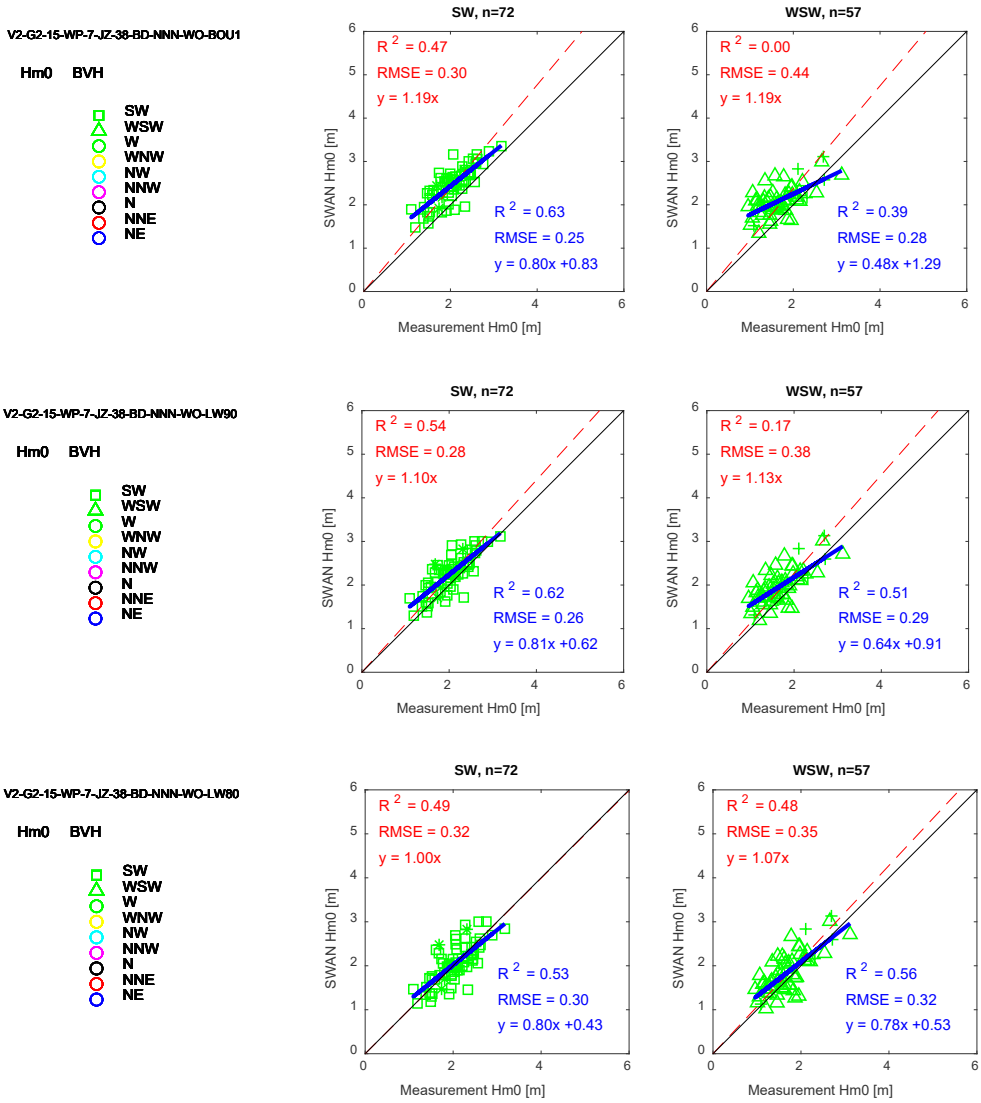

Figure 6.58 – Sensitivity of boundary condition input for SW and WSW (upper: basic case, middle: wind from the land is reduced to 90 %, lower: reduced to 80%) – significant wave height Hm0

Summary of wave/wind boundary condition for SW and WSW

As seen in the results above, switching off western wave boundary for WSW direction (less than 2% for all locations) is limited compared to other measures (i.e. switching off the western boundary for SW, and wind speed reduction for wind direction from landward). Therefore it is not recommended to apply switching off western wave boundary for WSW direction in order to avoid extra complexity. The time lag and the water level correction do not influence to the quality of the output but this will be considered in the final calculation anyway considering about the conclusion from section 6.2.13.

Here below is the summary of the recommended settings.

- Take into account the time lag and water level correction
- Wind input from the land (wind direction from 67.5 to 247.5 deg) is reduced to 80%
- Swithcing off the wave input at the western lateral boundary for waves from SW (wave direction from 258.75 to 236.25 deg)
- Breakwater of Ostend included

6.5.3 Wave/wind boundary condition for NE

Time lag and water level input

Following to the same step as conducted in the last section, we first investigate the influence of the time lag and water level correction (i.e. instead of using the water level from OST, geographically closest water level measurement ZBG is used).

The result shows that the estimated significant wave heights are reduced and qualitatively become closer to the 1:1 line.

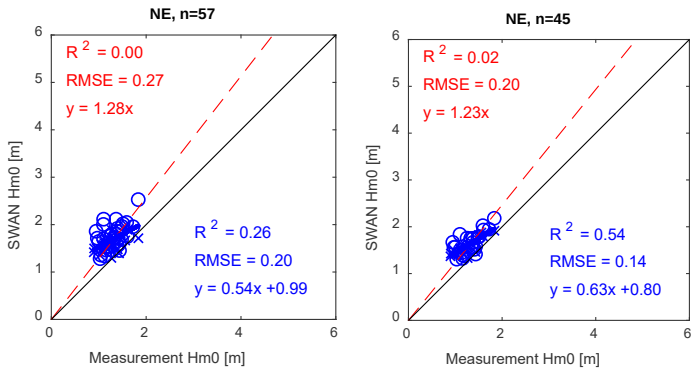

Figure 6.59 – Influence of the time lag and water level correction for NE at BVH (left: basic case, right: time lag + water level correction) – significant wave height Hm0

Decrease wind speed blowing from the land

In order to reduce the estimation value, the input of wind speed is decreased for the wind direction 45 to 67.5 degree in addition to 67.5 to 247.5 deg (see section 6.5.2). In these wind directions, the wind speed might be smaller than one observed in the offshore since the wind blows from the land (i.e. Walcheren in Zeeland) – BVH is located at 45 deg line from Westkapelle, even though the distance is long. Wind speed of again 80% is applied for the wind direction 45-67.5 deg and the result is shown in Figure 6.58.

The slope 'a' of y=ax is reduced by this measure but the upper cloud stay the same: it will not be an effective measure to reduce the wave height compared to the time lag and water level input correction shown above.

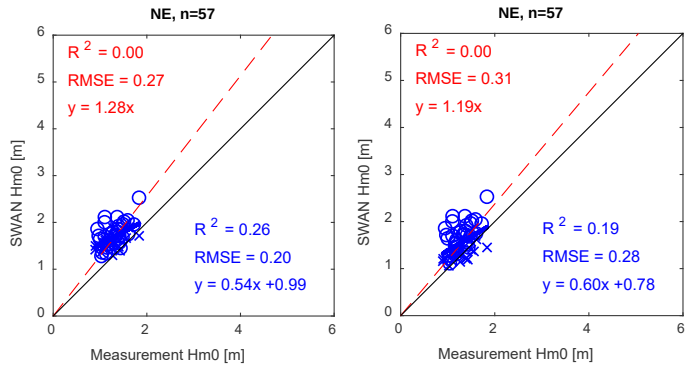

Figure 6.60 – Influence of the time lag and water level correction for NE at BVH (left: basic case, right: 80% wind speed reduction for wind direction 45-67.5 deg) – significant wave height Hm0

Summary of wave/wind boundary condition for NE

As seen in the results above, the wind speed reduction do not improve estimation significantly. Therefore it is not recommended to apply it. On the other hand, the time lag and the water level correction gives an effective change in contrast to the wind speed reduction.

Here below is the summary of the recommended settings.

- Take into account the time lag and water level correction

6.6 Further screening

6.6.1 Screening and comparison

From the investigation till here, it is concluded that following settings will lead to good estimation being at the same time computationally not too demanding to decide the hydraulic boundary conditions at the -5m TAW, see below:

- Version: 41.20.AB
- Bathymetry input: BCP2015 (BCP2020 for SA21)
- Grid size: 250x250 m (250x125 m is recommended in SA21)
- Offshore wave input: WHI (alternatively AKZ)
- Wind input: MP7 (alternatively MP0)
- Wind drag: default
- GEN3: Komen
- TRIADS: on/off, to be investigated
- Bottom friction: JONSWAP 0.038
- Spectrum resolution: 38 bins for frequency and 36 bins for the range of 360 degree for direction
- Breaking formula: Westhuysen/Ruessink, to be investigated
- Time lag: taking into account the theoretical time lag calculated from the distance and group wave velocity
- Time lag for water level: selection of the closest water level location
- Number of iteration: Default (iteration finishes at 99.5 % accuracy with maximum number of iteration 50).
- Western wave boundary is off for wave direction SW
- Wind limitation: Wind from the land (67.5-247.5 degree) is reduced to 80%
- Object: Ostend breakwater is implemented as objects (transmission and reflection zero)

Based on the screening above, further comparison in terms of Triads and breaking formula is conducted here.

6.6.2 Triads

The influence of Triads is again investigated here using the screened settings. Figure 6.60 and Figure 6.61 show the comparison of Triads based on the screened settings (Breaking formula Westhuysen), significant wave height and mean wave period respectively. Figure 6.62 and Figure 6.63 show the comparison of Triads based on the selected settings (Breaking formula Ruessink), significant wave height and mean wave period respectively.

As can be seen, the differences of the significant wave height are limited while the differences of the mean wave period are significant. However this result (i.e. big change in wave period) is inconsistent to the findings in the sensitivity analysis earlier: in the basic case the difference was only 2%. In order to check the validity of the result, the point which had a big influence of the triads - the red box depicted in Figure 6.61 is further investigated by means of extra iteration (force to iterate 50 times).

Table 6.25 shows the estimation compared to observation of significant wave height and mean wave period. As can be seen wave height and wave period stay the same in case of triad off. This is consistent to the findings in the sensitivity analysis of numerics. However, the iteration gives lower results both for Hm0 and Tm02 when triad is activated. In fact, the underestimation of mean wave period shown in Figure 6.61 and Figure 6.63 are even not saturated ones, and thus further underestimation is expected.

Therefore it is clear that it is better to put triads off (in SA21).

Table 6.25 – Estimation of significant wave height and mean wave period by different iterations – triads off and on

Triads	Parameter	SWAN - Default iteration	SWAN - Iteration 50	Observation
Off	Hm0 [m]	3.69	3.69	3.61
	Tm02 [s]	7.86	7.88	7.96
On	Hm0 [m]	3.55	3.33	3.61
	Tm02 [s]	6.43	5.69	7.96

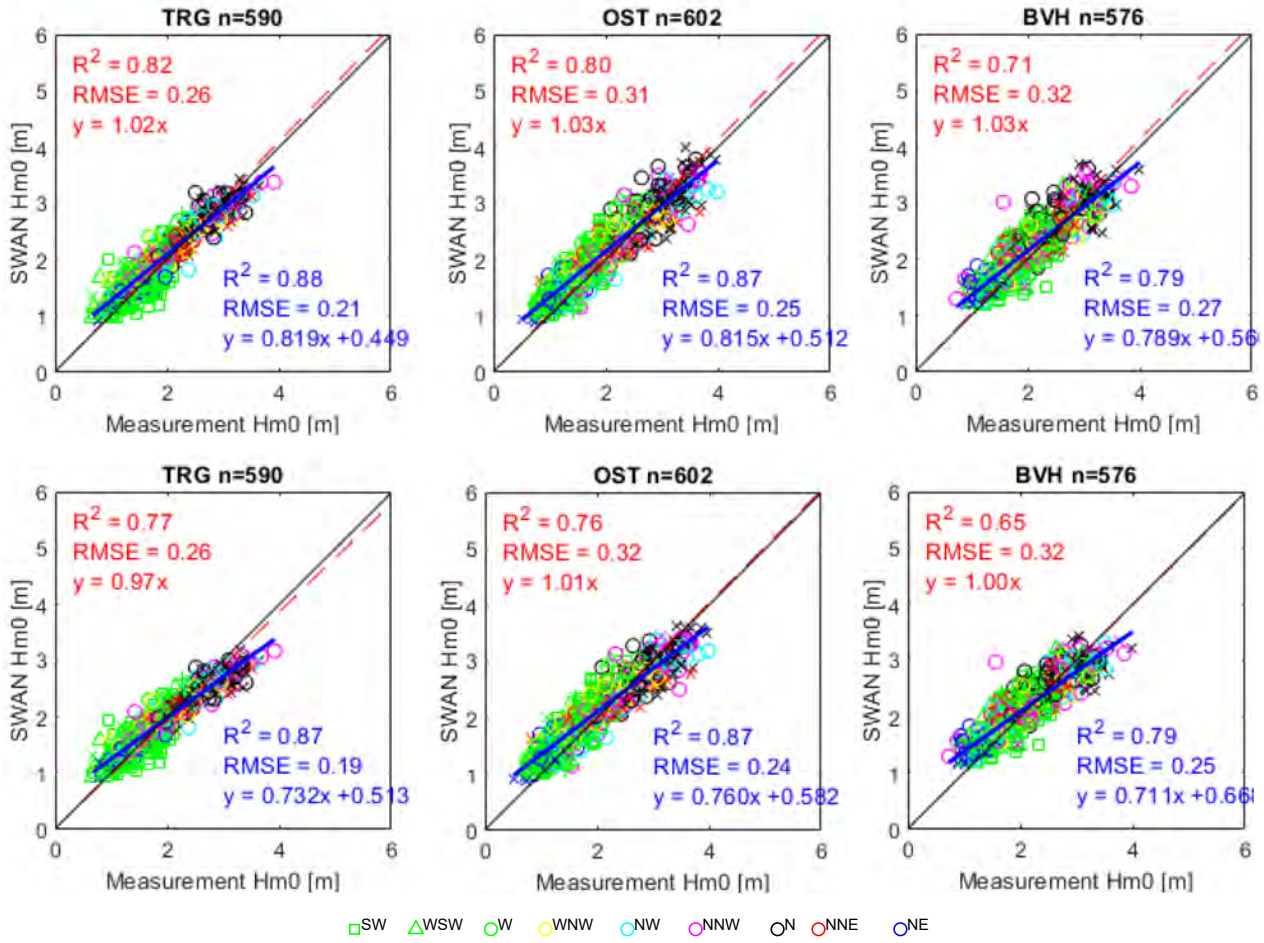

Figure 6.61 – Comparison of Triads based on the selected settings (Top: Breaking Westhuysen+TRIADS off, Bottom: Breaking Westhuysen+TRIADS on) – significant wave height Hm0

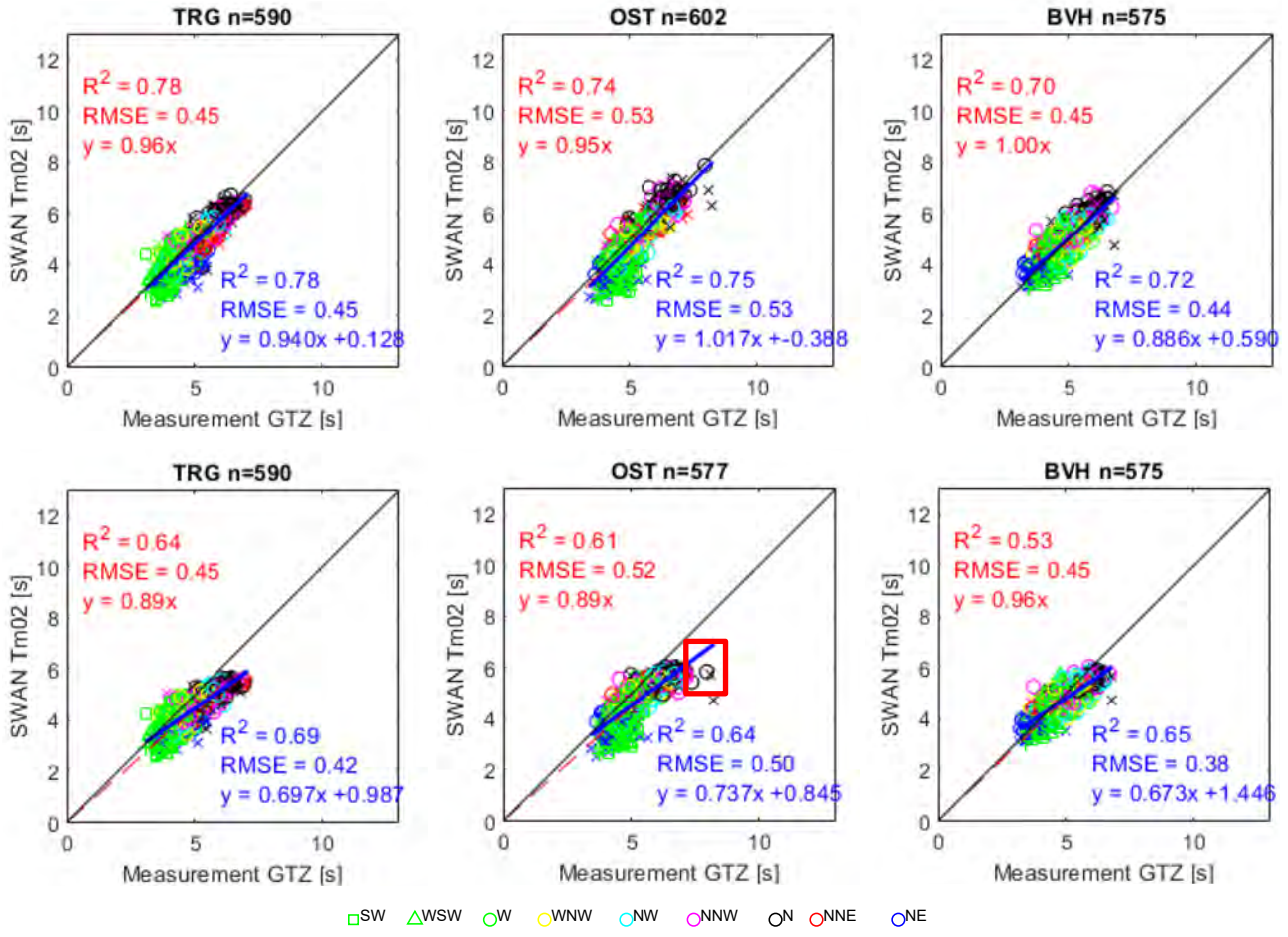

Figure 6.62 – Comparison of Triads based on the selected settings (Top: Breaking Westhuysen+TRIADS off, Bottom: Breaking Westhuysen+TRIADS on) – mean wave period Tm02

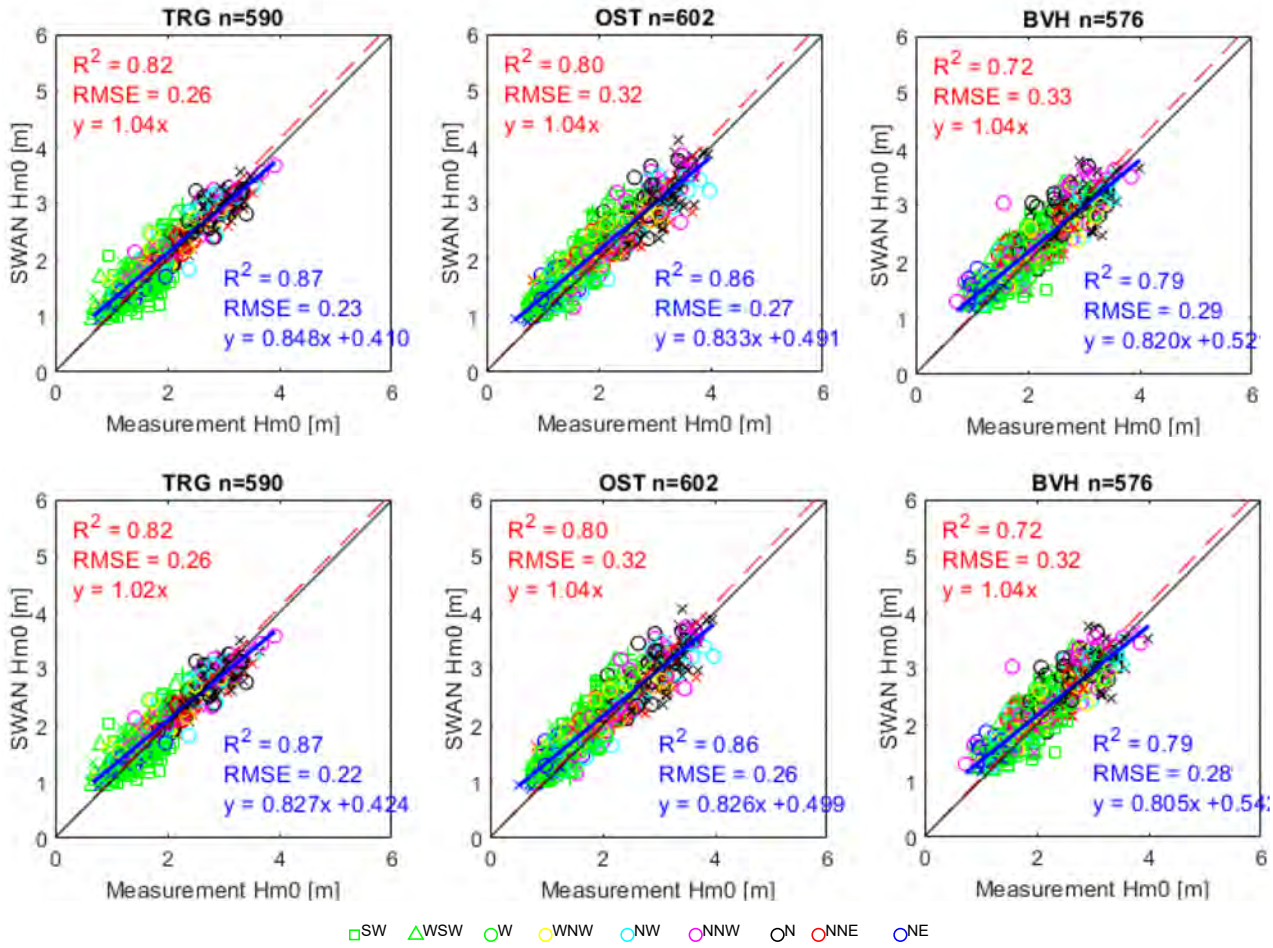

Figure 6.63 – Comparison of Triads based on the selected settings (Top: Breaking Ruessink+TRIADS off, Bottom: Breaking Ruessink+TRIADS on) – significant wave height Hm0

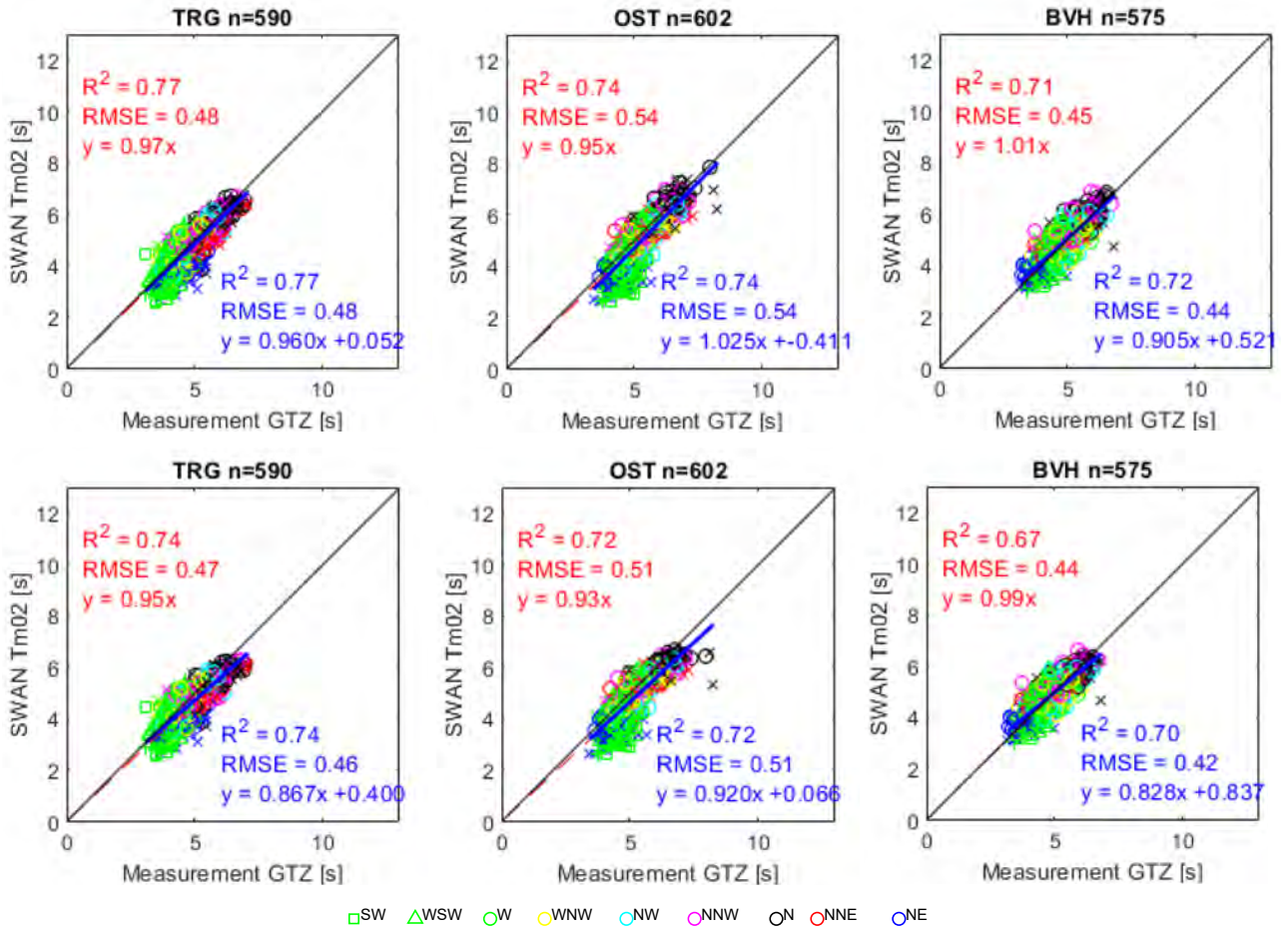

Figure 6.64 – Comparison of Triads based on the selected settings (Top: Breaking Ruessink+TRIADS off, Bottom: Breaking Ruessink+TRIADS on) – mean wave period Tm02

6.6.3 Breaking formula

Breaking formula is a critical input for SA21. The investigation till here indicates that the breaking formula of Westhuysen and Ruessink is equally good for the estimation of significant wave height and mean wave period at the location of TRG, OST and BVH. Figure 6.64 shows comparison of breaking formula based on the selected settings (triads off). As can be seen, the performance of both models is good – all the points are located close to 1:1 line. Therefore it is rather difficult to judge which model is better for SA21. In this section these settings are applied to extreme wave/wind conditions.

The same setting as shown in the sensitivity analysis of grid size (Section 6.2.3, grid size 250x250) is used here: Water level=7.0 m TAW, Hm0=5 m, Tp=12 s, wave dir=NNW, wind speed=26 m/s (and 10 m/s to check the sensitivity), wind dir=NNW, based on the screened settings. Figure 6.65 and Figure 6.66 show the comparison of Westhuysen and Ruessink for the wind speed of 26 m/s and 10 m/s at HBC output points in SA15, respectively. Figure 6.67 shows the comparison of Westhuysen and Ruessink for the wind speed of 26 m/s in 1500 m line. Note that the output of the basic case (section 6.1) is also shown here to compare with the present results.

Westhuysen gives a higher significant wave height everywhere at HBC output points in SA15 when wind speed=26 m/s is applied (Figure 6.65), however, the result becomes opposite when the wind speed is low (i.e. 10 m/s, Figure 6.66). It implies that the Westhuysen method is more sensitive to the wind input. In the different output point (i.e. 1500 m line, Figure 6.67), Ruessink become slightly higher around point 120.

Figure 6.68 shows wave height estimation accuracy in relation to the wind speed, under a criteria Hm0_SWAN/d>0.35 both for Westhuysen and Ruessink method. Number of the plot is zero for BVH because of its deeper location, so no data H_SWAN/d>0.35. As can be seen in the figure, Ruessink does not underestimate for wind speed up to 21 m/s.

Taking into account that Ruessink is implemented in the standard SWAN (while Westhuysen formula is not), Ruessink's method is recommended for SA21.

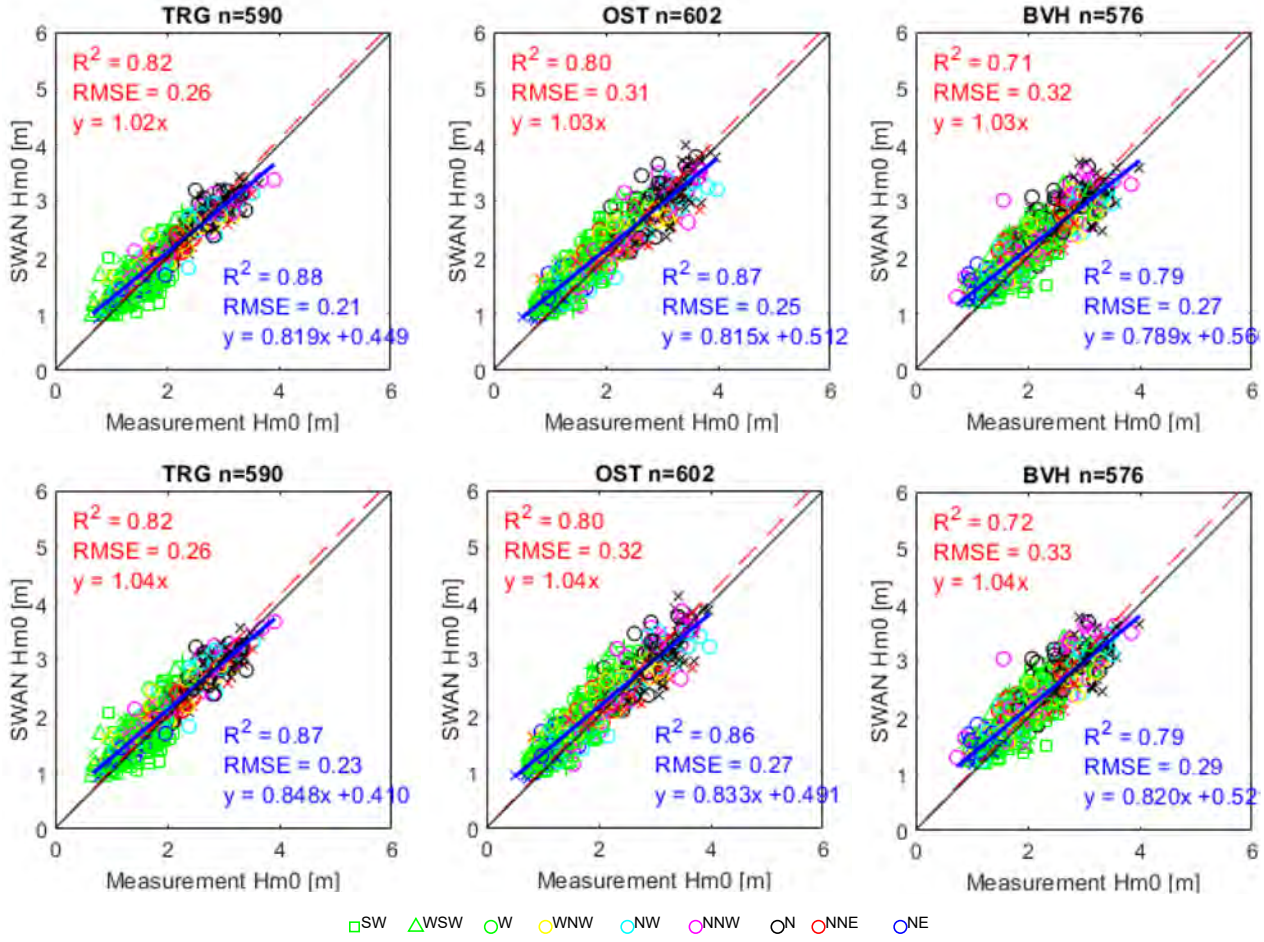

Figure 6.65 – Comparison of Breaking formula based on the selected settings (Top: Breaking Westhuysen, Bottom: Breaking Ruessink) – significant wave height Hm0

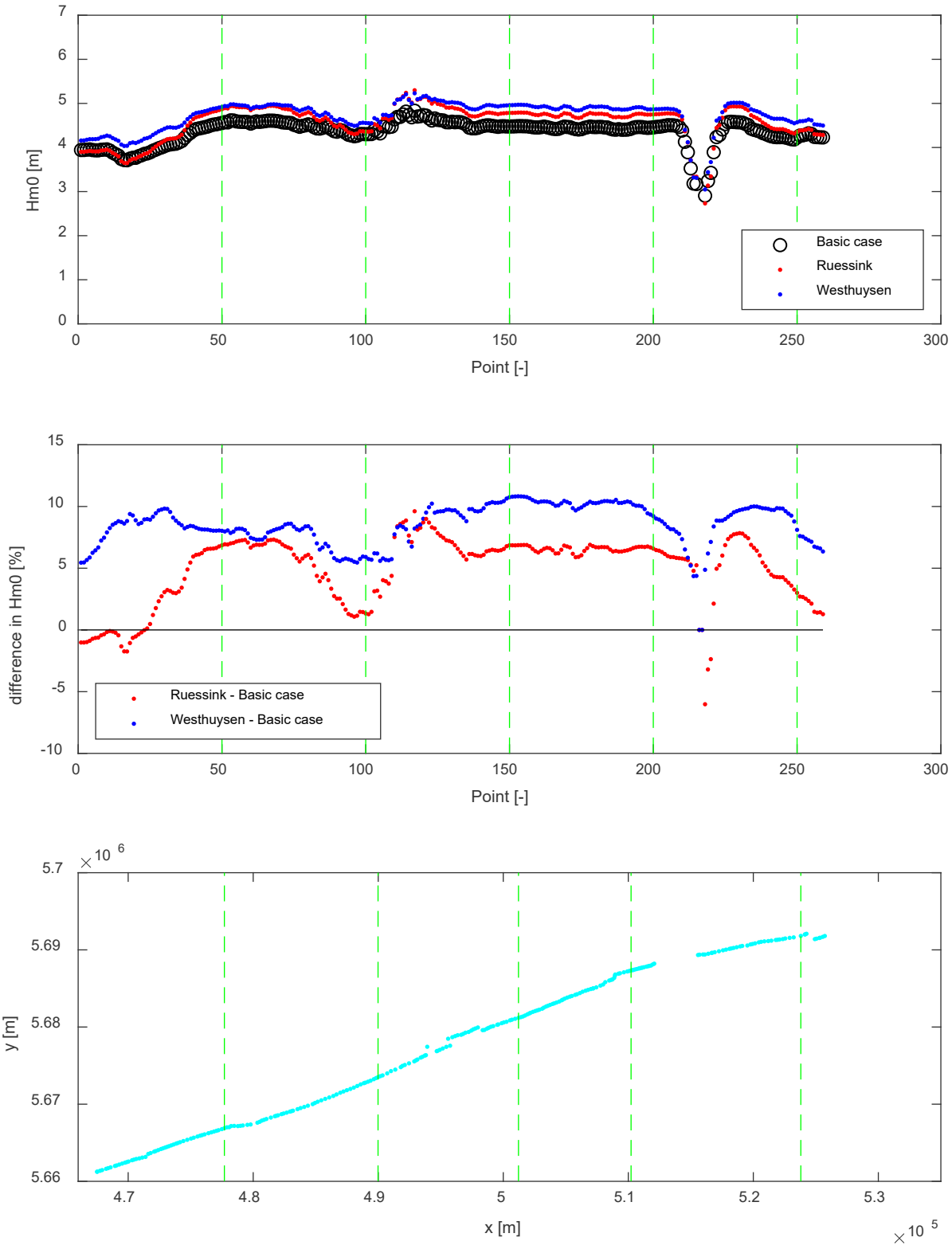

Figure 6.66 – Estimation of Hm0 in extreme conditions at HBC output points in SA15 (wind 26 m/s)

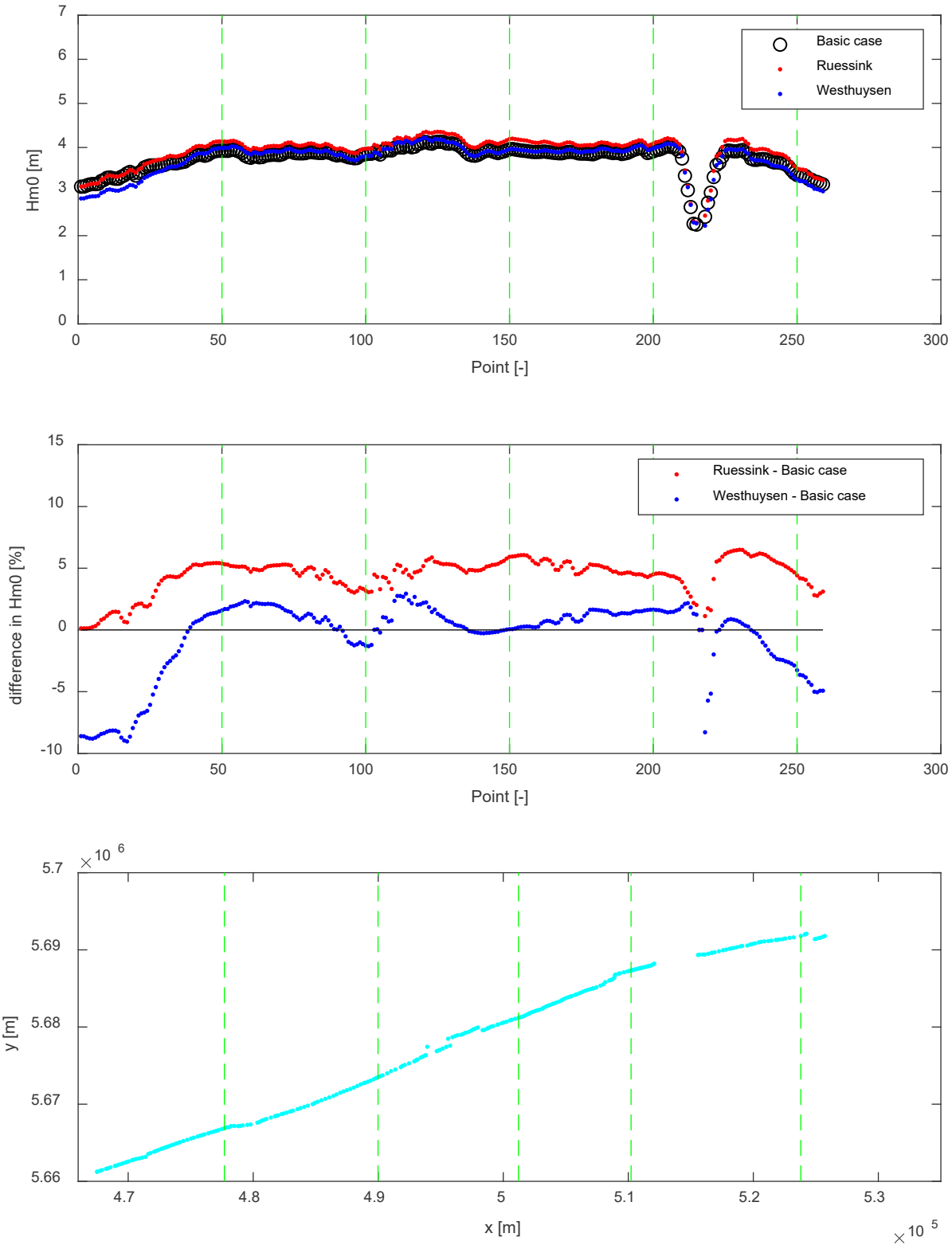

Figure 6.67 – Estimation of Hm0 in extreme conditions at HBC output points in SA15 (wind is reduced to 10 m/s)

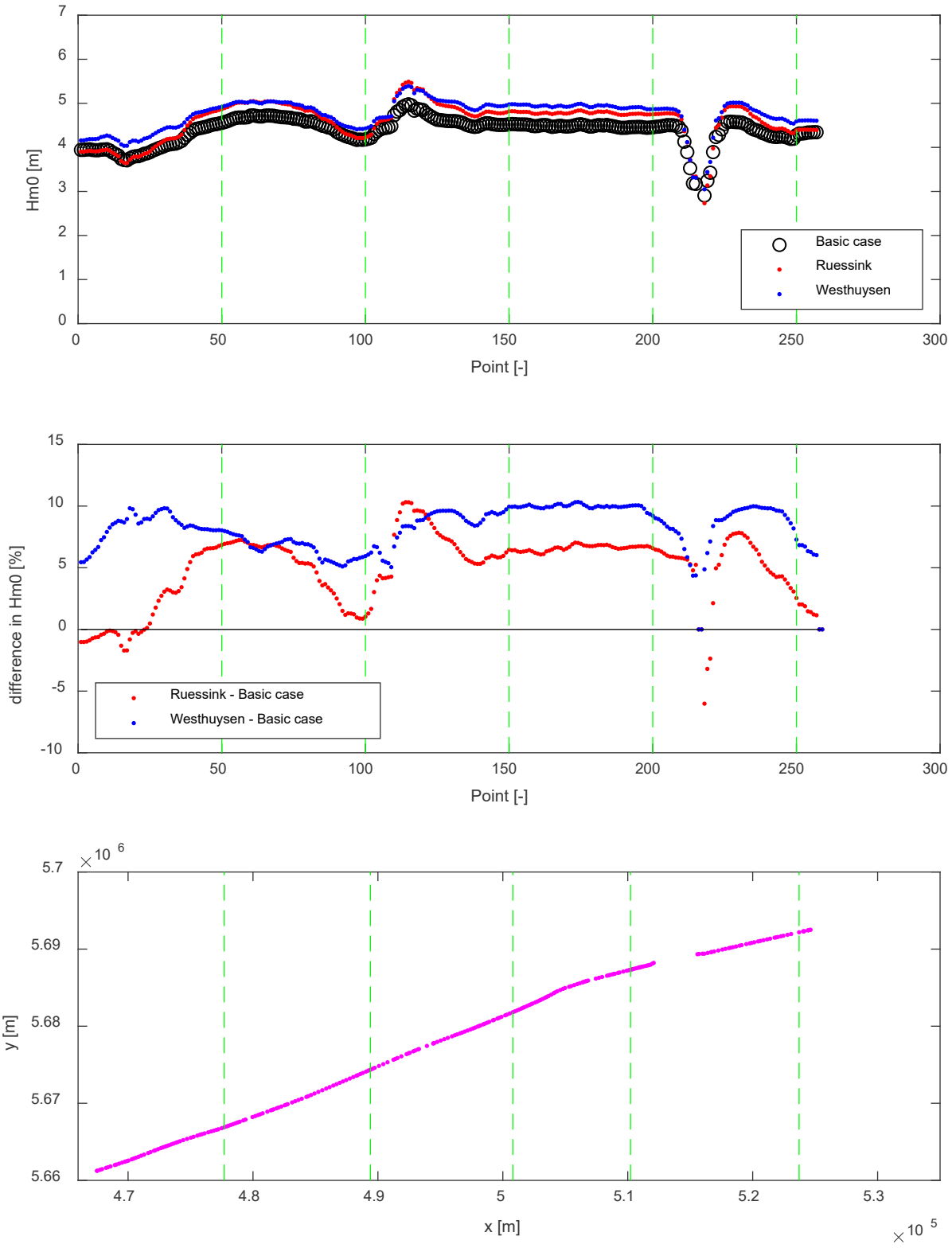

Figure 6.68 – Estimation of Hm0 in extreme conditions at 1500 m line (wind 26 m/s)

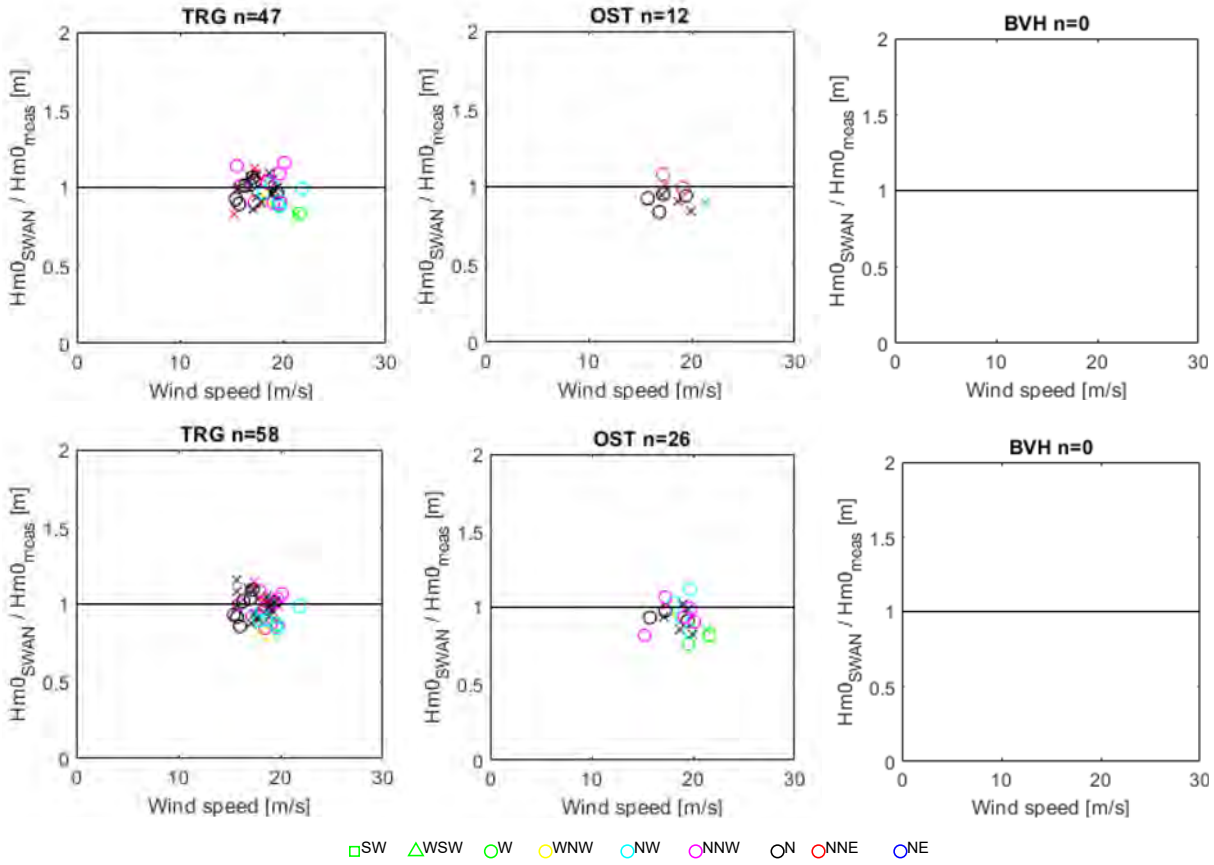

Figure 6.69 – Wave height estimation accuracy in a function with wind speed, under a criteria Hm0_SWAN/d>0.35
(Top: Westhuysen, bottom: Ruessink)

6.6.4 Conclusion of validation and detailed analysis

It is concluded that breaking formula Ruessink without triads is a good choice for SA21. Here below is the summary of the settings best suited for the validation case selected in this study.

- Version: 41.20.AB
- Bathymetry input: BCP2015 (BCP2020 is used in SA21)
- Grid size: 250x250 m (note that 250x125 m is recommended in SA21)
- Offshore wave input: WHI (alternatively AKZ)
- Wind input: MP7 (alternatively MP0)
- Wind drag: default
- GEN3: Komen
- TRIADS: off
- Bottom friction: JONSWAP 0.038
- Spectrum resolution: 38 bins for frequency and 36 bins for the range of 360 degree for direction
- Breaking formula: Ruessink
- Time lag: taking into account the theoretical time lag calculated from the distance and group wave velocity
- Time lag for water level: selection of the closest water level location
- Number of iteration: 101% accuracy with 50 iteration (note that the default setting for iteration was used for the result shown here since the calculated value is already saturated in the validation runs)
- Western wave boundary is off for wave direction SW
- Wind limitation: Wind from the land (67.5-247.5 degree) is reduced to 80%
- Object: Ostend breakwater is implemented as objects (transmission and reflection zero)

Figure 6.69 shows the overall analysis of significant wave height Hm0 and mean wave period Tm02 respectively. Figure 6.70, Figure 6.71 and Figure 6.72 show the directional analysis of significant wave height, and Figure 6.73, Figure 6.74 and Figure 6.75 show the directional analysis of mean wave period. Ruessink *et al.* (2003) indicated in their abstract that BJ is overestimating wave height while their setting solve this overestimation. Looking into the details of the Ruessink's study, the range of significant wave height is up to 1.5 m (max error is 60%). It is consistent with our study: the basic case setting (BJ 0.73) for the lower wave height (Hm0<2m) is overestimating the wave height as shown in Figure 6.3 (see example TRG, plots below Hm0~2m are located above the 1:1 line = overestimation), while the Ruessink's setting minimised this overestimation as indicated in Figure 6.70. As shown here estimation points for all the directions are situated around the 1:1 line for significant wave height and mean wave period Tm02. The quality of the estimation of highly angled waves is less compared to the ones coming from more transverse directions but it is still acceptable. It can be concluded that SWAN with the selected settings gives reasonable significant wave height and mean wave period.

Figure 6.76, Figure 6.77 and Figure 6.78 show the relationship between estimated Tps and observed Tp, estimated Tm-1,0 and observed Tp, estimated Tm02 and observedTp, respectively. These included some scatters, especially for the extreme wave directions (e.g. SW, WSW) in TRG. These directions in TRG must have flatter spectrum and that might be the reason that there is no clear relationship between mean wave period and peak wave period. However, other directions have clear correlation with measured Tp.

Figure 6.79 shows the relationship between estimated wave direction and observed wave direction. The number of the points is smaller since the directional data is limited. The DIR output of SWAN (mean wave direction) is slightly better than pdir (peak wave direction) but the definition of REM (wave direction of highest energy component) is more closer to pdir. However the peak value can be jumped one bin to the other easily and also depends on the resolution of the bin. This might be a reason that the estimation results of pdir do not show the best performance. Due to the same reason we prefer to use tps instead of tp. Further investigation will be useful (e.g. checking the whole 3D spectrum shape). The result indicated that SWAN gives reasonable estimation for wave direction in general.

Figure 6.80 shows the relationship between estimated directional spreading using SWAN (DSPR: the standard deviation of directional spreading width calculated from the entire 3D spectrum, and SEM: directional spreading at the highest energy frequency component by) and observed one (SEM). The result indicated that the SEM output gives a slightly better representation compared to the DSPR output while in general there is a big scatter to estimate the directional spreading. Note that the quality of the result is the same as the basic case. Further investigation is necessary/useful to explain why SWAN estimation gives so much scatter for directional spreading.

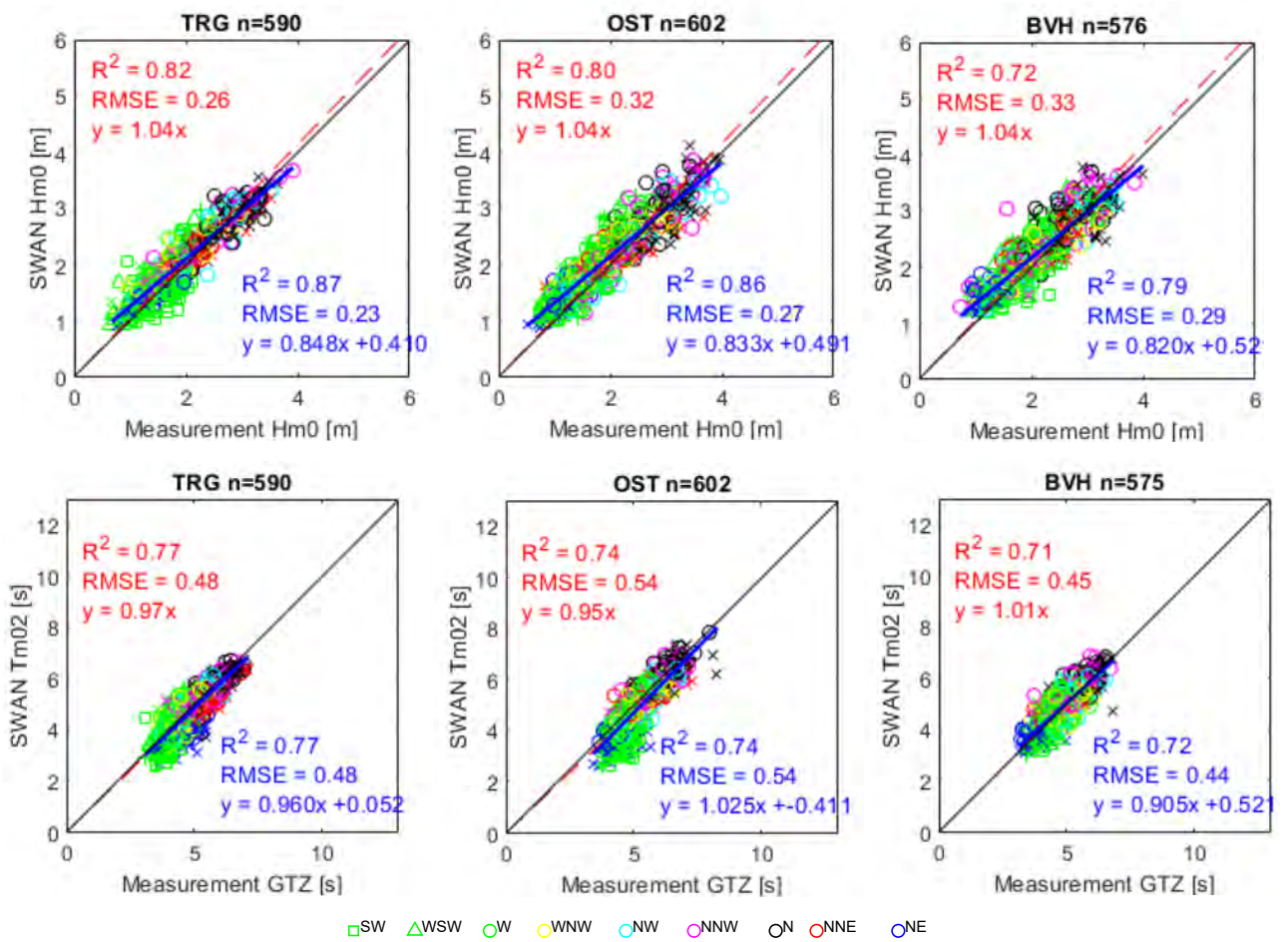

Figure 6.70 – Model performance of the best case for the validation – Hm0 (top) and Tm02 (bottom)

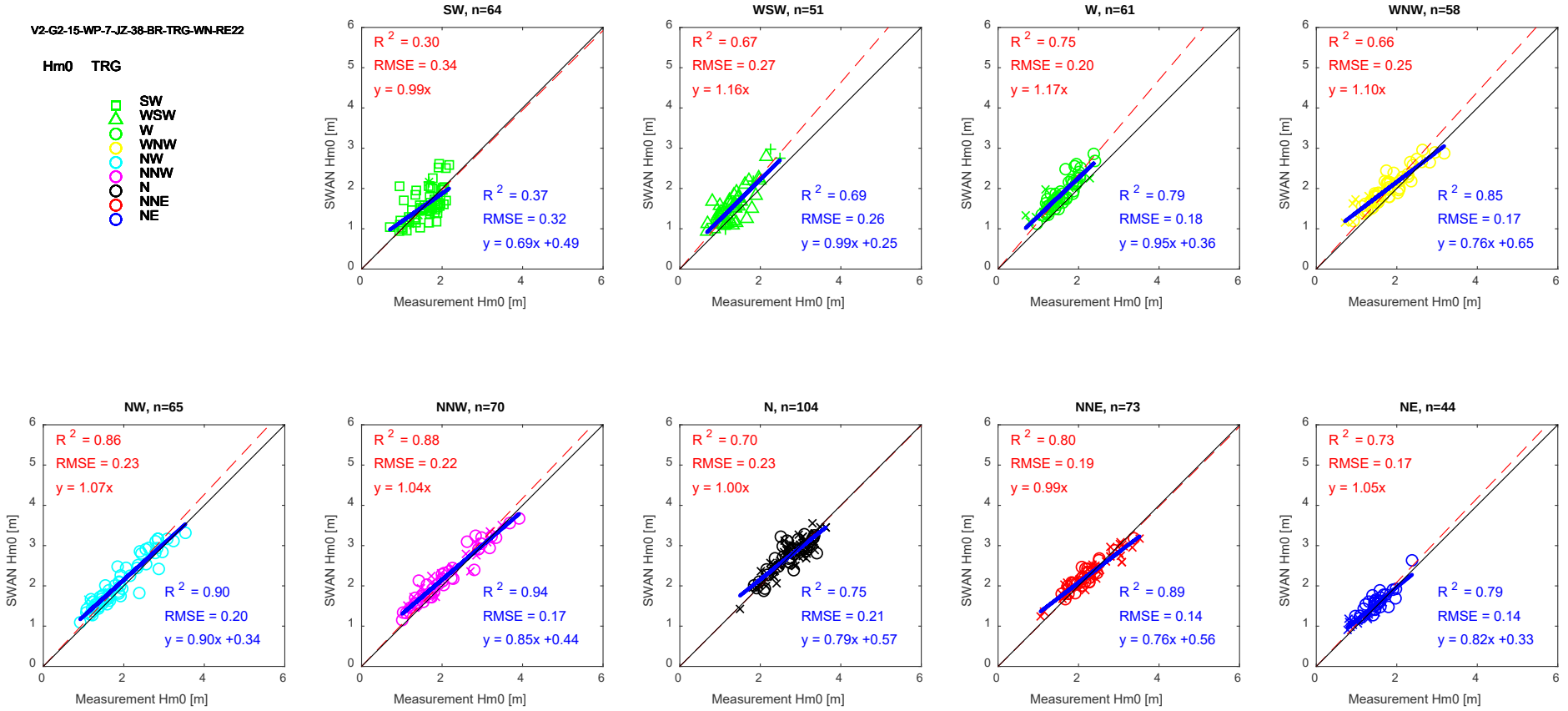

Figure 6.71 – Model performance of the best case for validation (TRG) - significant wave height Hm0

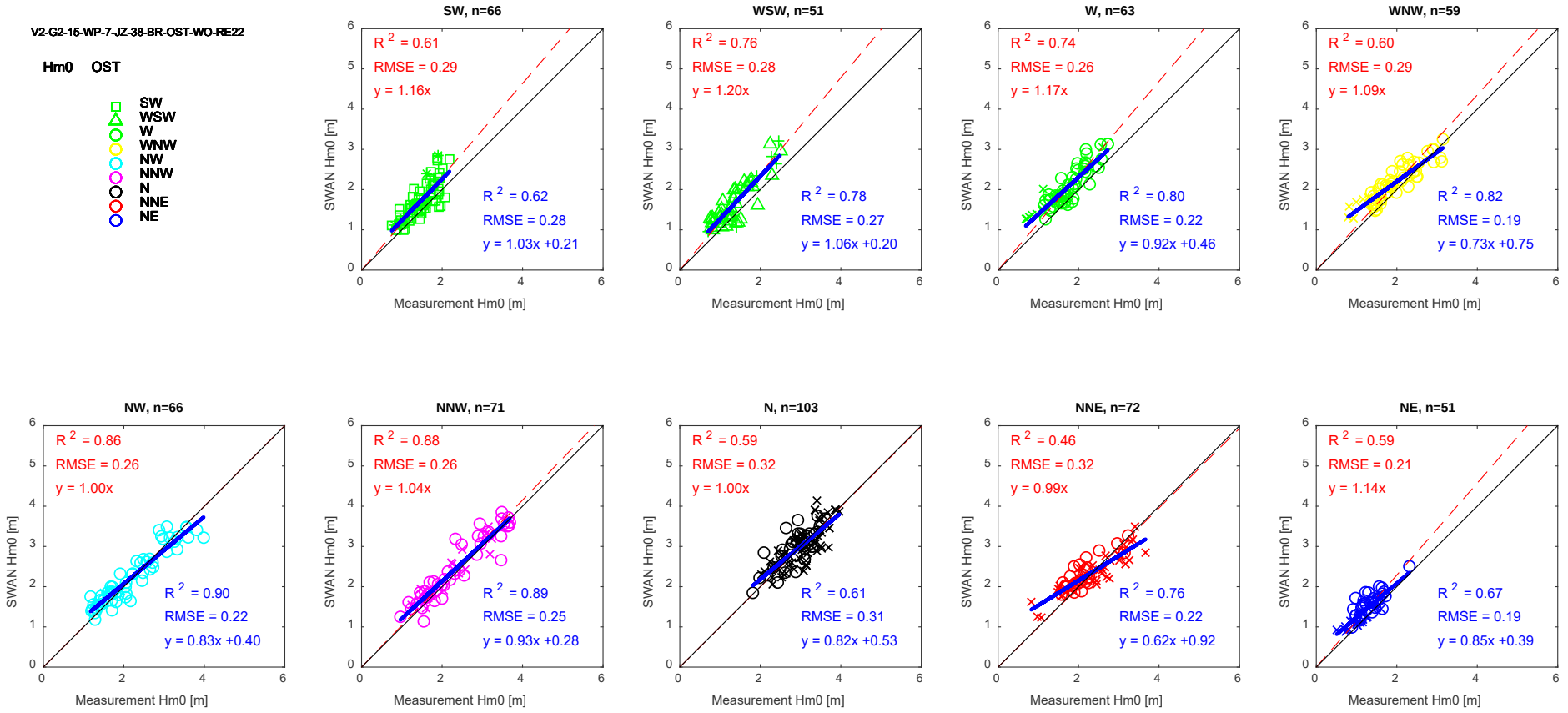

Figure 6.72 – Model performance of the best case for the validation (OST) – significant wave height Hm0

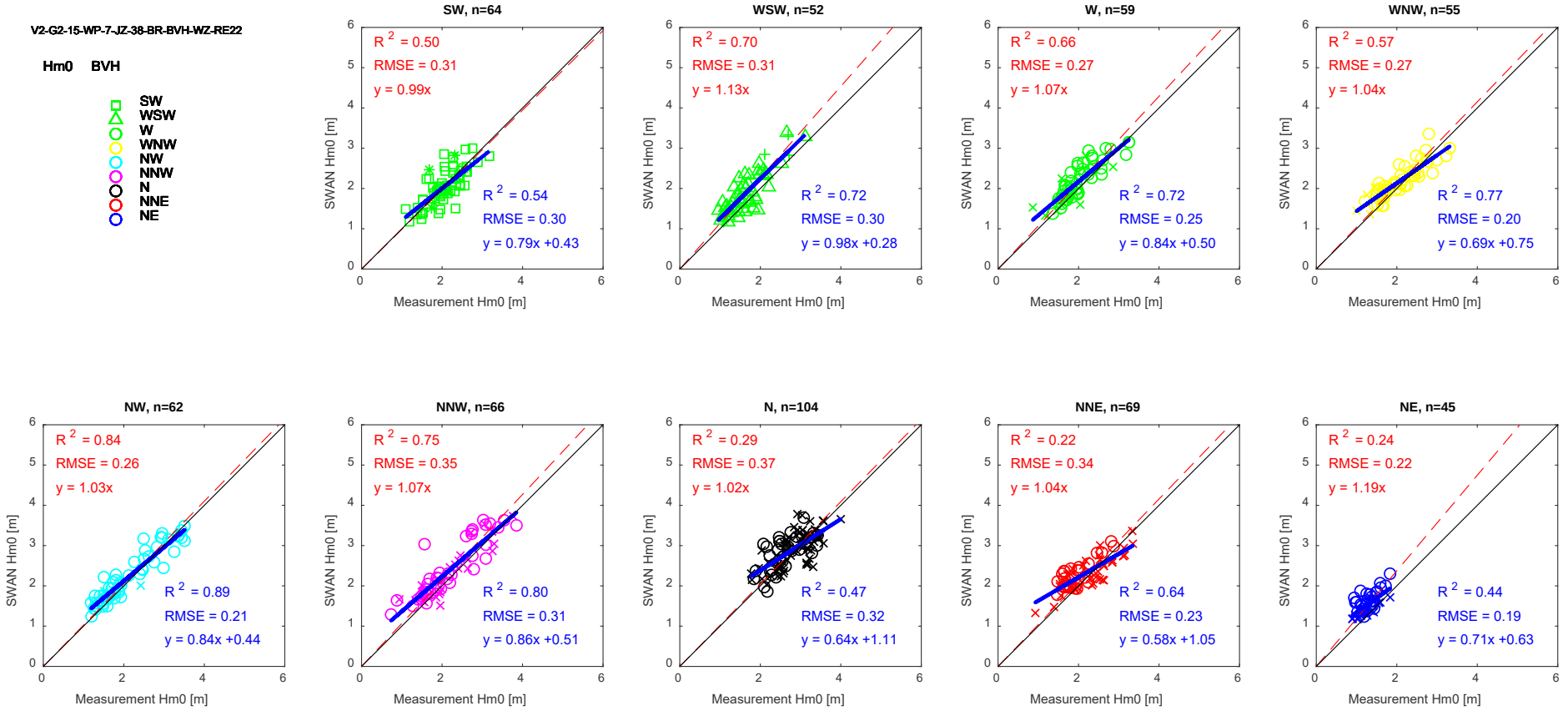

Figure 6.73 -- Model performance of the best case for the validation (BVH) – significant wave height Hm

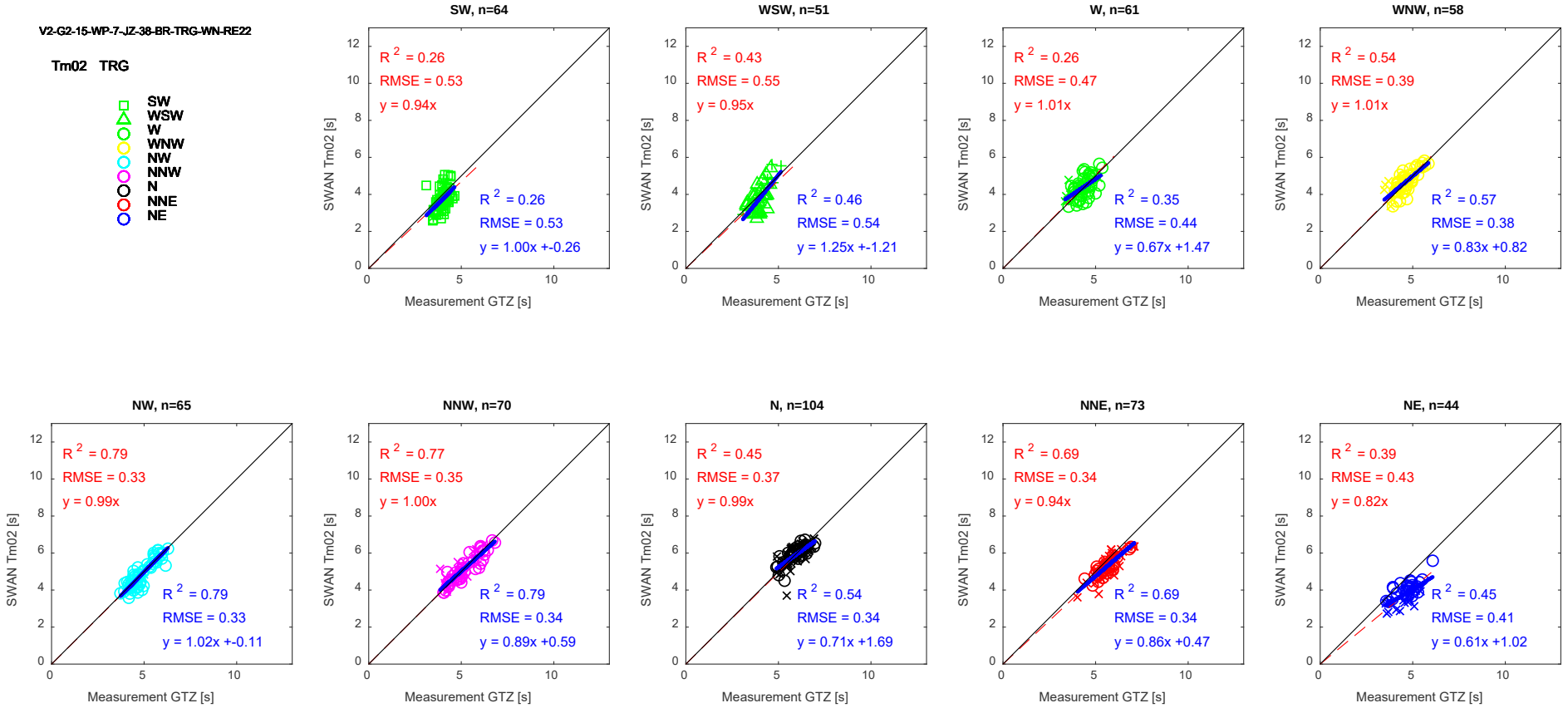

Figure 6.74 – Model performance of the best case for the validation (TRG) – mean wave period Tm02

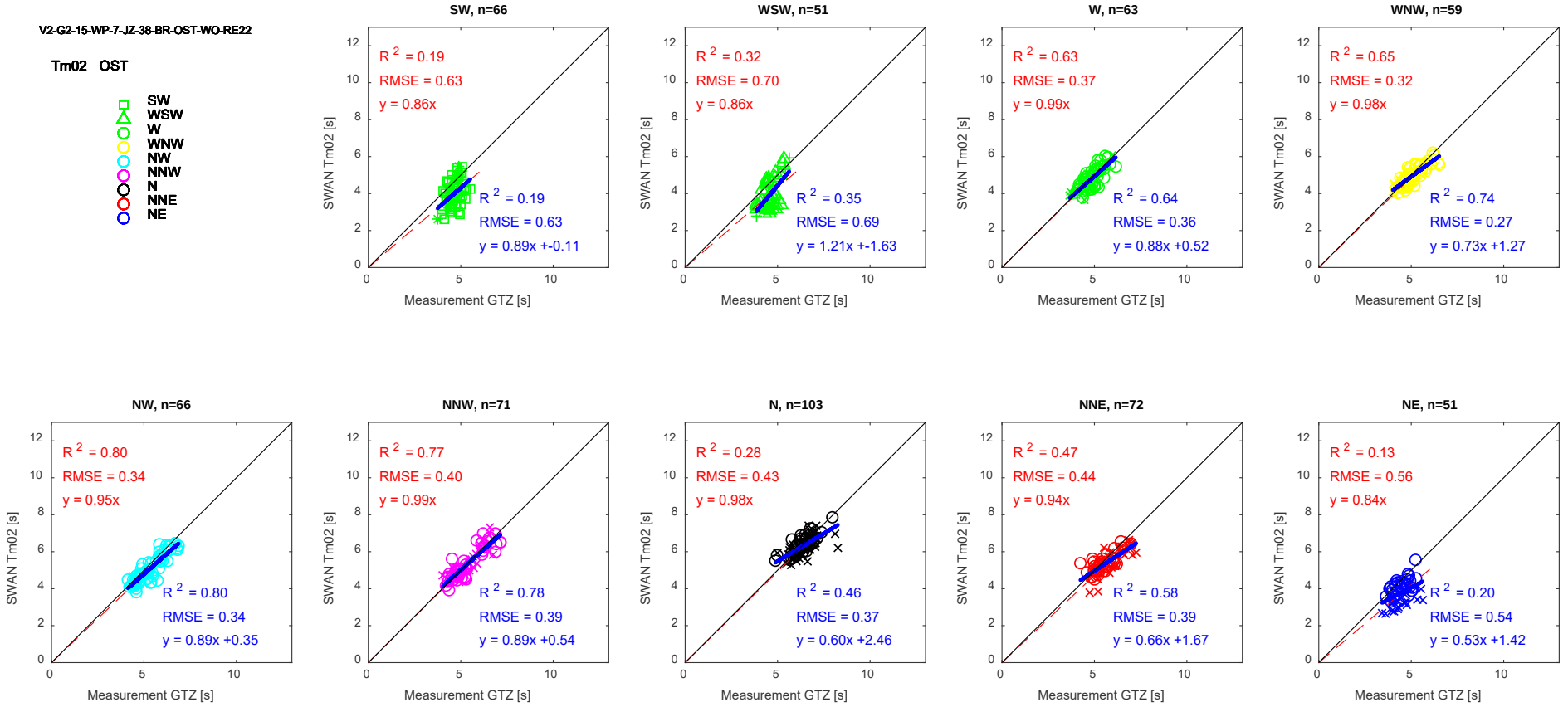

Figure 6.75 – Model performance of the best case for the validation (OST) – mean wave period Tm02

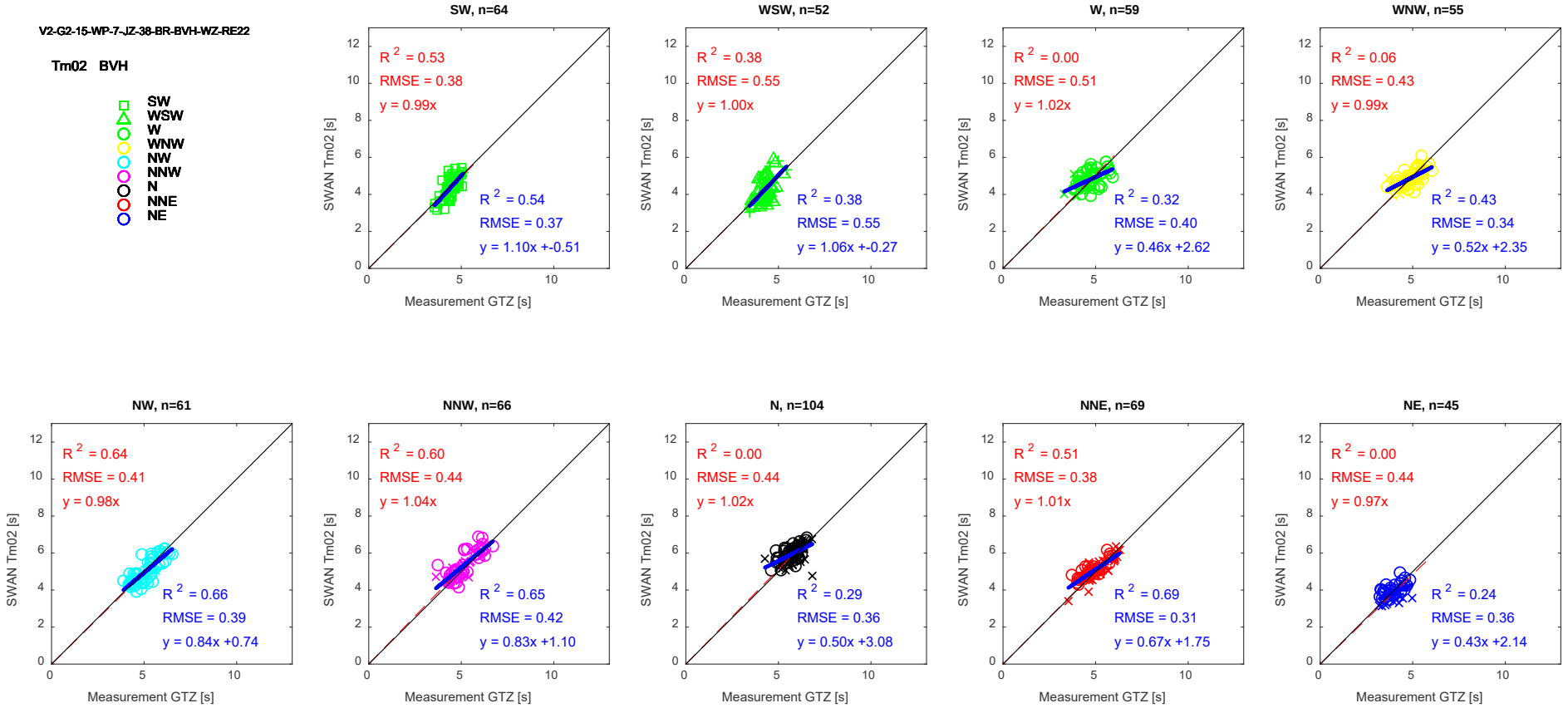

Figure 6.76 – Model performance of the best case for the validation (BVH) – mean wave period Tm02

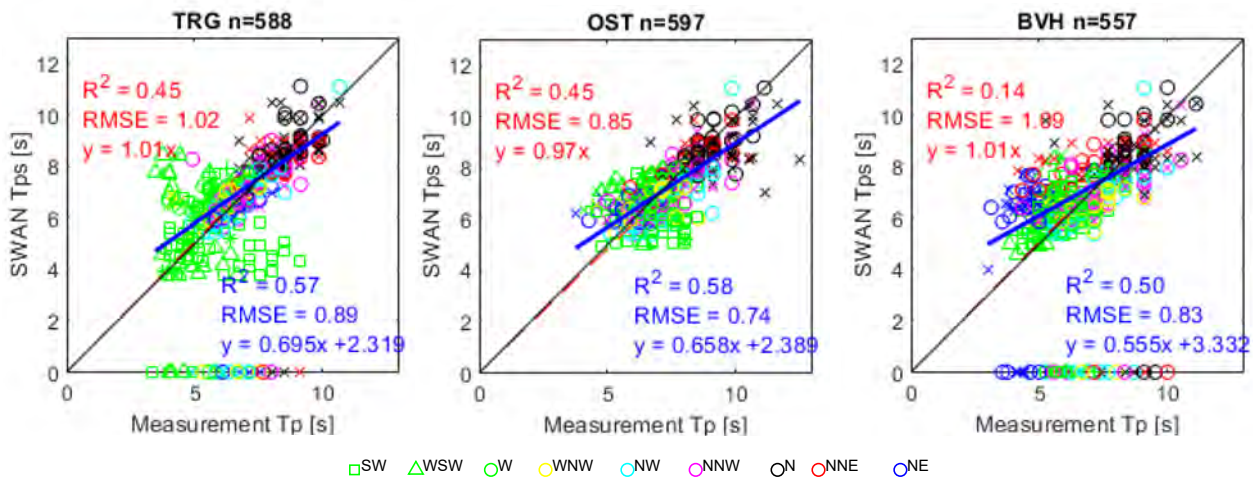

Figure 6.77 – Model performance of the best case for the validation – SWAN smoothed wave period Tps vs measured Tp

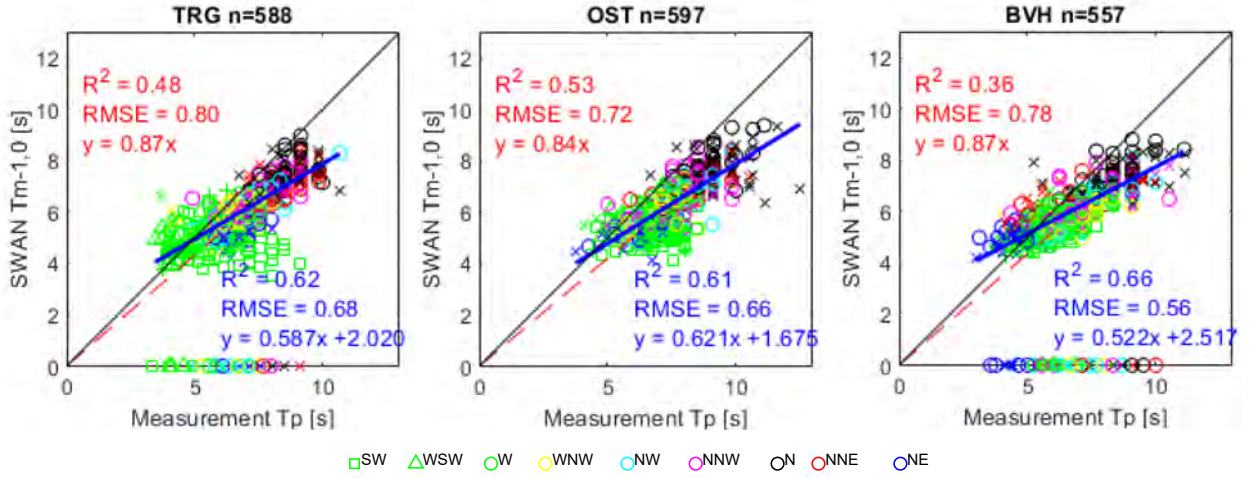

Figure 6.78 – Model performance of the best case for the validation – SWAN spectral period Tm-1,0 vs measured Tp

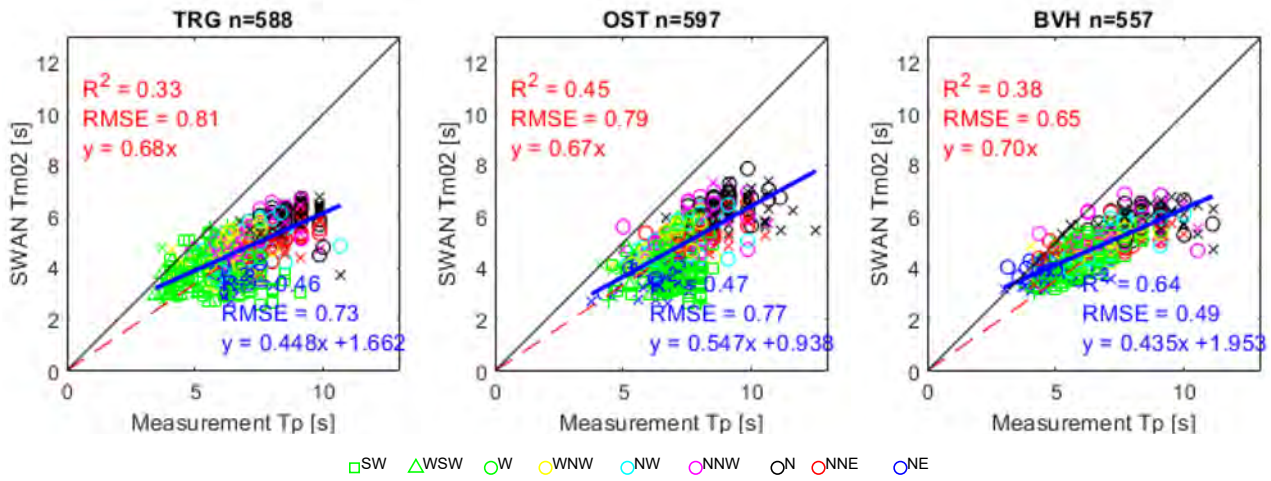

Figure 6.79 – Model performance of the best case for the validation – SWAN mean wave period Tm02 vs measured Tp

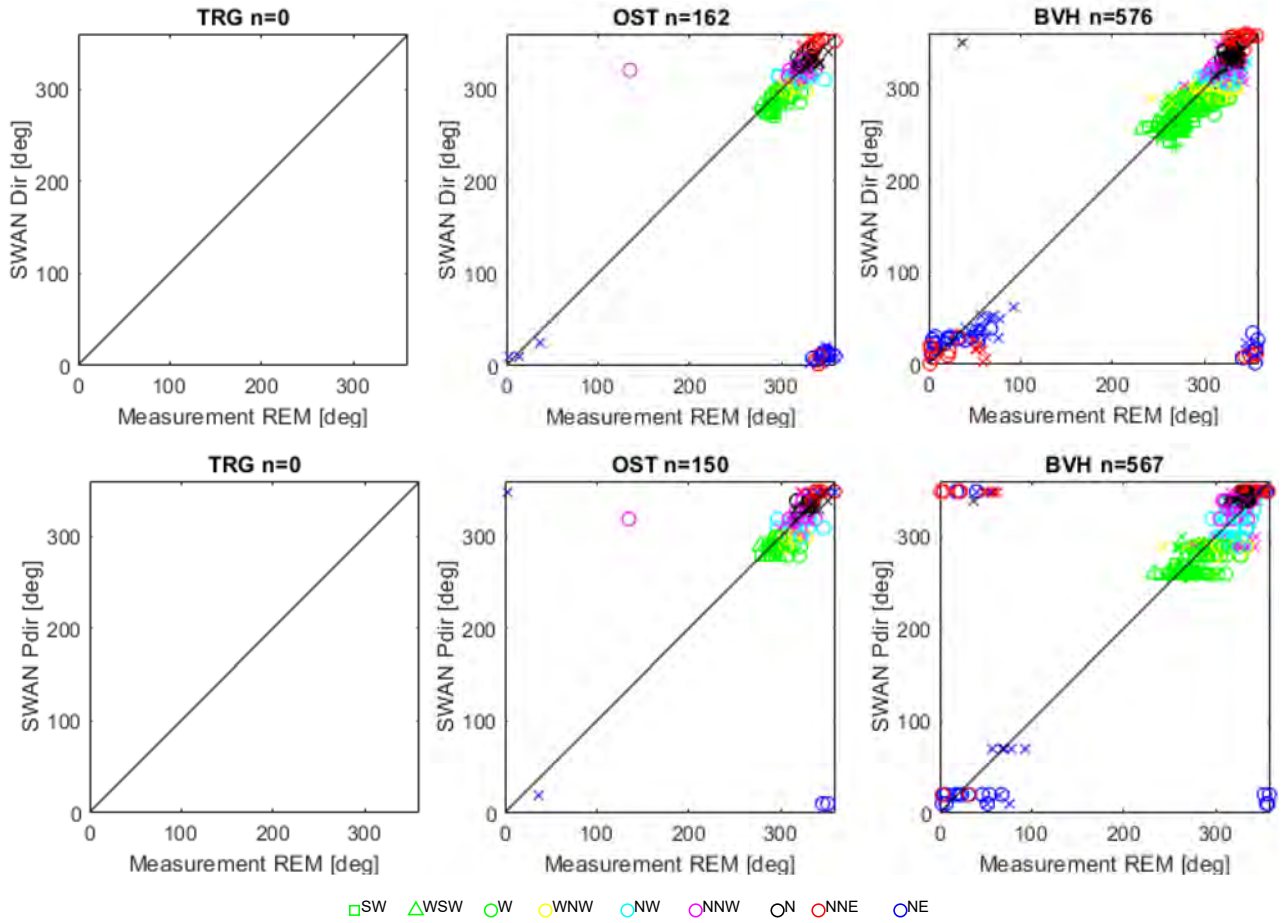

Figure 6.80 – Model performance of the best case for the validation – SWAN dir vs measured dir and pdir

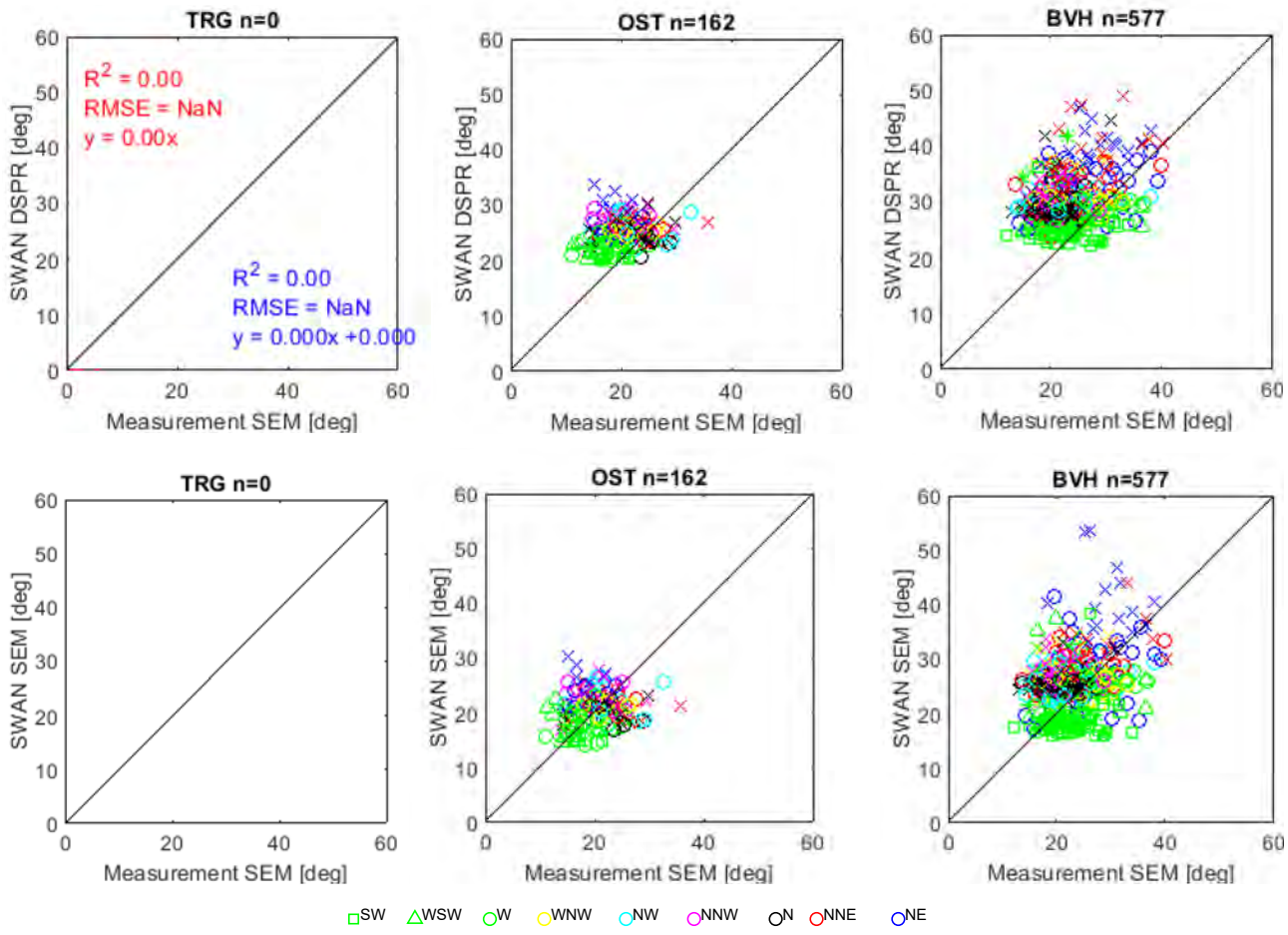

Figure 6.81 – Model performance of the best case for the validation – SWAN DSPR vs measured SEM, and SWAN SEM vs measured SEM

6.6.5 Quality of the present model compared to Ortega & Monbaliu (2015)

The result quality of the calibrated setting in the present study (see section 6.6.4) is compared to the one in Ortega & Monbaliu (2015) . Trappeger's result of this study is compared to be able to judge the differences since TRG is the only common place.

As statistical parameters, bias and RMSE are first evaluated here. The bias and RMSE in Ortega & Monbaliu (2015) is based on 1:1 line and thus red value (y=ax) form is used in the present study. The bias is 0.07-0.12 (depending on the model settings) for the period of Dec 2013 – Feb 2015 and RMSE is 0.19-0.21. In the present study the bias is 0.04 and RMSE is 0.26. Note that this RMSE value 0.26 is not the same evaluation as one in Ortega & Monbaliu (2015) since it is not based on 1:1 line. However the value should not be changed a lot since the bias is small. Statistical parameter (based on y=ax form) is somewhat important however the most important evaluation for SA21 is the evaluation for the cloud of the higher wave heights. For example the bias in the basic case (before the calibration) gives -0.01 which is better value as a statistical value. As can be seen in the basic setting case, the cloud of the lower wave height was overestimated and the higher one was underestimated. That is why fine tuning was necessary. Eventually, after the tuning, the wave height in the upper cloud is corrected and the entire cloud in the final configuration is very close to 1:1 line. Furthermore, the selection of the validation dataset is also different. On one hand, Ortega & Monbaliu (2015) used all the time series during 2 years while this study used selected storms (692 points, in which each direction has more than 60 cases). This 'artificial' selection might have influenced on the statistical value results.

In order to evaluate upper cloud results, four cases are selected based on Komijani *et al.*, (2016), see Table 6.26. The results are shown in Figure 6.80, the high waves are modelled accurately (model error up to ~15-20% at the peak) in the Broersbank study which fall into the cloud pf the plot of the present study (cfr Figure 6.69).

The model of Ortega & Monbaliu (2015) used unstationary mode and specturm input for wave boundary which would have given positive influence on the result while the present study has calibrated many different parameters. Further study will be useful to use Broersbank dataset and explore better parametrization.

Table 6.26 – Four largest event during the Broersbank measurement

storm nr	jaar	maand	stormperiode
1	2013	Dec.	5 Dec 00:00 tot 8 Dec 00:00
2	2014	Jul.	8 Jul 00:00 tot 12 Jul 00:00
3	2015	Nov.	21 Nov 00:00 tot 22 Nov 12:00
4	2016	Jan.	14 Jan 10:00 tot 16 Jan 00:00

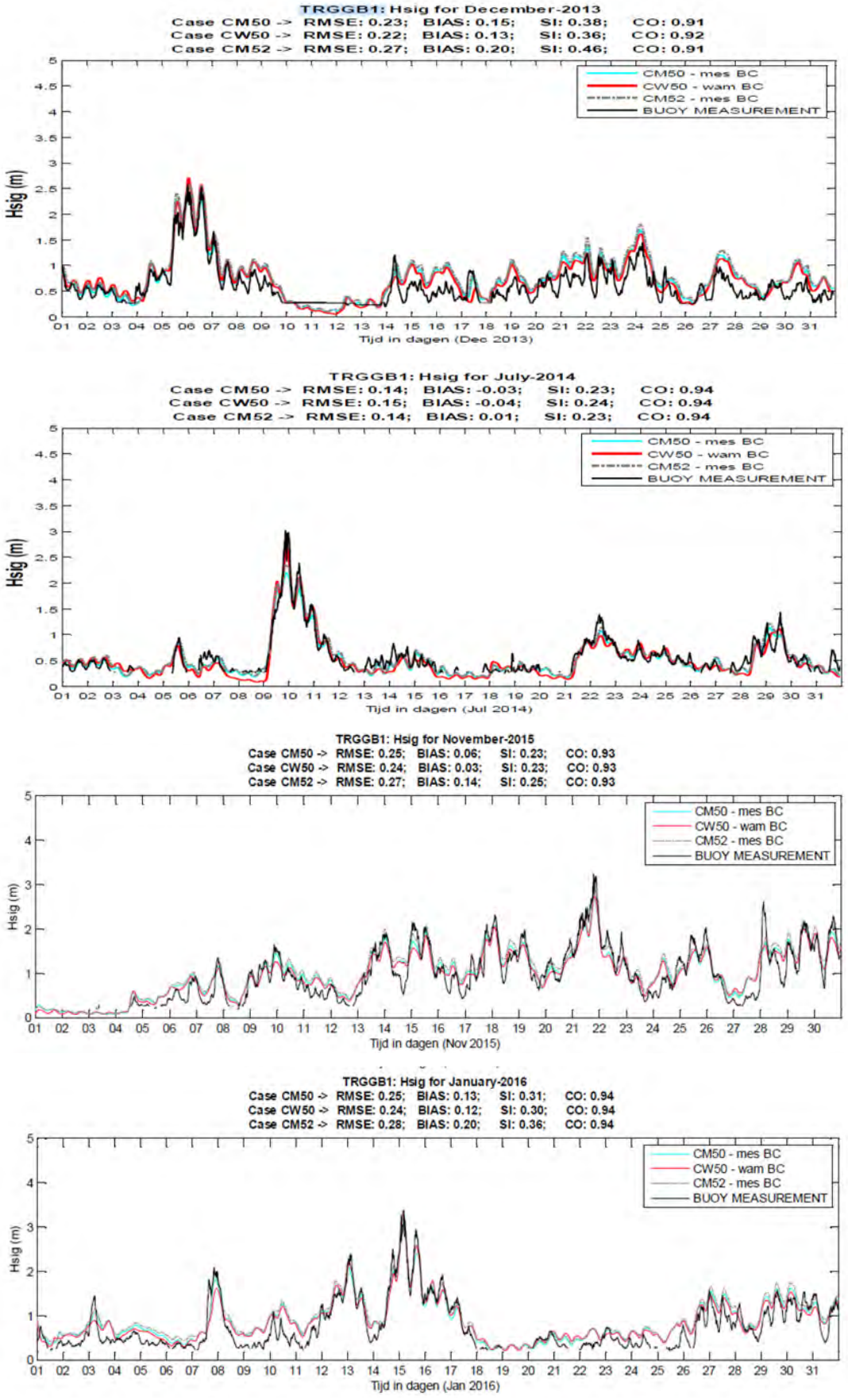

Figure 6.82 – Model performance of the selected four storms in the Broersbank study

7 Conclusions

7.1 General conclusions

In order to estimate appropriate wave boundary conditions nearshore, it is important to have a good model which can deal with wave generation by wind and wave propagation. In this report, the SWAN model and settings are investigated in order to estimate the wave boundary conditions nearshore, and more specifically at -5 m TAW or 1500m from the coast. The latter will be roughly the output locations in SA21, to be used as an input for further calculations (morphological calculation, wave propagation from that point to the toe, and wave overtopping).

SWAN has been selected for this purpose, considering the feasibility and reliability of different existing wave models. Relying on continued model developments and specific use of the model, it is still favourable to optimize SWAN (for SA21).

After the model selection a validation data set was (re-) organized and criteria for case selection were set. Compared to the last safety assessment (i.e. SA15), the number of validation cases has been increased from 209 to 692. On top, these 692 cases include enough cases for each considered wave/wind direction. By doing that, the model performance is evaluated for each wave direction, from SW to NE.

Based on the selected cases, a benchmark basic case and sensitivity analyses of various input parameters (e.g. grid resolution, bottom friction, time lag,..) were conducted.

A change of several input parameters (e.g. time lag, breaking formula, GEN3 setting, reduced wind speed) improved the SWAN estimation compared to the benchmark case, i.e. the slope and intercept parameters of the regression line and the scatter of the data were improved.

Further optimination has been conducted for highly angled wave/wind directions, and concluded that it is important to reduce the wind speed of winds blowing from the land (wind direction from 67.5 – 247.5 deg). For the wave direction SW, no wave boundary is used at the western wave boundary in the SWAN domain.

The breaking formulation plays the most important role for a good estimation of the higher waves, especially for those nearshore locations at a rather shallow depth. The higher waves often break on the sandbanks e.g. located in front of and at Trapegeer. Details of the breaking settings were further investigated using the breaking criterion expressed as Hmax/d. This investigation revealed that the breaking formula of Ruessink and Westhuysen give the most reasonable estimation. After further screening of the model setting and a test case study with extreme wave/wind conditions, we decided that Ruessink is the best suitable breaking formulation to be used in SA21. The result indicates that SWAN gives a good estimation in terms of significant wave height Hm0 and mean wave period Tm02 for the selected 692 cases of the higher wave climate. Therefore it has been concluded that t**he SWAN output can be used as it is (without using correction factors) to estimate wave boundary condition for SA21**.

In the following section further clarification of the input to be used in SA21 has been made.

7.2 Input for SA21

The SWAN input setting to be used in SA21 is shown below.

SET LEVEL X.XX ! Water level

SET NAUT ! Same settings as previous SAs

MODE STATIONARY ! Same settings as previous SAs

MODE TWOD ! Same settings as previous SAs

CGRID REG 438116 5639190 25.50 125000 39000 500 312 CIRCLE 36 0.025 0.85 37 ! dx=250 m, dy=125 m and the number of the frequency bin is 38.

INPGRID BOTTOM 438116 5639190 25.50 2500 780 50 50 EXC 999 ! BCP2020 (50x50 m input)

READINP BOTTOM -1.0 'wgs84_taw_swan2020_50m.dep' 4 0 FREE ! BCP2020

BOU SHAP JON 3.3 PEAK DEGREES ! Same settings as previous SAs

BOU SIDE N CCW CON PAR X.XX X.XX X.XX X.XX ! Hs, Tp, dir, spr input from WHI/AKZ

BOU SEGM IJ 500 160 500 312 CON PAR X.XX X.XX X.XX X.XX ! Hs, Tp, dir, spr input from WHI/AKZ

BOU SIDE W CCW CON PAR X.XX X.XX X.XX X.XX ! Hs, Tp, dir, spr input from WHI/AKZ (except SW)

GEN3 KOMEN ! New setting in SA21

Note that Whitecapping, Quadruplet is automatically included if no declaration OFF WCAP, OFF QUAD. Triads was not activated.

BREAK RUESSINK ! Breaking formula of Ruessink is activated

FRIC JON 0.038 ! Bottom friction values 0.038

OBST TRANSM 0 REFL 0 LINE 494291.1 5676640.5 494523.0 5676661.3 ! Breakwater Ostend

OBST TRANSM 0 REFL 0 LINE 494523.0 5676661.3 494783.6 5676213.4 ! Breakwater Ostend

OBST TRANSM 0 REFL 0 LINE 494041.2 5676494.0 493892.7 5676224.8 ! Breakwater Ostend

OBST TRANSM 0 REFL 0 LINE 493892.7 5676224.8 494166.6 5675959.2 ! Breakwater Ostend

WIND X.XX X.XX! Wind input MP7/MP0. u is at 10 m level from the sea surface. Reduction factor of 80% need to be used for the wind from the land (67.5 – 247.5 deg).

NUM STOPC npnts 101 STAT mxitst 50! force to calculate 50 iterations

7.3 Recommendation for future study

In this report the SWAN validation has been conducted in ther aforementioned settings. One of the difficulties were due to the stationary mode setting. Due to the nature of the SWAN simulation in the safety assessment, stationary mode was selected a priori. However to discuss further the optimum settings of the paramters, unstationary mode can be a good option.

The other aspect is that the modelling has been conducted only considering parameter input in this study. Still of interest to see the difference between using the spectra and using parameters only. It is interesting to collect all the available spectrum inputs and can be tested if the result can be improved.

Even though the performance of the validated model is in general very good in terms of wave height, wave period and direction, the quality of the estimation result of the directional spreading is not good. Further investigation is necessary since the comparison is based on the parameter at this moment and yet the spectrum shape has not been compared.

Finally, breaking formula is the one which needs to be explored more. The present study used Ruessink but the Salmon's studies can still be explored. To discuss further, the Broersbank dataset is very useful.

8 References

Battjes, J.A.; Stive, M.J.F. (1985). Calibration and Verification of a Dissipation Model for Random Breaking Waves., ***in***: (1985). *Proceedings of the Coastal Engineering Conference*, 1. ISBN 0872624382. pp.649–660. doi:10.9753/icce.v19.44

Booij, N.; Ris, R.C.; Holthuijsen, L.H. (1999). A third-generation wave model for coastal regions 1 . Model description and validation *104*: 7649–7666

De Mulder, T.; Monbaliu, J.; Mostaert, F. (2004). Veiligheidsniveau Vlaanderen kustverdediging: opmaak van een numerieke golfdatabank voor de Vlaamse kust. *WL Rapporten*, 644. Waterbouwkundig Laboratorium/KU Leuven: Antwerpen

De Roo, S.; Trouw, K.; Ruiz Parrado, I.; Willems, P.; Suzuki, T.; Verwaest, T.; Mostaert, F. (2016). Het hydraulisch randvoorwaardenboek 2014: achtergrondrapport. Versie 4.0. *WL Rapporten*, 14_014_3. Waterbouwkundig Laboratorium: Antwerpen. XXIII, 104 + 96 p. appendices pp.

Groeneweg, J.; van Gent, M.; van Nieuwkoop, J.; Toledo, Y. (2015). Wave propagation into complex coastal systems and the role of nonlinear interactions. *J. Waterw. Port, Coast. Ocean Eng. 141*(*5*). doi:10.1061/(ASCE)WW.1943-5460.0000300

Holthuijsen, L.H.; Herman, A.; Booij, N. (2003). Phase-decoupled refraction-diffraction for spectral wave models. *Coast. Eng. 49*(*4*): 291–305. doi:10.1016/S0378-3839(03)00065-6

IMDC. (2007). Leidraad Toetsen 2007 - Project: Geïntegreerd Kustveiligheidsplan. 149 pp.

International Marine and Dredging Consultants. (2005). Afstemming Vlaamse en Nederlandse voorspelling golfklimaat op ondiep water: deelrapport 1. Voorbereiding tijdsreeksen met randvoorwaarden. Waterbouwkundig Laboratorium: Antwerpen

International Marine and Dredging Consultants. (2006). Afstemming Vlaamse en Nederlandse voorspelling golfklimaat op ondiep water: deelrapport 2. Voortzetting validatie numeriek model: tekst. Waterbouwkundig Laboratorium en Hydrologisch Onderzoek: Antwerpen

International Marine and Dredging Consultants. (2009a). Afstemming Vlaamse en Nederlandse voorspelling golfklimaat op ondiep water: deelrapport 3. Ontwikkeling van post processing tools. Waterbouwkundig Laboratorium: Antwerpen

International Marine and Dredging Consultants. (2009b). Afstemming Vlaamse en Nederlandse voorspelling golfklimaat op ondiep water: deelrapport 4. Technisch wetenschappelijke bijstand: traject golfklimaat. Waterbouwkundig Laboratorium: Antwerpen

International Marine and Dredging Consultants. (2009c). Afstemming Vlaamse en Nederlandse voorspelling golfklimaat op ondiep water: deelrapport 5. Rapportage jaargemiddelde golfklimaat. Waterbouwkundig Laboratorium: Antwerpen

International Marine and Dredging Consultants. (2009d). Afstemming Vlaamse en Nederlandse voorspelling golfklimaat op ondiep water - Deelrapport 4 : Technisch Wetenschappelijke Bijstand : Traject Onderzoek

Janssens, J.; Delgado, R.; Verwaest, T.; Mostaert, F. (2013). Morfologische trends op middellange termijn van strand, vooroever en kustnabije zone langsheen de Belgische kust: deelrapport in het kader van het Quest4Dproject. *WL Rapporten*, 814_02. Waterbouwkundig Laboratorium: Antwerpen

Kolokythas, G.K.; Fonias, S.; Wang, L.; De Maerschalck, B.; Vanlede, J.; Mostaert, F. (2018). Modelling Belgian Coastal zone and Scheldt mouth area: sub report 7. Progress report 3: Model developments: hydrodynamics, waves and idealized modelling. Version 4.. *FHR reports*, 15_068_7. Flanders Hydraulics Research: Antwerp

Komijani, H.; Ortega, H.; Zhang, Q. (2016). Opstellen van een hydrodynamische modellensuite TELEMAC-TOMAWAC voor de Broersbank. 1–137 pp.

Miani, M.; Vanneste, D. (2019). Update SWAN-2D wave model for flood risk calculations.. *WL Memo's*, 16_122_2. Flanders Hydraulics Research: Antwerp

Nabi Allahdadi, M.; He, R.; Neary, V.S. (2019). Predicting ocean waves along the US east coast during energetic winter storms: Sensitivity to whitecapping parameterizations. *Ocean Sci. 15*(*3*): 691–715. doi:10.5194/os-15-691-2019

Ortega, H.; Monbaliu, J. (2015). Monitoring Broersbank modelstudie -resultaten modellering december 2013 - February 2015

Ruessink, B.G.; Walstra, D.J.R.; Southgate, H.N. (2003). Calibration and verification of a parametric wave model on barred beaches. *Coast. Eng.* ISBN 3130253114 *48*(*3*): 139–149. doi:10.1016/S0378-3839(03)00023-1

Salmon, J.E.; Holthuijsen, L.H. (2015). Modeling depth-induced wave breaking over complex coastal bathymetries. *Coast. Eng. 105*: 21–35. doi:10.1016/j.coastaleng.2015.08.002

Salmon, J.E.; Holthuijsen, L.H.; Zijlema, M.; van Vledder, G.P.; Pietrzak, J.D. (2015). Scaling depth-induced wave-breaking in two-dimensional spectral wave models. *Ocean Model. 87*: 30–47. doi:10.1016/j.ocemod.2014.12.011

Suzuki, T.; De Roo, S.; Altomare, C.; Zhao, G.; Kolokythas, G.K.; Willems, M.; Verwaest, T.; Mostaert, F. (2016). Toetsing kustveiligheid-2015 - Methodologie: toetsingsmethodologie voor dijken en duinen. Versie 10. *WL Rapporten*, 14_014. Waterbouwkundig Laboratorium: Antwerpen

Technum; IMDC; Alkyon. (2002). Structureel herstel van de kustverdediging te Oostende en verbetering van de haventoegang anar de haven van Oostende: Hydrodynamische randvoorwaarden voor het ontwerp. Waterstanden en golfklimaat. Technum: Oostende. 264 pp.

The SWAN team. (2019a). SWAN scientific and technical document version 41.31

The SWAN team. (2019b). SWAN user manual version 41.31. 143 pp.

Van Der Westhuysen, A.J. (2010). Modeling of depth-induced wave breaking under finite depth wave growth conditions. *J. Geophys. Res. Ocean. 115*(*1*): 1–19. doi:10.1029/2009JC005433

Vlaamse Hydrografie. (2014a). Overzicht locaties en parameters van de golfmeetboeien. 6 pp.

Vlaamse Hydrografie. (2014b). Overzicht van de locaties en parameters met winddata. 7 pp.

Yan, L. (1987). An improved wind input source term for third generation ocean wave modelling, WR-No 87-8. 1–22 pp. Available at: http://publicaties.minienm.nl/documenten/an-improved-wind-input-source-term-for-third-generation-ocean-wa%0Apapers2://publication/uuid/3D3F948F-8ED5-4866-9E0A-743D454BA05C

Zijlema, M.; Vledder, G.; Holthuijsen, L. (2012). Bottom friction and wind drag for wave models. *Coast. Eng. 65*: 19–26. doi:10.1016/j.coastaleng.2012.03.002

Appendix A ALD.mat

Integrating all the available datasets (e.g. data from CD-Rom and MVB), a mat file 'ALD.mat' has been created. This file contains time and partly processed measurement data (see below for the details) every 30 min for the period from 01-Jul-1990 00:00:00 to 31-Oct-2019 23:30:00. Note that some of available data contain more data points in time (e.g. water level data is every 5 min), however such detailed information was omitted in this file.

Data tree and explanation

```
ALD.mat
|
ALD
|
| <time>
|-- ALD.Time{1,1} ! Serial date number 727015 to 7.37729979166e+05 (514320 data)
|                       Date and time 01-Jul-1990 00:00:00 to 31-Oct-2019 23:30:00 (every 30 min)
|
| <data at Westhinder>
|-- ALD.WHI.Hm0 ! significant wave height Hm0 [m]
|-- ALD.WHI.TPE   ! peak wave period Tp [s]
|-- ALD.WHI.GTZ   ! average wave period* [s]     *average wave period is mostly comparable to Tm02
|-- ALD.WHI.REM  ! main wave direction [degree]
|-- ALD.WHI.SEM  ! directional spreading [degree]
|
| <water levels: OST-Oostende (main), NPT-Nieuwpoort, ZLD-Zeebrugge>
|-- ALD.OST.WTL  ! water level [m]
|-- ALD.NPT.WTL  ! water level [m]
|-- ALD.ZLD.WTL  ! water level [m]
|
| <wind data: MP7-Westhinder (main), MP0-Wandelaar>
|-- ALD.MP7.dir    ! wind direction [degree]
|-- ALD.MP7.vel    ! wind speed [m/s] at 10 m height from the mean water level at the time (all corrected)
|-- ALD.MP0.dir    ! wind direction [degree]
|-- ALD.MP0.vel    ! wind speed [m/s] at 10 m height from the mean water level at the time (all corrected)
|
| <data at Akkaert>
|-- ALD.AKZ.Hm0; ALD.AKZ.TPE; ALD.AKZ.GTZ; ALD.AKZ.REM; ALD.AKZ.SEM;
|
| <data at Trapegeer>
|-- ALD.TRG.Hm0; ALD.TRG.TPE; ALD.TRG.GTZ
|
| <data at Oostende>
|-- ALD.OST.Hm0; ALD. OST.TPE; ALD. OST.GTZ; ALD.OST.REM; ALD.OST.SEM;
|
| <data at Bol van Heist>
|-- ALD.BVH.Hm0; ALD.BVH.TPE; ALD.BVH.GTZ; ALD.BVH.REM; ALD.BVH.SEM;
```

Original files and each period

The original files used to make the ALD.mat file are shown below. Note that the ALD.mat contains only one data for each time step. If two data is available at the same time step (e.g. Directional waverider data and wavec data, wind data), one higher value was selected.

- Water levels
  - OST
    - OSTVL_19920101_20020206.txt (1992-2002)
      Time in GMT; Water level
    - WL_OST.mat (2000-2014)
      Time in GMT; Water level
    - Gemeten Waterstanden OST_2011_2019.txt (2011- end June 2019)
      Time in GMT; Water level
    - OHM.WS5_001_OSTVL0WS5005_2019.txt (Jan 2019-end Oct 2019)
      Time in GMT; Water level
  - NPT
    - Gemeten Waterstanden NPT_2000_2010.txt (2000- 2010)
      Time in GMT; Water level
    - Gemeten Waterstanden NPT_2011_2019.txt (2011-end Oct 2019)
      Time in GMT; Water level
  - ZLD
    - Gemeten Waterstanden ZLD_2000_2010.txt (2000- 2010)
      Time in GMT; Water level
    - Gemeten Waterstanden ZLD_2011_2014.txt (2011- Oct 2014)
      Time in GMT; Water level
    - Gemeten Waterstanden ZLD_2014_2019.txt (Dec 2014-end Oct 2019)
      Time in GMT; Water level
- Waves
  - WHI
    - WAVES_WHI.mat (1990-2014)
      WHIDW0_1_20060101_20130731.txt
      Time in GMT; E10; GTZ; GEM; HLF; HM0; HM1; HMM; REM; RHF; RLF; SEM; TPE; TZW
      WHIDW1_1_20130801_20141031.txt
      Time in GMT; E10; GTZ; GEM; HLF; HM0; HM1; HMM; REM; RHF; RLF; SEM; TPE; TZW
      WHIDB0_1_19900701_20111231.txt
      Time in GMT; GEM; GTZ; HLF; HM0; HM1; HMM
      WHIDB0_2_19950801_20111231.txt
      Time in GMT; REM; RHF; RLF
      WHIDB0_3_19900701_20111231.txt
      Time in GMT; E10; TPE; SEM
    - WHI_2014_2019.txt (2014-end Oct 2019)
      Time in GMT; HM0; TPE; GTZ; SEM; REM; RLF; RHF
  - AKZ
    - WAVES_AKZ.mat (1990-2014)
      AKZDW1_1_20120701_20141031.txt
      Time in GMT; E10; GTZ; GEM; HLF; HM0; HM1; HMM; REM; RHF; RLF; SEM; TPE; TZW
      AKZGB0_1_19940101_20120630.txt
      Time in GMT; H33; H01; H10; GTZ; E10; TPE; HLF; GEM
    - AKZ_2014_2019.txt (2014-end Oct 2019)

Time in GMT; HM0; TPE; GTZ; SEM; REM; RLF; RHF

- TRG
  - TRGGB0_1_19940101_20140131.txt (1994- Jan 2014)
    Time in GMT; H33; H01; H10; GTZ; E10; TPE; HLF; GEM
  - TRGGB1_1_20140201_20141031.txt (Feb 2014-Oct 2014)
    Time in GMT; H33; H01; H10; GTZ; E10; TPE; HLF; GEM
  - TRG_2014_2018.txt (2014-2018)
    Time in GMT; HM0; TPE; GTZ
  - TRG_2018_2019.txt (2018-end Oct 2019)
    Time in GMT; HM0; TPE; GTZ
- OST
  - OSTGB0_1_19970401_20140131.txt (1997-2014)
    Time in GMT; H33; H01; H10; GTZ; E10; TPE; HLF; GEM
  - OSTGB1_1_20140201_20141031.txt (Feb 2014 – Oct 2014)
    Time in GMT; H33; H01; H10; GTZ; E10; TPE; HLF; GEM
  - OST_2014_2015.txt (2014-2015)
    Time in GMT; HM0; TPE; GTZ
  - OST_2016_2019.txt (2016-end Oct 2019)
    Time in GMT; HM0; TPE; GTZ; SEM; REM; RLF; RHF
- BVH
  - BVHDW0_1_20050401_20130731.txt (2005-2013)
    Time in GMT; E10; GTZ; GEM; HLF; HM0; HM1; HMM; REM; RHF; RLF; SEM; TPE; TZW
  - BVHDW1_1_20130801_20141031.txt (2013-2014)
    Time in GMT; E10; GTZ; GEM; HLF; HM0; HM1; HMM; REM; RHF; RLF; SEM; TPE; TZW
  - BVHDB0_1_19930601_20050331.txt ~Hm0, GTZ (1993-2005)
    Time in GMT; GEM; GTZ; HLF; HM0; HM1; HMM
  - BVHDB0_2_19950801_20050331.txt ~REM (1995-2005)
    Time in GMT; REM; RHF; RLF
  - BVHDB0_3_19930601_20050331.txt ~TPE,SEM (1993-2005)
    Time in GMT; E10; TPE; SEM
  - BVH_2014_2019.txt (2014-end Oct 2019)
    Time in GMT; HM0; TPE; GTZ; SEM; REM; RLF; RHF

- Wind
  - MP7
    - WIND_MP7.mat (1993-2014)*
      *all the data converted from raw data (measured at 26.15 m TAW) to 10 m height from mean sea level data
      Time in GMT; WRS; WVC
    - MP7_2014_2019.txt (2014-end Oct 2019)
      Time in GMT; WRS; WVC
  - MP0
    - WIND_MP0.mat (1993-2014)**
      **all the data converted from raw data (measured at 19.2 – 25.7 m TAW in different periods) to 10 m height from mean sea level data
      Time in GMT; WRS; WVC
    - MP0_2014_2019.txt (2014-end Oct 2019)
      Time in GMT; WRS; WVC

Appendix B Output locations in xy coordinate

The output x-y locations in the WGS84UTM31 coordinate are obtained by SuperTrans matlab script available in OpenEarth (https://www.deltares.nl/en/software/openearth) and summarized in

Table B.0.1 – Selected locations in xy-coordinates

Code	Location	Position N (WGS84)	Position E (WGS84)	X coordinate (WGS84UTM31)	Y coordinate (WGS84UTM31)
TRG	Trapegeer	51° 8'15.04"N	2°34'58.97"E	470723.8	5665106.3
OST	Oostende Oosterstaketsel	51°14'48.60"N	2°55'39.60"E	494847.0	5677183.9
AKZ	Akkaert	51°25'5.40"N	2° 48'4.20"E	486069.0	5696254.8
BVH	Bol van Heist	51°23'30.60"N	3° 12'1.50"E	513840.8	5693326.4
WHI	Westhinder*	51°22'51.72"N	2° 26'20.82"E	460860.6	5692255.5

FOR THE SIMPLICITY, WE USE ONLY DIR.WAVERIDER LOCATION FOR WHI (DIFFERENT LOCATIONS FOR DIFFERENT SONSORS)

Appendix C Influence of higher fmax

Not only the number of the frequency bins but also the value of fmax can also influence to the result.

Figure C.1 and Figure C.2 show the influence of fmax based on the best case for the validation (see section 6.6.4), significant wave height and mean wave period respectively. Table C.1 and Table C.2 show the estimation value using y=ax+b regression line for significant wave height and mean wave period. Note that the best case uses fmax=0.85 Hz corresponding to 38 bins while higher fmax case uses fmax=1.506 Hz corresponding to 44 bins.

As shown in the results, there is no influence to the wave height. On the other hand, 2-3% difference can be seen in the estimated value using y=ax+b regression line for the mean wave period. It is a minor difference therefore bin 38 is still valid. Note that bin 38 settings lead slightly better estimation value.

Figure C.3 show the influence of fmax under the extreme wave/wind conditions (see similar exercise in section 6.6.3).

The difference in Hm0 is 0% and the difference in Tm02 is maximum 1 % except for the nebouring grid points of Zeebrugge.

Note that the difference of the fmax is not so sensitive because *the wave parameters in the output of SWAN are computed from the wave spectrum over the prognostic part of the spectrum with the diagnostic tail added* (The SWAN team, 2019b).

From those analysis, it can be again concluded that the influence of fmax is negligible for the higher wave climate. Note that the influence of higher fmax might be important for mild wave climate.

Table C.0.1 – Influence of fmax to the best case for the validation (upper: 0.85 Hz = best case, lower 1.506 Hz) – Hm0

Location	Case	Y=ax			Y=ax+b					
		Slope 'a'	R^2	RMSE	Slope 'a'	Intcpt 'b'	R^2	RMSE	Est_x=5	Ratio
TRG	Best case	**1.04**	0.82	0.26	0.85	0.41	0.87	0.23	4.65	-
	fmax 1.506	**1.04**	0.82	0.26	0.85	0.41	0.87	0.23	4.65	**1.00**
OST	Best case	**1.04**	0.80	0.32	0.83	0.49	0.86	0.27	4.66	-
	fmax 1.506	**1.04**	0.80	0.32	0.83	0.49	0.86	0.27	4.66	**1.00**
BVH	Best case	**1.04**	0.72	0.33	0.82	0.52	0.79	0.29	4.62	-
	fmax 1.506	**1.04**	0.72	0.33	0.82	0.52	0.79	0.29	4.62	**1.00**

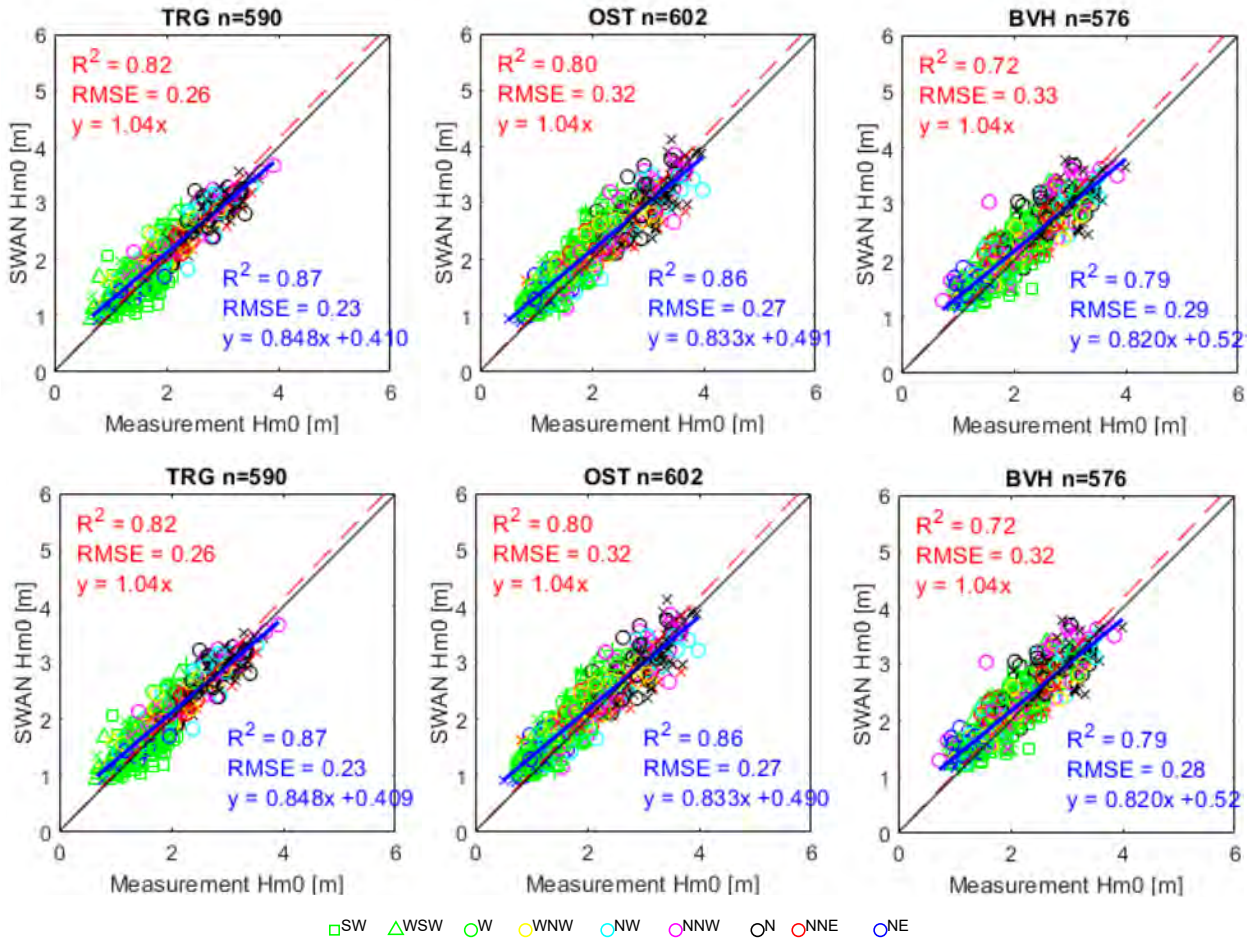

Figure C.0.1 – Influence of fmax to the best case for the validation (upper: 0.85 Hz = best case, lower 1.506 Hz) – Hm0

Table C.0.2 – Influence of fmax to the best case for the validation (upper: 0.85 Hz = best case, lower 1.506 Hz) – Tm02

Location	Case	Y=ax			Y=ax+b					
		Slope 'a'	R^2	RMSE	Slope 'a'	Intcpt 'b'	R^2	RMSE	Est_x=11	Ratio
TRG	Best case	**0.97**	0.77	0.48	0.96	0.05	0.77	0.48	10.61	-
	fmax 1.506	**1.00**	0.79	0.42	0.90	0.47	0.79	0.41	10.40	**0.98**
OST	Best case	**0.95**	0.74	0.54	1.03	-0.41	0.74	0.54	10.86	-
	fmax 1.506	**0.97**	0.75	0.49	0.96	0.07	0.75	0.49	10.58	**0.97**
BVH	Best case	**1.01**	0.71	0.45	0.91	0.52	0.72	0.45	10.48	-
	fmax 1.506	**1.02**	0.70	0.43	0.85	0.87	0.73	0.41	10.23	**0.98**

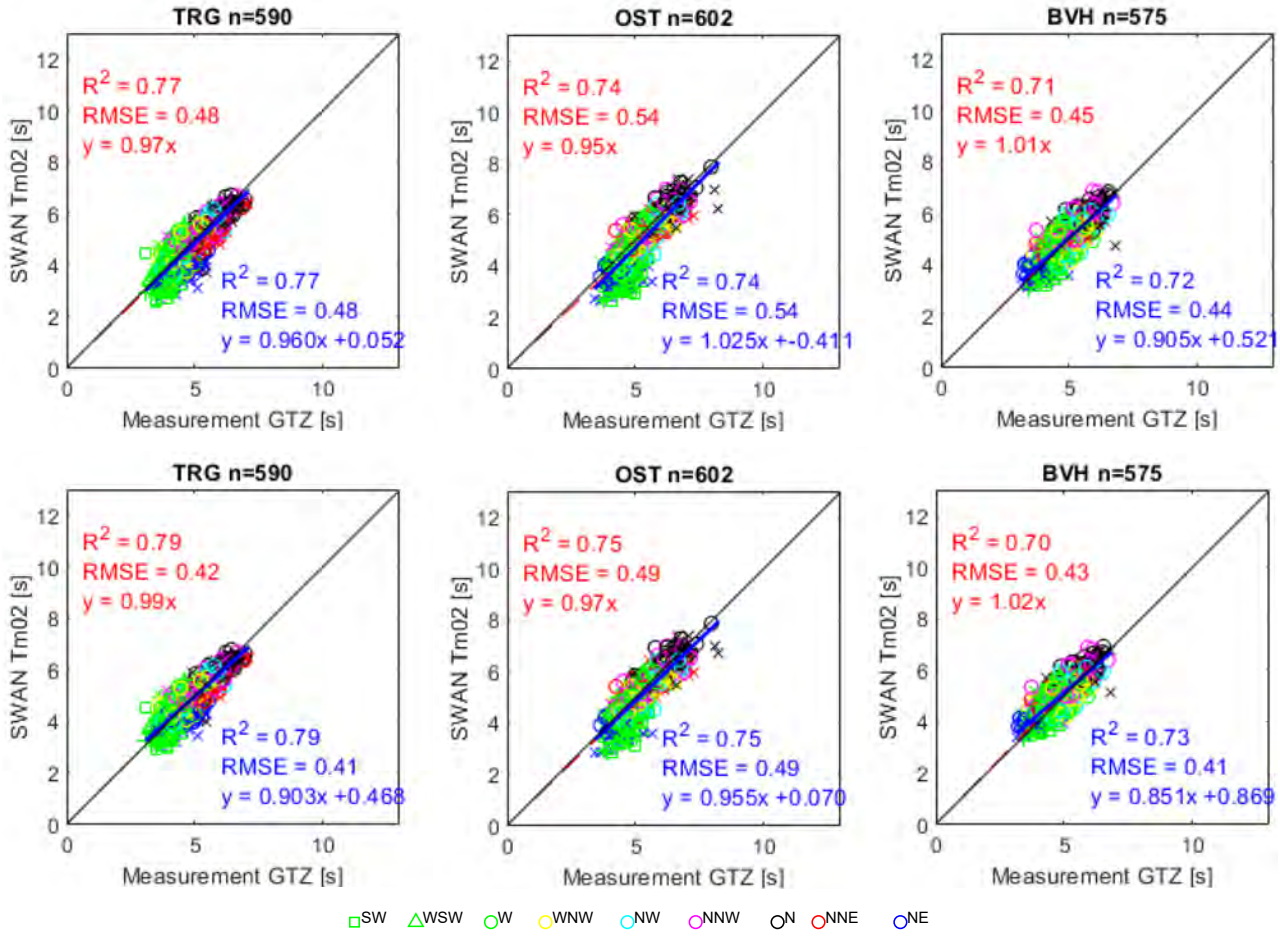

Figure C.0.2 – Influence of fmax to the best case best for the validation (upper: 38, lower 44 bins) - Tm02

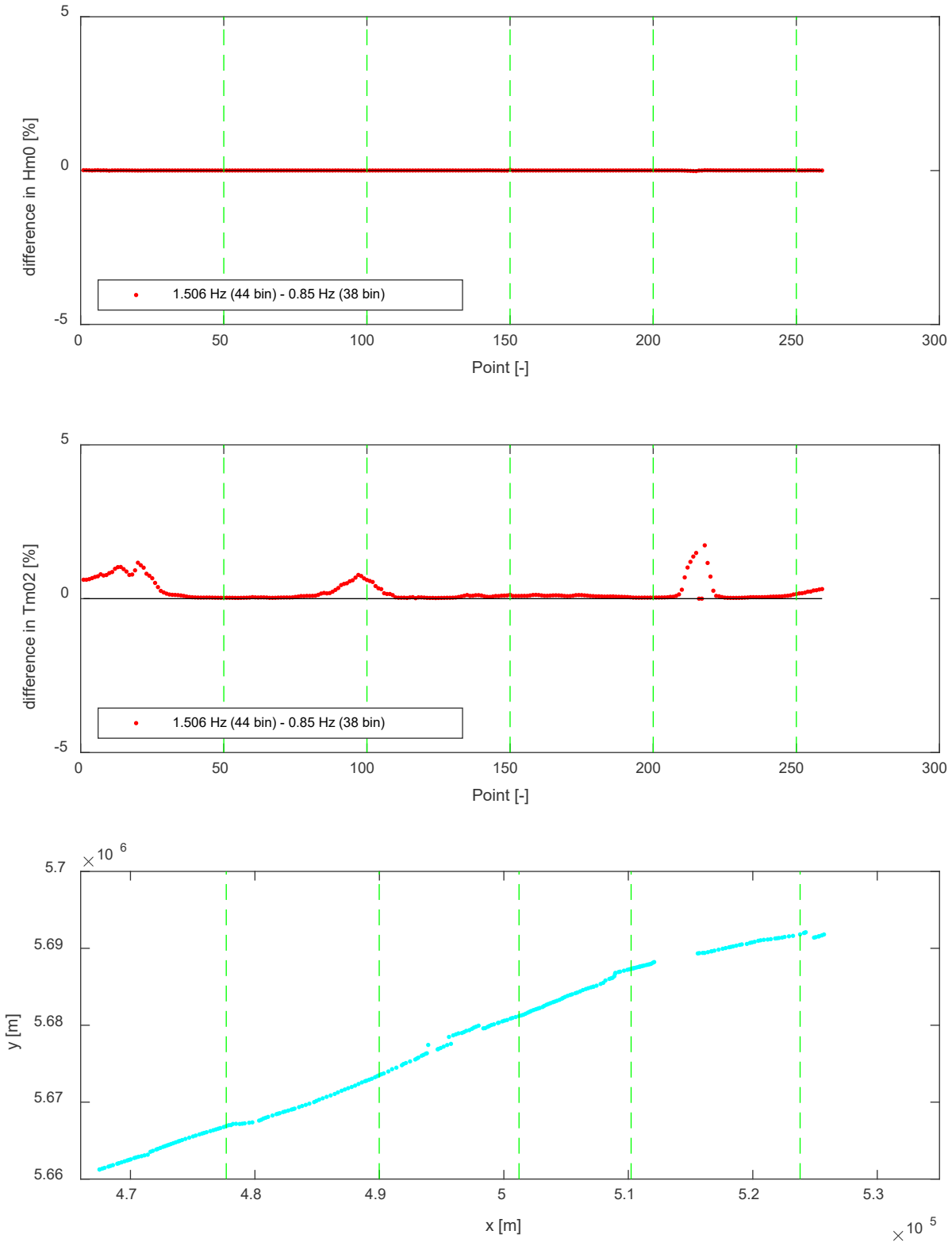

Figure C.0.3 – Influence of fmax for the extreme wave/wind condition (upper: fmax=0.85 Hz & 38 bins, middle: fmax=1.506 Hz & 44 bins, lower: location of HBC output points in SA15) – Hm0

DEPARTMENT **MOBILITY & PUBLIC WORKS**
Flanders hydraulics

Berchemlei 115, 2140 Antwerp
T +32 (0)3 224 60 35
F +32 (0)3 224 60 36
flanders.hydraulics@vlaanderen.be
www.flandershydraulics.be